DUCT DESIGN IMPACTS ON ENERGY CONSUMPTIONS AND LIFE CYCLE COSTS FOR RESIDENTIAL CENTRAL HEATING AND COOLING SYSTEMS

A Dissertation

by

PENG YIN

Submitted to the Office of Graduate and Professional Studies of
Texas A&M University
in partial fulfillment of the requirements for the degree of

DOCTOR OF PHILOSOPHY

Chair of Committee,	Michael B. Pate
Committee Members,	Dennis L. O'Neal
	Bryan P. Rasmussen
	Jorge L. Alvarado
Head of Department,	Andreas A. Polycarpou

August 2015

Major Subject: Mechanical Engineering

ABSTRACT

In this study, a series of laboratory measurements was conducted on residential air handling units (AHUs) and air conditioners to characterize their performance at typical installed conditions. In addition, performance models of blowers and air conditioners were developed from the laboratory measurements and integrated with building energy simulations to predict the energy consumption and the life cycle cost of ductworks with respect to different climates (Chicago, IL and Austin, TX), duct materials (e.g., sheet metal and flex ducts), flow resistances, and blower types (e.g. PSC and ECM blowers).

The experimental results showed that PSC and ECM blowers have distinct airflow, power, and efficiency performance in response to increases in the external static pressure (ESP). The building energy simulation results showed that increasing the duct flow resistance from 0.3 to 0.9 in. w.g. (75 to 225 Pa) decreased airflow rates of PSC blowers and consequently decreased the annual blower electricity consumptions by 11% for the Austin home and 16% for the Chicago home. However, in systems with ECM blowers the same increase in the duct flow resistance increased the annual blower electricity consumptions by about 60% for both the Austin home and the Chicago home, primarily because ECM blowers maintained constant airflow rates over a range of pressures. For the same increase in the duct flow resistance, the electricity consumptions of condensing units in systems with PSC blowers increased by 2.7% for the Austin home and 5.5% for the Chicago home, while the electricity increase in systems with ECM

blowers were less dramatic, being 1.6% for the Austin home and 1.5% for the Chicago home. Also, the simulation results indicated that although the cost-effectiveness of a specific duct design is shown to be heavily dependent on initial duct fabrication and installation costs, the use of lower flow resistance ductworks generally leads to lifetime savings in the presence of supply and return leakages of 10%. Specifically, the lifetime savings is achieved in 6 out of 8 simulated cases for the Chicago home and all of the simulated cases for the Austin home by using ductworks at lower flow resistances.

DEDICATION

To my parents and my wife.

ACKNOWLEDGEMENTS

I would like to thank my committee chair, Dr. Pate, and my committee members, Dr. O'Neal, Dr. Rasmussen, and Dr. Alvarado, for their guidance and support throughout the course of this research.

Thanks also go to my friends and colleagues and the staff at Riverside Energy Efficiency Laboratory (REEL) for making my time at Texas A&M University a great experience.

Finally, thanks to my parents for their encouragement and to my wife for her patience and love.

NOMENCLATURE

A	Dependent variable
ACCA	Air Conditioning Contractors of America
ach	air change per hour
AFUE	Annual fuel utilization efficiency
AHU	Air handling unit
AHRI	Air-Conditioning, Heating and Refrigeration Institute
ASHRAE	American Society of Heating, Refrigerating, and Air-Conditioning Engineers
ASP	Available static pressure
$C_1, C_2 \dots C_n$	Empirical coefficients
C_d	Discharge coefficient
C_L	Leakage constant
$c_{p_{a1}}$	Specific heat of air entering the indoor side, Btu/lb_m·°F (J/kg·°C)
$c_{p_{a2}}$	Specific heat of air leaving the indoor side, Btu/lb_m·°F (J/kg·°C)
CapModCurve	Capacity modifier curve
CFA	Conditioned floor are, ft^2 (m^2)
COP	Coefficient of performance
COP_{rated}	Coefficient of performance at the rating condition
$Cost_n$	n^{th} year energy cost, USD
DB	Dry-bulb temperature, °F (°C)

DOE	Department of Energy
E_{AE}	Average annual auxiliary electrical energy consumption, kWh
E_i	Power input, indoor side, W
ECM	Electronically commutated motor
EER	Energy efficiency ratio, Btu/(W·h)
EIA	U.S. Energy Information Administration
EIRModCurve	Energy input ratio modifier curve
ELA	Effective leakage area, ft^2 (m^2)
ESP	External static pressure, in. w.g. (Pa)
FF	Flow fraction
FR	Friction factor
g	Inflation rate
h_{a1}	Enthalpy, air entering the indoor side, Btu/lb_m (J/kg)
h_{a2}	Enthalpy, air leaving the indoor side, Btu/lb_m (J/kg)
h_{r1}	Enthalpy, refrigerant entering the indoor side, Btu/lb_m (J/kg)
h_{r2}	Enthalpy, refrigerant leaving the indoor side, Btu/lb_m (J/kg)
HVAC	Heating, ventilation, and air-conditioning
IGain	Internal heat gain, Btu/day (kW)
IECC	International Energy Conservation Code
K	Conversion factor for the latent cooling calculation, 63660 for I-P unit and 2.47×10^6 for SI unit.
LBNL	Lawrence Berkeley National Laboratory

N_{br}	Number of bedroom
N_L	Leakage exponent
PNNL	Pacific Northwest National Laboratory
PSC	Permanent split capacitor
PV	Present value
PV_{total}	Total present value over lifetime
$\dot{Q}$	Blower airflow rate, ft^3/min (m^3/s)
$\dot{Q}(\%)$	Percentage airflow change, %
$\dot{Q}_{25}$	Blower airflow rate at 0.1 in. w.g. (25 Pa), ft^3/min (m^3/s)
$\dot{Q}_{known}$	Know blower airflow rate at any pressure, ft^3/min (m^3/s)
$\dot{Q}_L$	Leakage airflow rate, ft^3/min (m^3/s)
$\dot{Q}_{Lr}$	Rated leakage airflow rate, ft^3/min (m^3/s)
$\dot{Q}_{max}$	Maximum system airflow rate, ft^3/min (m^3/s)
$\dot{Q}_{mi}$	Airflow rate, indoor, measured, ft^3/min (m^3/s)
$\dot{q}_{lci}$	Latent cooling capacity, indoor side, Btu/h (W)
$\dot{q}_{sci}$	Sensible cooling capacity, indoor side, Btu/h (W)
$\dot{q}_{tc}$	Total cooling capacity, Btu/h (W)
$\dot{q}_{tc,rated}$	Total cooling capacity at the rating condition, Btu/h (W)
$\dot{q}_{tci_a}$	Total cooling capacity, indoor side, air side, Btu/h (W)
$\dot{q}_{tci_r}$	Total cooling capacity, indoor side, refrigerant side, Btu/h (W)
REEL	Riverside Energy Efficiency Laboratory

R^2	Coefficient of determination
r_L	Effective leakage ratio
SHR	Sensible heat ratio
SHR_{rated}	Sensible heat ratio at the rating condition
SHRModCurve	Sensible heat ratio modifier curve
SIR	Savings-to-investment ratio
t_{a1}	Dry-bulb temperature of air entering the indoor side, °F, (°C)
t_{a2}	Dry-bulb temperature of air leaving the indoor side, °F, (°C)
T_{DB_o}	Dry-bulb temperature of air entering the outdoor side, °F (°C)
T_{WB_i}	Wet-bulb temperature of air entering the indoor side, °F (°C)
TEL	Total effective length, ft (m)
TXV	Thermostatic expansion valve
U_A	Combined uncertainty for the dependent variable A
$u_{h_{r1}}$	Uncertainty of the refrigerant enthalpy entering indoor side, Btu/lb_m (J/kg)
$u_{h_{r2}}$	Uncertainty of the refrigerant enthalpy leaving indoor side, Btu/lb_m (J/kg)
$U_{q_{tci_r}}$	Combined uncertainty for the total cooling capacity at the refrigerant side
U_{x_i}	Uncertainty for the independent variable x_i
u_{w_r}	Uncertainty of refrigerant mass flow rate, lb_m/h (kg/s)

v_n	Specific volume of air, ft^3/lb_m (m^3/kg)
VFD	Variable frequency drive
W	Blower power, W
$\dot{w}_r$	Mass flow rate, refrigerant, lb_m/h (kg/s)
WB	Wet-bulb temperature, °F (°C)
x_i	i^{th} independent variable
ΔP_s	Static differential pressure, in. w.g. (Pa)
ΔP_{sr}	Static differential pressure at the reference condition, in. w.g. (Pa)
η	Overall efficiency
ρ	Air density, lb_m/ft^3 (kg/m^3)
ω_1	Humidity ratio, air entering the indoor side
ω_2	Humidity ratio, air leaving the indoor side

TABLE OF CONTENTS

Page

LIST OF FIGURES

Page

LIST OF TABLES

Page

1. INTRODUCTION

1.1 Background

In the United States, substantially high duct flow resistances widely exist in residential central heating, ventilating, and air-conditioning (HVAC) systems. The duct flow resistance is quantified in terms of the external static pressure (ESP), which is the sum of external flow resistances in an air distribution system that a blower in an air handling unit (AHU) has to work against, such as the pressure drops caused by ducts, duct fittings, cooling coils, heat exchangers, return grilles, supply registers, and air filters. Figure 1 shows static pressure changes with gradients referenced to the atmospheric pressure in an air handling unit (AHU) and its adjacent ducts.

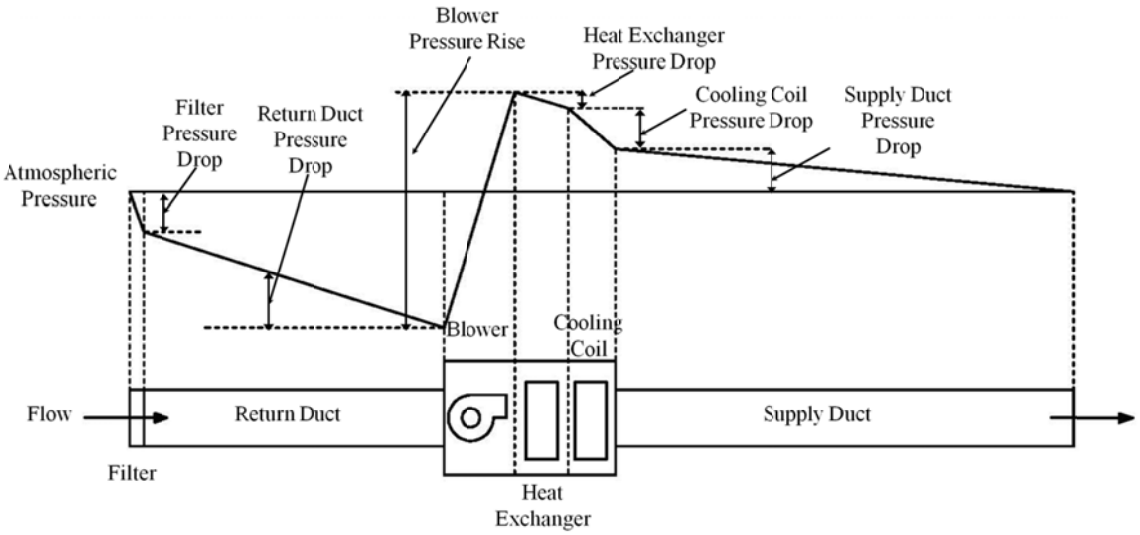

Figure 1 Theoretical static pressure changes for a typical residential central HVAC system

National standards specify a range of external static pressures (ESPs) for testing and rating residential forced-air heating and cooling equipment. For example, the unitary air-conditioning and air-source heat pump equipment up to 65 kBtu/h (19 kW) are tested within an external static pressure range of 0.1 to 0.2 in. w.g. (25 to 50 Pa) based on the unit capacity in accordance with the Air-Conditioning, Heating and Refrigeration Institute (AHRI) Standard 210/240 (AHRI 2008). Also, gas furnaces are rated within a pressure range of 0.18 to 0.33 in. w.g. (45 to 82 Pa) following the American Society of Heating, Refrigerating, and Air-Conditioning Engineers (ASHRAE) Standard 103 (2007c).

However, extensive field measurements have indicated that many residential systems operate at much higher external static pressures (ESPs). Table 1 summarizes the external static pressure (ESP) measurements in over 800 field surveys from 22 studies (DOE 2014). It shows that the external static pressure (ESP) in installed conditions varies from 0.31 to 1.12 in. w.g. (77 to 279 Pa) with a weighted average of 0.5 in. w.g. (125 Pa), which is well above the pressures specified in AHRI Standard 210/240 (AHRI 2008) and ASHRAE Standard 103 (ASHRAE 2007c) for equipment testing and rating. The excess external static pressures (ESPs) observed in the field measurements imply that the equipment performance determined at the laboratory settings may not be achievable at installed conditions due to the impacts of excess duct flow resistances on the performance of blowers and air conditioners.

Table 1 Summary of field measurements of external static pressure (DOE 2014)

No.	Study	Sample Size	Measured ESP, in. w.g. (Pa)	Note
1	Blasnik et al. 1995 study	40	0.41 (103)	1
2	Blasnik et al. 1996 study	28	0.48 (120)	1
3	Parker 1997 study	9	0.55 (138)	1
4	Proctor et al. 1995 study	40	0.53 (133)	1
5	Proctor et al. 1996 study	36	0.51 (128)	1
6	Proctor et al. 1998 Study	15	0.45 (113)	1
7	Proctor 1998 study	36	0.42 (105)	1
8	Proctor 2005 study	78	0.48 (120)	1
9	Proctor et al. 2007 study	4	1.01 (253)	1,2
10	Proctor 2000 study	5	0.50 (125)	1
11	Proctor 2001 study	69	0.54 (135)	1
12	Proctor 2003 study	69	0.53 (133)	1
13	Proctor 1996a study	8	0.45 (113)	1
14	Proctor 1996b study	92	0.31 (78)	1,2
15	Wilcox et al. 2006 study	51	0.77 (193)	1
16	Dickenhoff 1998 study	13	0.51 (128)	1
17	Ueno 2008 study	4	0.9 (225)	1,2
18	Ueno 2009 study	1	1.12 (280)	1,2
19	Pigg 2005 study	37	0.53 (133)	1
20	Pigg 2007 study	76	0.73 (183)	1
21	Baylon et al. 2005 study	148	0.36 (90)	1,2
22	Pigg 2003 study	31	0.55 (138)	1
	Weighted Average	890	0.5 (125)	

Note: 1= ESP measured including coil
2= ESP measured including filter

1.2 Impacts of Excess Ductwork Flow Resistance on Equipment Performance

1.2.1 Impact on Blower Performance

Excess duct flow resistances directly affect the blower airflow and power performance, although this impact varies with blower types, namely blowers driven by permanent split capacitor (PSC) motors and electrically commutated motors (ECMs). For example, Walker and his colleague (Walker 2004, Walker and Lutz 2005, Walker 2006, Walker 2008) conducted a series of laboratory tests on one PSC blower and one

ECM blower to quantify the airflow and power performance with respect to external static pressure (ESP) changes. Their results show that airflow rates of the PSC blower at 1 in. w.g. (250 Pa) are less than half of the airflow rates at 0 in. w.g. (0 Pa), while the ECM blower is capable of maintaining relatively constant airflow rates over the entire pressure range.

Also, their results show that as a result of increasing the external static pressure (ESP), the PSC blower power consumption decreases due to airflow reductions, while the ECM blower power consumption increases as the ECM blower maintains airflow rates. For example, at a pressure of 0.2 in. w.g. (50 Pa), the ECM blower used 60% less power than the PSC blower with power measurements of 750 W for the PSC blower versus 300 W for the ECM blower. However, at a pressure of 0.5 in. w.g. (125 Pa), the PSC blower used less power than the ECM blower, showing 550 W for the PSC blower versus 600 W for the ECM blower. Due to the pressure increase from 0.2 to 0.5 in. w.g. (50 to 125 Pa), the power of the PSC blower decreased by 27% from 750 W to 550 W, while the power of the ECM blower doubled from 300 W to 600 W

1.2.2 Impact on Air Conditioner Performance

It is important to note that the above laboratory measurements (Walker 2004, Walker and Lutz 2005, Walker 2006, Walker 2008) focused only on blower energy consumptions in the presence of excess duct flow resistances. Of even more importance is the impact of excess duct flow resistance on non-blower energy consumptions, which makes up 80-95% of the total energy use in a residential central HVAC system (Parker

et al. 2005, Stephens et al. 2010). The non-blower energy use that has not been thoroughly investigated in any of the above studies includes condensing unit electricity consumptions in cooling seasons and natural gas consumptions in heating seasons with respect to different types of system blowers (i.e., PSC or ECM blowers). The effect of different blower types on the non-blower energy use is made more obvious when one consider the fact that increases in the flow resistance reduce airflow rates of PSC blowers, resulting in decreasing cooling capacities and coefficients of performance (COP) because of insufficient evaporator airflows (Palani et al. 1992, Breuker and Braun 1998, Siegel et al. 2002, Kim et al. 2009, Palmiter et al. 2011, Mowris et al. 2012). The negative effect of insufficient airflows is well documented, with one experimental study (Rodriguez et al. 1996) reporting that a 50% airflow reduction would lead to a decrease of 15% in the total cooling capacity and 14% in the COP for an air conditioner with a thermostatic expansion valve (TXV). For the same airflow reduction, the impact on a non-TXV unit was even more severe, showing a decrease of about 25% in the total capacity and 22% in the COP.

Relative to PSC blowers, ECM blowers have better performance in terms of maintaining constant airflow rates over a pressure range, but the power of ECM blowers can significantly increase with the excess flow resistance. More importantly, this increased blower power imposes an additional cooling load on a system and tends to offset the sensible capacity by reducing the temperature difference between the supply and return air (Kendall 2004). Based on a combined approach of experimental measurements and empirical modeling, Yin et al. (2014a) quantified this effect by

showing that the heat gain from an ECM blower in a 60 kBtu/h (17.6 kW) air conditioner could decrease the sensible cooling capacity by up to 1.9% and the sensible COP by as much as 6.6%. Capturing this effect is of special importance because most residential air conditioning systems are controlled by thermostats that can only sense the sensible load. For a given sensible load, system runtime will increase with this reduced sensible capacity, and thus, result in more energy consumptions. Yin et al. (2014b) evaluated this energy penalty by integrating building energy simulations with experimental performance measurements taken on a residential air conditioner with an ECM blower and found that increases in the flow resistance from 0.3 to 0.9 in. w.g. (75 Pa to 225 Pa) could decrease the airflow rate of the ECM blower by 11.2% in the heating mode and 17.7% in the cooling mode. Furthermore, the combined effects of decreasing airflows and increasing blower powers increased the annual system runtime by 6.8% and condensing unit electricity consumption by 7.5%.

1.3 Impacts of Excess Ductwork Flow Resistance on Duct Leakages

Beyond the aforementioned impacts on the performance of blowers and air conditioners, excess ductwork flow resistances can increase duct leakages, which widely exist in residential air distribution systems (Bryan and Perez 2001, Kinney 2005, Modera 2005, Boudreaux et al. 2011, Stephens et al. 2011). For example, the group of Energy Performance of Buildings at Lawrence Berkeley National Laboratory took more than 30,000 duct leakage measurements from 28 states and showed that an average duct

leakage rate for a single-family house is 0.07 ft^3/min per ft^2 at 0.1 in. w.g. (0.36 L/s per m^2 at 25 Pa), accounting for 18% of the airflow rate from an AHU (LBNL 2013b).

Because it is a common practice to place ducts outside of conditioned spaces, such as unconditioned attics, unconditioned basements, and crawl spaces, duct leakages have been recognized for years as a major source of energy loss in residential buildings (Modera 1993, Parker et al. 1993). It results in a loss of the conditioned air to the outside on the supply side and the infiltration of unconditioned air into the system on the return side. Several filed measurements quantified the energy impact of duct leakages in residential central HVAC systems. For example, the results of duct leakage testing and energy efficiency auditing on 43 homes in Louisiana show that an average energy cost due to duct leakages is $280/year per home, which is approximately 30% of the annual heating and cooling energy bill (Witriol et al. 2008). Another study recently conducted on 10 houses in the mixed-humid climate show that the energy cost due to duct leakages is in a range of 1.8 to 18.5% of the annual utility bills (Boudreaux et al. 2011).

Extensive duct leakage tests confirm that duct leakages can be represented by Equation (1) (ASHRAE 2009a)

$$\dot{Q}_L = C_L \Delta P_s^{N_L} \tag{1}$$

where ΔP_s is the static differential pressure between the interior and exterior of duct walls, while C_L and N_L are leakage constant and leakage exponent, respectively, both of which are empirical coefficients and dependent on the geometry of a leakage hole. Equation (1) indicates that duct leakages are sensitive to pressures. Increases in the duct pressure will result in exponential increases in the duct leakage, which means more

energy losses are expected for systems operating at excess duct pressures compared with systems running at lower duct pressures.

1.4 Research Objective and Significance

Severely restrictive duct designs are considered to be the primary cause of substantially high flow resistances in residential air distribution systems (Parker et al. 1997, Proctor and Parker 2000, Ueno 2010, Shapiro et al. 2012). The undersized ductwork indeed reduces the initial duct fabrication and installation costs, but meanwhile it increases system operating costs because of the impacts of excess duct flow resistance on the blower and air conditioner performance. Several studies have tried to quantify the energy impacts of excess duct flow resistance for the purpose of ductwork design and optimization (Lutz et al. 2006, Franco et al. 2008); however, these studies have been primarily limited to blower energy use only. The impact on energy consumptions of non-blower components, such as electricity consumptions of condensing units in cooling seasons and natural gas consumptions of furnaces in heating seasons, has not been thoroughly investigated, although non-blower energy consumptions take up to 80-95% of the energy use in residential heating and cooling systems (Parker et al. 2005, Stephens et al. 2010). Of greater importance, the excess flow resistances in restrictive duct systems not only affect the performance of blowers and air conditioners, but also increase duct leakages, which are a major source of energy losses in residential buildings reported by Parker et al. (1993) and Modera (1993). But the effect of excess flow resistances on duct leakages has not been taken into consideration when economically

evaluating duct designs in previous studies conducted by Franco et al. (2008) and Lutz et al.(2006).

Therefore, the objective of this study reported herein is to comprehensively evaluate energy and economic impacts of duct designs for residential central HVAC systems in response to various combinations of blower types (i.e., PSC and ECM blowers), duct flow resistances, duct materials (i.e., sheet metal and flex ducts), and climates. A series of laboratory experiments were conducted on residential air handling units (AHUs) and air conditioners to characterize their performance at typical installed conditions. For the air handling unit (AHUs) testing, the airflow, power, and overall efficiency of six PSC and six ECM blowers were measured over a pressure range of 0.1 to 1.2 in. w.g. (25 to 300 Pa). For the air conditioner testing, the cooling performance characterized in terms of cooling capacities, condensing unit power, and sensible heat ratios (SHRs) were determined over an airflow range of 1000 to 2250 ft^3/min (0.47 to 1.06 m^3/s). In addition to experimental performance evaluations, empirical models that describe the blower and air conditioner performance at different operating conditions were developed from the laboratory measurements and integrated with building energy simulations to investigate the impact of duct flow resistances on annual electricity consumptions of blowers and condensing units as well as natural gas consumptions of furnaces. With considering the energy loss caused by duct leakages respect to different duct flow resistances, the cost-effectiveness of each duct design was assessed in terms of 15-year life cycle costs (LCCs), which includes both initial duct fabrication/installation costs and consequential lifetime operating costs of heating and cooling equipment.

By determining the effects of blower types (i.e., PSC and ECM blowers), duct flow resistances, duct materials (i.e., sheet metal and flex ducts), and local climates on energy consumptions and life cycle costs (LCCs) of duct designs, the study reported herein can facilitate the constructions of residential air distribution systems with the lowest cost of ownership. In addition, the collected experimental data and empirical models of blowers and air conditioners can be used by HVAC engineers for residential system designs and equipment selections. Moreover, this study have several broader impacts on the residential sector of HVAC&R industry, including supporting the development of improved components and providing professionals with efficient, long-term, and cost-effective solutions when they face numerous tradeoffs and challenges associated with designing residential air distribution systems.

2. EXPERIMENTAL PERFORMANCE EVALUATIONS AND EMPIRICAL MODEL DEVELOPMENTS OF RESIDENTIAL FURNACE BLOWERS WITH PSC AND ECM MOTORS

2.1 Overview

The study reported herein is to experimentally evaluate and compare the performance of blowers driven by permanent split capacitor (PSC) motors and electronically commutated motors (ECMs) in residential non-weatherized, non-condensing gas furnaces. As a first step, twelve different commercially available residential furnace blowers from four manufacturers were selected, with six having PSC blowers and the other six having ECM blowers. Then, these blowers were tested in a well-instrumented laboratory facility with a nozzle airflow chamber. The furnace blower performance was characterized in terms of measured airflow rates and blower powers over a pressure range of 0.1 to 1.2 in. w.g. (25 to 300 Pa). Overall blower efficiencies were also determined from the airflow, pressure, and power measurements. The results of this study showed that PSC and ECM blowers have significantly distinct airflow and power performance in response to increasing external static pressures (ESPs). In addition to performance evaluations, empirical models that describe the airflow and efficiency behaviors of the PSC and ECM blowers with respect to external static pressures (ESPs) were developed from the experimental data taken over the pressure range of 0.1 to 1.2 in. w.g. (25 to 300 Pa). Of special importance, these empirical models can be used for the investigation of energy consumptions in residential central HVAC systems with PSC and ECM blowers at various operating conditions.

2.2 Introduction

In the United States, over 60% of homes have central warm-air furnaces for space heating and cooling, and furnace blowers account for an annual electricity use of 3.81×10^{10} kWh nationwide, which is 2.6% of the site electricity consumption and 1.1% of the total energy use in the residential sector (EIA 2009). Traditionally, these blowers have been driven by permanent split capacitor (PSC) motors, which are split-phase alternate current (AC) induction motors with starting capacitors. Recently, a growing number of manufacturers have started to provide blowers equipped with electrically commutated motors (ECMs), which are brushless direct current (DC) motors with permanent magnet rotors and ball bearings.

Compared with traditional PSC blowers, advantages of using ECM blowers are capabilities of maintaining constant airflow rates over a pressure range and of using less power at conditions of low flow resistances. For example, Biermayer et al. (2004) showed in a series of laboratory experiments that ECM blowers had less airflow decreases compared with PSC blowers as the flow resistance was increased. Also, Walker and his colleague (Walker 2004, Walker and Lutz 2005, Walker 2006, Walker 2008) conducted a series of laboratory measurements on the power consumptions of PSC and ECM blowers. Their results showed that power consumptions of the PSC blower decreased as a result of increasing the flow resistance. In contrast, power consumptions of the ECM blower increased with the increasing flow resistance.

Although previous experimental studies, such as laboratory measurements performed by Biermayer et al. (2004) and by Walker and his colleague (Walker 2004,

Walker and Lutz 2005, Walker 2006, Walker 2008), provide important information for characterizing the performance of PSC and ECM blowers, the breadth of currently available data may not be adequate for the development of national appliance rating standards and public policies due to the fact that only a small sample of furnace blowers has been tested (Walker 2008). For instance, the results reported by Biermayer et al. (2004) were based on only one PSC and one ECM blower, while the Walker's studies (Walker 2004, Walker and Lutz 2005, Walker 2006, Walker 2008) measured only one PSC blower and two ECM blowers.

Another concern arising out of having only a few experimental studies is whether the findings are typical enough to draw conclusions that can be applied in all cases. For example, Lutz et al. (2006) and Franco et al. (2008) reported measurements of constant airflow rates of an ECM blower over a pressure range of 0 to 1.0 in. w.g. (0 to 250 Pa). However, recent experimental results showed that even for an ECM blower increases in the flow resistance could result in airflow reductions as much as 25%, with increasing airflow reductions at conditions of higher blower speeds and higher flow resistances (Yin et al. 2014a). The discrepancy of airflow measurements from ECM blowers in two different studies indicates significant performance variations, even for the same category of blower type. Hence, it is necessary to extend laboratory measurements to more PSC and ECM blowers over a larger range of operating conditions in order to further characterize the blower performance.

The study reported herein experimentally evaluates and compares the performance of PSC and ECM blowers. A total of twelve (12) different commercially

available furnace blowers, namely six PSC blowers and six ECM blowers, were tested in a well-instrumented laboratory setting. Blower airflow and power measurements were conducted over a range of external static pressures (ESPs) and blower speeds. The blower overall efficiencies were also calculated based on the measured airflow, pressure, and power data. In addition to experimental evaluations, empirical models that characterize PSC and ECM blower airflow and overall efficiency behaviors as a function of the external static pressure (ESP) were developed from the statistical analysis of the experimental data.

2.3 Test Method

All twelve (12) blowers tested in this study are from residential non-weatherized, non-condensing gas furnaces made by four major manufacturers in the United States. Out of the twelve units, six are PSC blowers while the other six are ECM blowers. All blowers are designed with forward-curved blades, although the blower wheel dimensions vary from unit to unit. Table 2 summarizes the key characteristics of blower assemblies that were tested in this study.

Table 2 Characteristics of furnaces and blowers tested in this study

Blower	Manufacturer	Blower Motor	Motor Size, hp (W)	Blower Wheel Size, in. (mm)	Speed	Heating Output Capacity, kBtu/h (kW)	Add-on Cooling Capacity, kBtu/h (kW)
Blower #1	A	PSC	1/3 (249)	10 × 6 (254 × 152)	4 speeds	High: 54 (15.83) Low: 36 (10.55)	36 (10.55)
Blower #2	A	ECM	1/2 (373)	10 × 6 (254 × 152)	4 speeds	High: 54 (15.83) Low: 36 (10.55)	36 (10.55)
Blower #3	A	PSC	1/3 (249)	10 × 6 (254 × 152)	4 speeds	54 (15.83)	36 (10.55)
Blower #4	A	PSC	1/3 (249)	10 × 7 (254 × 178)	4 speeds	48 (14.07)	36 (10.55)
Blower #5	A	ECM	3/4 (559)	11 × 8 (279 × 203)	4 speeds	54 (15.83)	48 (14.07)
Blower #6	A	PSC	1/3 (249)	10 × 6 (254 × 152)	3 speeds	54 (15.83)	36 (10.55)
Blower #7	B	ECM	1/2 (373)	10 × 8 (254 × 203)	3 speeds	58 (17.00)	24-36 (7.03-10.55)
Blower #8	B	PSC	1/3 (373)	10 × 10 (254 × 254)	4 speeds	High: 74 (21.69) Low: 58 (17.00)	18-36 (5.28-10.55)
Blower #9	B	ECM	1/2 (373)	10 × 10 (254 × 254)	4 speeds	High: 97 (28.43) Low: 85 (24.91)	30-42 (8.79-12.31)
Blower #10	C	PSC	1/3 (249)	10 × 6 (254 × 152)	4 speeds	56 (16.41)	36 (10.55)
Blower #11	C	ECM	3/4 (559)	10 × 10 (254 × 254)	4 speeds	92 (26.96)	24-60 (7.03-17.58)
Blower #12	D	ECM	1/2 (373)	11 × 8 (279 × 203)	4 speeds	High: 47 (13.77) Low: 24 (7.03)	36 (10.55)

2.3.1 Experimental Setup

The experimental setup developed for testing these blowers was constructed with the ability to provide accurate measurements of pressure, airflow rate, and blower power. Figure 2 is a schematic of the experimental test setup, which includes a test unit, supply and return ducts, and a nozzle airflow chamber, with all components in the horizontal position. Because the focus of this study is the blower performance only and the fact that the evaluation of heating and cooling performance is beyond the project scope, burners were not operating during the tests nor were the cooling coils installed. Conditioned laboratory air at a uniform and constant temperature was used in all tests. To simulate field installations, supply and return ducts with the same cross-sectional dimensions as the supply and return air openings on the furnaces were built and attached to the test units by following the requirements in ANSI/ASHRAE Standard 37 (2009b). Following the specifications in this standard, the length of the supply duct is 2.5 equivalent diameters, and the length of the return duct is 1.5 equivalent diameters. In addition, static pressure taps that were made according to ANSI/ASHRAE Standard 51 (2007b) were installed at the center of each surface on both supply and return ducts so that average static pressures could be measured.

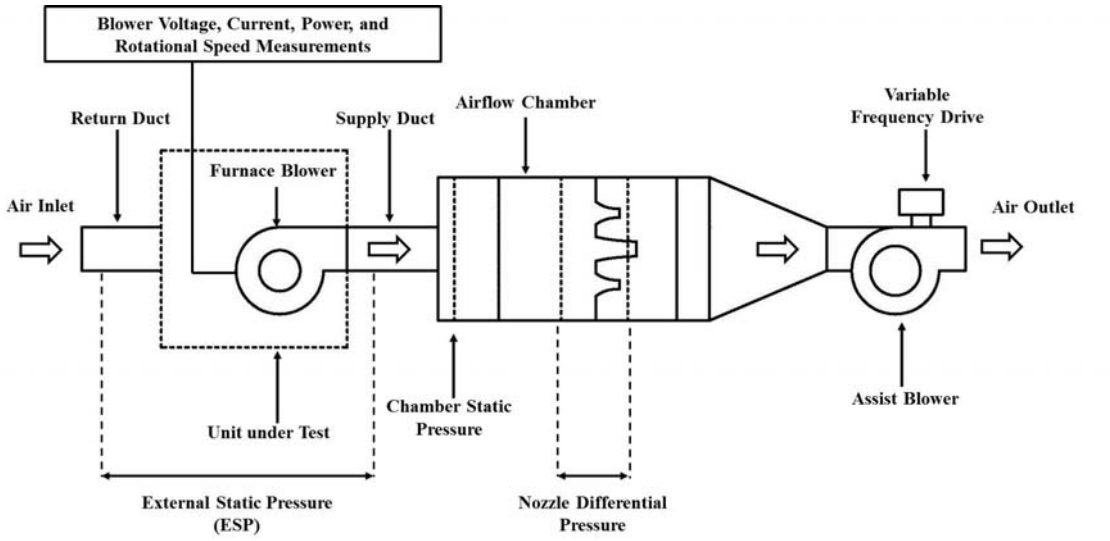

Figure 2 Experimental setup with nozzle airflow chamber for airflow testing

Blower airflow rates were measured by using a nozzle airflow chamber that was built in accordance with the requirements of ANSI/ASHRAE Standard 51 (2007b). This chamber has a nozzle board consisting of one 1-in. (25 mm), one 3-in. (76 mm), and four 5-in. (127 mm) nozzles, which allows the same chamber to be used for the airflow measurement over an airflow range of 11 to 3300 ft^3/min (0.005 to 1.557 m^3/s). An assist blower, which is controlled by a variable frequency drive (VFD), is attached to this chamber and used to achieve variable external static pressures (ESPs). Ambient conditions were monitored by a stand-alone psychrometric station that featured two temperature transmitters, for dry-bulb (DB) temperature and wet-bulb (WB) temperature measurements, as well as a barometric transmitter. Air pressures were measured by using pressure transmitters with a 4-20 mA output, and the supply voltage to the furnace blower was stabilized at 115 ±0.5 V by using a variable transformer.

2.3.2 Test Procedures

For each unit, the airflow rate and blower power were measured over an external static pressure (ESP) range of 0.1 to 1.2 in. w.g. (25 to 300 Pa) by using an incremental change of 0.1 in. w.g. (25 Pa) at each blower speed. Before initiating airflow tests, blowers were run for a 30-minute warm-up period in order to obtain steady-state conditions. The corresponding airflow rates through the known open-nozzle areas in the airflow chamber were calculated at each of the 12 pressure points by using measurements of pressure and temperature averaged over a 5-second interval. The measured airflow data were then converted to standard air with an air density of 0.075 lb_m/ft^3 (1.2 kg/m^3) so that the airflow performance of different units could be directly compared, regardless of environmental conditions occurring during data collections. While taking airflow measurements, the blower rotational speed was measured by using a non-contact digital tachometer, and the electrical performance was measured by using a power quality analyzer. The simultaneously measured and recorded electrical data included voltage, current, power factor, and both real and apparent power. Table 3 shows the instruments used in the airflow tests, along with their specifications and accuracies.

Table 3 Instrument specifications and accuracies

Measurement	Sensor Type	Accuracy
Barometric pressure	Barometer, 600-1100 mb (0.6-1.1×10^5 Pa)	±1.5%
Ambient DB and WB temperature Airflow chamber DB temperature	Temperature transmitter, 20-120°F (-6.7-48.9°C)	±0.3% Full Scale
External static pressure (ESP)	Air pressure transmitter, 0-3 in. w.g. (0-747 Pa)	±0.25% Full Scale
Chamber nozzle differential pressure	Air pressure transmitter, 0-3 in. w.g. (0-747 Pa)	±0.25% Full Scale
Voltage	Power quality analyzer, 0-1000 V	±0.6 V
Current	Power quality analyzer, 0.01-5 A	±0.5% Reading
Power	Power quality analyzer	±1% Reading
Power factor	Power quality analyzer, 0-1	±0.1% Reading
Blower rotational speed	Tachometer, 5 – 999990 round/min	±0.50 round/min

2.3.3 Uncertainty Analysis

Uncertainties in the calculated airflow rate and overall efficiency were estimated based on instrument accuracies associated with temperature, pressure, and power measurements, along with the Kline and McClintock (1953) method described in Equation (2)

$$U_A = \sqrt{\sum_{i=1}^{j} \left(\frac{\partial A}{\partial x_i} \cdot U_{x_i} \right)^2} \quad (2)$$

where U_A is the combined uncertainty for the dependent variable A, x_i is one of the independent variables that affect the dependent variable A, and U_{xi} is the uncertainty for the independent variable x_i. Depending on operating conditions and the calculated terms of airflow rate and overall efficiency, the measured parameters of temperature, pressure, and power contribute differently to the combined uncertainties in the airflow and efficiency results. Table 4 summarizes percentage contributions of different measurements to the combined uncertainties in airflow and efficiency results. As can be seen in Table 4, the measurement of nozzle differential pressure contributes to 85-90%

of the uncertainties in the airflow results, followed by the measurement of barometric pressure with a percentage of 8-10%. For the efficiency results, measurements of blower power and external static pressure (ESP) are the most important factors that influence the combined uncertainties. In general, at a confidence level of 95%, the combined uncertainty in the calculated airflow rate was within ±1%, and the combined uncertainty in the calculated overall efficiency was within ± 7%.

Table 4 Contributions of experimental measurements to combined uncertainties in airflow and efficiency

Parameter	Barometric pressure	Ambient DB	Ambient WB	Chamber DB	External static pressure (ESP)	Nozzle differential pressure	Blower Power
Airflow Rate	8-10%	0.01%	0.05-0.1%	1-1.5%	0.01%	85-90%	-
Overall Efficiency	0.1-0.5%	0.01%	0.05-0.1%	0.05-0.1%	25-95%	0.1-4.5%	1-65%

2.4 Experimental Results and Data Analysis

The airflow and power performance of the twelve (12) blowers were determined over an external static pressure (ESP) range of 0.1 to 1.2 in .w.g. (25 to 300 Pa) by using the experimental setup and testing procedures that were described earlier in Section 2.3. Furthermore, blower overall efficiencies were calculated based on the measured airflow, pressure, and power data. This section presents the experimental results and discusses the performance characteristics of PSC and ECM blowers with respect to these important parameters, namely the airflow rate, blower power, and overall efficiency.

2.4.1 Airflow Results and Analysis

Airflow measurements over a range of pressures and blower speeds for Blower #8 (PSC blower) and Blower #9 (ECM blower) are shown in Figure 3. The airflow and power performance of the other ten (10) blowers were also measured, but the results from Blower #8 and Blower #9 are presented as an example of typical PSC and ECM blower performance. It should be noted that the measured airflow rate at the medium high speed of Blower #9 at the lowest pressure of 0.1 in. w.g. (25 Pa) falls outside of the design range. Therefore, the results of airflow, power, and efficiency at this specific point for this specific blower were excluded from the data analysis.

Airflow results presented in Figure 3 show the different airflow performance of PSC and ECM blowers in response to pressure changes in spite of having the same blower wheel size and housing configurations. As a result of increasing the external static pressure (ESP), airflow rates of the PSC blower decrease in all blower speeds. For example, the airflow rate at the high speed decreases by 46.5% from 1780 to 954 ft^3/min (0.84 to 0.45 m^3/s) as the external static pressure (ESP) is increased from 0.1 to 0.9 in. w.g. (25 to 225 Pa). In contrast to the PSC blower that has decreasing airflow rates with increasing pressures, the ECM blower maintains relatively constant airflow rates over a pressure range, which is represented by the more horizontal airflow curves in Figure 3. For instance, the airflow rate of the ECM blower at the high speed decreases less than 1% as the pressure is increased, showing 1423 ft^3/min (0.671 m^3/s) at 0.1 in. w.g. (25 Pa) versus 1415 ft^3/min (0.667 m^3/s) at 0.9 in. w.g. (225 Pa). However, as the external static pressure (ESP) goes above 0.9 in. w.g. (225 Pa), airflow decreases of as much as 24%

relative to the measurement at 0.1 in. w.g. (25 Pa) occur in the medium high and high speeds. Even so, this airflow decreases for the ECM blower at the higher pressure is still less dramatic than the airflow reductions associated with the PSC blower over the same pressure range.

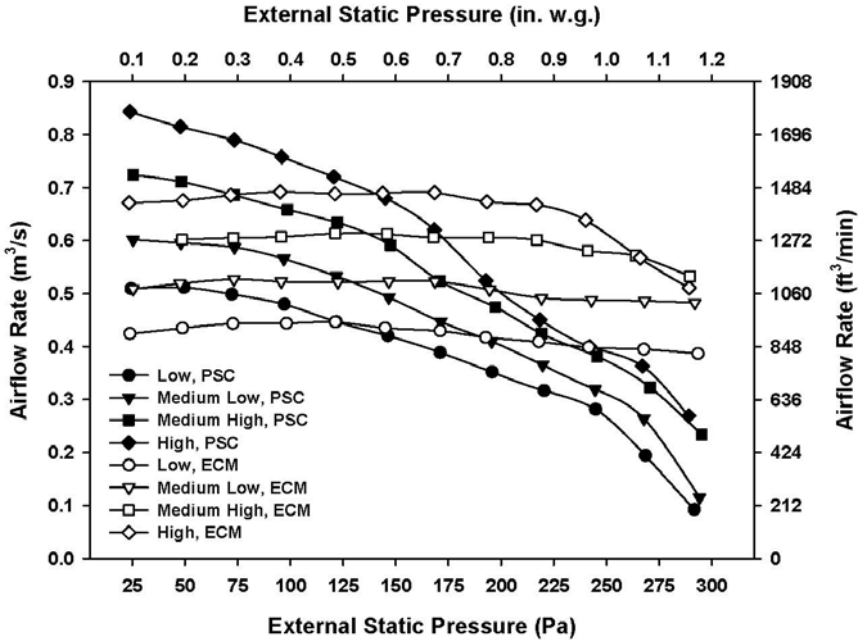

Figure 3 Airflow comparison of PSC and ECM blowers over a range of external static pressure

As mentioned earlier, one purpose of this study is to characterize the typical performance of PSC and ECM blowers, namely the airflow, power, and overall efficiency, based on extensive laboratory measurements performed on the six PSC and six ECM blowers. However, given the fact that each blower is designed differently in

terms of airflow rates, blower speeds, and motor sizes, it is difficult to describe the typical blower performance as a function of external static pressures (ESPs) by using direct airflow and power measurements. Therefore, the measured airflow rates of the twelve tested blowers were first transformed into a non-dimensional format by following the method described in Equation (3).

$$\text{Performance change (\%)} = \frac{\text{Performance}_{esp} - \text{Performance}_{25}}{\text{Performance}_{25}} \times 100\% \quad (3)$$

where Performance_{25} represents the airflow and power measurements at 0.1 in. w.g. (25 Pa), and Performance_{esp} is the airflow and power measurements at other external static pressures (ESPs). Next, the data for percentage performance changes were categorized by blower type and summarized in tables that show the observed 25%, 50% (the median), and 75% percentiles along with minimum and maximum values in the percentage performance changes. In addition to tables, the data of percentage performance changes were graphically presented in box-and-whisker plots, with the bottom and top of the box showing the 25% and 75% percentiles and the band inside the box representing the 50% percentile (the median). The ends of the whiskers represent the minimum and maximum values in the percentage performance changes at each pressure setting.

Following the method described in Equation (3), percentage airflow changes over a pressure range of 0.1 to 1.2 in .w.g. (25 to 300 Pa) for the six PSC and the six ECM blowers were calculated and are shown in Figure 4 and Figure 5, respectively. In addition, these percentage changes are summarized in Table 5. A comparison between Figure 4 and Figure 5 indicates that increases in the external static pressure (ESP) have

less airflow impacts on ECM blowers than on PSC blowers, which is consistent with the observation in Figure 3. For example, Table 5 shows that even at the highest test pressure in this study of 1.2 in. w.g. (300 Pa), the median airflow decrease relative to the airflow rates at 0.1 in. w.g. (25 Pa) for ECM blowers is only 10%, while PSC blowers have a median airflow decrease of 84% at the same pressure. Moreover, for both PSC and ECM blowers, airflow changes due to pressure increases vary significantly. For instance, as a result of increasing pressures from 0.1 to 1.2 in .w.g. (25 to 300 Pa), the airflow decreases for PSC blowers vary from 61% to 97%, while the airflow decrease for ECM blowers range from 0.3% to 49% for the same pressure increases. The variations in the airflow performance may be caused by various designs from different manufacturers, such as blower wheel dimensions, motor sizes, furnace housings, and control mechanisms.

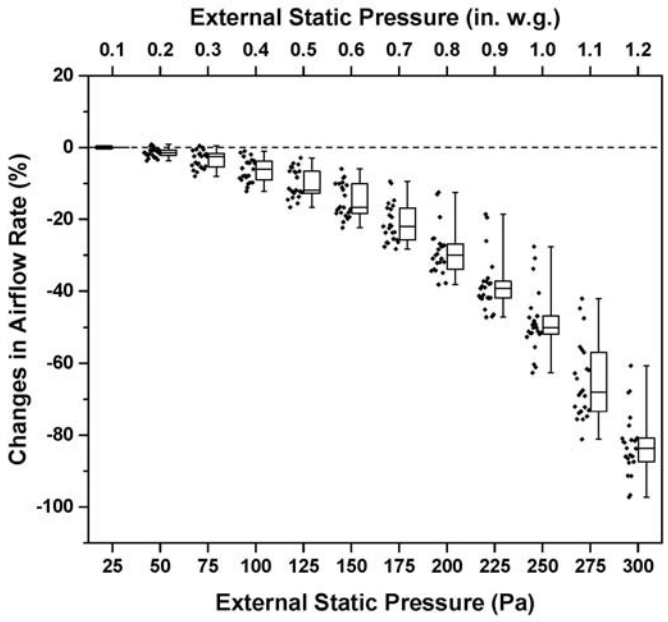

Figure 4 Percentage airflow changes for six PSC blowers over a range of external static pressures

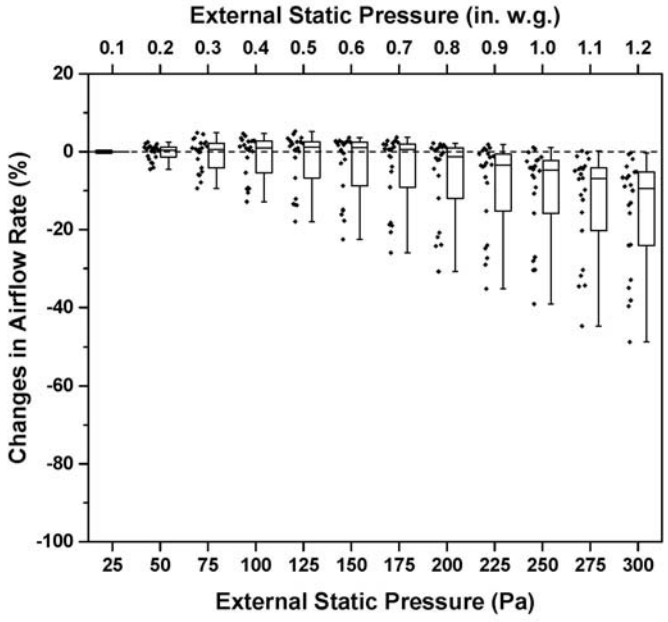

Figure 5 Percentage airflow changes of six ECM blowers over a range of external static pressures

Table 5 Percentage changes in airflow with ESP for PSC and ECM blowers

Blower Type	Statistical Measure	External Static Pressure, in. w.g. (Pa)											
		0.1 (25)	0.2 (50)	0.3 (75)	0.4 (100)	0.5 (125)	0.6 (150)	0.7 (175)	0.8 (200)	0.9 (225)	1.0 (250)	1.1 (270)	1.2 (300)
PSC	Minimum (%)	0	-3.7	-8.0	-12.2	-16.7	-22.4	-28.3	-38.2	-47.3	-62.6	-81.1	-97.3
	25% Percentile (%)	0	-2.2	-5.3	-8.7	-12.5	-18.2	-25.6	-32.6	-42.0	-52.0	-73.1	-87.5
	50% Percentile (%)	0	-1.3	-2.6	-5.9	-11.7	-16.6	-21.9	-29.8	-40.2	-50.6	-68.4	-83.7
	75% Percentile (%)	0	-0.7	-1.7	-4.1	-6.6	-10.4	-17.1	-27.2	-37.4	-47.3	-60.4	-80.9
	Maximum (%)	0	0.9	0.5	-1.0	-2.9	-6.0	-9.4	-12.5	-18.6	-27.6	-42.1	-60.7
ECM	Minimum (%)	0	-4.5	-9.4	-12.8	-18.0	-22.5	-25.9	-30.8	-35.2	-39.1	-44.6	-48.7
	25% Percentile (%)	0	-1.3	-3.6	-4.4	-5.4	-7.3	-8.1	-10.5	-13.4	-14.6	-19.1	-24.0
	50% Percentile (%)	0	0.4	0.6	1.0	1.2	1.1	0.6	-1.2	-3.5	-4.7	-6.9	-9.5
	75% Percentile (%)	0	1.2	2.2	2.7	2.5	2.5	1.9	1.0	-0.6	-2.3	-4.2	-5.4
	Maximum (%)	0	2.5	4.9	4.7	5.2	3.6	3.7	2.2	1.9	1.1	0.2	-0.3

2.4.2 Power Results and Analysis

Blower power measurements over a range of pressures and blower speeds are presented in Figure 6 for Blower #8 (PSC blower) and #9 (ECM blower). It should be noted that these are the same two blowers whose airflow results were compared earlier. As can be seen in Figure 6, the blower power behaviors with respect to pressure changes are quite different for PSC and ECM blowers. For the PSC blower, the power consumption continuously decreases with increasing pressures. For example, the power

decreases by 40.5% from 740 to 440 W at the high speed as the external static pressure (ESP) is increased from 0.1 to 0.9 in. w.g. (25 to 225 Pa). The same trend is also observed at other speeds but to a lesser degree. Unlike the PSC blower, increasing pressures lead to increases in the ECM blower power. For instance, the blower power at the high speed almost doubles from 320 to 630 W as a result of a pressure increase from 0.1 to 0.9 in. w.g. (25 to 225 Pa).

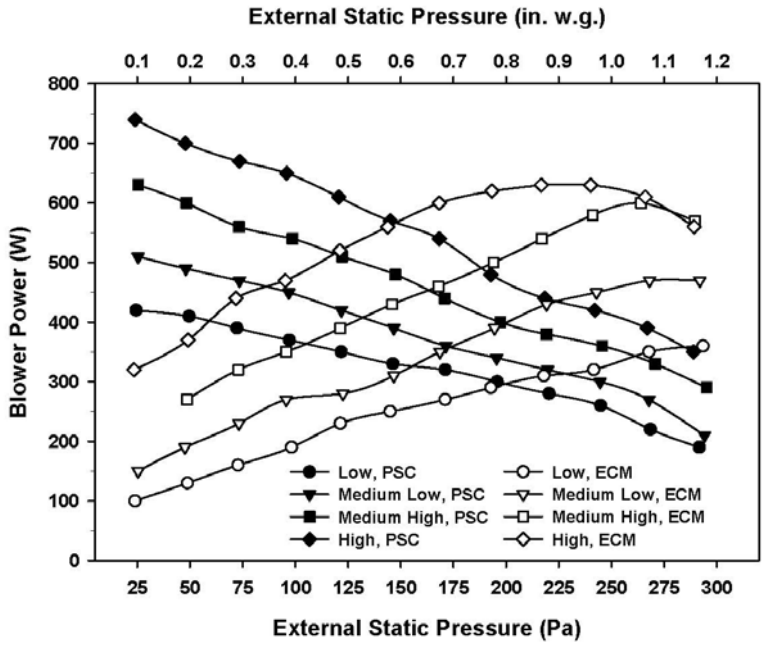

Figure 6 Power comparison of PSC and ECM blowers over a range of external static pressure

Following the same approach described in Equation (3), percentage power changes over a pressure range of 0.1 to 1.2 in. w.g. (25 to 300 Pa) are graphically

presented in Figure 7 and Figure 8 for the six PSC and six ECM blowers, respectively. Furthermore, these percentage power changes are summarized in Table 6. A comparison between Figure 7 and Figure 8 shows that the power consumptions of PSC and ECM blowers behave differently with respect to increasing pressures. Specifically, increasing pressures result in decreasing power consumptions of PSC blowers, while power consumptions of ECM blowers continuously increase as the pressure is increased. For example, the statistical summary of results presented in Table 6 shows that the median percentage change for PSC blower power is a decrease of 57% as a result of a pressure increase from 0.1 to 1.2 in. w.g. (25 to 300 Pa), while the median percentage change for ECM blower power is an increase of 208% for the same pressure increase. These results are consistent with the trends previously shown in Figure 6. It should also be noted that power changes for ECM blowers have a greater degree of scatter compared to that of PSC blowers. For instance, at the external static pressure of 1.2 in. w.g. (300 Pa), power decreases for PSC blowers vary within a range of 38 to 66% relative to the measurements at 0.1 in. w.g. (25 Pa), while power increases for ECM blowers are in a range of 40 to 383%. The wider range of percentage power changes for ECM blowers found in this study can be attributed to considerable differences among ECM units in terms of housing designs, delivered airflow rates, motor sizes, and speed control mechanisms.

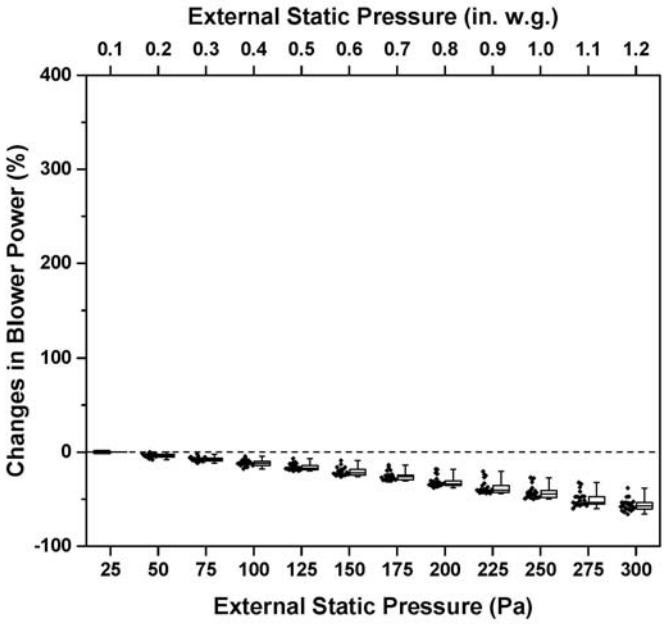

Figure 7 Percentage power changes of six PSC blowers over a range of external static pressures

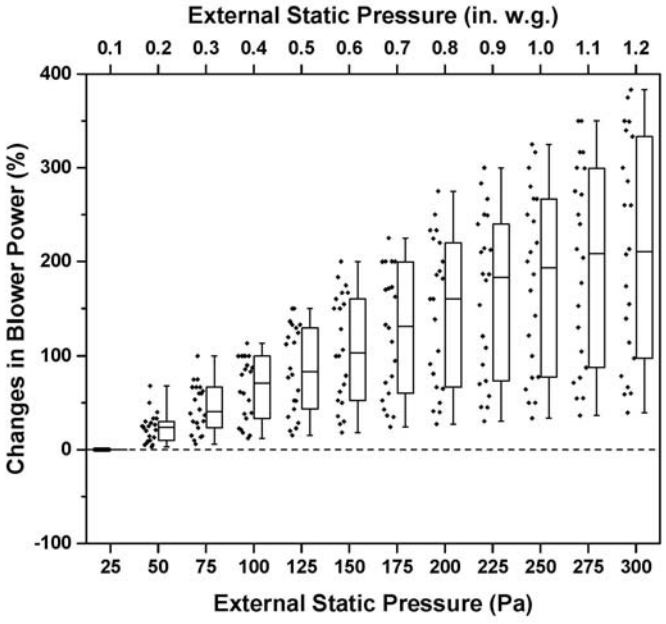

Figure 8 Percentage power changes of six ECM blowers over a range of external static pressures

Table 6 Percentage changes in power with ESP for PSC and ECM blowers

Blower Type	Statistical Measure	External Static Pressure, in. w.g. (Pa)											
		0.1 (25)	0.2 (50)	0.3 (75)	0.4 (100)	0.5 (125)	0.6 (150)	0.7 (175)	0.8 (200)	0.9 (225)	1.0 (250)	1.1 (270)	1.2 (300)
PSC	Minimum (%)	0	-8.1	-11.6	-17.7	-20.2	-26.0	-30.6	-38.0	-44.0	-50.0	-60.0	-66.0
	25% Percentile (%)	0	-5.1	-9.4	-14.3	-18.8	-24.4	-29.4	-35.7	-42.9	-48.2	-55.3	-60.4
	50% Percentile (%)	0	-3.8	-7.8	-11.8	-16.9	-22.0	-25.9	-34.0	-40.3	-44.6	-53.6	-57.1
	75% Percentile (%)	0	-2.5	-6.3	-9.8	-14.3	-18.5	-24.4	-30.5	-35.6	-40.7	-47.3	-53.7
	Maximum (%)	0	0.1	-2.3	-4.5	-6.8	-9.1	-13.6	-18.2	-20.5	-27.3	-32.4	-38.2
ECM	Minimum (%)	0	3.0	6.0	12.1	15.3	18.3	24.3	27.3	30.4	33.6	36.4	39.5
	25% Percentile (%)	0	10.0	23.3	33.3	43.3	52.5	60.0	66.7	73.3	77.5	87.5	97.5
	50% Percentile (%)	0	23.2	38.6	61.6	60.0	100.0	130.0	160.0	180.0	186.4	204.0	207.6
	75% Percentile (%)	0	30.0	66.7	99.8	130.0	160.0	199.5	220.0	240.0	266.7	299.5	333.3
	Maximum (%)	0	68.2	100.0	113.6	150.0	200.0	225.0	275.0	300.0	325.0	350.0	383.3

2.4.3 Overall Efficiency Results and Analysis

Fan and motor efficiencies are often required for the calculation of blower power, but separate fan and motor efficiencies are rarely provided by furnace manufacturers. Specifically, for blowers with small fractional horsepower motors as found in residential furnaces, fans and motors are typically evaluated as a unit rather than separately. Therefore, the fan/motor overall efficiency was calculated based on the measurements of airflow, pressure, and power by following Equation (4)

$$\eta = \frac{\dot{Q}\Delta P_S}{W} \times 100\% \quad (4)$$

where η is the overall efficiency, the $\dot{Q}$ is the measured blower airflow rate, the ΔP is the measured external static pressure across the test units, and the W is the measured blower power. Another interpretation of this efficiency equation is that the ideal work into the working fluid (i.e., air) is divided by the actual work into the unit.

The overall efficiencies for Blower #8 (PSC blower) and #9 (ECM blower) are plotted in Figure 9 against external static pressures (ESPs) in a range of 0.1 to 1.2 in. w.g. (25 to 300 Pa). The results presented in Figure 9 show that the overall efficiency mostly increases with increasing pressures for both the PSC and ECM blowers. However, unlike the ECM blower, the PSC blower has a maximum efficiency of 25% at a pressure of 1.0 in. w.g. (250 Pa), and then the efficiency drops sharply to a range of 10 to 20% as the pressure increases further. Also, for any given external static pressure, efficiencies of the PSC blower at all speeds collapse into a small range, which indicates that the overall efficiency of the PSC blower is independent of blower speeds. However, for the ECM blower at the same pressure, efficiencies are increased as the blower speed is decreased. For example, at 1.0 in. w.g. (250 Pa), the efficiency of 30% at the low speed is 13% higher than the efficiency of 26% at the high speed.

The results presented in Figure 9 can also be used to compare PSC and ECM blower efficiencies. It can be seen in Figure 9 that the ECM blower has higher efficiencies compared with the PSC blower at pressures below 0.5 in. w.g. (125 Pa). For example, the overall efficiencies of the ECM blower at 0.5 in. w.g. (125 Pa) are in the range of 16 to 23% depending on the blower speed, while the efficiencies of the PSC

blower at the same pressure are 14 to 15%, which is approximately 12% to 34% lower than the efficiencies of the ECM blower. The above example is at a mid-range pressure; however, the efficiency advantage of the ECM blower becomes marginal as a result of increasing external static pressures (ESPs). For instance, the efficiencies of the ECM blower at a pressure of 1.0 in. w.g. (250 Pa) for all speeds, except for the low speed, are essentially the same as the efficiencies of the PSC blower, with efficiencies being 23-26% for PSC blowers versus 24-26% for ECM blowers.

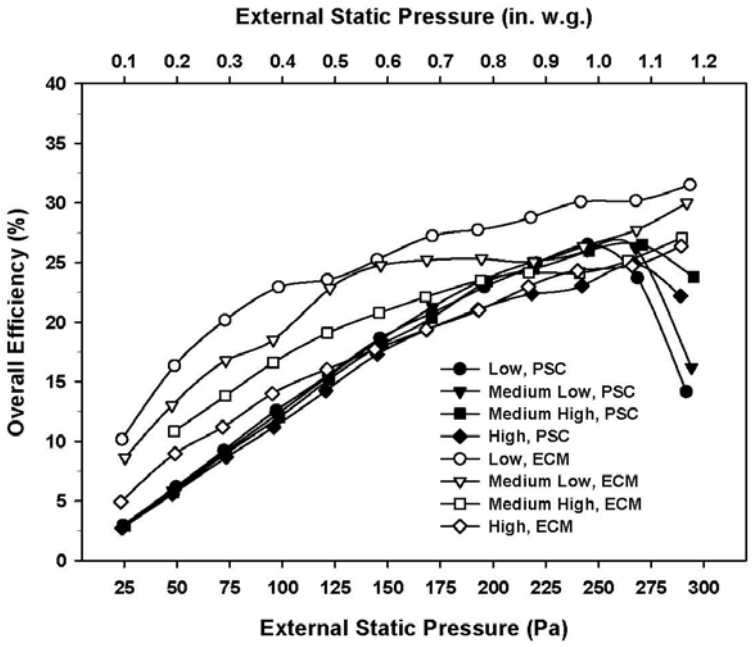

Figure 9 Efficiency comparison of PSC and ECM blowers over a range of external static pressures

Overall efficiencies for the six PSC and six ECM blowers tested were determined by using Equation (4) along with the experimental measurements of airflow rate, blower power, and external static pressure (ESP). These results are graphically presented in Figure 10 and Figure 11 for PSC and ECM blowers, respectively. In addition, the statistical efficiency results are summarized in Table 7, which shows the values of 25%, 50% (median), and 75% percentiles along with the minimum and maximum efficiencies in a pressure range of 0.1 to 1.2 in. w.g. (25 to 300 Pa). The efficiency behaviors of PSC and ECM blowers in Figure 10 and Figure 11 are consistent with the trends previously shown in Figure 9. For example, results in Figure 10 and Figure 11 show that ECM blowers tend to have higher efficiencies than PSC blowers, especially at lower pressures. For instance, Table 7 shows that the efficiencies of PSC blowers at 0.2 in. w.g. (50 Pa) vary from 4.6 to 6.2% with a median efficiency of 5.7%, while efficiencies of ECM blowers are in a range of 8.7 and 23.0% with a median efficiency of 15.2%. A simple comparison of these median values indicates that ECM blowers are almost three times more efficient than PSC blowers at 0.2 in. w.g. (50 Pa). However, at a higher pressure of 0.9 in. w.g. (225 Pa), the median efficiency of 29.7% for ECM blowers is only 20% higher than the median efficiency of 24.5% for PSC blowers.

Moreover, as discussed previously, one can observe in Figure 10 and Figure 11 that ECM blowers have greater levels of scatter in the overall efficiencies compared to the scatter in PSC blower efficiencies. This larger scatter for ECM blowers is not surprising considering that ECM blowers tend to have higher efficiencies at lower speeds, while efficiencies of PSC blowers are independent of blower speeds. Of special

importance, various designs in ECM blowers from different manufacturers may add the variability to this efficiency results.

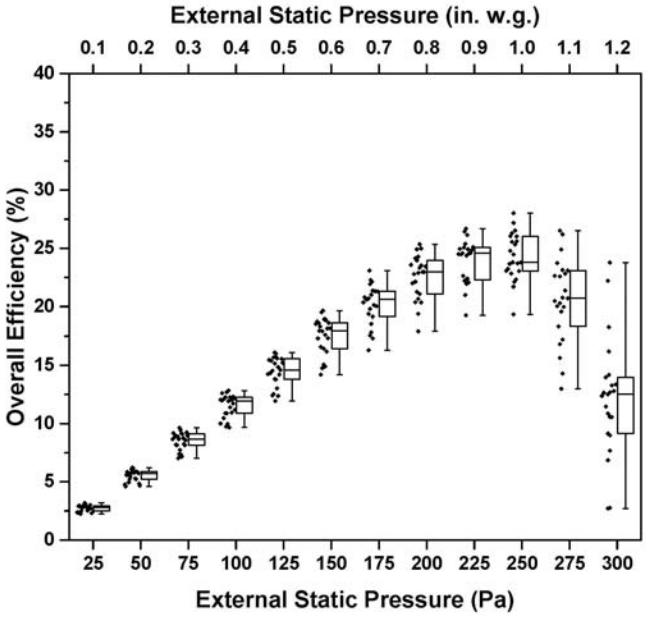

Figure 10 Overall efficiencies of six PSC blowers over a range of external static pressures

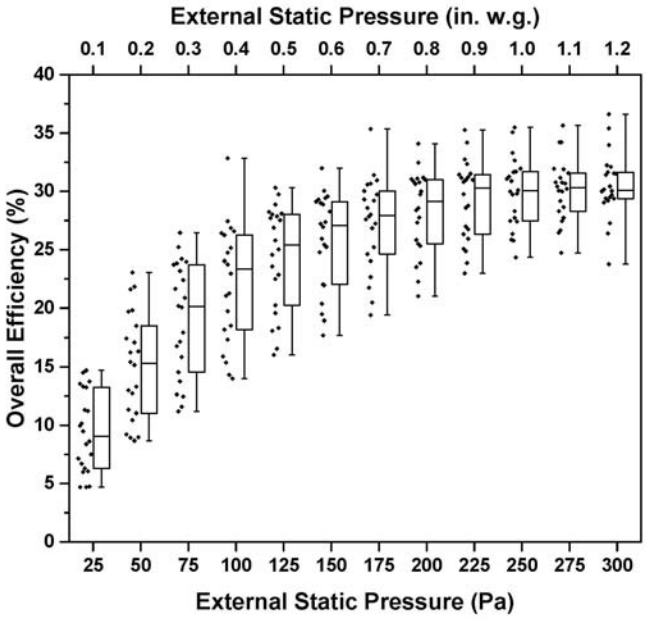

Figure 11 Overall efficiencies of six ECM blowers over a range of external static pressures

Table 7 Overall efficiencies of PSC and ECM blowers varying with ESP

Blower Type	Statistical Measure	External Static Pressure, in. w.g. (Pa)											
		0.1 (25)	0.2 (50)	0.3 (75)	0.4 (100)	0.5 (125)	0.6 (150)	0.7 (175)	0.8 (200)	0.9 (225)	1.0 (250)	1.1 (270)	1.2 (300)
PSC	Minimum (%)	2.3	4.6	7.0	9.7	11.9	14.2	16.3	17.9	19.2	19.3	13.0	2.7
	25% Percentile (%)	2.5	5.2	8.1	10.9	13.8	16.5	19.2	21.2	22.3	23.1	19.0	9.8
	50% Percentile (%)	2.8	5.7	8.7	11.9	14.6	18.0	20.6	23.0	24.6	23.8	20.7	12.5
	75% Percentile (%)	2.9	5.9	9.1	12.2	15.5	18.6	21.3	23.8	25.0	25.8	23.0	13.7
	Maximum (%)	3.2	6.2	9.6	12.8	16.1	19.6	23.1	25.3	26.7	28.0	26.5	23.8
ECM	Minimum (%)	4.7	8.7	11.2	14.0	16.0	17.7	19.4	21.0	23.0	24.1	24.7	23.7
	25% Percentile (%)	6.2	10.9	14.2	17.8	19.9	22.0	24.3	25.4	26.1	27.4	28.0	29.3
	50% Percentile (%)	8.6	15.2	20.1	22.9	25.0	26.9	27.9	28.6	29.7	30.0	30.2	30.0
	75% Percentile (%)	12.3	18.0	23.4	25.7	27.9	29.1	29.9	30.9	31.3	31.7	31.4	31.6
	Maximum (%)	14.7	23.0	26.5	32.8	30.3	32.0	35.3	34.1	35.3	35.5	35.7	36.6

2.5 Empirical Model Development

In the above experimental studies and comparative analysis, the performance of six PSC and six ECM blowers were investigated in terms of airflow rates, blower power, and overall efficiencies over a pressure range of 0.1 to 1.2 in. w.g. (25 to 300 Pa). In addition to performance evaluations, another important goal of the study reported herein is to develop empirical models that can be used to characterize the typical airflow and energy performance of PSC and ECM blowers. In this section, empirical models of

airflow and efficiency were developed for both PSC and ECM blowers based on the experimental results. Due to significant blower design variations from different manufacturers, such as multiple blower speeds, airflow ranges, and blower wheel dimensions, measurements of airflow and overall efficiency vary at any given external static pressure (ESP) even for blowers with the same motor type. These variations indicate that it is impractical to use a single curve or correlation to represent the performance characteristics of the entire category of PSC blowers or ECM blowers. However, it was found that comprehensive performance representations of both airflow and efficiency could be developed from the statistical results presented previously in Table 5 and Table 7. Specifically, three best-fit curves were generated by using the 25%, 50% (median), and 75% percentiles in the corresponding statistical results of airflow and efficiency over an external static pressure (ESP) range of 0.1 to 1.2 in. w.g. (25 to 300 Pa). Because the developed models are designed to capture typical airflow and efficiency behaviors of PSC and ECM blowers, extreme performance that are characterized by the minimum and maximum values in airflow and efficiency measurements were not used for the model development.

2.5.1 Development of Airflow Models

The purpose of the airflow models is to characterize the airflow behaviors of PSC and ECM blowers as a function of external static pressures (ESPs). However, because the direct airflow measurements from each blower at any given pressures vary over a wide range due to different blower designs and speed settings, it is difficult to correlate

direct airflow measurements of PSC and ECM blowers with external static pressures (ESPs). Therefore, rather than using direct airflow measurements, percentage airflow changes relative to the airflow measurements at 0.1 in. w.g. (25 Pa) calculated according to Equation (3) were used for the model development.

The 25%, 50% (median), and 75% percentile statistical results for the percentage airflow changes presented previously in Figure 4 and Figure 5 and summarized in Table 5 were fitted into a second order polynomial by taking the percentage airflow changes as the dependent variable and the external static pressure (ESP) as the only independent variable, as shown in Equation (5)

$$\dot{Q}(\%) = C_1 + C_2 \times ESP + C_3 \times ESP^2 \quad (5)$$

Consequently, three airflow curves presenting the three statistical percentiles were generated for each type of blowers so that comprehensive descriptions of airflow behaviors as a function of the external static pressure (ESP) can be developed. These airflow models for PSC and ECM blowers share the same format but with different empirical coefficients, which were determined from a regression analysis by using the least-squares approach. Figure 12 and Figure 13 show these airflow model curves for PSC and ECM blowers respectively. Also, shown in Figure 12 and Figure 13 are the statistical results of the percentage airflow changes that were previously presented in Table 5 and used here to develop the model. The empirical coefficients and the R^2 values for these airflow models are shown in Table 8 for both PSC and ECM blowers.

The airflow curves generated from the developed models and plotted in Figure 12 and Figure 13 have good agreement with the experimental data. Further evidence of

this good agreement is presented in Table 8, which shows that the R^2 values for PSC blower models are all above 0.99 while the R^2 values for ECM blower models are all above 0.98. The results in Figure 12 and Figure 13 as well as the high R^2 values as listed in Table 8 indicates that the developed airflow models are capable of predicting PSC and ECM blower airflow performance as a function of the external static pressure (ESP) over a pressure range of 0.1 to 1.2 in. w.g. (25 to 300 Pa).

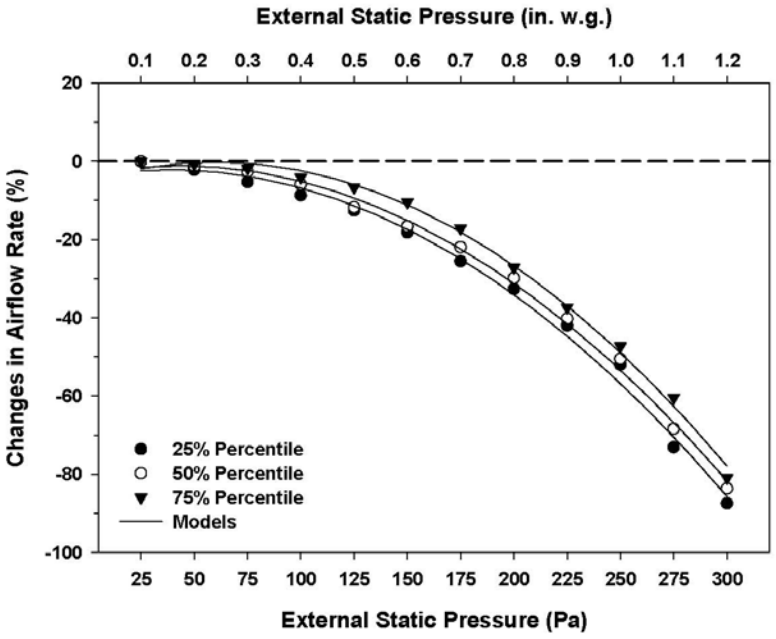

Figure 12 Percentage airflow changes as a function of ESP for PSC blowers

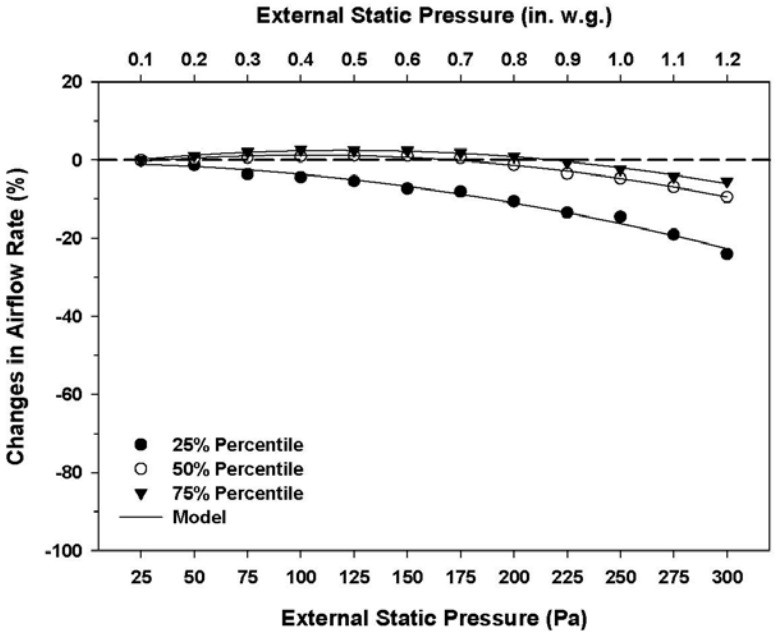

Figure 13 Percentage airflow changes as a function of ESP for ECM blowers

Table 8 Empirical coefficients and R^2 values for airflow models

Blower Type	Percentile	C_1 (-)	C_2 (Pa^{-1})	C_3 (Pa^{-2})	R^2
PSC	25%	-3.918	0.0934	- 0.00122	0.994
	50%	-3.389	0.105	- 0.00122	0.997
	75%	-5.053	0.162	-0.00135	0.997
ECM	25%	-0.649	-0.00798	-0.000218	0.985
	50%	-1.654	0.0576	-0.000279	0.989
	75%	-1.275	0.0642	-0.000267	0.989

2.5.2 Development of Efficiency Models

As the next step to characterize the performance of PSC and ECM blowers, efficiency models were developed from the experimental data over an external static pressure (ESP) range of 0.1 to 1.2 in. w.g. (25 to 300 Pa). Following the same approach used previously to develop airflow models, the statistical efficiency results for both PSC and ECM blowers shown in Figure 10 and Figure 11 and Table 7 were used for the model development. Specifically, the 25%, 50% (median), and 75% percentile results for the efficiencies were fitted into a third-order polynomial shown in Equation (6), with the efficiency as the dependent variable and the external static pressure as the independent variable.

$$\eta = C_1 + C_2 \times ESP + C_3 \times ESP^2 + C_4 \times ESP^3 \quad (6)$$

Similar to the airflow models in Equation (5) developed previously, the efficiency models for PSC and ECM blowers have the same format, but with different empirical coefficients, which were found by applying the least-squares approach to the data in Table 7.

Efficiency curves as a function of the external static pressure (ESP) generated from these models are shown in Figure 14 and Figure 15 for PSC and ECM blowers, respectively. As can be seen, the efficiency curves in Figure 14 and Figure 15 are consistent with the statistical efficiency results that were used to develop the correlations. In addition, the empirical coefficients for the efficiency models of PSC and ECM blowers are tabulated in Table 9, along with R^2 values. The R^2 values in Table 9 are all in a range of 0.97 to 0.99, which along with results shown in Figure 14 and Figure

15 is strong evidence that the developed efficiency models can provide accurate performance representations of PSC and ECM blowers. Therefore, these efficiency models along with the airflow models that were developed in the previous section can be used to predict energy consumptions of PSC and ECM blowers in future studies, dealing with building energy simulations and equipment performance modeling.

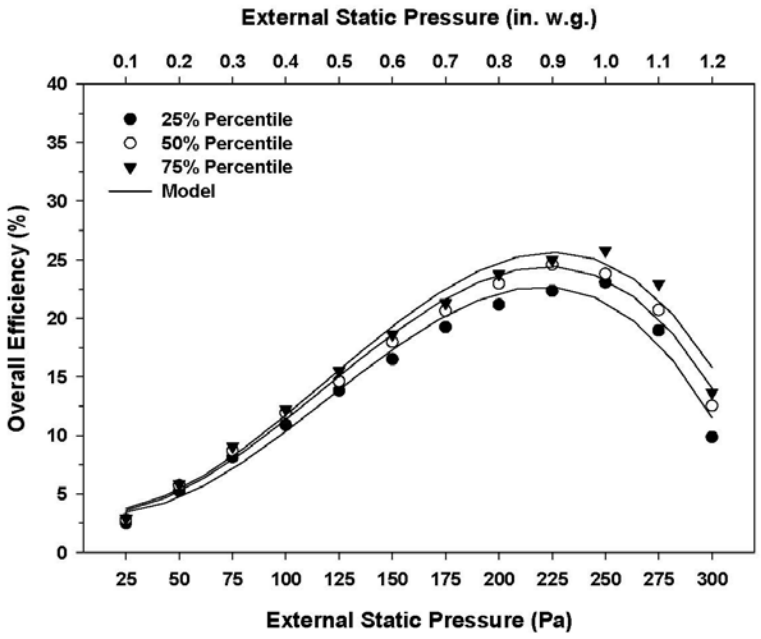

Figure 14 Overall efficiencies as a function of ESP for PSC blowers

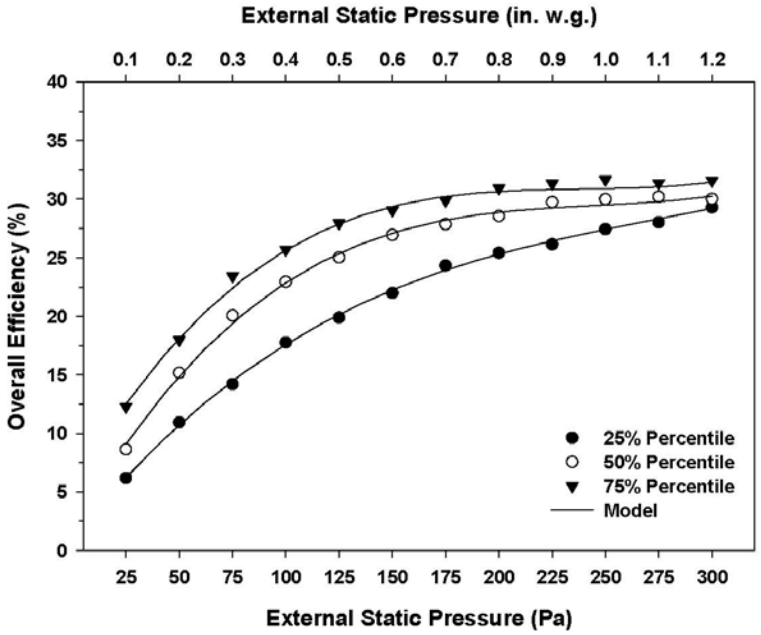

Figure 15 Overall efficiencies as a function of ESP for ECM blowers

Table 9 Empirical coefficients and R^2 values for efficiency models

Blower Type	Percentile	C_1 (-)	C_2 (Pa^{-1})	C_3 (Pa^{-2})	C_4 (Pa^{-3})	R^2
PSC	25%	3.824	-0.0536	0.00165	-0.00000462	0.977
	50%	3.528	-0.0334	0.00156	-0.00000444	0.989
	75%	3.687	-0.0346	0.00160	-0.00000450	0.982
ECM	25%	0.962	0.228	-0.000702	0.000000853	0.999
	50%	1.846	0.320	-0.00127	0.00000173	0.997
	75%	5.426	0.315	-0.00131	0.00000183	0.996

2.5.3 Model Application

The value of the empirical models developed and presented herein is that they can be used by HVAC engineers to determine the typical blower airflow and efficiency behaviors as a function of external static pressures (ESPs). For example, the airflow model provides an approach to characterize blower airflow performance over a pressure range of 0.1 to 1.2 in. w.g. (25 to 300 Pa) for both PSC and ECM blowers based on the knowledge of a single airflow rate at any external static pressure (ESP). The procedure for determining the airflow performance is to use Equation (5), along with appropriate coefficients from Table 8, for the calculation of percentage airflow change at the known pressure relative to the airflow rate at the pressure of 0.1 in. w.g. (25 Pa). Next, utilizing the airflow rate at 0.1 in. w.g. (25 Pa), one can easily calculate the median airflow rate for a PSC blower or an ECM blower, along with statistical bounds, namely 25% and 75% percentiles that one might expect.

It should be noted that it is not necessary to know the airflow rate at 0.1 in. w.g. (25 Pa), rather one can use any point on the airflow curve as long as one knows an airflow rate at a known pressure. For example, the percentage airflow change at any known pressure can be calculated by using Equation (5) in conjunction with coefficients in Table 8. And then, the airflow rate at 0.1 in. w.g. (25 Pa) can be calculated from the airflow rate at the known pressure and the corresponding percentage airflow change, as shown in Equation (7).

$$\dot{Q}_{25} = \frac{\dot{Q}_{known}}{1-\dot{Q}(\%)} \tag{7}$$

With the knowledge of the airflow rate at 0.1 in. w.g. (25 Pa), the full airflow curve can be determined from the developed airflow model by using coefficients from Table 8.

In addition to the prediction of airflow performance, the developed efficiency model, which correlates the over efficiencies of both PSC and ECM blowers with external static pressures (ESPs), can be used to calculate blower power consumptions over a pressure range of 0.1 to 1.2 in. w.g. (25 to 300 Pa). Before one can determine the blower power consumption at a known pressure, the airflow rate at the known pressure should be known or calculated by using the developed airflow model. As the next step, the blower overall efficiency at the known pressure is determined according to Equation (6) along with coefficients from Table 9. With the knowledge of both airflow rate and overall efficiency at the known pressure, Equation (4) can be rearranged into Equation (8) and used for the calculation of blower power.

$$W = \frac{\dot{Q}\Delta P_s}{\eta} \times 100\% \tag{8}$$

2.6 Conclusions

In this study, the performance of six PSC and six ECM blowers from four different manufacturers were experimentally evaluated over a range of blower speeds in a well-instrumented laboratory environment with a nozzle airflow chamber. Airflow and blower power measurements were taken over an external static pressure (ESP) range of 0.1 to 1.2 in. w.g. (25 to 300 Pa), and then blower overall efficiencies were determined from the measured airflow, pressure, and power data. Also, the airflow, power, and efficiency data were statistically analyzed and presented in terms of 25%, 50% (median),

75% percentiles, along with the minimum and maximum values at each external static pressure (ESP) in a range of 0.1 to 1.2 in. w.g. (25 to 300 Pa). To complement the experimental investigation, empirical models that characterize the airflow and efficiency behaviors of PSC and ECM blowers as a function of external static pressures (ESPs) were developed from the statistical analysis of airflow and efficiency results. The major findings are summarized below:

- The airflow performance responding to changes in the external static pressure (ESP) for PSC and ECM blowers are significantly different. Specifically, airflow rates for PSC blowers decrease as the external static pressure (ESP) is increased, while ECM blowers are able to maintain relatively constant airflow rates regardless of pressure changes.
- Power consumptions of PSC blowers decrease as the external static pressure (ESP) is increased because of the substantial airflow reductions that occur. In contrast, ECM blowers require more power to maintain airflow rates at higher flow resistances.
- The overall efficiencies of both PSC and ECM blowers increase with increasing external static pressures (ESPs). For PSC blowers, all speeds essentially have the same level of efficiencies, while ECM blowers tend to have higher efficiencies at lower speeds. In addition, for the same pressure, ECM blowers tend to have higher efficacies than PSC blowers, especially at the low end of the pressure.
- Among blowers with the same motor type, there are great variations in the performance of airflow, power, and efficiency with respect to changes in the

external static pressure (ESP). These performance variations are because of varying designs of housings, blower wheel dimensions, airflow ranges, motor sizes, and speed control mechanisms.

The experimental data taken and analyzed in this study reported herein provides essential and necessary information for the development of rating standards to regulate electricity consumptions of PSC and ECM blowers. Also, of great importance, the airflow and efficiency models developed and reported herein provide an effective approach to predict typical PSC and ECM blower performance based on external static pressures. These models can be used by HVAC engineers for residential system designs and equipment selections. Also, the developed airflow and efficiency models can be easily integrated with building energy simulations for future studies that evaluates the savings potential of ECM blowers over PSC blowers in residential central HVAC systems.

3. IMPACT OF DUCT FLOW RESISTANCE ON RESIDENTIAL HEATING AND COOLING ENERGY USE IN SYSTEMS WITH PSC AND ECM BLOWERS

3.1 Overview

Extensive field measurements indicate that excess duct flow resistances widely exist in residential air distribution systems and directly affect the blower airflow and power performance. More importantly, the excess flow resistance also indirectly impacts equipment efficiencies and cooling capacities, and thus, affects cooling energy consumptions. However, the energy impact of excess duct flow resistance on a system is still unclear because of complex relationships among duct flow resistances, airflow rates, blower efficiencies, system runtime, condensing unit electricity consumptions, and furnace natural gas consumptions. In addition, the different performance characteristics of PSC blowers and ECM blowers add more complexity to these relationships. Therefore, the objective of this study is to provide understanding and solutions to these complex relationships by quantifying the impact of duct flow resistance on residential heating and cooling energy use in systems with PSC and ECM blowers. Experimentally determined cooling performance results for a unitary air conditioner were integrated with building energy simulations of two homes (Austin, TX and Chicago, IL) to predict the annual space heating and cooling energy use for ductworks with four different levels of flow resistance of 0.3, 0.5, 0.7, and 0.9 in. w.g. (75, 125, 175, and 225 Pa) in two extreme climate conditions. An analysis of these predictions shows that increasing the duct flow resistance from 0.3 to 0.9 in. w.g. (75 to 225 Pa) decreased airflow rates of

PSC blowers and consequently decreased the annual blower electricity consumptions by 11% for the Austin home and 16% for the Chicago home. However, in systems with ECM blowers the same increase in the duct flow resistance increased the annual blower electricity consumptions by about 60% for both the Austin home and the Chicago home, primarily because ECM blowers maintained constant airflow rates over a range of pressures. In addition, the system electricity savings of ECM blowers relative to PSC blowers decreased from 17% to 9% for the Austin home and from 27% to 13% for the Chicago home as a result of increasing the duct flow resistance from 0.3 to 0.9 in. w.g. (75 to 225 Pa).

3.2 Introduction

Substantially high duct flow resistances widely exist in residential central heating, ventilating, and air-conditioning (HVAC) systems due to combinations of inappropriate designs and installations, undersized ducts, and pressure drops caused by major system restrictions, such as cooling coils, heating elements, filters, supply registers, and return grilles. This excess duct flow resistance directly affects the blower power as documented in the past studies of laboratory blower power measurements over a pressure range of 0 to 1.2 in. w.g. (0 to 300 Pa) conducted by Walker and his colleague (Walker 2004, Walker and Lutz 2005, Walker 2006, Walker 2008). These studies demonstrated that the power of blowers with permanent split capacitor (PSC) motors is decreased with increasing pressures due to decreases in airflow rates, while the power of blowers driven by electronically commuted motors (ECMs) is increased as airflow rates

are maintained. For example, at a pressure of 0.2 in. w.g. (50 Pa), which represents the flow resistance of ideal ducts, the ECM blower used 60% less power than the PSC blower with power measurements of 750 W for the PSC blower versus 300 W for the ECM blower. However, at a pressure of 0.5 in. w.g. (125 Pa), which represents the flow resistance of real-world duct installations, the PSC blower used less power than the ECM blower, showing 550 W for the PSC blower versus 600 W for the ECM blower. Due to the pressure increase from 0.2 to 0.5 in. w.g. (50 to 125 Pa), the power of the PSC blower decreased by 27% from 750 W to 550 W, while the power of the ECM blower doubled from 300 W to 600 W (Walker 2008).

In addition to the experimental results reported by Walker and his colleague (Walker 2004, Walker and Lutz 2005, Walker 2006, Walker 2008), Lutz et al. (2006) and Franco et al. (2008) took the performance comparison of PSC and ECM blowers a step further by simulating the blower energy use at different duct flow resistances. For example, in a comparison of blower energy consumptions at different duct flow resistances of 0.3, 0.5, and 0.8 in. w.g. (75, 125, and 200 Pa), along with 16 house locations in the U.S., they showed that the blower electricity savings from ECM blowers relative to PSC blowers decreased with increasing duct flow resistances and varied widely with weather conditions. Specifically, they found that nationally ECM blowers consumed 45% less electricity at the low flow resistance of 0.3 in. w.g. (75 Pa) , 35% less electricity at the medium flow resistance of 0.5 in. w.g. (125 Pa), and 6% less at the high flow resistance of 0.8 in. w.g. (200 Pa) compared to PSC blowers.

It is important to note that the above laboratory measurements (Walker 2004, Walker and Lutz 2005, Walker 2006, Walker 2008), along with the simulation results from Lutz et al. (2006) and Franco et al. (2008) focused only on blower energy consumptions in the presence of excess duct flow resistances. Of even more importance is the impact of excess duct flow resistance on non-blower energy consumptions, which makes up 80-95% of the total energy use in a residential central HVAC system (Parker et al. 2005, Stephens et al. 2010). The non-blower energy use that has not been thoroughly investigated in any of the above studies includes condensing unit electricity consumptions in cooling seasons and natural gas consumptions in heating seasons with respect to different types of system blowers (i.e., PSC or ECM blowers). The effect of different blower types on the non-blower energy use is made more obvious when one consider the fact that increases in the flow resistance reduce airflow rates of PSC blowers, resulting in decreasing cooling capacities and coefficients of performance (COP) because of insufficient evaporator airflows (Palani et al. 1992, Breuker and Braun 1998, Siegel et al. 2002, Kim et al. 2009, Palmiter et al. 2011, Mowris et al. 2012). The negative effect of insufficient airflows is well documented, with one experimental study (Rodriguez et al. 1996) reporting that a 50% airflow reduction would lead to a decrease of 15% in the total cooling capacity and 14% in the COP for an air conditioner with a thermostatic expansion valve (TXV). For the same airflow reduction, the impact on a non-TXV unit was even more severe, showing a decrease of about 25% in the total cooling capacity and 22% in the COP.

Relative to PSC blowers, ECM blowers have better performance in terms of maintaining constant airflow rates over a pressure range, but the power of ECM blowers can significantly increase with the excess flow resistance. More importantly, this increased blower power imposes an additional cooling load on a system and tends to offset the sensible capacity by reducing the temperature difference between the supply and return air (Kendall 2004). Based on a combined approach of experimental measurements and empirical modeling, Yin et al. (2014a) quantified this effect by showing that the heat gain from an ECM blower in a 60 kBtu/h (17.6 kW) air conditioner could decrease the sensible cooling capacity by up to 1.9% and the sensible COP by as much as 6.6%. Capturing this effect is of special importance because most residential air conditioning systems are controlled by thermostats that can only sense the sensible load. For a given sensible load, system runtime will increase with this reduced sensible capacity, and thus, result in more energy consumptions. Yin et al. (2014b) evaluated this energy penalty by integrating building energy simulations with experimental performance measurements taken on a residential air conditioner with an ECM blower and found that increases in the flow resistance from 0.3 to 0.9 in. w.g. (75 Pa to 225 Pa) could decrease the airflow rate of the ECM blower by 11.2% in the heating mode and 17.7% in the cooling mode. Furthermore, the combined effects of decreasing airflows and increasing blower powers increased the annual system runtime by 6.8% and the condensing unit electricity consumption by 7.5%.

Although previous studies have identified energy impacts of excess duct flow resistances on blowers and air conditioners separately, the system-level energy effect

caused by excess duct flow resistances in residential central HVAC systems is still unclear, especially for the non-blower energy consumptions, because of the complex relationships among duct flow resistances, airflow rates, blower efficiencies, system runtime, condensing unit electricity consumptions, and furnace natural gas consumptions. More importantly, these relationships vary with the type of installed blowers, namely PSC or ECM blowers. Therefore, the objective of the study reported herein is to comprehensively quantify the impact of excess duct flow resistances on the heating and cooling energy use in residential central HVAC systems by using a combined approach of experimental measurements performed on HVAC systems and building energy simulations that provides heating and cooling loads for the specific buildings at specific ambient conditions.

As a first step, empirical correlations linking cooling performance and evaporator airflow rates were developed over an airflow range of 1000 to 2250 ft^3/min (0.47 to 1.06 m^3/s) from well-instrumented laboratory measurements. Then, these experimental results were integrated with public-domain building energy simulation models to estimate the annual electricity consumptions of blowers and condensing units as well as furnace natural gas consumptions in residential central HVAC systems as a consequence of PSC and ECM blowers that were paired with ductworks of different flow resistances.

3.3 Experimental Study

Although several studies have investigated air conditioner cooling performance at reduced evaporator airflow conditions, none of them have provided empirical curves

or correlations relating the cooling performance with evaporator airflow rates, even though this relationship is required so that system energy penalties caused by airflow reductions with PSC and ECM blowers can be accurately determined for ductworks with excess flow resistances. Hence, the purpose of the experimental study part of the project reported herein is to characterize the cooling performance of a typical air conditioner for a range of evaporator airflows, which serves as an important input for the building energy simulation study developed later. The unit tested in this study is a 60 kBtu/h (17.6 kW) R410a unitary air conditioner with a nominal airflow rate of 2000 ft^3/min (0.94 m^3/s). Well-instrumented laboratory measurements were taken on both the air side and the refrigerant side to determine the cooling performance in terms of cooling capacities, condensing unit powers, and sensible heat ratios (SHRs) with respect to airflow rates that varied from 1000 to 2250 ft^3/min (0.47 to 1.06 m^3/s).

3.3.1 Experimental Setup

All laboratory tests were conducted in two identical, heavily-insulated environmental control rooms (i.e. psychrometric chambers) that were capable of achieving controllable indoor and outdoor ambient conditions. ANSI/ASHRAE Standard 37 (2009b) and AHRI Standard 210/240 (2008) were used as guidelines for the experimental setup and testing procedures. The cooling capacity at any given airflow rate was determined by using two independent methods, namely the indoor air enthalpy method and the refrigerant enthalpy method.

For the indoor air enthalpy method, the cooling capacities were calculated based on air enthalpy changes and airflow rates through the evaporator coil. The enthalpy changes were determined by measuring the dry-bulb (DB) and wet-bulb (WB) temperatures of the supply and return air. Specifically, two 12-element type-T thermocouple grids were installed upstream and downstream of the evaporator to determine the average DB temperature of the air side. Psychrometric stations with sampling devices built in accordance with ASHRAE 41.1 (ASHRAE 1996) were used to measure the average WB temperature. Evaporator airflow rates were measured by using a nozzle airflow chamber that was built in accordance with the requirements of ANSI/ASHRAE Standard 51 (ASHRAE 2007b). This nozzle airflow chamber was equipped with multiple nozzles of different sizes to cover an airflow measurement range of 200 to 4000 ft^3/min (0.09 to 1.89 m^3/s). An assist blower controlled by a variable frequency drive (VFD) was attached to the nozzle chamber and used to obtain variable airflow rates. In addition to air-side DB and WB temperature measurements on the evaporator, the condenser inlet air DB and WB temperatures were measured and averaged by using an air sampling unit as described in ASHRAE 41.1 (1996).

For using the refrigerant enthalpy method, refrigerant-side cooling capacities were calculated from refrigerant enthalpy changes and mass flow rates. Refrigerant enthalpy changes were determined by measuring the refrigerant temperatures and pressures entering the TXV and leaving the indoor coil. Refrigerant temperature measurements were made by inserting T-type thermocouple probes into the centerline of copper elbows. Elastomeric pipe insulations were installed 2 in. (51 mm) before and

after each temperature measurement point in order to minimize the measurement errors carried by the ambient temperature. Pressure transducers were directly connected to the refrigerant stream to obtain accurate pressure measurements. The refrigerant mass flow rate was recorded by a coriolis mass flow meter installed at the bottom of a vertical downward loop in the liquid line. After the refrigerant-side instrument installation, the refrigeration system was sealed, vacuumed, and charged with 9.9 lb_m (4.5 kg) of R410a by following the manufacturer's instructions.

3.3.2 Test Procedures

Cooling performance tests were conducted at six different evaporator airflow rates ranging from 1000 to 2250 ft^3/min (0.47 to 1.06 m^3/s) by using airflow increments of 250 ft^3/min (0.12 m^3/s). The same temperature settings were maintained in all tests based on the "A Test" condition prescribed by AHRI Standard 210/240 (2008), namely 80°F (26.7°C) for the indoor DB, 67°F (19.4°C) for the indoor WB, and 95°F (35°C) for the outdoor DB.

For each test, after reaching the target indoor and outdoor temperatures as specified in AHRI Standard 210/240 (2008), the psychrometric room reconditioning apparatus and the test unit were continuously operated for one hour at steady state. Then, the air-side and refrigerant-side measurements were taken and recorded at equal intervals of 30 seconds until completing a 30-minute testing period. Air properties, such as the density, specific heat, enthalpy, humidity ratio, and relative humidity, were calculated by using equations in ASHRAE Handbook-Fundamental (ASHRAE 2009a). The

REFPROP software developed by National Institute of Standards and Technology (NIST 2007) was used for the enthalpy calculation of R410a. A customized computer program was used to perform real-time calculations of psychrometrics, refrigerant enthalpies, and cooling capacities based on measurements of temperatures, pressures, and mass flow rates for both air and refrigerant sides. While measuring the cooling performance, the power consumptions of compressor, condenser fan, and indoor blower were simultaneously and individually measured.

Test results were considered valid only if the two cooling capacities as determined from the two independent methods, namely the indoor air enthalpy method and the refrigerant enthalpy method, agreed to within 6% based on the guidelines provided by AHRI Standard 210/240 (2008). Once a test was completed, calculation results were saved into a spreadsheet, along with the measured raw data. Table 10 shows the instruments used in the experimental study and their accuracies.

Table 10 Instrument specifications and accuracies

Measurement	Instrument Specifications	Accuracies
Barometric pressure	Barometer, 600-1100 mb a (0.6-1.1×10^5 P)	±0.15%
Air DB temperature	Calibrated RTD probe, 32-140°F (0-60°C)	±0.4°F (±0.2°C)
Air WB temperature	Calibrated RTD probe, 32-140°F (0-60°C)	±0.4°F (±0.2°C)
Airflow chamber temperature	Calibrated RTD probe, 32-140°F (0-60°C)	±0.4°F (±0.2°C)
Refrigerant temperature	Calibrated thermocouple, 32-140°F (0-60°C)	±0.4°F (±0.2°C)
Refrigerant pressure	Gauge pressure transmitter 0-1000 psi (0-6.9×10^6 Pa)	±0.3% Full Scale
Refrigerant mass flow rate	Coriolis mass flow meter 0-26 lb_m/min (0-12 kg/min)	±0.2% Reading
External static pressure	Air pressure transmitter, 0-1 in. w.g. (0-250 Pa)	±0.25% Full Scale
Airflow chamber static pressure	Air pressure transmitter, 0-3 in. w.g. (0-750 Pa)	±0.25% Full Scale
Chamber nozzle differential pressure	Air pressure transmitter, 0-3 in. w.g. (0-750 Pa)	±0.25% Full Scale
Compressor power	Power transducer, 0-4 kW	±0.2% Full Scale
Indoor blower power Condenser fan power	Power transducer, 0-1 kW	±0.2% Full Scale
Voltage	Voltage transducer, 0-300 V	±0.25% Full Scale

3.3.3 Data Reduction and Uncertainty Analysis

A series of calculations was performed by using the measurements of temperature, pressure, mass flow rate, and power to characterize the cooling performance in terms of the total cooling capacity, condensing unit power, and sensible heat ratio (SHR). For example, the air-side sensible, latent, and total capacities were determined according to Equations (9) to (11), respectively.

$$\dot{q}_{sci} = \frac{\dot{Q}_{mi}(c_{pa1}t_{a1} - c_{pa2}t_{a2})}{v_n} + E_i \tag{9}$$

$$\dot{q}_{lci} = \frac{\dot{Q}_{mi}K(\omega_1 - \omega_2)}{v_n} \tag{10}$$

$$\dot{q}_{tci_a} = \frac{\dot{Q}_{mi}(h_{a1} - h_{a2})}{v_n} + E_i \tag{11}$$

The refrigerant-side cooling capacity was calculated by using Equation (12).

$$\dot{q}_{tci_r} = \dot{w}_r(h_{r2} - h_{r1}) \tag{12}$$

In addition, the sensible heat ratio (SHR), defined as the ratio of the sensible cooling capacity to the total cooling capacity, was calculated by using Equation (13).

$$SHR = \frac{\dot{q}_{sci}}{\dot{q}_{tci_a}} \tag{13}$$

It should be noted that the above performance parameters are based on the gross cooling performance, which is determined without considering the heating effect caused by the indoor blower.

The combined uncertainties in the above calculated terms, namely cooling capacities and the SHR, were resulted from instrument accuracies associated with measurements of temperature, pressure, mass flow rate, and power. The Kline and McClintock (1953) method was used to estimate the uncertainty propagation. For example, the uncertainty for the refrigerant-side cooling capacity was determined as following

$$U_{q_{tci_r}} = \sqrt{\left(\frac{\partial q_{tci_r}}{\partial h_{r2}} \cdot u_{h_{r2}}\right)^2 + \left(\frac{\partial q_{tci_r}}{\partial h_{r1}} \cdot u_{h_{r1}}\right)^2 + \left(\frac{\partial q_{tci_r}}{\partial \dot{w}_r} \cdot u_{\dot{w}_r}\right)^2} \tag{14}$$

The $u_{h_{r2}}$ and $u_{h_{r1}}$ terms are uncertainties associated with refrigerant enthalpies, which are dependent on the uncertainties of the refrigerant temperature and pressure measurements, while the $u_{\dot{w}_r}$ term is the uncertainty of the refrigerant mass flow rate based on the flow meter's accuracy. At a confidence level of 95%, the combined uncertainties in the final results were calculated and summarized in Table 11.

Table 11 Uncertainties for calculated terms

Calculated Term	Uncertainty at 95% confidence interval
Evaporator airflow rate	±1.0%
Air enthalpy	±1.0%
Air humidity ratio	±1.5%
Sensible cooling capacity	±1.5%
Latent cooling capacity	±10.0%
Total cooling capacity, air side	±3.0%
Total cooling capacity, refrigerant side	±1.0%
Sensible heat ratio (SHR)	±3.5%

3.3.4 Experimental Results

The cooling performance was characterized in terms of the total cooling capacity, condensing unit power, and SHR, all of which were determined from the experimental measurements of temperature, pressure, mass flow rate, and power along with the calculations performed in Equations (9) to (13). To investigate airflow impacts on the cooling performance, three performance parameters, namely the total cooling capacity, condensing unit power, and SHR, were plotted against the evaporator airflow rate. Figure 16 shows the total cooling capacity and the condensing unit power consumption over an airflow range of 1000 to 2250 ft^3/min (0.47 to 1.06 m^3/s). As can be seen in Figure 16, variations in evaporator airflow rates affect these two performance parameters differently. For example, the condensing unit power, which is the sum of power consumptions of the compressor and the condenser fan, remains almost constant over the entire airflow range, with only a 3% increase from 4.27 to 4.40 kW in response to increasing airflows from 1000 to 2250 ft^3/min (0.47 to 1.06 m^3/s). In contrast, the total cooling capacity continuously increases with increasing airflow rates, showing a 20%

increase in the total cooling capacity from 50.5 to 60.4 kBtu/h (14.8 to 17.7 kW) as the airflow rate is increased from 1000 to 2250 ft^3/min (0.47 to 1.06 m^3/s).

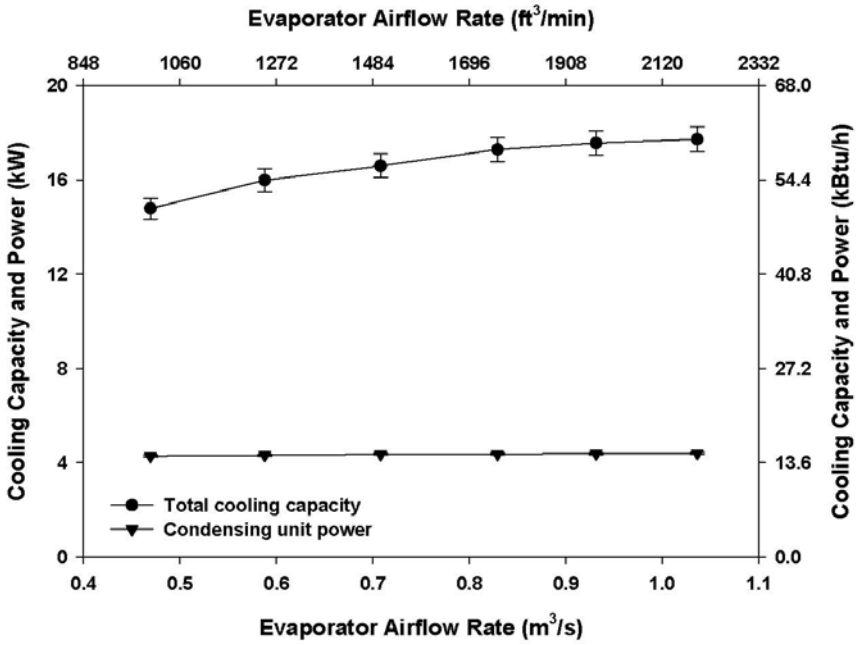

Figure 16 Cooling capacity and power consumption for a range of evaporator airflow

Figure 17 shows the behavior of SHR with changes of evaporator airflow rates. As can be seen, increasing airflows lead to increases in SHR. For instance, SHR is increased by 29% from 0.62 to 0.80 as a result of airflow increases from 1000 to 2250 ft^3/min (0.47 to 1.06 m^3/s). Due to decreases in the contact time between the air stream

and the cooling coil at conditions of increased airflow rates, part of latent cooling is converted to sensible cooling and consequently results in continuous increases in SHR.

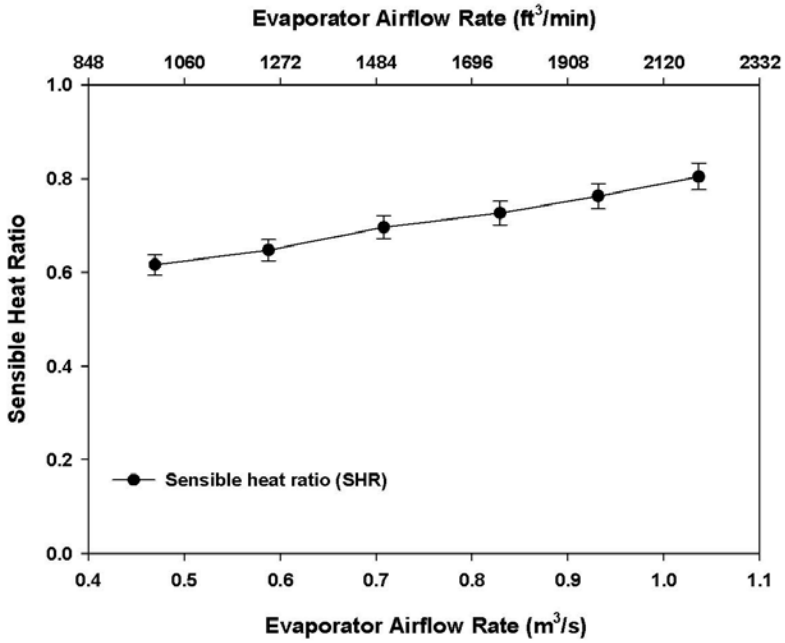

Figure 17 SHR for a range of evaporator airflow

3.3.5 Model Development

As mentioned earlier, the purpose of the experimental study phase of the research presented in this paper is to develop empirical models that can then be used to characterize the performance of residential air conditioners at different airflow and temperature conditions for simulation studies. Previous studies in the literature (Henderson et al. 2000, Kruis 2010, LBNL 2014) modeled the air conditioner

performance by using the rated performance data and a group of empirical curves. The rated performance data refers to the nominal airflow rate, total cooling capacity, SHR, and COP at the "A Test" condition specified in AHRI Standard 210/240 (2008), namely indoor temperatures at 80°F (26.7°C) DB / 67°F (19.4°C) WB and the outdoor temperature at 95°F (35°C) DB. Empirical curves that are modifier curves of cooling capacity, energy input ratio, and SHR as functions of flow fraction (FF) and temperatures were used in the past studies to account for variations in evaporator and condenser heat exchanger performance under varying environmental and building conditions. Specifically, these curves were used to calculate the actual cooling performance at conditions that deviate from the rating condition of airflow rate and temperature. Using the rated performance data and empirical curves, the actual cooling capacity at any airflow and temperature conditions is calculated as

$$\dot{q}_{tc} = \dot{q}_{tc,rated} \cdot \text{CapModCurve(FF)} \cdot \text{CapModCurve}(T_{wb_i}, T_{db_o}) \quad (15)$$

In a similar way, the electricity consumption of the condensing units is calculated by using the following equation

$$Power = \frac{\dot{q}_{tc,rated}}{COP_{rated}} \cdot \text{EIRModCurve(FF)} \cdot \text{EIRModCurve}\left(T_{wb_i}, T_{db_o}\right) \quad (16)$$

Also, the SHR at specific airflow rates and temperatures is calculated as

$$SHR = SHR_{rated} \cdot \text{SHRModCurve(FF)} \cdot \text{SHRModCurve}(T_{wb_i}, T_{db_o}) \quad (17)$$

The same approach as documented in the literature (Henderson et al. 2000, Kruis 2010, LBNL 2014) and as described above was used in this study for modeling the air conditioner performance. The performance at the rating condition was experimentally determined, while the corresponding empirical curves were derived from both the

experimental data and the manufacturer's catalog data. The modifier curves of cooling capacity (CapModCurve(FF)), energy input ratio (EIRModCurve(FF)), and SHR (SHRModCurve(FF)) as a function of the flow fraction were directly derived from the experimental results. As a first step, the measured total cooling capacity, condensing unit power, and SHR were normalized against the corresponding results at the rated airflow rate of 2000 ft^3/min (0.94 m^3/s) at the "A Test" condition. Then, these normalized results were fitted into second order polynomials as shown in Equation (18) with the independent variable of flow fraction, which is the ratio of the actual airflow rate to the rated airflow rate.

$$\begin{Bmatrix} \text{CapModCurve (FF)} \\ \text{EIRModCurve (FF)} \\ \text{SHRModCurve (FF)} \end{Bmatrix} = C_1 \cdot FF^2 + C_2 \cdot FF + C_3 \quad (18)$$

The coefficients for Equation (18) were estimated from a regression analysis by using the least-squares approach, and they are summarized in Table 12, along with R^2 values ranging from 0.97 to 0.99.

Table 12 Coefficients and R^2 for performance modifier curves as a function of flow fraction

Performance parameters	Empirical coefficients			R^2
	C_1	C_2	C_3	
CapModCurve	-0.406	0.925	0.481	0.996
EIRModCurve	-0.0497	0.123	0.928	0.978
SHRModCurve	0	0.403	0.601	0.996

Figure 18 shows the results of normalized total cooling capacity, condensing unit power, and SHR plotted against the flow fraction, along with the resulting empirical curves. As can be seen in Figure 18, the developed curves have good agreement with the experimental data. Also, the high R^2 values above 0.97 listed in Table 12 indicates that the developed curves are capable of charactering the behaviors of total cooling capacity, condensing unit power, and SHR over an airflow range of 1000 to 2250 ft^3/min (0.47 to 1.06 m^3/s).

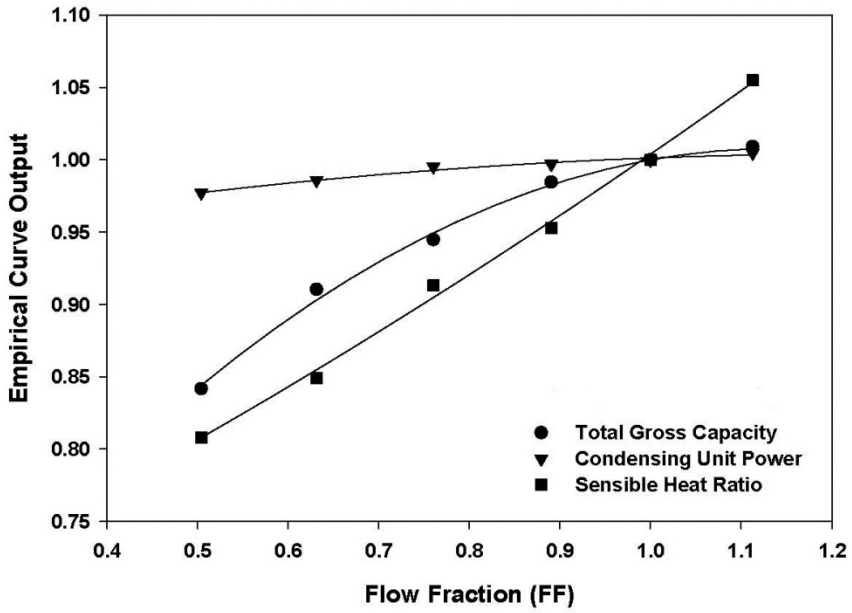

Figure 18 Normalized performance and empirical curves

The modifier curves of cooling capacity (CapModCurve(T_{WB_i}, T_{DB_o})), energy input ratio (EIRModCurve(T_{WB_i}, T_{DB_o})), and SHR (SHRModCurve(T_{WB_i}, T_{DB_o})) as

functions of indoor WB and outdoor DB temperatures were derived from the manufacturer's catalog data, which include power consumptions, total and sensible cooling capacities at various combined conditions of the indoor WB temperature in a range of 57 to 72 °F (13.8 to 22.2 °C) and the outdoor DB temperature in a range of 75 to 125 °F (23.9 to 51.7 °C). Similar to the development of modifier curves as functions of the flow fraction, the catalog data at various combined indoor WB temperature and outdoor DB temperature conditions were normalized against the measured performance data at the "A Test" condition with an airflow rate of 2000 ft^3/min (0.94 m^3/s). Then, the normalized results of total cooling capacity, energy input ratio, and SHR were fitted into Equation (19), with indoor WB and outdoor DB being independent variables.

$$\left\{\begin{matrix}\text{CapModCurve}\left(T_{WB_i}, T_{DB_o}\right)\\ \text{EIRModCurve}\left(T_{WB_i}, T_{DB_o}\right)\\ \text{SHRModCurve}\left(T_{WB_i}, T_{DB_o}\right)\end{matrix}\right\} = \mathrm{C}_1 + \mathrm{C}_2 \cdot T_{WB_i} + \mathrm{C}_3 \cdot T_{WB_i}^2 + \mathrm{C}_4 \cdot T_{DB_o} + \mathrm{C}_5 \cdot T_{DB_o}^2 + \mathrm{C}_6 \cdot T_{WB_i} \cdot T_{DB_o} \quad (19)$$

As before, the empirical coefficients in Equation (19) were estimated from a regression analysis on the normalized results by using the least-squares approach, and they are shown in Table 13, along with the R^2 values for the developed performance curves. As noted, the R^2 values in Table 13 are all above 0.9, which indicates the developed empirical curves are in good agreement with the normalized catalog data.

Table 13 Coefficients and R^2 values for performance modifier curves as functions of temperature

Performance parameters	Empirical coefficients						R^2
	C_1	C_2 (°C^{-1})	C_3 (°C^{-2})	C_4 (°C^{-1})	C_5 (°C^{-2})	C_6 (°C^{-2})	
CapModCurve	1.666	-6.78×10^{-2}	2.94×10^{-3}	-3.03×10^{-3}	-7.79×10^{-6}	-5.14×10^{-4}	0.999
EIRModCurve	0.516	-1.05×10^{-2}	4.11×10^{-4}	1.27×10^{-2}	9.69×10^{-5}	-4.61×10^{-5}	0.999
SHRModCurve	2.022	-2.52×10^{-2}	-1.72×10^{-3}	-4.48×10^{-3}	4.50×10^{-5}	3.04×10^{-4}	0.904

3.4 Building Energy Simulation

The second important step, which follows the first step of developing cooling performance curves, required for investigating the impact of excess duct flow resistances on residential heating and cooling energy use is the development of 16 building energy simulations in EnergyPlus (LBNL 2013a). Also in this step, the simulations were integrated with the empirical performance curves in Equations (18) and (19) and corresponding coefficients in Table 12 and Table 13, along with performance models of PSC and ECM blowers that were developed in the previous study (DOE 2014). This section provides detailed information on the building model development and an extensive discussion of simulation results.

3.4.1 Building Model Development

Two building models were developed to represent typical residential dwellings in the Midwestern region (cold climate) and the Southern region (hot climate) of the United States. Specifically, Chicago, IL, and Austin, TX were selected as the representative locations in each region. Considering the great impact of local climates on the residential heating and cooling energy use (Franco et al. 2008), the selection of these two regions

with extreme climate conditions provides the best opportunity for comparing the regional energy consequences of different duct flow resistances.

Both the Chicago and Austin homes were simulated as single-story buildings consisting of rectangular conditioned zones topped with unconditioned attics. The Chicago home had dimensions of 90 ft × 35 ft × 8 ft (27.3 m × 10.8 m × 2.4 m) with an unconditioned basement, while the Austin home was a slab-on-grade house with dimensions of 87 ft × 35 ft × 8 ft (26.4 m × 10.8 m × 2.4 m). Both homes were assumed to have four bedrooms. The thermal and physical properties of the building envelop, such as exterior walls, floors, roofs, windows, doors, ceilings, attics, and underground walls, were directly adopted from the residential prototype building models developed by the Pacific Northwest National Laboratory (Mendon and Taylor 2014, PNNL 2015) according to the 2012 International Energy Conservation Code (ICC 2011). Table 14 summarizes the characteristics of the Chicago and Austin homes that were simulated in the study reported herein.

Table 14 Characteristics of simulated homes

Building characteristics	Chicago home	Austin home
Climate zone	5A	2A
Number of bedrooms	4	4
Floor area, ft^2 (m^2)	3150 (293)	3045 (283)
Foundation type	unconditioned basement	slab on grade
Wall insulation, $ft^2 \cdot °F \cdot h/Btu$ ($m^2 \cdot K/W$)	20 (3.5)	13 (2.3)
Ceiling insulation, $ft^2 \cdot °F \cdot h/Btu$ ($m^2 \cdot K/W$)	49 (8.6)	38 (6.7)
Floor insulation, $ft^2 \cdot °F \cdot h/Btu$ ($m^2 \cdot K/W$)	30 (5.3)	13 (2.3)
Window U-value, $Btu/h \cdot ft^2 \cdot °F$ ($W/m^2 \cdot K$)	0.32 (1.8)	0.40 (2.3)
Window SHGC	0.4	0.25
Door U-value, $Btu/h \cdot ft^2 \cdot °F$ ($W/m^2 \cdot K$)	0.32 (1.8)	0.4 (2.3)
Underground wall insulation, $ft^2 \cdot °F \cdot h/Btu$ ($m^2 \cdot K/W$)	15 (2.6)	0

Infiltration, ventilation, and internal heat gains were also determined and added to the simulated buildings. The 2012 IECC (ICC 2011) specifies an infiltration rate of five air changes per hour (ach) for Climate Zone 2 and three air changes per hour (ach) for Climate Zone 5, respectively, at a pressure of 0.2 in. w.g. (50 Pa). These infiltration rates were converted into effective leakage areas (ELA) at a pressure of 0.016 in. w.g. (4 Pa) by using Equation (20), resulting in an effective leakage area (ELA) of 1.09 ft^2 (0.1 m^2) for the Chicago home and 1.76 ft^2 (0.16 m^2) for the Austin home for the simulation purpose.

$$ELA = 0.186 \cdot \dot{Q}_{Lr} \frac{\sqrt{\rho / 2\Delta P_{sr}}}{C_d} \tag{20}$$

In addition, a constant rate of 0.15 air changes per hour (ach) was added to the conditioned space in both the Chicago and Austin homes to account for occupancy-caused infiltrations, such as door/window openings and exhaust fans (ASHRAE 2007a).

A ventilation rate of 69 ft^3/min (0.033 m^3/s) for the Chicago home and a rate of 68 ft^3/min (0.032 m^3/s) for the Austin home were determined according to Equation (21) from the 2012 IECC (ICC 2011) with an assumption of four bedrooms in each home.

$$\text{Ventilation } (ft^3/\text{min}) = 0.01 \times CFA + 7.5 \times (N_{br} + 1) \tag{21}$$

Heat gains from lights, equipment, and occupants were estimated according to Equation (22) based on the 2012 IECC (ICC 2011), leading to an internal heat gain of 109 kBtu/day for the Chicago home and 107 kBtu/day for the Austin home.

$$\text{IGain (Btu/day)} = 17900 + 23.8 \times \text{CFA} + 4104 \times \text{N}_{\text{br}} \tag{22}$$

In addition, 20% of the internal heat gain was assumed to be latent load while the rest was sensible load (ASHRAE 2007a). A daily internal heat-gain profile was adopted from ASHRAE Standard 90.2 (2007a) so that the hourly heat again could be calculated by multiplying the daily overall heat gain by the corresponding fraction factor from the profile.

3.4.2 Equipment Selection and Performance Modeling

After establishing the building models, load calculations were performed in EnergyPlus (LBNL 2013a) for the purpose of equipment selection. The climate design conditions of 99% heating dry-bulb temperature and 1% cooling dry-bulb temperature, with mean coincident wet-bulb temperatures, were taken from the ASHRAE handbook (ASHRAE 2009a) for Chicago, IL and Austin, TX and used for the whole house load calculation at each location. Following the 2012 IECC (ICC 2011), thermostats were set at 72°F (22.2°C) for heating and 75°F (23.9°C) for cooling. A heating oversizing factor of 1.3 and a cooling oversizing factor of 1.1 were applied to the calculated loads, which resulted in a heating load of 83 kBtu/h (24.3 kW) and a sensible cooling load of 37 kBtu/h (10.8 kW) for the Chicago home along with a heating load of 65 kBtu/h (18.9 kW) and a sensible cooling load of 42 kBtu/h (12.3 kW) for the Austin home.

Based on the results from load calculations, appropriate heating and cooling equipment were identified. For the Chicago home, a 93 kBtu/h (27.3 kW) gas furnace and an air conditioner of 48 kBtu/h (14.1 kW) total cooling capacity were selected. The same type of equipment was chosen for the Austin home, with the heating and cooling

capacities being 72 kBtu/h (21.1 kW) and 60 kBtu/h (17.6 kW), respectively. For the purpose of simplification, duct leakages were assumed to be zero at both locations. The detailed heating and cooling equipment characteristics for both homes are presented in Table 15.

Table 15 Characteristics of heating and cooling equipment in simulations

	Chicago, IL	Austin, TX
Heating equipment	Gas furnace 93 kBtu/h (27.3 kW) output 80% AFUE	Gas furnace 72 kBtu/h (21.1 kW) output 80% AFUE
Cooling equipment	Air conditioner 48 kBtu/h (14.1 kW) SHR=0.77 COP=4.01	Air conditioner 60 kBtu/h (17.6 kW) SHR=0.77 COP=4.01
Duct leakage	0	0

A series of performance parameters were input into EnergyPlus (LBNL 2013a) so that the performance of gas furnaces, air conditioners, and blowers could be accurately modeled. The heating performance of gas furnaces was determined from the nominal output heating capacity and the annual fuel utilization efficiency (AFUE), both of which were assumed to be constant and independent of airflow rates. The air conditioner cooling performance at different combined conditions of temperatures and airflow rates were determined by using the empirical curves developed earlier and shown in Equations (18) and (19). Specifically, modifier curves of cooling capacity, energy input ratio, and SHR as functions of temperatures and flow fractions, along with

the performance data at the rating condition, were used to determine the actual cooling capacities and power consumptions.

The typical airflow and power performance of PSC and ECM blowers over a pressure range were determined from the DOE's "virtual model" (DOE 2014), which is developed based on broad reviews of a large quantity of performance data for both PSC and ECM blowers from various manufacturers. This model correlates airflow rates (ft^3/min) and efficacies (Watts per ft^3/min) with external static pressures (in. w.g.) by fitting manufacturers' catalog data into a second order polynomial, as shown in Equation (23).

$$Airflow\ and\ Efficacy = C_1 \times ESP^2 + C_2 \times ESP + C_3 \quad (23)$$

Although the DOE's "virtual model" (DOE 2014) does not provide the blower power as a function of external static pressures explicitly, the blower power can be calculated by using the airflow and efficacy at the same external static pressure.

Blowers with nominal airflow rates of 1600 ft^3/min (0.76 m^3/s) and 2000 ft^3/min (0.94 m^3/s) were selected for the Chicago and Austin homes, respectively, so that they are compatible with the pre-sized heating and cooling equipment. As noted, Table 16 lists the corresponding coefficients (C_1, C_2, and C_3) used in Equation (23) for the PSC and ECM blowers that were selected for simulations. In addition, the airflow and power performance of the selected PSC and ECM blowers in both cooling and heating speeds were plotted against the external static pressure and are shown in Figure 19 and Figure 20.

Table 16 Coefficients of airflow and efficacy curves for blowers

Blower	Location	Performance	Cooling Speed			Heating Speed		
			C_1	C_2	C_3	C_1	C_2	C_3
PSC blower	Chicago home	Airflow	-570	49	1718	-570	49	1500
		Efficacy	0.19	-0.2	0.55	0.19	-0.2	0.55
	Austin home	Airflow	-570	49	2118	-570	49	1883
		Efficacy	0.19	-0.2	0.57	0.19	-0.2	0.57
ECM blower	Chicago home	Airflow	-103	99	1576	-103	99	1464
		Efficacy	-0.01	0.25	0.13	-0.01	0.25	0.13
	Austin home	Airflow	-103	99	1976	-103	99	1832
		Efficacy	-0.01	0.25	0.15	-0.01	0.25	0.15

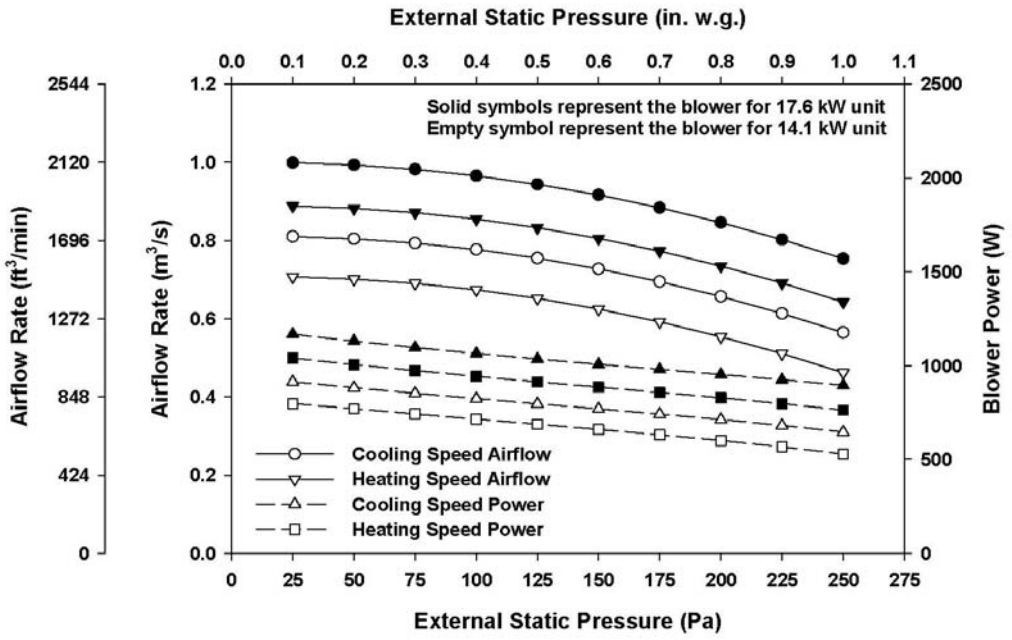

Figure 19 Airflow and power performance of PSC blowers from the DOE's virtual model

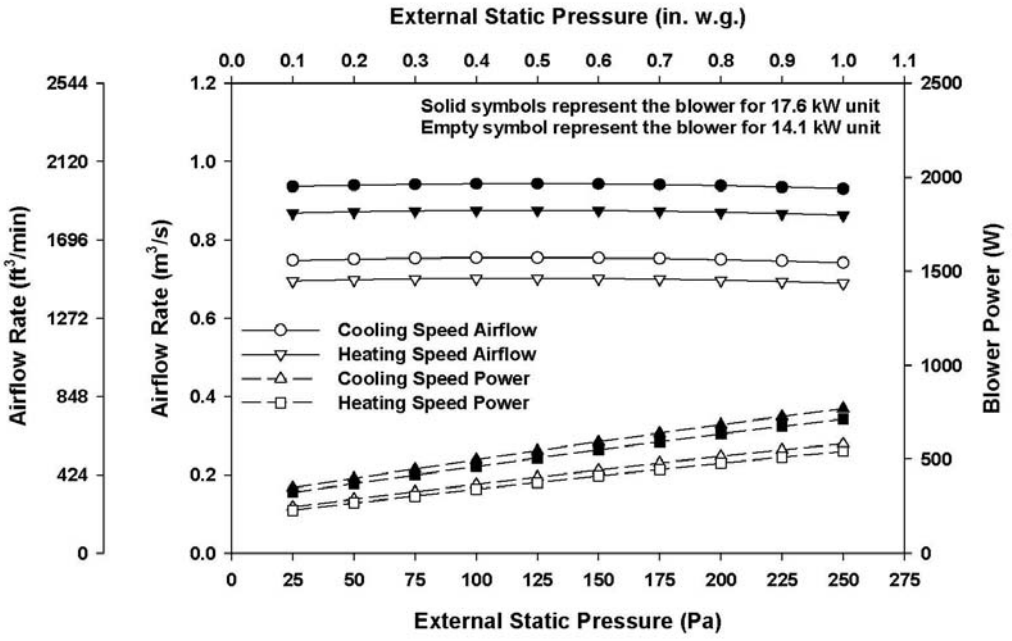

Figure 20 Airflow and power performance of ECM blowers from DOE's virtual model

3.4.3 System Performance Determination for Different Duct Flow Resistance

After selecting gas furnaces, air conditioners, and blowers for the Chicago and Austin homes, system performance, such as airflow rates, blower powers, cooling capacities, condensing unit powers, and SHRs, at different levels of duct flow resistance were determined, resulting in annual energy consumptions as a function of the ductwork flow resistance. As a first step, four reference system curves that describe the relationship between airflow rates and system flow resistances were generated at design pressures of 0.3, 0.5, 0.7, and 0.9 in. w.g. (75, 125, 175, and 225 Pa), which represent low, medium-low, medium-high, and high flow resistance ductworks, respectively. Then, airflow curves for PSC and ECM blowers were plotted and intersected with these

system curves at the design pressures for the cooling speed, which is shown in Figure 21 as an example. The intersections of the blower airflow curves and the ductwork system curves are operating points, which represent unique operating conditions of airflows and pressures when a blower is connected to a ductwork of a specific flow resistance.

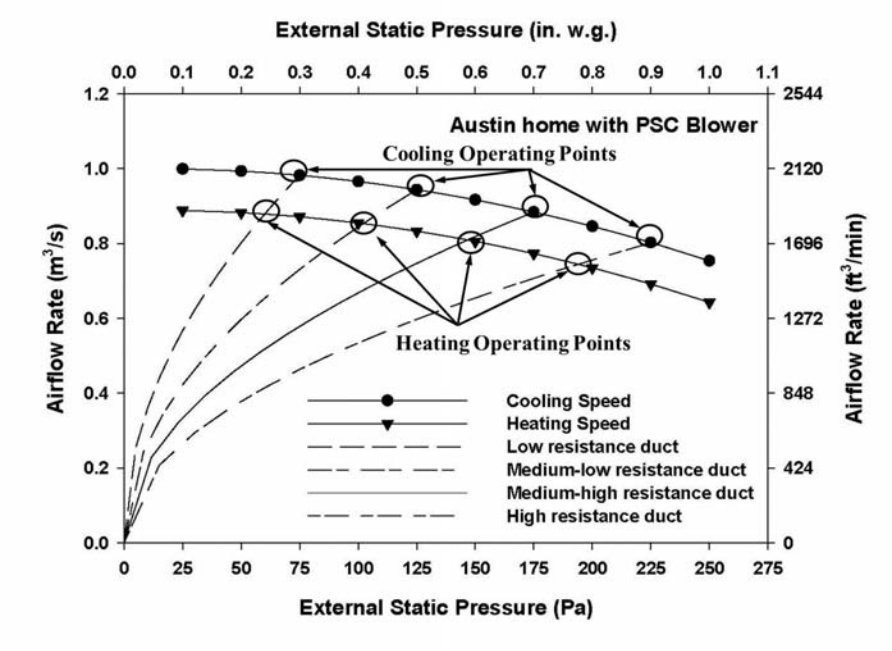

Figure 21 Example of system and fan curves interaction

Following the approach demonstrated in Figure 21, eight operating points were determined for each of the Chicago and Austin homes respectively with combinations of two blower types (i.e., PSC and ECM blowers) and four duct flow resistances (i.e., low, medium-low, medium-high, and high). At each point, the duct pressure, airflow rate, and

blower power were estimated. Also, blower overall efficiencies that are required by EnergyPlus (LBNL 2013a) for the modeling of blower power performance were calculated by using Equation (4) along with the results of duct pressure, airflow rate, and blower power at each operating point. Table 17 shows the performance of PSC and ECM blowers at each operating point that were used in the simulations. In addition, the standby power was assumed to be 5 W for PSC blowers and 9 W for ECM blowers.

The blower performance data in Table 17 were input into EnergyPlus (LBNL 2013a) for the simulation of PSC and ECM blowers at various duct flow resistances. Moreover, the knowledge of actual airflow rate enabled the calculation of actual cooling performance at each operating point, which is calculated from the rated data in conjunction with the developed empirical curves according to Equations (15) to (17).

Table 17 Blower performance data at each operating point

Home	Type	Duct flow resistance	Performance data							
			Cooling mode				Heating mode			
			Duct pressure, in. w.g. (Pa)	Airflow, ft^3/min (m^3/s)	Power, W	η %	Duct pressure, in. w.g. (Pa)	Airflow, ft^3/min (m^3/s)	Power, W	η %
Austin, TX	PSC	Low	0.3 (75)	2077 (0.98)	1097	6.7	0.24 (60)	1865 (0.88)	992	5.3
		Medium low	0.5 (125)	1992 (0.94)	1035	11.4	0.41 (102)	1801 (0.85)	940	9.3
		Medium high	0.7 (175)	1865 (0.88)	980	15.8	0.59 (147)	1716 (0.81)	889	13.4
		High	0.9 (225)	1695 (0.80)	925	19.5	0.78 (194)	1568 (0.74)	835	17.3
	ECM	Low	0.3 (75)	1992 (0.94)	447	15.8	0.26 (64)	1843 (0.87)	396	14.2
		Medium low	0.5 (125)	1992 (0.94)	545	21.7	0.43 (108)	1865 (0.88)	475	19.9
		Medium high	0.7 (175)	1992 (0.94)	639	25.8	0.61 (151)	1865 (0.88)	552	24.0
		High	0.9 (225)	1992 (0.94)	727	28.9	0.77 (193)	1843 (0.87)	623	27.0
Chicago, IL	PSC	Low	0.3 (75)	1674 (0.79)	853	7.0	0.23 (57)	1483 (0.7)	762	5.2
		Medium low	0.5 (125)	1610 (0.76)	796	11.9	0.4 (100)	1420 (0.67)	715	9.4
		Medium high	0.7 (175)	1483 (0.7)	741	16.4	0.58 (145)	1335 (0.63)	666	13.7
		High	0.9 (225)	1293 (0.61)	681	20.3	0.77 (192)	1208 (0.57)	611	17.8
	ECM	Low	0.3 (75)	1589 (0.75)	326	17.3	0.26 (65)	1483 (0.7)	288	15.8
		Medium low	0.5 (125)	1589 (0.75)	404	23.4	0.43 (108)	1483 (0.7)	351	21.6
		Medium high	0.7 (175)	1589 (0.75)	479	27.5	0.61 (152)	1483 (0.7)	413	25.8
		High	0.9 (225)	1589 (0.75)	549	30.6	0.79 (197)	1483 (0.7)	474	29.0

3.4.4 Simulation Results

By integrating the performance models of blowers and air conditioners with the established building models, a total of 16 simulations were conducted using EnergyPlus

(LBNL 2013a) to predict the annual heating and cooling energy use in the Chicago and Austin homes for various combinations of blower types and duct flow resistances. Table 18 shows the number of variations in each key parameter and the total number of accomplished simulation runs. The energy impact of duct flow resistance was evaluated in terms of the electricity consumptions of indoor blowers and condensing units, along with natural gas consumptions of furnaces. For the purpose of comparisons, the simulation results of the low-flow resistance ductwork were used as a baseline scenario, and then changes at other conditions of flow resistance relative to the results at the low-flow resistance were determined.

Table 18 Variations in key parameters and number of simulation runs

Parameter	Description	Number of variations
Blower type	PSC and ECM blowers	2
Duct flow resistance	Low, medium-low, medium-high, and high	4
Location	Austin, TX and Chicago, IL	2
Total number of simulation runs		16

3.4.4.1 Blower Electricity Consumption

The energy impact of duct flow resistance varies with blower types, namely PSC and ECM blowers. Table 19 summarizes the annual blower electricity consumptions in the standby, cooling, and heating modes at different levels of duct flow resistance for the Austin home and the Chicago home. On account of differing local climates, the blower electricity consumptions in the heating and cooling modes are different for the Austin

home and the Chicago home. For example, the Austin home uses a significant amount of electricity in the cooling mode, showing about 71-77% of the total annual blower electricity consumption in the cooling mode and 21-22% in the heating mode, while the Chicago home consumes more electricity in the heating mode than in the cooling mode, showing 35-41% for cooling and 56-59% for heating. It should be emphasized again that the above comparisons are for blower electricity comparisons only and do not include the energy used by other system components.

Table 19 Annual blower electricity consumptions

Location	Blower Type	Duct flow resistance	Operating Mode			
			Standby, kWh	Cooling, kWh	Heating, kWh	Total, kWh
Austin, TX	PSC	Low*	34.4	1572	440.4	2046.8
		Medium low	34.4 (-0.1%)	1497.5 (-4.7%)	420.5 (-4.5%)	1952.4 (-4.6%)
		Medium high	34.2 (-0.4%)	1442.1 (-8.3%)	400.6 (-9.0%)	1876.9 (-8.3%)
		High	33.9 (-0.9%)	1407.7 (-10.5%)	374.5 (-15.0%)	1816.1 (-11.3%)
	ECM	Low*	62.1	603.8	181.6	847.5
		Medium low	62.0 (-0.1%)	748.6 (24.0%)	216.9 (19.4%)	1027.5 (21.2%)
		Medium high	62.0 (-0.1%)	891.2 (47.6%)	251.1 (38.3%)	1204.3 (42.1%)
		High	62.0 (-0.1%)	1031.6 (70.9%)	282.3 (55.5%)	1375.9 (62.3%)
Chicago, IL	PSC	Low*	34.4	607	904.6	1545.9
		Medium low	34.2 (-0.3%)	575.7 (-5.2%)	851.0 (-5.9%)	1460.9 (-5.5%)
		Medium high	34.1 (-0.3%)	553 (-8.9%)	794.3 (-12.2%)	1381.4 (-10.6%)
		High	33.9 (-0.9%)	536.7 (-11.6%)	730.6 (-19.2%)	1301.2 (-15.8%)
	ECM	Low*	61.5	223.6	358.6	643.7
		Medium low	61.5 (0.0%)	278.2 (24.4%)	436.7 (21.8%)	776.4 (20.6%)
		Medium high	61.4 (-0.1%)	331.2 (48.1%)	514.4 (43.4%)	907.1 (40.9%)
		High	61.3 (-0.2%)	381.5 (70.6%)	592.3 (65.2%)	1035.1 (60.8%)

* Baseline scenario of the low-flow resistance ductwork.

Values in parenthesis are percentage changes relative to the baseline scenario.

The energy impact of duct flow resistance on blower electricity consumptions is characterized by the percentage changes relative to the baseline results of the low-flow resistance ductwork. These percentage changes are tabulated in Table 19 and also graphically presented in Figure 22, both of which show that annual electricity consumptions of PSC and ECM blowers are distinctly different in response to increasing the duct flow resistance. Because of decreasing airflow rates, PSC blowers consume less electricity when paired with ductworks of higher flow resistances. For example, the blower electricity consumption for the Austin home is decreased by 10.5% in the cooling mode and 15.0% in the heating mode as the duct flow resistance is increased from the lowest level to the highest level, which in turn leads to an 11.3% decrease in the annual blower electricity consumption. This impact is even greater for the Chicago home, showing decreases of 11.6% in the cooling mode, 19.2% in the heating mode, and 15.8% in the annual blower electricity consumption as the duct flow resistance is increased from the lowest level to the highest level.

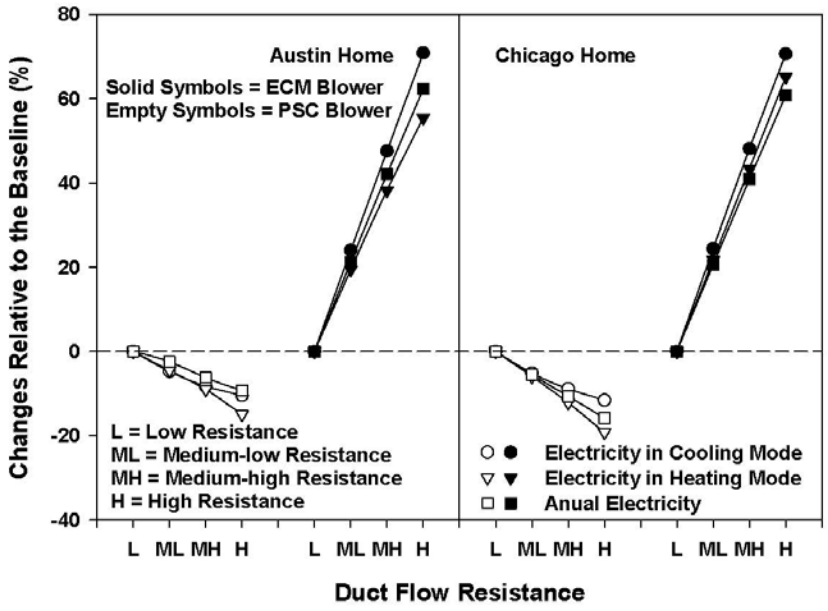

Figure 22 Percentage changes in annual blower electricity consumptions relative to the baseline

Compared with PSC blowers, the energy impact of the increasing duct flow resistance on ECM blowers is in the opposite direction, showing increases in the blower electricity consumption and of a greater magnitude. The reason for the increasing electricity use is because ECM blowers require additional power in order to maintain constant airflow rates at conditions of a higher flow resistance. For instance, the high flow resistance ductwork for the Austin home increases the blower electricity consumption by 70.9% in the cooling mode, 55.5% in the heating mode, and 62.3% in the annual consumption relative to the baseline results of the low flow resistance. A comparable incremental change due to increasing duct flow resistances is also observed for the Chicago home when paired with ECM blowers.

3.4.4.2 Condensing Unit Electricity and Natural Gas Consumptions

It is important to note that the system airflow rates vary with the duct flow resistance, which consequently has impacts on system cooling and heating energy use. In addition to blower energy consumptions analyzed in the previous section, the annual electricity consumption of condensing units and the natural gas consumption of furnaces for the Austin and Chicago homes at different levels of flow resistance are summarized in Table 20. Also, the percentage changes in electricity and natural gas consumptions relative to the baseline results of the low-flow resistance ductwork are shown in Figure 23.

Table 20 Annual consumptions of condensing unit electricity and natural gas

Location	Blower Type	Duct flow resistance	Annual energy consumption	
			Condensing unit electricity consumption, kWh	Natural gas consumption, 1000 ft^3
Austin, TX	PSC	Low*	5869.1	39.0
		Medium low	5893.3 (0.4%)	39.1 (0.2%)
		Medium high	5945.6 (1.3%)	39.2 (0.5%)
		High	6028.4 (2.7%)	39.3 (0.8%)
	ECM	Low*	5696.5	40.2
		Medium low	5724.8 (0.5%)	40.0 (-0.4%)
		Medium high	5756.5 (1.1%)	39.9 (-0.8%)
		High	5789.0 (1.6%)	39.7 (-1.2%)
Chicago, IL	PSC	Low*	2222.5	134.4
		Medium low	2243.3 (0.9%)	134.7 (0.2%)
		Medium high	2283.4 (2.7%)	134.9 (0.4%)
		High	2344 (5.5%)	135.2 (0.6%)
	ECM	Low*	2121.3	136.9
		Medium low	2130.8 (0.4%)	136.6 (-0.3%)
		Medium high	2141.5 (0.9%)	136.2 (-0.5%)
		High	2153.4 (1.5%)	135.8 (-0.8%)

* Baseline scenario of the low-flow resistance ductwork.

Values in parenthesis are percentage changes relative to the baseline scenario.

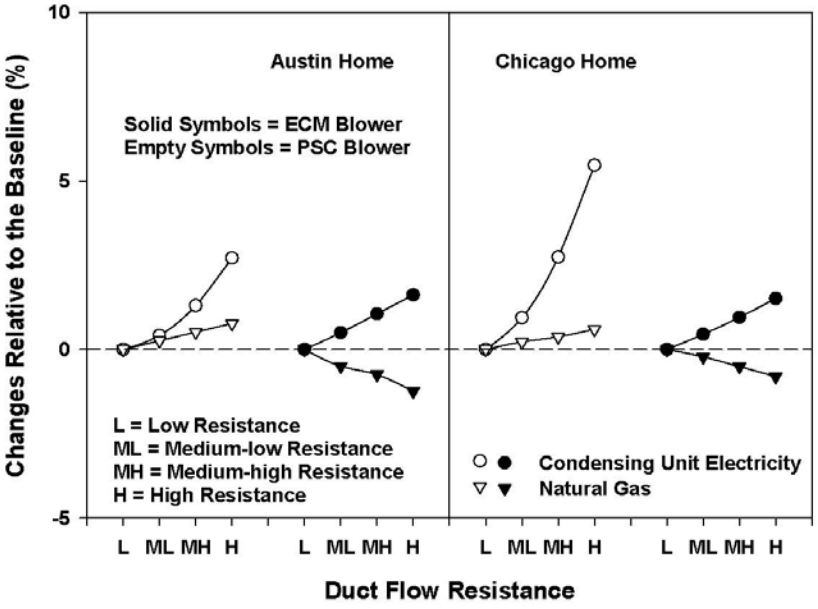

Figure 23 Percentage changes in annual consumptions of condensing unit electricity and natural gas

Both Table 20 and Figure 23 show that the percentage changes in non-blower energy consumptions caused by increasing the duct flow resistance are relatively small compared with the energy impact on blowers previously shown in Table 19 and Figure 22. As a result of increasing the duct flow resistance from the lowest level to the highest level, the condensing unit electricity consumption is increased by up to 5.5% in systems with PSC blowers and 1.6% in systems with ECM blowers. The impact of increasing the duct flow resistance is even smaller on natural gas consumptions, showing ±1.5% changes. The reason that the increasing duct flow resistance does not result in comparable system energy changes as large as blower electricity consumptions is

because the electricity use of condensing units was about 2-3 times higher than blower electricity consumptions.

In addition, Table 20 and Figure 23 reveal that increasing the duct flow resistance leads to increases in condensing unit electricity consumptions in systems with both PSC and ECM blowers but with different magnitudes. For example, because of decreases in cooling capacities that are caused by reduced airflow rates, the condensing unit electricity consumptions in systems with PSC blowers is consistently increased by up to 2.7% for the Austin home and 5.5% for the Chicago home in response to ductworks with increasing flow resistances. The corresponding increases in systems with ECM blowers are less dramatic due to the capability of ECM blowers to maintain a constant airflow rate over a pressure range, showing up to 1.6% increase for the Austin home and 1.5% increase for the Chicago home. The incremental changes in systems with ECM blowers are mainly caused by increased blower electricity consumptions responding to higher flow-resistance ductworks, which imposes an additional cooling load to systems and consequently leads to increases in condensing unit electricity consumptions.

The impacts of duct flow resistance on natural gas consumptions are different for systems with PSC and ECM blowers. For example, Table 20 and Figure 23 show that in systems with PSC blowers the natural gas consumption is increased by up to 0.8% for the Austin home and 0.6% for the Chicago home as a result of increasing the duct flow resistance. These incremental changes are consequences of decreased blower electricity consumptions in the heating mode shown in Table 19 and Figure 22, which leads to less

heat gains from PSC blowers. Therefore, in order to satisfy a constant heating load, additional natural gas is consumed for the compensation of decreased blower heat gains. However, in systems with ECM blowers, the natural gas consumption is consistently decreased by up to 1.2% for the Austin home and 0.8% for the Chicago home when paired with ductworks of a higher flow resistance, as shown in Table 20 and Figure 23. Unlike PSC blowers, the electricity consumption of ECM blowers in the heating mode is increased by 55% for the Austin home and 65% for the Chicago home as a result of a higher flow resistance, which consequently leads to an increased motor heat gain. With a constant heating load, this increased motor heat gain tends to offset the natural gas consumption.

3.4.4.3 Electricity Savings in Systems with ECM Blowers

Another observation from the tabulated results in Table 19 and Table 20 is that systems with ECM blowers have less electricity consumptions compared to systems with PSC blowers at the same level of duct flow resistance. In order to quantify the impact of duct flow resistance on this electricity savings, the savings from blowers and condensing units, along with the total system electricity savings, when using ECM blowers compared to using PSC blowers were determined and summarized in Table 21,. In addition to the results presented in Table 21, the electricity savings with respect to the duct flow resistance are plotted in Figure 24.

Table 21 Annual electricity savings in systems with ECM blowers

Location	Duct flow resistance	Annual electricity savings relative to systems with PSC blowers						
		Blower		Condensing Unit		Total		Percentage savings from blowers
		kWh	%	kWh	%	kWh	%	%
Austin, TX	Low	1199.3	58.6	172.6	2.9	1371.9	17.3	87.4
	Medium low	924.9	47.4	168.5	2.9	1093.4	13.9	84.6
	Medium high	672.6	35.8	189.1	3.2	861.7	11.0	78.1
	High	440.2	24.2	239.4	4.0	679.6	8.7	64.8
Chicago, IL	Low	902.2	58.4	101.2	4.6	1003.4	26.6	89.9
	Medium low	684.5	46.9	112.5	5.0	797	21.5	85.9
	Medium high	474.4	34.3	141.9	6.2	616.3	16.8	77.0
	High	266.1	20.5	190.6	8.1	456.7	12.5	58.3

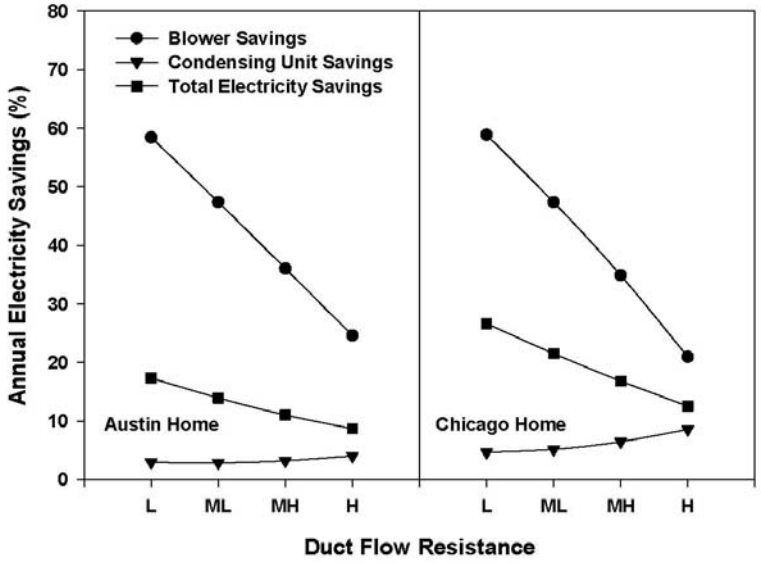

Figure 24 Annual electricity savings in systems with ECM blowers relative to systems with PSC blowers

Both Table 21 and Figure 24 show that the electricity savings from systems with ECM blowers compared to systems with PSC blowers vary with the duct flow

resistance. Although the savings from condensing units tends to increase for higher flow-resistance ductworks, the blower and total electricity savings is decreased with the increasing duct flow resistance. For example, at the condition of low flow resistance, ECM blowers in both homes use approximately 60% less electricity than PSC blowers, with blower electricity savings of 1199.3 kWh for the Austin home and 902.2 kWh for the Chicago home. However, increases in the duct flow resistance dramatically decrease this 60% savings potential because of the decreased electricity consumption of PSC blowers as their airflow rates decrease and the increased electricity consumption of ECM blowers as it maintains constant airflow rates. When the duct flow resistance is increased from the lowest to the highest level, the savings potential of ECM blowers relative to PSC blowers diminishes from 58.6% to 24.2% for the Austin home with blower electricity savings of 440.2 kWh and from 58.4% to 20.5% for the Chicago home with blower electricity savings of 266.1 kWh. Consequently, total system savings for ECM blowers decreases from 17.3% to 8.7% for the Austin home and from 26.6% to 12.5% for the Chicago home, which is the result of 60 to 90% of the total electricity savings being from ECM blower operations. In addition, at the same level of duct flow resistance, the use of ECM blowers is more effective for the Chicago home than for the Austin home based on a higher percentage savings in the total electricity consumptions.

3.5 Conclusions

In this study, the impact of duct flow resistance on residential heating and cooling energy use was investigated by using laboratory experiments and building

energy simulations. As a first step, the cooling performance of a unitary air conditioner was measured and evaluated over an airflow range of 1000 to 2250 ft^3/min (0.47 to 1.06 m^3/s), and then the experimental results were integrated with public-domain building simulation models, along with airflow and efficiency data for PSC and ECM blowers. A total of 16 simulations were conducted for various combinations of blower types, duct flow resistances, and locations, followed by a detailed result comparison of the flow resistance impact on electricity and natural gas consumptions in systems with PSC and ECM blowers in the climates of Austin, TX and Chicago, IL. As a result of increasing duct flow resistances from the lowest level to the highest level, simulation results show that

- The electricity consumption of PSC blowers decreased by 11% for the Austin home and 16% for the Chicago home due to airflow decreases, while the electricity consumption of ECM blowers increased by 62% for the Austin home and 61% for the Chicago home as ECM blowers maintain airflow rates.
- Electricity consumptions of condensing units in systems with PSC blowers increased by 2.7% for the Austin home and 5.5% for the Chicago home, while the electricity increase in systems with ECM blowers were less dramatic, being 1.6% for the Austin home and 1.5% for the Chicago home.
- Natural gas consumptions increased by 0.6-0.8% in systems with PSC blowers and decreased by 0.8-1.2% in systems with ECM blowers, mainly because in the latter case the increase in blower electricity consumptions contributed to space heating, then offsetting the natural gas consumption.

- Total electricity savings in systems with ECM blowers relative to systems with PSC blowers dramatically decreased from 17.3% to 8.7% for the Austin home and 26.6% to 12.5% for the Chicago home.
- Results also indicate that 60 to 90% of the total electricity savings in systems with ECM blowers relative to the systems with PSC blowers were from ECM blower operations with the rest from condensing unit operations.
- Moreover, the use of ECM blowers was more effective in the Chicago home in terms of a higher percentage savings in electricity consumptions compared to the Austin home at the same duct flow resistance in this simulation study.

In summary, this study quantified the impact of duct flow resistance on residential heating and cooling energy consumptions in two different climate regions. The results provide further understanding of how the excess duct flow resistance affects the residential space heating and cooling energy consumptions. In addition, the results can also be used for the development of cost-effective designs for residential central air distribution systems.

4. ENERGY IMPACT AND LIFE CYCLE COSTS OF DUCT DESIGNS FOR RESIDENTIAL CENTRAL HVAC SYSTEMS WITH PSC AND ECM BLOWERS

4.1 Overview

The purpose of this study is to comprehensively evaluate energy impacts and life cycle costs of duct designs for residential central HVAC systems. Based on two contrasting climate conditions, namely climates in Chicago, IL and Austin, TX, building energy simulations were performed to predict the heating and cooling energy use in systems with PSC and ECM blowers that were paired with ductworks of varying flow resistances and duct materials. In addition to the energy use, the life cycle cost of each duct design was determined over a 15-year lifetime. Depending on the specific duct design, the annual energy costs in the Chicago home increased by 12-20% for systems with ECM blowers and 3-9% for systems with PSC blowers as the flow resistance increased from 0.3 to 0.8 in. w.g. (75 to 200 Pa). In the Austin home for the same flow resistance increases, the annual energy costs increased by 19-22% for systems with ECM blowers and 7-9% for systems with PSC blowers. Although the cost-effectiveness of a specific duct design is shown to be heavily dependent on initial duct fabrication and installation costs, the use of lower flow resistance ductworks generally leads to lifetime savings in the presence of supply and return leakages of 10%. Specifically, the lifetime savings is achieved in 6 out of 8 simulated cases for the Chicago home and all of the simulated cases for the Austin home.

4.2 Introduction

Blowers with electronically commuted motors (ECMs) have recently gained increased usage in residential air handling units (AHUs) because of the potential for electricity savings over the more traditional permanent split capacitor (PSC) motors. For example, Sachs and Smith (2004) demonstrated that ECM blowers were capable of reducing the annual electricity consumption by 67 to 82% compared with PSC blowers based on the comparison of Average Annual Auxiliary Electrical Energy Consumption (E_{AE}) for 107 furnaces with capacities varying from 26 to 130 KBtu/hr (7.6 to 38.1 kW). Following the same approach, Kendall (2004) estimated blower electricity savings of 38 to 42% for single-stage furnaces and 63 to 67% for two-stage furnaces as a result of using ECM blowers.

The blower electricity savings indicated by these reported results are based on the blower operation at ideal duct pressures ranging from 0.18 to 0.33 in. w.g. (45 to 82 Pa) (ASHRAE 2007c); however, much of the benefits of using ECM blowers is lost in undersized duct systems with excess flow resistances (Ueno 2010), which are common in real-world installations. For instance, Walker (2008) compared the power performance of one PSC and one ECM blower over a range of pressures and blower speeds in a laboratory environment and showed that at an external static pressure of 0.2 in. w.g. (50 Pa), which is representative of ideal ducting, the ECM blower consumed 60% less power in the cooling mode and 45% less power in the heating mode relative to the PSC blower. Unfortunately, this savings substantially decreased at a higher external static pressure of 0.5 in. w.g. (125 Pa), which represents typical field installations.

Specifically, the 60% less power was reduced to only 8% less power in the cooling mode, and the 45% less power was reduced to 5% less power in the heating mode compared with the PSC blower. These experimental results show that the benefit of using ECM blowers is strongly tied to the proper design and installation of duct systems.

The same conclusion was also drawn by Lutz et al. (2006) and Franco et al. (2008) from their simulation studies, which compared the blower energy consumption of PSC and ECM blowers at different duct flow resistances of 0.3, 0.5, and 0.8 in. w.g. (75, 125, and 200 Pa) in 16 house locations across the United States. Their results showed that the electricity savings from ECM blowers relative to PSC blowers decreased with the increasing duct flow resistance and varied with weather conditions. For example, they reported that on a national basis, ECM blowers compared with PSC blowers consumed 45% less electricity with ducts at the low flow resistance of 0.3 in. w.g. (75 Pa), 35% less electricity at the medium flow resistance of 0.5 in. w.g. (125 Pa), and 6% less at the high flow resistance of 0.8 in. w.g. (200 Pa). As one can observe from the above studies, the advantage of electricity savings from using ECM blowers over PSC blowers decreases as the duct flow resistance is increased, meaning that ECM blower electricity savings are over-estimated because of the excess flow resistance in the real-world duct installations.

Due to combinations of restricted duct designs, inappropriate installations, dirty filters, and fouled evaporators, most real-world residential duct systems have a flow resistance ranging from 0.3 to 1.1 in. w.g. (75 to 275 Pa) with a weighted average around 0.5 in. w.g. (125 Pa) (DOE 2014). These flow resistances represented by external static

pressures are much higher than the typical laboratory testing conditions of 0.18 to 0.33 in. w.g. (45 to 82.5 Pa) for residential heating and cooling equipment performance ratings according to ASHRAE Standard 103 (ASHRAE 2007c) and AHRI 210/240 (AHRI 2008).

As discussed previously, without appropriate duct designs to limit the system flow resistance, the use of ECM blowers becomes less cost-effective compared with PSC blowers. As an example, a project of replacing PSC blowers with ECM blowers in residential air handlers conducted in North Carolina projected an economic simple payback period of approximately 31 years when ECM blowers were operating in the auto mode and 7 years in the continuous circulation mode based on the ECM blower electricity savings relative to PSC blowers (Murray and Fitzpatrick 2012). Another project that included eight homes in Syracuse, New York estimated a savings-to-investment ratio (SIR) of 0.63, which implies a negative net present value (NPV), by using the ECM blower electricity savings over an assumed 15-year lifetime as a result of replacing PSC blowers with ECM blowers (Aldrich and Williamson 2014). The economic analysis presented in both of these studies show that there may not be a justification for replacing PSC blowers with ECM blowers in real-world duct systems that have excess flow resistances. Furthermore, it can be concluded from the above studies that the use of ECM blowers is energy efficient and cost-effective only when they are paired with low-resistance ductworks. However, the duct systems with the lower flow resistance usually cost more because of the requirement for larger size ducts.

As a result, the higher duct cost may offset blower electricity savings so that there is no net savings.

The impact of duct flow resistance on residential heating and cooling energy use should be evaluated from a system standpoint. For example, the previous studies that dealt with PSC and ECM blower comparisons only focused on blower electricity consumptions without considering the energy consumption of non-blower components, such as the electricity consumption of condensing units or the natural gas consumption of furnaces. The lack of emphasis on the other components and the whole system is surprising given the fact that the energy consumption of non-blower components is 80-95% of the total energy use in a residential central HVAC system (Parker et al. 2005, Stephens et al. 2010). Again, realizing that past studies have only focused on blower electricity consumptions and neglected non-blower energy consumptions reinforces the need for a system approach for analyzing energy consumptions associated with different blower types and ducting designs.

Only recently has a study of the system energy consumption as a function of the duct flow resistance and blower types been first performed and reported by Yin et al. (Yin et al. 2014b), who investigated the effect of duct flow resistance on the energy use in a residential central HVAC system with an ECM blower by integrating experimental results with building energy simulations. The study reported by Yin et al. (2014b) showed that as a result of increasing the duct flow resistance from 0.3 to 0.9 in. w.g. (75 to 225 Pa), airflow rates decreased by 11% in the heating mode and 18% in the cooling mode. Of special importance, these airflow reductions led to an increase of 7% in the

annual condensing unit electricity consumption and 6% in the total system electricity consumption due to the combined effects of decreasing airflows and increasing blower powers. Also, in an earlier section of this report, the impact of duct flow resistance on annual electricity consumptions of blowers and condensing units was quantified and compared for systems with PSC and ECM blowers for two contrasting climates in Chicago, IL and Austin, TX, respectively. Results from this earlier section indicated that when the duct flow resistance was increased from 0.3 to 0.9 in. w.g. (75 to 225 Pa), the annual electricity consumption of condensing units in systems with PSC blowers increased by 3% for the Austin home and 6% for the Chicago home, while condensing unit electricity increases for systems with ECM blowers were less dramatic, being 1.6% for the Austin home and 1.5% for the Chicago home. In addition, the total electricity savings in systems with ECM blowers relative to systems with PSC blowers decreased from 17% to 9% for the Austin home and 27% to 13% for the Chicago home as a result of increasing the duct flow resistance from 0.3 to 0.9 in. w.g. (75 to 225 Pa). By showing that the excess duct flow resistance can affect both blowers and condensing unit electricity consumptions, the above studies confirm the necessity of investigating the impact of duct flow resistance on the energy use from a system standpoint.

The excess pressure in restrictive duct systems not only affects the performance of blowers and air conditioners, but it also increases duct leakages that widely exist in residential dwellings and have been recognized as an additional source of energy loss (Bryan and Perez 2001, Kinney 2005, Modera 2005, Boudreaux et al. 2011, Stephens et al. 2011). Because of the assumption of zero duct leakages in building energy

simulations, neither the study conducted and reported by Yin et al. (2014b) nor the analysis reported earlier considered or assessed the energy consequences of duct leakages at excess duct pressures. In fact, because the duct leakage effect was neglected, these studies may have possibly underestimated the negative effect of high flow resistance ducts as found in actual real-world ducting systems.

The study reported herein comprehensively evaluates the energy and economic impacts of duct designs for residential central HVAC systems with different blower types, namely PSC and ECM blowers, by using empirical blower models in conjunction with building energy simulations. Duct systems with three levels of flow resistance that were made from flexible ducts and sheet metal ducts were individually designed and integrated with code-compiled building models. Building energy simulations were performed in a heating-dominated (Chicago, IL) region and a cooling-dominated (Austin, TX) region in order to fully explore climate impacts. Energy losses caused by duct leakages with respect to different duct pressures were also simulated. It is understood that complex relationships exist among duct pressures, airflow rates, equipment performance, energy consumptions, and annual operating costs. Therefore, the cost-effectiveness of each duct design was assessed in terms of life cycle costs over a 15-year lifetime with considerations of both initial duct fabrication/installation costs and consequential lifetime operating costs.

4.3 Annual Energy Consumption Analysis

As the first step to determine the ductwork life cycle costs, annual energy consumptions resulted from different duct designs were predicted by using building energy simulations, along with empirical performance curves that were developed in earlier sections of this report. This section provides detailed information on the building model development, duct designs, equipment modeling, and analysis of simulation results.

4.3.1 Building Model Development

Two building models were developed to represent typical residential dwellings in the Upper Midwestern region (cold climate) and the Southern region (hot climate) of the United States. Specifically, Chicago, IL, and Austin, TX were selected as the representative locations in each region. The selection of these two regions allows us to explore the regional impacts, such as climates and local costs of labor, duct material, and energy, on designs of residential air distribution systems. Both the Chicago and the Austin homes were rectangular-shaped, single-story 1800 ft^2 (167.2 m^2) buildings with one conditioned zone and topped with an unconditioned attic. Both homes were designed with the same dimensions of 60 ft × 30 ft × 8 ft (18.3 m × 9.2 m × 2.4 m). The foundation type was an unconditioned basement for the Chicago home and slab-on-grade for the Austin home, both of which are typical building constructions in each region. Each home was also assumed to have three bedrooms with a gas furnace for heating and an air conditioner for cooling. The thermal and physical properties of building envelops,

such as exterior walls, floors, roofs, windows, doors, ceilings, attics, and underground walls, were directly adopted from the residential prototype building models developed by the Pacific Northwest National Laboratory (2015) according to 2012 International Energy Conservation Code (ICC 2011). It should be noted that the two homes are not being compared to each other in this study so there is no need for similar locations; rather it is more important to represent regional building and construction practices. Table 22 summarizes the characteristics of the Chicago and Austin homes.

Table 22 Summary of building characteristics

	Chicago home	Austin home
Climate zone	5A	2A
Floor area, ft^2 (m^2)	1800 (167.2)	1800 (167.2)
Foundation type	unconditioned basement	slab on grade
Number of bedrooms	3	3
Wall insulation, ft^2·°F·h/Btu (m^2·K/W)	20 (3.5)	13 (2.3)
Ceiling insulation, ft^2·°F·h/Btu (m^2·K/W)	49 (8.6)	38 (6.7)
Floor insulation, ft^2·°F·h/Btu (m^2·K/W)	30 (5.3)	13 (2.3)
Window U-value, Btu/h· ft^2·°F (W/m^2·K)	0.32 (1.8)	0.40 (2.3)
Window SHGC	0.4	0.25
Door U-value, Btu/h· ft^2·°F (W/m^2·K)	0.32 (1.8)	0.4 (2.3)
Underground wall insulation, ft^2·°F·h/Btu (m^2·K/W)	15 (2.6)	0
Heating and cooling temperature set point, °F (°C)	72 (22.2) for heating 75 (23.9) for cooling	72 (22.2) for heating 75 (23.9) for cooling
Single-stage gas furnace, kBtu/hr (kW)	48 (14.07) output 80% AFUE	42 (12.3) output 80% AFUE
Single-stage air conditioner, kBtu/hr (kW)	30 (8.79) , 4.01 COP SHR=0.77	36 (10.55), 4.01 COP SHR=0.77
Duct insulation, h-ft^2-F/Btu (m^2·K/W)	R8, 8.62 (1.518)	R8, 8.62 (1.518)

Infiltration, ventilation, and internal heat gains were also determined and added to the simulated buildings by using the same approach shown in Section 3.4. Parameters

and calculations used for modeling the effect of infiltration, ventilation, and internal heat gains are summarized in Table 23.

In addition, 20% of the internal heat gain was assumed to be latent load while the rest was sensible load (ASHRAE 2007a). A daily internal heat-gain profile was adopted from ASHRAE Standard 90.2 (2007a) so that the hourly heat again could be calculated by multiplying the daily overall heat gain by the corresponding fraction factor from the profile.

Table 23 Summary of parameters for infiltration, ventilation, and internal heat gains

Parameters	Parameter value		Reference
	Chicago home	Austin home	
Effective leakage area (ELA), ft^2 (m^2)	0.62 (0.058)	1.03 (0.096)	Equation (20)
Occupancy-caused infiltration, air change per hour	0.15	0.15	(ASHRAE 2007a)
Ventilation, ft^3/min (m^3/s)	48 (0.023)	48 (0.023)	Equation (21)
Internal heat gains, kBtu/day (kW)	73 (0.89)	73 (0.89)	Equation (22)

4.3.2 Duct Design and Modeling

Duct designs were performed by following the procedures described in ACCA Manual D (Rutkowski 2011). Based on extensive field duct pressure measurements reported in previous studies (Walker 2008, DOE 2014), pressures of 0.3, 0.5, and 0.8 in. w.g. (75, 125, and 200 Pa) were used as design pressures to represent ductworks with low, medium, and high flow resistances, respectively. It should be noted that these pressures are total external static pressures (ESPs) at the blower outlet, including

pressure drops caused by both duct and non-duct components, such as air filters, cooling coils, return grilles, and supply registers. Available ESPs for duct designs were calculated from the total ESP by subtracting the fixed pressure drop of 0.26 in. w.g. (65 Pa) due to non-duct components (Wilcox et al. 2006, Rutkowski 2011). At each design pressure, air distribution systems made from flexible ducts and rigid sheet metal ducts were individually developed and evaluated. In systems of the same duct material, the design parameters, such as duct layouts, length of duct runs, numbers of supply registers and return grilles, remained the same, and only the duct sizes were varied. For example, systems with lower pressure drops used larger size ducts, which also resulted in larger duct surface areas and the use of more duct materials, along with higher construction and installation costs. The corresponding duct design pressures and duct surface areas are summarized in Table 24.

Table 24 Surface areas of designed ductwork

Material	Blower Type	Flow resistance in. w.g. (Pa)	Total duct surface area ft^2 (m^2)	
			Chicago home	Austin home
Flexible	PSC blower	0.3 (75)	1126 (105)	1199 (111)
		0.5 (125)	814 (76)	819 (76)
		0.8 (200)	581 (54)	686 (64)
	ECM blower	0.3 (75)	1034 (96)	1136 (106)
		0.5 (125)	817 (76)	882 (82)
		0.8 (200)	683 (63)	723 (67)
Sheet metal	PSC blower	0.3 (75)	868 (81)	1030 (96)
		0.5 (125)	602 (56)	665 (62)
		0.8 (200)	521 (48)	525 (49)
	ECM blower	0.3 (75)	864 (80)	867 (81)
		0.5 (125)	602 (56)	670 (62)
		0.8 (200)	521 (48)	580 (54)

Duct leakages were simulated by using the airflow network model (Gu 2007) in EnergyPlus (LBNL 2013a) so that the energy impact of duct leakages could be predicted. Duct leakages were simulated as a function of the effective leakage ratio and the differential pressure from the duct interior to the exterior (LBNL 2014), as shown in Equation (24).

$$\dot{Q}_L = r_L \cdot \dot{Q}_{max} \cdot \rho \cdot \left(\frac{\Delta P_s}{\Delta P_{sr}}\right)^{0.65} \quad (24)$$

The effective leakage ratio (r_L) is defined as the ratio of the leakage airflow rate to the total system airflow rate at a reference differential pressure of 0.1 in. w.g. (25 Pa). In this study, an effective leakage ratio of r_L=0.1 was used for duct leakage modeling on both supply and return sides. It should be noted that the actual duct leakage is dependent on duct differential pressures, meaning that as the actual duct differential pressure deviates from the reference condition of 0.1 in. w.g. (25 Pa), the actual duct leakage also varies accordingly.

4.3.3 Equipment Modeling

Blowers with nominal airflow rates of 1000 and 1200 ft^3/min (0.49 and 0.57 m^3/s) were selected for the Chicago home and the Austin home, respectively, so that the blowers would be compatible with the pre-sized heating and cooling equipment. At each location, both PSC and ECM blowers with the same nominal airflow rate were chosen. Therefore, a total of four blowers with combinations of two nominal airflow rates and two motor types were utilized in this study.

The accurate performance representations of PSC and ECM blowers with respect to pressure changes are critical to investigate the energy impact of duct flow resistance. In this study, the airflow rates and overall efficiencies of PSC and ECM blowers over a pressure range of 0.1 to 1.2 in. w.g. (25 to 300 Pa) were characterized by using the empirical models and performance curves developed in Section 2 of this report, which are shown in Figure 25 and Figure 26. The operating points, representing actual airflow rates and overall efficiencies when blowers are connected to a specific duct design, were determined from these performance curves at the design duct flow resistance of 0.3, 0.5, and 0.8 in. w.g. (75, 125, and 200 Pa). Table 25 summarizes the airflow and overall efficiency at each operating point.

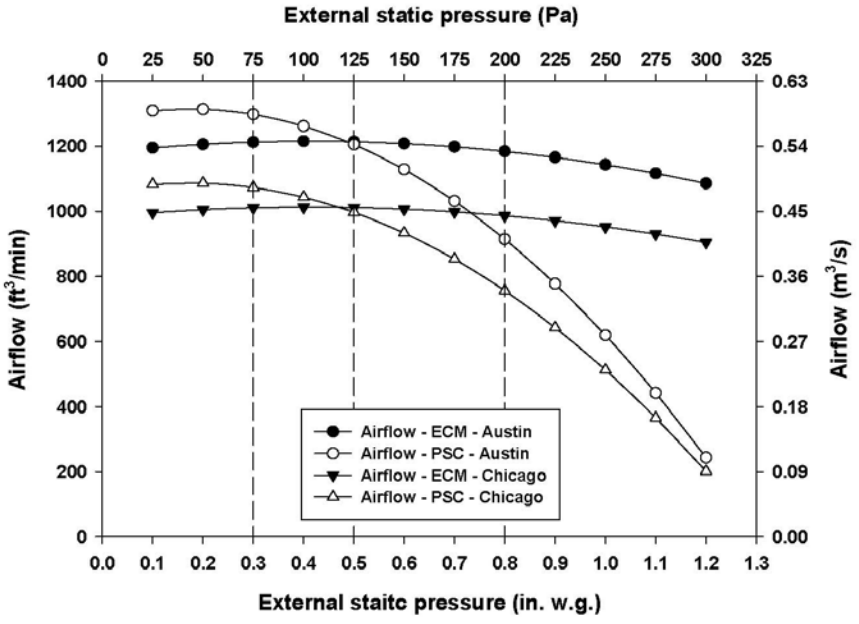

Figure 25 Blower airflow curves as a function of pressures

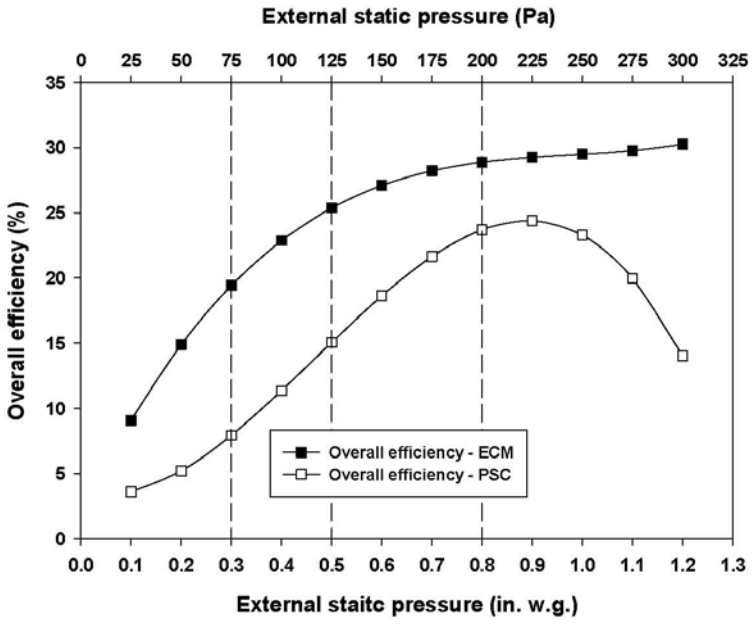

Figure 26 Blower efficiency curves as a function of pressures

Table 25 Airflow rate and overall efficiency at each operating point

Home Location	Blower Type	Duct flow resistance in. w.g. (Pa)	Airflow rate ft^3/min (m^3/s)	Overall efficiency %
Chicago home	PSC blower	0.3 (75)	1074 (0.51)	7.9
		0.5 (125)	997 (0.47)	15.1
		0.8 (200)	757 (0.36)	23.7
	ECM blower	0.3 (75)	1011 (0.48)	19.4
		0.5 (125)	1012 (0.48)	25.4
		0.8 (200)	987 (0.47)	28.9
Austin home	PSC blower	0.3 (75)	1298 (0.61)	7.9
		0.5 (125)	1206 (0.57)	15.1
		0.8 (200)	915 (0.43)	23.7
	ECM blower	0.3 (75)	1213 (0.57)	19.4
		0.5 (125)	1214 (0.57)	25.4
		0.8 (200)	1184 (0.56)	28.9

As discussed earlier, in addition to impacting the blower performance, the duct flow resistance also affects both air conditioner cooling capacities and operating efficiencies because of their dependency on evaporator airflow rates. In order to capture the airflow impact on the cooling performance, the same group of empirical curves as developed and used in Section 3 of this dissertation were used herein, as was shown in Equations (18) and (19) along with the tabulated coefficients in Table 12 and Table 13. This group of empirical performance curves, namely cooling capacity, energy input ratio, and sensible heat ratio (SHR) as functions of flow fractions (FFs) and temperatures, accounts for variations in evaporator and condenser heat exchanger performance under varying environmental and building conditions.

Both the Chicago home and Austin home used single-stage gas furnaces for space heating with a constant annual fuel utilization efficiency (AFUE) of 80%, which was assumed to be independent of variations in airflow rates.

4.3.4 Simulation Results

A group of parameters obtained from duct designs and equipment modeling (e.g., surface areas, effective leakage ratios, overall duct thermal resistances, flow resistance of duct designs, airflow rates and overall efficiencies of blowers) as well as air conditioner empirical performance curves was integrated with established building models to predict annual energy consumptions at different combined conditions of duct flow resistance and blower types. A total of 24 simulations were conducted by using EnergyPlus (LBNL 2013a) with the TMY3 weather file of Austin, TX and Chicago, IL.

(Wilcox and Marion 2008). Table 26 shows the number of variations in each key parameter and the total number of simulation runs.

Table 26 Variations in key parameters and number of simulation runs

Parameter	Description	Number of variations
Blower type	PSC and ECM blowers	2
System flow resistance	0.3, 0.5, and 0.8 in. w.g. (75, 125, and 200 Pa)	3
Duct material	Flexible and sheet metal	2
Location	Austin, TX and Chicago, IL	2
Total number of simulation runs		24

The energy impact of duct flow resistance was characterized in terms of the electricity consumptions of blowers and condensing units along with the natural gas consumptions of furnaces. In addition, the annual energy costs at both locations were calculated by using the average local rates reported by U.S. Energy Information Administration (EIA), which are 10.3 cents /kWh of electricity and \$8.20 per 1000 ft^3 of natural gas for Illinois, and 11.36 cents/kWh of electricity and \$10.53 per 1000 ft^3 of natural gas for Texas (EIA 2014a, EIA 2014b). For the purpose of comparison, results at the low flow resistance of 0.3 in. w.g. (75 Pa) were used as the baseline scenario. The annual energy consumptions and utility costs at other conditions were determined and expressed in terms of percentage changes relative to the results at the low flow resistance of 0.3 in. w.g. (75 Pa).

Figure 27 and Figure 28 show the impacts of increasing system flow resistance on energy consumptions and annual costs in the presence of 10% duct leakages for the Chicago and Austin homes, respectively. In addition to Figure 27 and Figure 28, simulation results of energy consumptions categorized by blowers, condensing units, and furnaces are tabulated in Table 27, along with annual energy costs and percentage changes relative to the baseline results at the low flow resistance of 0.3 in. w.g. (75 Pa).

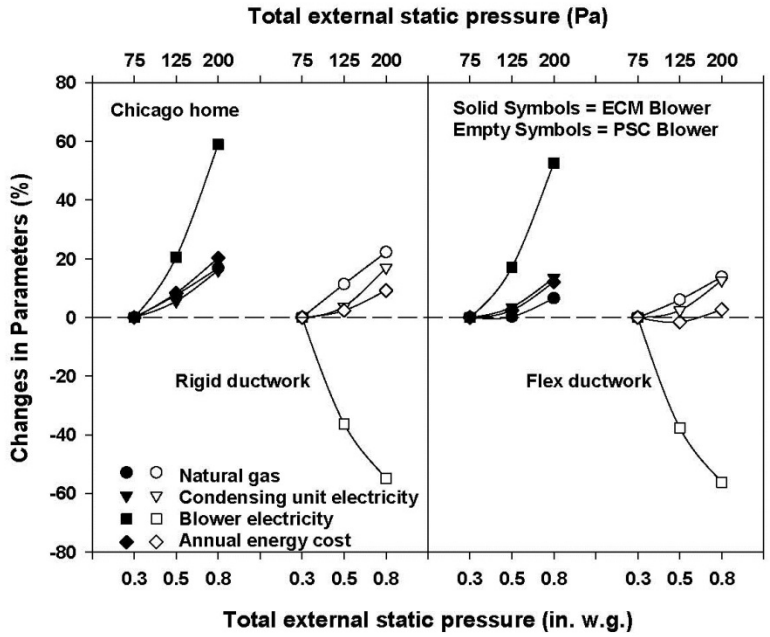

Figure 27 Parameter changes for the Chicago home with duct leakages

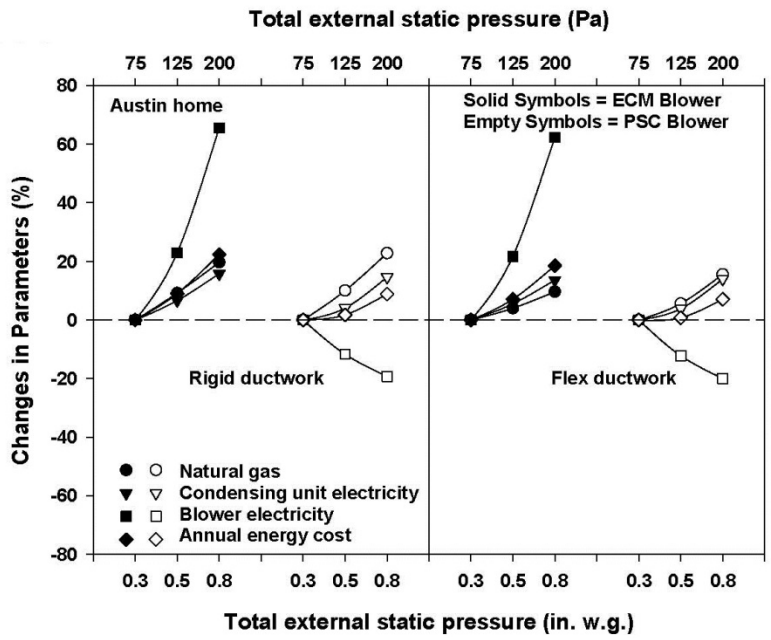

Figure 28 Parameter changes for the Austin home with duct leakages

Table 27 Annual energy consumption and cost resulting from varying ductworks

Location	Blower type	Duct material	Duct flow resistance, in. w.g. (Pa)	Annual energy consumption and cost			
				Blower electricity, kW	Condensing electricity, kW	Natural gas, 1000 ft^3	Annual cost, USD
Chicago home	ECM	Sheet metal	0.3 (75)*	573	1464	58	681
			0.5 (125)	691 (21%)	1545 (6%)	62 (8%)	738 (8%)
			0.8 (200)	911 (59%)	1699 (16%)	67 (17%)	820 (20%)
		Flex	0.3 (75)*	580	1509	58	693
			0.5 (125)	679 (17%)	1563 (4%)	58 (1%)	710 (2%)
			0.8 (200)	885 (53%)	1714 (14%)	62 (7%)	777 (12%)
	PSC	Sheet metal	0.3 (75)*	1089	1502	56	725
			0.5 (125)	694 (-36%)	1558 (4%)	62 (11%)	742 (2%)
			0.8 (200)	491 (-55%)	1756 (17%)	68 (22%)	792 (9%)
		Flex	0.3 (75)*	1096	1542	55	727
			0.5 (125)	682 (-38%)	1580 (2%)	59 (6%)	716 (-2%)
			0.8 (200)	480 (-56%)	1738 (13%)	63 (14%)	746 (3%)
Austin home	ECM	Sheet metal	0.3 (75)*	672	3929	13	654
			0.5 (125)	826 (23%)	4189 (7%)	14 (9%)	714 (9%)
			0.8 (200)	1112 (66%)	4549 (16%)	15 (20%)	801 (22%)
		Flex	0.3 (75)*	678	4012	12	662
			0.5 (125)	826 (22%)	4233 (6%)	13 (4%)	709 (7%)
			0.8 (200)	1102 (62%)	4559 (14%)	13 (10%)	785 (19%)
	PSC	Sheet metal	0.3 (75)*	1399	4123	12	755
			0.5 (125)	1235 (-12%)	4290 (4%)	13 (10%)	769 (2%)
			0.8 (200)	1129 (-19%)	4725 (15%)	15 (23%)	822 (9%)
		Flex	0.3 (75)*	1404	4160	12	757
			0.5 (125)	1232 (-12%)	4319 (4%)	12 (6%)	762 (1%)
			0.8 (200)	1122 (-20%)	4741 (14%)	14 (16%)	810 (7%)

* Baseline scenario at the flow resistance of 0.3 in. w.g. (75 Pa).
Values in parenthesis are percentage changes relative to the baseline for the same blower type and duct material.

Table 27 indicates that the energy cost of blowers, condensing units, and furnaces contribute differently to the annual energy cost. For example, 63 to 71% of the annual energy cost for the Chicago home is from the furnace natural gas consumption because of the heating-dominated climate. The electricity consumption of condensing units in the Chicago home accounts for 24 to 26% of the annual energy cost, while the blower electricity consumption is only 7 to 17% of the annual energy cost depending on specific ductworks and blower types. However, for the Austin home, the largest portion

of the annual energy cost, namely 62 to 69%, is from the electricity consumption of condensing units because of the cooling-dominated climate, followed by the furnace natural gas consumption and the blower electricity consumption, which are 16 to 20% and 12 to 20%, respectively. The above analysis shows that local climates have a significant impact on the space heating and cooling energy use, which in turn influences the cost-effectiveness of duct designs.

It can also be observed from Figure 27 and Figure 28 along with Table 27 that the annual energy consumptions (i.e., electricity and natural gas) and costs at both locations increase in systems with ECM blowers as the system flow resistance is increased from 0.3 to 0.8 in. w.g. (75 to 200 Pa). For example, compared with the baseline results at the low flow resistance of 0.3 in. w.g. (75 Pa), the use of sheet metal ductwork at the high flow resistance of 0.8 in. w.g. (200 Pa) in the Chicago home increases the blower electricity consumption by 59%, the condensing unit electricity consumption by 16%, and the natural gas consumption by 17%. The corresponding energy consequences for the Austin home are increases of 66% in the blower electricity consumption, 16% in the condensing unit electricity consumption, and 20% in the natural gas consumption. Even more importantly, the annual energy cost increases by 20% for the Chicago home and 22% for the Austin home as the duct flow resistance is increased from 0.3 in. w.g. (75 Pa) to 0.8 in. w.g. (200 Pa). As can be seen in Table 27, increases in annual energy consumptions and costs of a similar magnitude also occur in systems using flexible ductworks as the flow resistance is increased from 0.3 to 0.8 in. w.g. (75 to 200 Pa).

For systems with PSC blowers, the increasing duct flow resistance decreases the blower electricity consumption, which is the result of decreasing airflows, while it increases both the condensing unit electricity consumption and the natural gas consumption. For instance, relative to the baseline results at the low flow resistance of 0.3 in. w.g. (75 Pa), the blower electricity consumption decreases by 55% for the Chicago home and 19% for the Austin home as a result of using sheet metal ductworks with the high flow resistance of 0.8 in. w.g. (200 Pa). In contrast, the sheet metal ductworks at the high flow resistance of 0.8 in. w.g. (200 Pa) leads to increases of 17% in the condensing unit electricity consumption for the Chicago home and 15% for the Austin home, along with increases of 22% in the natural gas consumption for the Chicago home and 23% for the Austin home. Compared with the results at the low flow resistance of 0.3 in. w.g. (75 Pa), the annual energy cost increases by 9% for both the Chicago home and the Austin home when using sheet metal ductworks with the high flow resistance of 0.8 in. w.g. (200 Pa). Similar results of energy consumptions and annual costs are also found in systems using flexible ductworks as the flow resistance is increased.

4.4 Life Cycle Cost Analysis

The life cycle cost analysis requires assessing initial duct fabrication/installation costs and lifetime operating costs resulting from a specific duct design. The duct costs were estimated based on the results from a literature review. While the lifetime operating costs were predicted from the simulation results of annual energy costs and the

procedures in 2013 Energy Price Indices and Discount Factors for Life-Cycle Cost Analysis (Rushing et al. 2013). The cost-effectiveness of each ductwork was evaluated in terms of the life cycle cost over an assumed 15-year lifetime.

4.4.1 Determination and Analysis of Duct Fabrication and Installation Costs

The accurate estimation of duct fabrication and installation costs is critical for the life cycle cost analysis. But securing a reasonable duct cost is difficult given the fact that duct costs depend on a number of factors, such as home sizes, home layout, number of registers, location of installations, and accessibility. More importantly, labor and material costs vary greatly by geographical regions, which add more complexity in the cost estimation. In order to simplify the duct cost estimation, this study eliminates excessive duct design variables by maintaining the same duct layout and only varying duct sizes for systems with different flow resistances. Therefore, the duct surface area, which is the only difference among duct designs of the same material, is considered as the primary factor in the cost determination. After a broad literature review, the data reported by Stephens (2014) were selected, which provides fabrication/installation costs of ductworks made from flexible and sheet metal ducts by contractors in Chicago, IL and Austin, TX. After grouping these duct cost data by material and plotting them against duct surface areas, correlations between duct costs and surface areas were developed, as shown in Figure 29. By using the corresponding correlations, duct costs for various combinations of material and flow resistances were estimated for the Chicago and Austin homes as a function of duct surface areas. It should be noted that the costs of

ductworks for the Chicago home were determined by using the correlations according to the Chicago contractor, while the costs of ductworks for the Austin home were determined by using the correlations according to the Austin contractor.

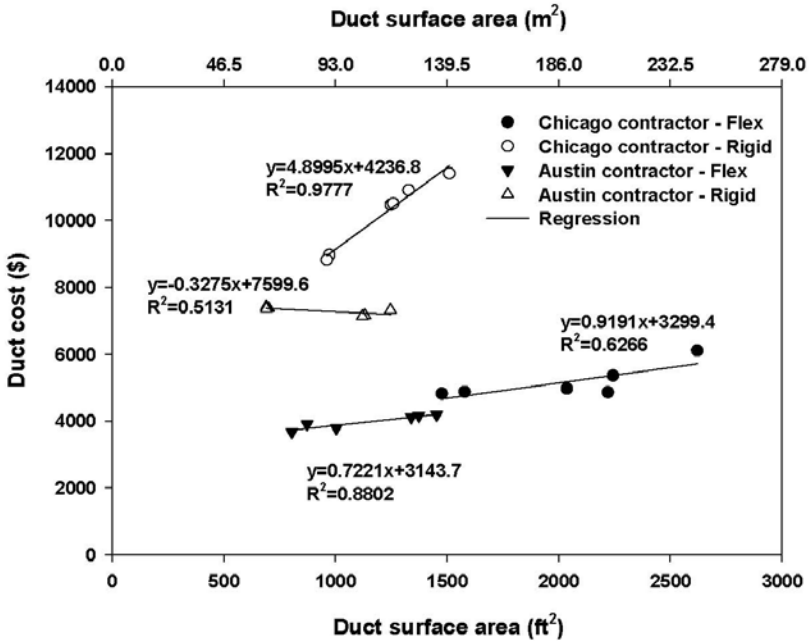

Figure 29 Estimated ductwork costs as a function of surface area

Table 28 summarizes the estimated ductwork costs for both the Chicago and Austin homes. Also, in each category of the same duct material and blower type, the premium costs, defined as differences relative to the cost of ductworks with the high flow resistance of 0.8 in. w.g. (200 Pa), are calculated and tabulated in Table 28. Results in Table 28 indicate that at the same level of flow resistance, ductworks made from rigid

sheet metal are 75-105% more expensive than flexible ductworks. For example, for the Chicago home, the cost of the sheet metal ductwork at the low flow resistance of 0.3 in. w.g. (75 Pa) is 96% higher than the flexible ductwork at the same flow resistance, with ductwork costs for the two cases being $8,488 versus $4,334.

Table 28 Ductwork costs and premium costs for the Chicago and Austin homes

Material	Blower Type	Duct flow resistance, in. w.g. (Pa)	Chicago home		Austin home	
			Ductwork costs (USD)	Premium costs (USD)	Ductwork costs (USD)	Premium costs (USD)
Flexible	PSC	0.3 (75)	4,334	500 (13%)	4,010	371 (9%)
		0.5 (125)	4,048	214 (6%)	3,735	96 (2%)
		0.8 (200)*	3,834	0	3,639	0
	ECM	0.3 (75)	4,250	322 (8%)	3,964	299 (8%)
		0.5 (125)	4,050	123 (3%)	3,781	115 (3%)
		0.8 (200)*	3,927	0	3,665	0
Sheet metal	PSC	0.3 (75)	8,488	1,698 (25%)	7,262	-166 (-2%)
		0.5 (125)	7,185	395 (6%)	7,382	-46 (-1%)
		0.8 (200)*	6,790	0	7,428	0
	ECM	0.3 (75)	8,470	1,680 (25%)	7,316	-94 (-1%)
		0.5 (125)	7,185	395 (6%)	7,380	-29 (-0.5%)
		0.8 (200)*	6,790	0	7,410	0

* Baseline scenario at the flow resistance of 0.8 in. w.g. (200 Pa).
Values in parenthesis are percentage changes relative to the baseline for the same blower type and duct material.

Based on the Chicago contractor's data, ductworks with lower flow resistances tend to have higher costs regardless of duct materials. For instance, for flexible ductworks with PSC blowers, the costs of ductworks with the flow resistance of 0.3 and 0.5 in. w.g. (75 and 125 Pa) are 13% and 5% higher respectively compared to the cost of the ductwork with the high flow resistance of 0.8 in. w.g. (200 Pa) made from the same material, which result in premium costs of $500 and $214 for ductworks with lower flow

resistances. Comparisons of sheet metal ductworks with PSC blowers yield corresponding cost increases of 25% and 6%, respectively, relative to the ductwork with the high flow resistance of 0.8 in. w.g. (200 Pa), resulting in premium costs of $1,698 and $395. Similar patterns in duct costs are also observed among ductworks for ECM blowers.

However, the trend of duct costs produced by using the Austin contractor's data is different from the trend revealed by the Chicago contractor's data. For example, the costs of flexible ductworks for PSC blowers with the flow resistances of 0.3 and 0.5 in. w.g. (75 and 125 Pa) are 10% and 3% higher respectively, compared to the cost of the flexible ductwork with the high flow resistance of 0.8 in. w.g. (200 Pa). In contrast, the costs of sheet metal ductworks for PSC blowers with the flow resistances of 0.3 and 0.5 in. w.g. (75 and 125 Pa) are 2% and 1% lower than the cost of the sheet metal ductwork with the high flow resistance of 0.8 in. w.g. (200 Pa). Similar cost variations are also observed in ductworks for ECM blowers. These variations in duct costs may be caused by varying regional labor and material expenses, which is important for evaluating the cost-effectiveness of duct designs at different locations.

4.4.2 Determination and Analysis of Lifetime Operating Costs

Lifetime operating costs due to different duct designs were determined by following the procedure outlined in 2013 Energy Price Indices and Discount Factors for Life-Cycle Cost Analysis (Rushing et al. 2013). In this procedure, the projected nominal price indices for electricity and natural gas in the residential sector from 2014 to 2043

are predicted based on the DOE energy price projections and presented in tables. The procedure also includes the effects of four alternative hypothetical rates of general price inflations: 2%, 3%, 4% and 5%. The future annual energy costs of electricity and natural gas were estimated by using the annual costs from simulations and the corresponding nominal price indices under an assumed inflation rate of 3%. Because the price indices are reported for the four Census regions (West, Midwest, Northeast and South), different price indices were applied to the Chicago and Austin homes, which took local and regional impacts on energy prices into consideration. The total operating costs over the lifespan of 15 years were converted into present values (PVs) according to Equation (25) with an assumed inflation rate of 3%.

$$PV_{total} = \sum_{n=1}^{15} \frac{Cost_n}{(1+g)^n} \tag{25}$$

The present values (PVs) of operating costs over an assumed 15-year lifetime for the Chicago and Austin homes are summarized in Table 29, which shows the results at three different levels of the duct flow resistance while considering the energy impact of duct leakages. In addition, the operating savings that results from using ductworks with lower flow resistances of 0.3 and 0.5 in. w.g. (75 and 125 Pa) relative to using ductworks with the high flow resistance of 0.8 in. w.g. (200 Pa) are calculated and tabulated in Table 29.

Table 29 Operating costs and savings resulting from different ductworks for the Chicago and Austin homes

Material	Blower Type	Duct flow resistance in. w.g. (Pa)	Chicago, IL		Austin, TX	
			Operating costs (USD)	Operating savings (USD)	Operating costs (USD)	Operating savings (USD)
Flexible	PSC blower	0.3 (75)	11,902	362 (3%)	12,016	853 (7%)
		0.5 (125)	11,746	517 (4%)	12,107	762 (6%)
		0.8 (200)*	12,263	0	12,869	0
	ECM blower	0.3 (75)	11,384	1,358 (11%)	10,523	1,944 (16%)
		0.5 (125)	11,654	1,088 (9%)	11,269	1,197 (10%)
		0.8 (200)*	12,742	0	12,467	0
Sheet metal	PSC blower	0.3 (75)	11,881	1,141 (9%)	11,997	1,069 (8%)
		0.5 (125)	12,196	826 (6%)	12,211	856 (7%)
		0.8 (200)*	13,022	0	13,067	0
	ECM blower	0.3 (75)	11,194	2,262 (17%)	10,403	2,327 (18%)
		0.5 (125)	12,128	1,328 (10%)	11,344	1,386 (11%)
		0.8 (200)*	13,456	0	12,730	0

* Baseline scenario at the flow resistance of 0.8 in. w.g. (200 Pa).
Values in parenthesis are percentage changes relative to the baseline for the same blower type and duct material.

Table 29 indicates that the use of ductworks at lower flow resistances is beneficial to 15-year operating costs as evidenced by the operating savings in all simulated cases. For example, in systems with PSC blowers for the Chicago home, the use of flexible ductworks with the lower flow resistances of 0.3 and 0.5 in. w.g. (75 and 125 Pa) leads to operating savings of $362 and $517, respectively, accounting for 3% and 4% of the 15-year operating cost resulting from using the flexible ductwork with the high flow resistance of 0.8 in. w.g. (200 Pa). The operating savings from using flexible ductworks at lower flow resistances in systems with ECM blowers for the Chicago home is even greater, with operating savings being $1,358 for the low flow resistance ductwork and $1,088 for the medium flow resistance ductwork. Generally, relative to the 15-year operating cost at the high flow resistance of 0.8 in. w.g. (200 Pa), the use of lower flow resistance ductworks results in the operating savings of 3-17% for the

Chicago home and 6-18% for the Austin home, depending on the specific duct designs and blower types.

It also can be observed from Table 29 that systems with ECM blowers for the Austin home always have lower 15-year operating costs compared to systems with PSC blowers for the same ductwork, flow resistance, and duct material. The same statement is true for the Chicago home for the two lower flow resistances of 0.3 and 0.5 in. w.g. (75 and 125 Pa), but for the high flow resistance of 0.8 in. w.g. (200 Pa), systems with PSC blowers result in lower 15-year operating costs than systems with ECM blowers. For example, the combination of a PSC blower with the flexible ductwork at the medium flow resistance of 0.5 in. w.g. results in an operating cost of $11,746, which is $92 higher than the operating cost from the same ductwork paired with an ECM blower. However, at the high flow resistance of 0.8 in. w.g. (200 Pa), the operating cost of the system with a PSC blower is $479 lower than the operating cost of the system with an ECM blower, with the operating cost being $12,263 versus $12,742. The same trends are also found in cases where sheet metal ductworks are used for the Chicago home.

4.4.3 Determination and Analysis of Life Cycle Costs

The impact of duct designs with different materials and flow resistances were evaluated for both the Chicago and Austin homes in terms of life cycle costs, which are the sum of initial duct fabrication/installation costs and present values (PVs) of operating costs over a 15-year lifetime. For the comparison purpose, the baseline scenario was the life cycle cost of ductworks at the high flow resistance of 0.8 in. w.g. (200 Pa), which

represents typical duct installations in real world (Franco et al. 2008, Walker 2008). The cost-effectiveness of ductworks at the other two lower flow resistances was determined and then expressed in terms of lifetime savings (or losses) relative to the baseline results. Table 30 summarizes life cycle costs and lifetime savings of ductworks with different flow resistances and materials. In addition, Figure 30 and Figure 31 show the lifetime savings relative to the baseline results at the high flow resistance of 0.8 in. w.g. (200 Pa) for the Chicago and Austin homes, respectively.

Table 30 Life cycle costs of ductworks for the Chicago and Austin homes

Material	Blower Type	Duct flow resistance in. w.g. (Pa)	Chicago, IL		Austin, TX	
			Life cycle costs (USD)	Lifetime savings (USD)	Life cycle costs (USD)	Lifetime savings (USD)
Flexible	PSC blower	0.3 (75)	16,236	-139 (-1%)	16,026	482 (3%)
		0.5 (125)	15,794	303 (2%)	15,843	666 (4%)
		0.8 (200)*	16,097	0	16,508	0
	ECM blower	0.3 (75)	15,634	1,035 (6%)	14,487	1,645 (10%)
		0.5 (125)	15,704	965 (5%)	15,050	1,082 (7%)
		0.8 (200)*	16,669	0	16,132	0
Sheet metal	PSC blower	0.3 (75)	20,369	-557 (-3%)	19,259	1,235 (6%)
		0.5 (125)	19,381	431 (2%)	19,593	902 (4%)
		0.8 (200)*	19,812	0	20,494	0
	ECM blower	0.3 (75)	19,664	581 (3%)	17,719	2,421 (12%)
		0.5 (125)	19,313	933 (5%)	18,725	1,415 (7%)
		0.8 (200)*	20,246	0	20,140	0

* Baseline scenario at the flow resistance of 0.8 in. w.g. (200 Pa).

Values in parenthesis are percentage changes relative to the baseline for the same blower type and duct material.

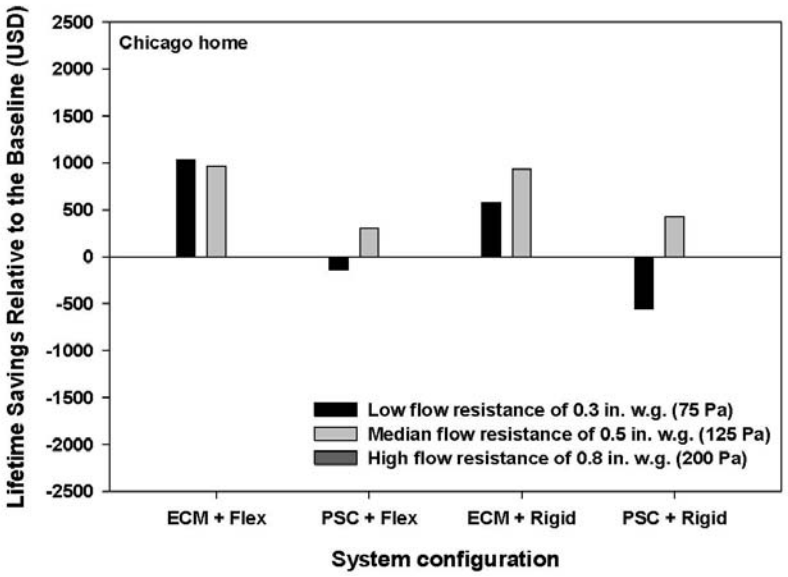

Figure 30 Lifetime savings for different ductworks in the Chicago home

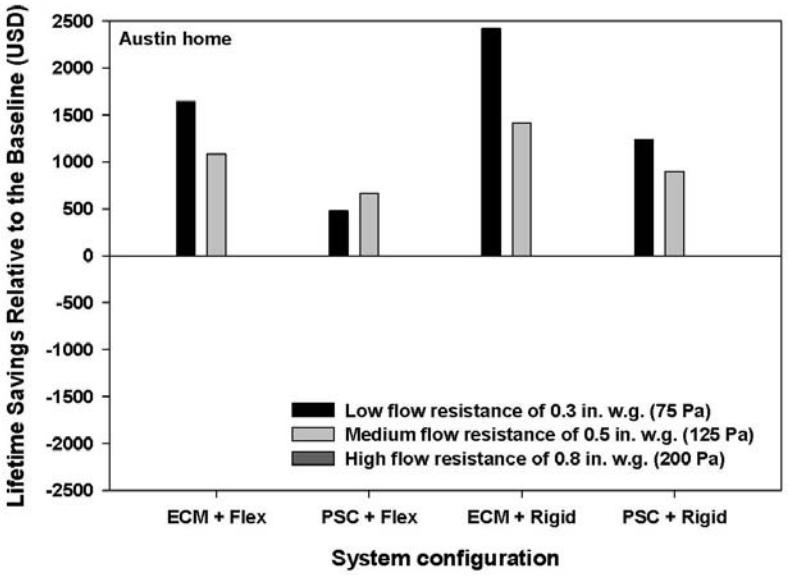

Figure 31 Lifetime savings for different ductworks in the Austin home

As shown in Figure 30 and Table 30, six out of eight simulated cases for the Chicago home result in lifetime savings, while two simulated cases result in lifetime losses. The lifetime savings range from $580 to $1030 for ductworks with the low flow resistance of 0.3 in. w.g. (75 Pa) and from $300 to $960 for ductworks with the medium flow resistance of 0.5 in. w.g. (125 Pa), depending on blower types and duct materials. The two combinations that lead to lifetime losses are the systems with PSC blowers paired with the low flow resistance ductworks of 0.3 in. w.g. (75 Pa), with a loss of $140 for the flexible ductwork and $560 for the sheet metal ductwork over a 15-year lifetime. Lifetime losses for these combinations of PSC blowers and low flow resistance ductworks are the consequences of higher premium duct costs, which are the result of larger size ducting, and relatively lower operating savings from using the low flow resistance ductworks. For instance, the cost of the flexible ductwork with the low flow resistance of 0.3 in. w.g. (75 Pa) is $500 higher than the cost of the ductwork with the high flow resistance of 0.8 in. w.g. (200 Pa) made from the same material, but the lifetime operating savings from using the low flow resistance ductwork is only $360 relative to the use of the high flow resistance ductwork. Consequently, the combination of the high premium duct cost of $500 and the relatively low savings of $360 in the operating cost results in a lifetime loss of $140 when compared with the use of high flow resistance ductwork. Similarly, for the combination of PSC blowers and the rigid ductwork, the high premium duct cost of $1,700 offsets the savings of $1,140 in the operating cost resulting from using the low flow resistance ductwork, and therefore leads to a lifetime loss of $560 relative to the use of high flow resistance ductwork.

It can also be observed from Figure 30 and Table 30 that using lower flow resistance ductworks is more cost-effective in systems with ECM blowers than that in systems with PSC blowers as evidenced by higher lifetime savings for systems with ECM blowers. For example, when paired with flexible ductworks with the medium flow resistance of 0.5 in. w.g. (125 Pa), the lifetime savings in systems with ECM blowers is $960, while the use of the same ductwork in systems with PSC blowers results in a lower lifetime savings of $300. The same comparison of sheet metal ductworks with the medium flow resistance of 0.5 in. w.g. (125 Pa) yields lifetime savings of $930 in systems with ECM blowers versus $430 in systems with PSC blowers. The higher lifetime savings from using lower flow resistance ductworks in systems with ECM blowers is primarily due to the higher operating savings in systems with ECM blowers than that in systems with PSC blowers when paired with ductworks of the same flow resistance and duct material, which can be observed in Table 29.

For the Austin home, the use of lower flow resistance ductworks leads to lifetime savings in all simulated cases, as shown in Figure 31 and Table 30. Depending on blower types and duct materials, lifetime savings vary from $480 to $2400 for the low flow resistance ductworks and from $660 to $1400 for the medium flow resistance ductworks. Again, systems with ECM blowers demonstrate higher lifetime savings than systems with PSC blowers when paired with ductworks of the same material and flow resistance. For example, when flexible ductworks are used, systems with ECM blowers have the lifetime savings of $1,645 at the low flow resistance of 0.3 in. w.g. (75 Pa) compared to the lifetime savings of $482 for PSC blowers at the same flow resistance.

Similarly, at the medium flow resistance of 0.5 in. w.g. (125 Pa), the savings for ECM blowers are $1,082 versus the lifetime savings of $482 at the same flow resistance for PSC blowers. The same conclusion is also true in cases where sheet metal ductworks are used at flow resistances of 0.3 and 0.5 in. w.g. (75 and 125 Pa), with the resulting lifetime savings being $2,421 and $1,415 for systems with ECM blowers versus $1,235 and $902 for systems with PSC blowers.

It was shown that the use of lower flow resistance ductworks brings lifetime savings in a majority of simulated cases over a 15-year lifetime, specifically six out of eight cases for the Chicago home and all cases for the Austin home. The above analysis indicates that lifetime savings are mainly dependent on premium duct costs and operating savings relative to the baseline results at the high flow resistance of 0.8 in. w.g. (200 Pa), with the operating savings for the larger ducts being greater in magnitude than the added cost of duct materials. Although the use of lower flow resistance ductworks can lead to lifetime savings in systems with both types of blowers, it is more cost-effective in systems with ECM blowers than PSC blowers as evidenced by higher lifetime savings as shown in Figure 30 and Figure 31 along with Table 30.

4.5 Sensitivity Analysis

The life cycle cost analysis in this study was based on a series of assumptions, with typical assumptions being values of cooling equipment COPs, heating equipment AFUEs, building envelop characteristics, equipment lifetime, blower performance, duct leakages and insulation levels, future energy prices, and inflation rates. Changes in any

of these assumptions may influence the final lifetime costs of duct designs. Among these assumptions, the impact of duct fabrication/installation costs is worth examining because duct costs vary significantly depending on geographic regions, designs, and materials. In addition, the analysis presented in the previous section indicates that duct costs can have a significant impact on the lifetime savings of duct designs. Therefore, a sensitivity analysis was performed in this section to analyze the impact of duct costs on duct life cycle costs.

In the previous analysis, life cycle costs and lifetime savings relative to the baseline results at the high flow resistance of 0.8 in. w.g. (200 Pa) were determined based on the local duct costs. Specifically, duct costs in the Chicago home was estimated according to the Chicago contractor, while duct costs in the Austin home was estimated according to the Austin contractor. In this section, lifetime savings over the 15-year lifetime of each duct design for the Chicago and Austin homes were estimated again by using the duct costs from both the Chicago and Austin contractors. Table 31 summarizes ductwork lifetime savings based on both Chicago and Austin contractors. In addition, the same information shown in Table 31 was plotted in in Figure 32 and Figure 33 for the Chicago home and the Austin home, respectively.

Table 31 Results of ductwork life cycle cost based on both Chicago and Austin contractors

Location	Material	Blower Type	Duct flow resistance in. w.g. (Pa)	Lifetime savings (USD) Based on the Chicago contractor	Lifetime savings (USD) Based on the Austin contractor
Chicago Home	Flexible	PSC blower	0.3	-139	-31
			0.5	303	349
			0.8	0	0
		ECM blower	0.3	1035	1105
			0.5	965	991
			0.8	0	0
	Sheet metal	PSC blower	0.3	-557	1254
			0.5	431	853
			0.8	0	0
		ECM blower	0.3	581	2374
			0.5	933	1354
			0.8	0	0
Austin Home	Flexible	PSC blower	0.3	381	482
			0.5	639	666
			0.8	0	0
		ECM blower	0.3	1563	1645
			0.5	1050	1082
			0.8	0	0
	Sheet metal	PSC blower	0.3	-1409	1235
			0.5	167	902
			0.8	0	0
		ECM blower	0.3	925	2421
			0.5	946	1415
			0.8	0	0

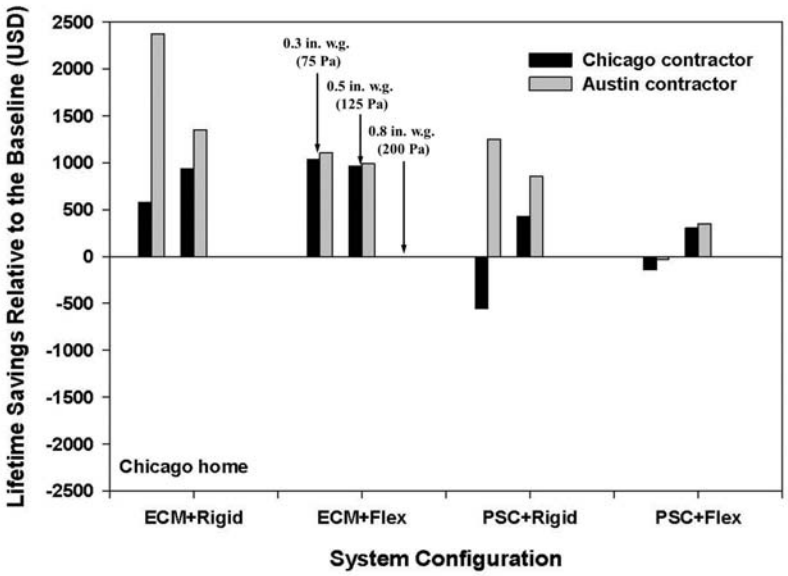

Figure 32 Lifetime savings of ductworks for the Chicago home according to both contractors

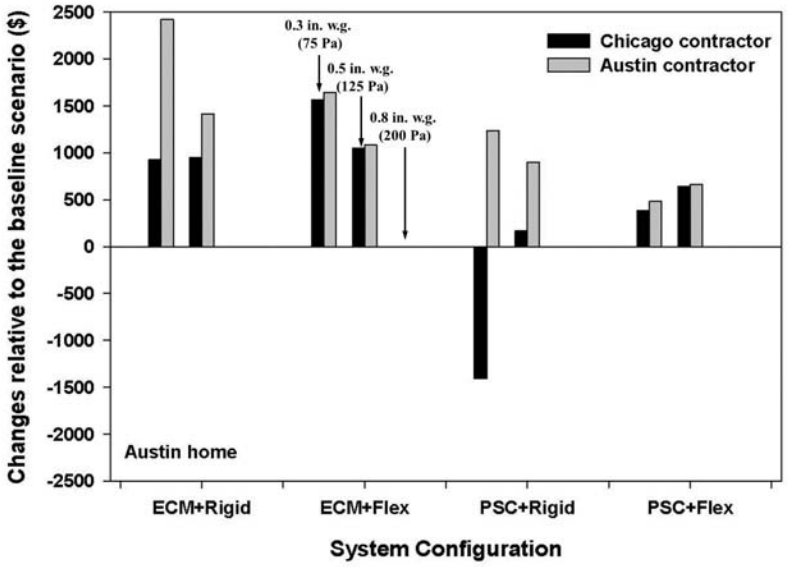

Figure 33 Lifetime savings of ductworks for the Austin home according to both contractors

Because of similar costs of flexible ductworks from both the Chicago contractor and the Austin contractor, Table 31 shows consistent results of lifetime savings in systems with flexible ductworks. For example, the combination of a PSC blower with the low flow resistance flexible ductwork for the Chicago home results in a lifetime loss of $139 based on the duct cost from the Chicago contractor. The result of negative lifetime savings remains based on the Austin contractor's duct cost, except for a lower loss of $31. However, dramatic changes in systems with sheet metal ductworks occur when different duct costs are used to calculate lifetime savings. For instance, the PSC+Rigid combination at the low flow resistance ductwork for the Chicago home results in a lifetime loss of $557 based on the duct cost from the Chicago contractor, but the same system configuration leads to lifetime savings of $1,254 based on the duct cost from the Austin contractor. The similar result is also observed for the Austin home, showing a transition from a lifetime loss of $1,409 to lifetime savings of $1,235 for the combination of PSC+Rigid when paired with the low resistance ductwork.

In addition, the amount of lifetime savings varies significantly according to the Chicago contractor and the Austin contractor. For example, by using the duct cost from the Chicago contractor, the combination of ECM+Rigid at the medium flow resistance of 0.5 in. w.g. (125 Pa) in the Chicago home leads to lifetime savings of $993. However, the lifetime savings for the same system configuration increased by 45% and becomes $1,354 based on the duct cost from the Austin contractor. Similar results are also found in other system configurations at both locations. Generally, lifetime savings based on the Austin contractor's duct costs are 3-27% higher for systems with flexible ductworks and

40-450% higher for systems with sheet metal ductworks compared with the lifetime savings according to the Chicago contractor's duct costs. These results suggest that the lifetime savings of duct designs is sensitive to the initial duct costs and can vary significantly with different contractors even for the same system configuration.

4.6 Conclusions

Excess operating pressures caused by restrictive ductworks have a great impact on energy use in residential central heating and cooling systems. These excess pressures not only affect blower airflow performance and energy consumptions, but also the cooling performance of air conditioning equipment. Excess operating pressures can also increase the duct leakage, which is a major source of energy loss that has not been thoroughly investigated in the past when evaluating the energy impact of duct designs. Therefore, in order to comprehensively assess the consequences of duct designs on both blower and non-blower energy use, a total of 24 building energy simulations was performed in this study for various combinations of duct flow resistance, blower types, duct materials, and home locations, namely a Chicago home and an Austin home. In addition, the cost-effectiveness of each duct design in the simulated cases was characterized in terms of life cycle costs over an assumed 15-year lifetime. The major findings are:

1. Compared to the use of ductworks with a low flow resistance of 0.3 in. w.g. (75 Pa), the use of ductworks with a high flow resistance of 0.8 in. w.g. (200 Pa) leads to increases in electricity consumptions of both blowers and

condensing units and natural gas consumptions of furnaces. Consequently, the annual energy costs are increased with increasing duct flow resistances. Specifically, simulation results show that annual energy costs in the Chicago home increased by 12-20% for systems with ECM blowers and 3-9% for systems with PSC blowers, depending on specific duct designs, as the flow resistance was increased from 0.3 to 0.8 in. w.g. (75 to 200 Pa). In the Austin home, the annual energy costs increased by 19-22% for systems with ECM blowers and 7-9% for systems with PSC blowers for the same flow resistance increase used in the Chicago home.

2. The use of lower flow resistance ductworks is beneficial to 15-year operating costs for both the Chicago and Austin homes. Compared to the results from the use of ductworks with the high flow resistance of 0.8 in. w.g. (200 Pa), the use of ductworks with the low flow resistance of 0.3 in. w.g. (75 Pa) for the Chicago home results in 15-year operating savings of 11-17% for systems with ECM blowers and 3-9% for systems with PSC blowers, depending on specific duct designs. The same comparison for the Austin home yields 15-year operating savings of 16-18% for systems with ECM blowers and 7-8% for systems with PSC blowers.
3. Lifetime savings over a 15-year period for all of the combinations of flow resistances, duct materials, and blower types analyzed in this study is especially important from an overall economic standpoint because it considers both operating costs and duct construction/installation costs. The

results show that lower flow resistance ductworks yield 15-year lifetime savings in 6 out of 8 simulated cases for the Chicago home and all of the simulated cases for the Austin home. For two cases in the Chicago home, the combination of high premium duct costs and relatively low consequential operating savings leads to lifetime losses relative to the use of high flow resistance ductworks.

4. Although using lower flow resistance ductworks can reduce life cycle costs for systems with both types of blowers, it is more cost-effective for systems with ECM blowers than systems with PSC blowers as evidenced by the higher lifetime savings that results from the use of lower flow resistance ductworks with ECM blowers.
5. The cost-effectiveness of a specific duct design largely depends on duct costs and can vary significantly with different contractors even for the same system configuration. Of special importance, it was found that duct construction/installation costs have a large effect on the lifetime savings over a 15-year period.

By determining the effects of blower types, duct flow resistances, and duct materials on energy consumptions and life cycle costs of duct designs, the study reported herein can facilitate the construction of residential air distribution systems with the lowest cost of ownership. In addition, the results generated herein can provide HVAC professionals with efficient, long-term, and cost-effective solutions as they face numerous tradeoffs and challenges associated with designing residential duct systems.

5. CONCLUSIONS

The ultimate goal of the study reported herein is to evaluate and compare the impact of different blowers, namely the more traditional technology of PSC blowers and the relatively new technology of ECM blowers, on energy consumptions and duct design practices for residential central heating and cooling systems by using both laboratory measurements and building energy simulations. In this study, the airflows, powers, and overall efficiencies of six PSC blowers and six ECM blowers were measured in a well-instrumented laboratory environment with a nozzle airflow chamber. In addition to experimental performance evaluations and comparative analysis, the airflow and efficiency models for both PSC blowers and ECM blowers were developed over an external static pressure range of 0.1 to 1.2 in. w.g. (25 to 300 Pa) from the statistical analysis of measured data. Besides developing the blower airflow and efficiency models, a correlation linking the air conditioner cooling performance with evaporator airflow rates was derived from laboratory experiments. Then, the performance models of blowers and air conditioners were integrated with building energy simulations to predict the system energy use, including the electricity consumptions of blowers and condensing units along with the natural gas consumptions of gas furnaces, as a result of using PSC blowers or ECM blowers at different duct flow resistances. Finally, a life cycle cost analysis of duct designs over a 15-year lifetime was performed over a range of design parameters, such as duct flow resistances, blower types, duct materials, and home locations, to comprehensively assess the energy consequences of duct designs for

residential central HVAC systems with PSC blowers and ECM blowers. The major findings are:

- The airflow performance responding to changes in the external static pressure (ESP) for PSC and ECM blowers are significantly different. Specifically, airflow rates for PSC blowers decrease as the external static pressure (ESP) is increased, while ECM blowers are able to maintain relatively constant airflow rates regardless of pressure changes.
- Power consumptions of PSC blowers decrease as the external static pressure (ESP) is increased because of the substantial airflow reductions that occur. In contrast, ECM blowers require more power to maintain airflow rates at higher flow resistances.
- The overall efficiencies of both PSC and ECM blowers increase with increasing external static pressures (ESPs). For PSC blowers, all speeds essentially have the same level of efficiencies, while ECM blowers tend to have higher efficiencies at lower speeds. In addition, for the same pressure, ECM blowers tend to have higher efficacies than PSC blowers, especially in the low pressure range.
- Among blowers with the same motor type, there are great variations in the performance of airflow, power, and efficiency with respect to changes in the external static pressure (ESP). These performance variations are because of varying designs of housings, blower wheel dimensions, airflow ranges, motor sizes, and speed control mechanisms.

- As a result of increasing the duct flow resistance from 0.3 to 0.9 in. w.g. (75 to 225 Pa), the electricity consumption of PSC blowers decreased by 11% for the Austin home and 16% for the Chicago home due to airflow decreases, while the electricity consumption of ECM blowers increased by 62% for the Austin home and 61% for the Chicago home as ECM blowers maintain airflow rates.
- For the same increase in the duct flow resistance, the electricity consumptions of condensing units in systems with PSC blowers increased by 2.7% for the Austin home and 5.5% for the Chicago home, while the electricity increase in systems with ECM blowers were less dramatic, being 1.6% for the Austin home and 1.5% for the Chicago home.
- Increasing the duct flow resistance from 0.3 to 0.9 in. w.g. (75 to 225 Pa) increased the natural gas consumptions by 0.6-0.8% in systems with PSC blowers and decreased by 0.8-1.2% in systems with ECM blowers, mainly because in the latter case the increase in blower electricity consumptions contributed to space heating, then offsetting the natural gas consumption.
- Total electricity savings in systems with ECM blowers relative to systems with PSC blowers dramatically decreased from 17.3% to 8.7% for the Austin home and 26.6% to 12.5% for the Chicago home as a result of increasing the duct flow resistance from 0.3 to 0.9 in. w.g. (75 to 225 Pa).
- Results also indicate that 60 to 90% of the total electricity savings in systems with ECM blowers relative to the systems with PSC blowers were from ECM blower operations with the rest from condensing unit operations.

- Moreover, the use of ECM blowers was more effective in the Chicago home in terms of a higher percentage savings in electricity consumptions compared to the Austin home at the same duct flow resistance in this simulation study.
- Compared to the use of ductworks with a low flow resistance of 0.3 in. w.g. (75 Pa), the use of ductworks with a high flow resistance of 0.8 in. w.g. (200 Pa) leads to increases in electricity consumptions of both blowers and condensing units and natural gas consumptions of furnaces. Consequently, the annual energy costs are increased with increasing duct flow resistances. Specifically, simulation results show that annual energy costs in the Chicago home increased by 12-20% for systems with ECM blowers and 3-9% for systems with PSC blowers, depending on specific duct designs, as the flow resistance was increased from 0.3 to 0.8 in. w.g. (75 to 200 Pa). In the Austin home, the annual energy costs increased by 19-22% for systems with ECM blowers and 7-9% for systems with PSC blowers for the same flow resistance increase used in the Chicago home.
- The use of lower flow resistance ductworks is beneficial to 15-year operating costs in both the Chicago and Austin homes. Compared to the results from the use of ductworks with the high flow resistance of 0.8 in. w.g. (200 Pa), the use of ductworks with the low flow resistance of 0.3 in. w.g. (75 Pa) in the Chicago home results in 15-year operating savings of 11-17% for systems with ECM blowers and 3-9% for systems with PSC blowers, depending specific duct designs. The same comparison in the Austin home yields 15-year operating

savings of 16-18% for systems with ECM blowers and 7-8% for systems with PSC blowers.

- Lifetime savings over a 15-year period for all of the combinations of flow resistances, duct materials, and blower types analyzed in this study is especially important from an overall economic standpoint because it considers both operating costs and duct construction/installation costs. The results show that lower flow resistance ductworks yield 15-year lifetime savings in 6 out of 8 simulated cases in the Chicago home and all of the simulated cases in the Austin home. For two cases in the Chicago home, the combination of high premium duct costs and relatively low consequential operating savings leads to lifetime losses relative to the use of high flow resistance ductworks.
- Although using lower flow resistance ductworks can reduce life cycle costs for systems with both types of blowers, it is more cost-effective for systems with ECM blowers than systems with PSC blowers as evidenced by the higher lifetime savings that results from the use of lower flow resistance ductworks with ECM blowers.
- The cost-effectiveness of a specific duct design largely depends on duct costs and can vary significantly with different contractors even for the same system configuration. Of special importance, it was found that duct construction/installation costs have a large effect on the lifetime savings over a 15-year period.

In summary, the study reported herein characterized the typical performance of PSC and ECM blowers and evaluated their impacts on energy use and duct design practices in residential central HVAC systems. The collected experimental data provide useful information for the development of rating standards to regulate electricity consumptions of PSC and ECM blowers. Of greater importance, the airflow and efficiency models reported herein provide an effective approach to predict typical PSC and ECM blower performance based on external static pressures. These models can be used by HVAC engineers for residential system designs, equipment selections, and blower performance modeling.

In addition, the results from building energy simulations determined the effects of blower types, duct flow resistances, and duct materials on energy consumptions and life cycle costs of duct designs. These results can facilitate the constructions of residential air distribution systems with the lowest cost of ownership and can provide HVAC professionals with efficient, long-term, and cost-effective solutions as they face numerous tradeoffs and challenges associated with designing residential duct designs.

REFERENCES

AHRI. 2008. AHRI Standard 210/240-2008, *Performance Rating of Unitary Air-Conditioning & Air-Source Heat Pump Equipment*. Arlington: Air-Conditioning, Heating, and Refrigeration Institute.

Aldrich, R., and J. Williamson. 2014. *Evaluation of retrofit variable-speed furnace fan motor*. DOE/GO-102014-4306. Golden, CO: National Renewable Energy Laboratory.

ASHRAE. 1996. ANSI/ASHRAE 41.1-1986 (RA 2006), *Standard Method for Temperature Measurement*. Atlanta: American Society of Heating, Refrigerating and Air-Conditioning Engineers, Inc.

ASHRAE. 2007a. ANSI/ASHRAE Standard 90.2-2007, *Energy-Efficiency Design of Low-Rise Residential Buildings*. Atlanta: American Society of Heating, Air-Conditioning and Refrigeration Engineers, Inc.

ASHRAE. 2007b. ANSI/ASHRAE Standard 51-2007, *Laboratory Methods of Testing Fans for Certified Aerodynamic Performance Rating*. Atlanta: American Society of Heating, Air-Conditioning and Refrigeration Engineers, Inc.

ASHRAE. 2007c. ANSI/ASHRAE Standard 103-2007, *Method of Testing for Annual Fuel Utilization Efficiency of Residential Central Furnaces and Boilers*. Atlanta: American Society of Heating, Refrigerating and Air-Conditioning Engineers, Inc.

ASHRAE. 2009a. Chapter 1, *ASHRAE Handbook-Fundamentals*. Atlanta: American Society of Heating, Refrigerating and Air-Conditioning Engineers, Inc.

ASHRAE. 2009b. ANSI/ASHRAE Standard 37-2009, *Methods of Testing for rating Electrically Driven Unitary Air-Conditioning and Heat Pump Equipment*. Atlanta: American Society of Heating, Air-Conditioning and Refrigeration Engineers, Inc.

Biermayer, P. J., J. Lutz, and A. Lekov. 2004. Measurement of airflow in residential furnaces. http://escholarship.org/uc/item/9x05g7d1.

Boudreaux, P., P. E. Christian, and R. Jackson. 2011. *Case studies of duct retrofits and guidelines for attic and crawl space duct sealing*. Report ORNL/TM-0000/00. Oak Ridge, TN: Oak Ridge National Laboratory.

Breuker, M. S., and J. E. Braun. 1998. Common faults and their impacts for rooftop air conditioners. *HVAC&R Research* 4(3): 303-16.

Bryan, J. A., and R. Perez. 2001. A residential duct leakage case study on "good cents" homes. *Proceedings of the First International Conference for Enhanced Building Operation*, Austin, TX.

CEC. 2012. *2013 Building Energy Efficiency Standards for Residential and Nonresidential Buildings*. Sacramento, CA: California Energy Commission.

DOE. 2014. Technical support document: energy efficiency program for consumer products and commercial and industrial equipment: residential furnace fans. http://www.regulations.gov/#!documentDetail;D=EERE-2010-BT-STD-0011-0111.

EIA. 2009. Residential Energy Consumption Survey. http://www.eia.gov/consumption/residential/data/2009/.

EIA. 2014a. Electric power monthly. http://www.eia.gov/electricity/monthly/epm_table_grapher.cfm?t=epmt_5_6_a

EIA. 2014b. Natural gas prices. http://www.eia.gov/dnav/ng/ng_pri_sum_a_epg0_prs_dmcf_m.htm

Franco, V., J. Lutz, A. Lekov, and L. Gu. 2008. *Furnace blower electricity: national and regional savings potential*. Report LBNL-417E. Berkeley, CA: Lawrence Berkeley National Laboratory.

Gu, L. 2007. Airflow network modeling in EnergyPlus. *Proceedings of 10th International Building Performance Simulation Association Conference and Exhibition*, Beijing, China: 964-71.

Henderson, H. I., D. Parker, and Y. J. Huang. 2000. Improving DOE-2's RESYS routine: user defined functions to provide more accurate part load energy use and humidity predictions. *Proceedings of ACEEE Summer Study on Energy Efficiency in Buildings*, Washington, DC.: 113-24.

ICC. 2011. *2012 International Energy Conservation Code*. Country Club Hills, IL: International Code Council.

Kendall, M. A. 2004. Energy-saving opportunities in residential air-handler efficiency. *ASHRAE Transactions* 110(1): 425-30.

Kim, M., W. V. Payne, P. A. Domanski, S. H. Yoon, and C. J. Hermes. 2009. Performance of a residential heat pump operating in the cooling mode with single faults Imposed. *Applied Thermal Engineering* 29(4): 770-78.

Kinney, L. 2005. Duct systems in southwestern homes: problems and opportunities. http://www.swenergy.org/publications/documents/DuctTech.pdf.

Kline, S. J., and F. A. McClintock. 1953. Describing Uncertainties in Single-Sample Experiments. *Mechanical Engineering* 75(1): 3-8.

Kruis, N. 2010. Reconcilling differences between residential DX cooling models in DOE-2 and EnergyPlus. *Proceedings of Fourth National Conference of IBPSA-USA*, New York City, NY: 134-41.

LBNL. 2013a. EnergyPlus, Version 8.1.0.009. Berkeley, CA: Lawrence Berkeley National Laboratory

LBNL. 2013b. Residential diagnostics database: duct leakage. https://sites.google.com/a/lbl.gov/resdb/duct-leakage-2.

LBNL. 2014. EnergyPlus enginnering reference. http://apps1.eere.energy.gov/buildings/energyplus/pdfs/engineeringreference.pdf.

Lutz, J., V. Franco, A. Lekov, and G. Wong-Parodi. 2006. *BPM motors in residential gas furnaces: what are the savings*. LBNL-59866. Berkeley, CA: Lawrence Berkeley National Laboratory.

Mendon, V., and Z. T. Taylor. 2014. Deevelopment of residential prototype building models and analysis system for large-scale energy efficiency studies using EnergyPlus. *Proceedings of 2014 ASHRAE/IBPSA-USA Building Simulation Conference*, Atlanta, GA: 457-64.

Modera, M. 1993. Characterizing the performance of residential air distribution systems. *Energy and Buildings* 20(1): 65-75.

Modera, M. 2005. ASHRAE standard 152 & duct leaks in houses. *ASHRAE Journal* March: 28-32.

Mowris, R., E. Jones, and R. Eshom. 2012. Laboratory measurements of HVAC installation and maintenance faults. *ASHRAE Transactions* 118(2): 165-72.

Murray, M., and S. Fitzpatrick. 2012. *Residential HVAC electronically commutated motor retrofit report.* Raleigh, NC: Advanced Energy.

NIST. 2007. REFPROP, Version 8.0. Boulder, CO: National Institute of Standard and Technology

Palani, M., D. L. O'Neal, and J. Haberl. 1992. The effect of reduced evaporator airflow on the performance of a residential central air conditioner. *Proceedings of the*

Eighth Symposium on Improving Building Systems in Hot and Humid Climates, Dallas, TX: 474-77.

Palmiter, L., J. Kim, B. Larson, P. W. Francisco, E. A. Groll, and J. E. Braun. 2011. Measured effect of airflow and refrigerant charge on the seasonal performance of an air-source heat pump using R-410A. *Energy and Buildings* 43(7): 1802-10.

Parker, D., P. Fairey, and L. Gu. 1993. Simulation of the effects of duct leakage and heat transfer on residential space-cooling energy use. *Energy and Buildings* 20(2): 97-113.

Parker, D. S., J. R. Sherwin, and B. Hibbs. 2005. Development of high-efficiency air conditioner condenser fans. *ASHRAE Transactions* 111(2): 511-20.

Parker, D. S., J. R. Sherwin, R. A. Raustad, and D. B. S. III. 1997. Impact of evaporator coil airflow in residential air-conditioning systems. *ASHRAE Transactions* 103(2): 395-405.

PNNL. 2015. Residential prototype building models. https://www.energycodes.gov/development/residential/iecc_models.

Proctor, J., and D. Parker. 2000. Hidden power drains: residential heating and cooling fan power demand. *Proceedings of the ACEEE Summer Study on Buildings*, Washington, DC., 1: 225-34.

Rodriguez, A. G., D. O'Neal, M. Davis, and S. Kondepudi. 1996. Effect of reduced evaporator airflow on the high temperature performance of air conditioners. *Energy and Buildings* 24: 195-201.

Rushing, A. S., J. D. Kneifel, and B. C. Lippiatt. 2013. Energy price indices and discount factors for life-cycle cost analysis-2013. http://www1.eere.energy.gov/femp/pdfs/ashb13.pdf.

Rutkowski, H. 2011. *Manual D : residential duct systems,* 3rd ed. Arlington, VA: Air Conditioning Contractors of America.

Sachs, H. M., and S. Smith. 2004. How much energy could residential furnace air handlers save. *ASHRAE Transactions* 110(1): 431-40.

Shapiro, C., R. Aldrich, and L. Arena. 2012. Retrofitting air conditioning and duct systems in hot, dry climates. http://apps1.eere.energy.gov/buildings/publications/pdfs/building_america/retrofit_ac_duct_systems.pdf.

Siegel, J., I. Walker, and M. Sherman. 2002. Dirty air conditioners: energy implication of coil fouling. *Proceedings of the ACEEE Summer Study on Energy Efficiency in Buildings*, Pacific Grove, CA, 1: 287-300.

Stephens, B. 2014. The impacts of duct design on life cycle costs of central residential heating and air-conditioning systems. *Energy and Buildings* 82: 563-79.

Stephens, B., A. Novoselac, and J. A. Siegel. 2010. The effects of filtration on pressure drop and energy consumption in residential HVAC systems. *HVAC&R Research* 16(3): 273-94.

Stephens, B., J. A. Siegel, and A. Novoselac. 2011. Operational characteristics of residential and light-commercial air-conditioning systems in a hot and humid climate zone. *Building and Environment* 46(10): 1972-83.

Ueno, K. 2010. ECM efficiency better (and worse) than you think. *Home Energy* May/June 34-38.

Walker, I. S. 2004. Improving Air Handler Efficiency in Houses. *Proceedings of the ACEEE Summer Study on Energy Efficiency in Buildings*, Pacific Grove, CA, 1: 341-52.

Walker, I. S. 2006. *Residential furnace blower performance*. Report 61467. Berkeley, CA: Lawrence Berkeley National Laboratory.

Walker, I. S. 2008. Comparing residential furnace blowers for rating and installed performance. *ASHRAE Transactions* 114(1): 187-95.

Walker, I. S., and J. D. Lutz. 2005. *Laboratory evaluation of residential furnace blower performance*. Report 0403. San Francisco, CA: Pacific Gas and Electric Company.

Wilcox, B., J. Proctor, R. Chitwood, and K. Nittler. 2006. Furnace fan watt and air flow in cooling and air distribution modes. http://www.energy.ca.gov/title24/2008standards/prerulemaking/documents/2006-07-12_workshop/reviewdocs/FAN_WATT_DRAW_AND_AIR_FLOW.pdf.

Wilcox, S., and W. Marion. 2008. *Users manual for TMY3 data sets*. NREL/TP-581-43156. Golden, CO: National Renewable Energy Laboratory.

Witriol, N. M., J. J. Erinjeri, E. Allouche, M. Katz, and R. Nassar. 2008. Cost due to duct leakage: return duct leakage VS supply duct leakage; and sealing energy ductwork thereby reducing energy usage in existing residential buildings. http://dnr.louisiana.gov/assets/docs/energy/programs/residential/La._Tech_DNR_Final_Report_2008-06-09.pdf.

Yin, P., J. F. Sweeney, and M. B. Pate. 2014a. The impact of an ECM blower on the system performance of a 5-ton air conditioner. *Proceedings of ASHRAE 2014 Annual Conference*, Seattle, WA.

Yin, P., J. F. Sweeney, and M. B. Pate. 2014b. Impact of external static pressure on residential heating and cooling energy use in hot climates. *Proceedings of 2014 ASHRAE/IBPSA-USA Building Simulation Conference*, Atlanta, GA: 410-16.

APPENDIX A AIR CONDITIONER PERFORMANCE TEST DATA

The performance test results for the 60 kBtu/h (17.6 kW) air conditioner, including airflow rates, cooling capacities, energy balances, and powers of the compressor, condenser fan, and indoor blower, are tabulated in Table 32.

Table 32 Performance test data for the air conditioner

Test No.	Test Condition	Airflow Rate, ft^3/min (m^3/s)	Net Total Cooling, Btu/h (kW)	Net Sensible Cooling, Btu/h (kW)	Indoor Blower Power, kW	Condenser Fan Power, kW	Compressor Power, kW	Total Cooling Refrigerant Side Btu/h (kW)	Energy Balance (%)
1	A Test	2196 (1.04)	57426 (16.83)	46200 (13.54)	0.89	0.22	4.17	58783	-2.4
2	A Test	1974 (0.93)	57052 (16.72)	43510 (12.75)	0.85	0.22	4.15	58352	-2.3
3	A Test	1758 (0.83)	56589 (16.59)	41126 (12.05)	0.70	0.22	4.14	55851	1.3
4	A Test	1500 (0.71)	54977 (16.11)	38290 (11.22)	0.48	0.22	4.15	55202	-0.4
5	A Test	1246 (0.59)	53657 (15.73)	34746 (10.18)	0.26	0.22	4.09	55257	-3.0
6	A Test	995 (0.47)	49341 (14.46)	30408 (8.91)	0.32	0.22	4.06	51322	-4.0

APPENDIX B AIR CONDITIONER GROSS COOLING PERFORMANCE DATA

The air conditioner gross cooling performance data are derived from the measured net cooling performance data by adding the blower power consumption to the total and sensible cooling capacities so that the heating effect caused by the indoor blower could be compensated. The gross cooling performance data are tabulated in Table 33.

Table 33 Gross cooling performance data for the air conditioner

Test No.	Airflow Rate, ft^3/min (m^3/s)	Gross Total Cooling, Btu/h (kW)	Gross Sensible Cooling, Btu/h (kW)	Gross SHR	Condensing Unit Power, kW	Gross Coefficient of Performance
1	2196 (1.04)	60472 (17.72)	49243 (14.43)	0.81	4.40	4.03
2	1974 (0.93)	59921 (17.56)	46376 (13.59)	0.77	4.37	4.01
3	1758 (0.83)	58993 (17.29)	43527 (12.76)	0.74	4.36	3.96
4	1500 (0.71)	56618 (16.59)	39928 (11.70)	0.71	4.37	3.81
5	1246 (0.59)	54552 (15.99)	35638 (10.44)	0.65	4.31	3.71
6	995 (0.47)	50441 (14.78)	31505 (9.23)	0.62	4.27	3.46

APPENDIX C AIR CONDITIONER COOLING PERFORMANCE DATA FROM THE MANUFACTURER'S CATALOG

Table 34 shows the manufacturer's catalog data along with the modified results that were used to generate the empirical cooling performance curves as a function of indoor WB and outdoor DB temperatures. For the calculation of gross total cooling capacities, gross sensible cooling capacities, and gross SHRs, a blower power consumption of 0.85 kW was added to the net total and sensible cooling capacities from the manufacturer's catalog data to account for the heating effect caused by the blower. Also, the same blower power consumption of 0.85 kW was removed from the manufacturer's total system power data to calculate the power consumption of the condensing unit.

Table 34 Manufacturer's catalog data

Indoor WB	Outdoor DB	Net total cooling capacity*	Net sensible cooling capacity*	Total system power*	Gross total cooling capacity	Gross sensible cooling capacity	Condensing unit power
°F (°C)	°F (°C)	Btu/h (kW)	Btu/h (kW)	kW	Btu/h (kW)	Btu/h (kW)	kW
57 (13.8)	75 (23.9)	60.39 (17.70)	60.39 (17.70)	4.33	63.31 (18.55)	63.29 (18.55)	3.47
62 (16.6)	75 (23.9)	61.11 (17.91)	55.94 (16.39)	4.33	64.03 (18.77)	58.84 (17.24)	3.47
63 (17.2)	75 (23.9)	62.07 (18.19)	45.41 (13.31)	4.34	64.99 (19.05)	48.31 (14.16)	3.48
67 (19.4)	75 (23.9)	66.6 (19.52)	46.95 (13.76)	4.38	69.52 (20.37)	49.85 (14.61)	3.52
72 (22.2)	75 (23.9)	72.91 (21.37)	37.66 (11.04)	4.43	75.83 (22.22)	40.56 (11.89)	3.57

Table 34 Continued

Indoor WB	Outdoor DB	Net total cooling capacity*	Net sensible cooling capacity*	Total system power*	Gross total cooling capacity	Gross sensible cooling capacity	Condensing unit power
°F (°C)	°F (°C)	Btu/h (kW)	Btu/h (kW)	kW	Btu/h (kW)	Btu/h (kW)	kW
57 (13.8)	85 (29.4)	56.8 (16.65)	56.8 (16.65)	4.74	59.72 (17.50)	59.70 (17.50)	3.88
62 (16.6)	85 (29.4)	57.07 (16.73)	53.59 (15.71)	4.74	59.99 (17.58)	56.49 (16.56)	3.88
63 (17.2)	85 (29.4)	57.83 (16.95)	43.39 (12.72)	4. 75	60.75 (17.80)	46.29 (13.57)	3.89
67 (19.4)	85 (29.4)	62.04 (18.18)	44.89 (13.16)	4.79	64.96 (19.04)	47.79 (14.01)	3.93
72 (22.2)	85 (29.4)	67.9 (19.90)	35.78 (10.49)	4.85	70.82 (20.76)	38.68 (11.34)	3.99
57 (13.8)	95 (35)	53.18 (15.59)	53.18 (15.59)	5.18	56.10 (16.44)	56.08 (16.44)	4.32
62 (16.6)	95 (35)	53.18 (15.59)	53.18 (15.59)	5.18	56.10 (16.44)	56.08 (16.44)	4.32
63 (17.2)	95 (35)	53.59 (15.71)	41.36 (12.12)	5.19	56.51 (16.56)	44.26 (12.97)	4.33
67 (19.4)	95 (35)	57.05 (16.72)	43.51 (9.94)	5.22	59.92 (17.56)	46.38 (13.59)	4.37
72 (22.2)	95 (35)	62.9 (18.43)	33.9 (14.51)	5.28	65.82 (19.29)	36.80 (10.79)	4.42
57 (13.8)	105 (40.6)	49.5 (14.51)	49.5 (14.51)	5.66	52.42 (15.36)	52.40 (15.36)	4.80
62 (16.6)	105 (40.6)	49.5 (14.51)	49.5 (14.51)	5.66	52.42 (15.36)	52.40 (15.36)	4.80
63 (17.2)	105 (40.6)	49.33 (14.46)	39.33 (11.53)	5.66	52.25 (15.31)	42.23 (12.38)	4.80
67 (19.4)	105 (40.6)	52.89 (15.50)	40.78 (11.95)	5.69	55.81 (16.36)	43.68 (12.80)	4.83
72 (22.2)	105 (40.6)	57.85 (16.95)	32.01 (9.38)	5.75	60.77 (17.81)	34.91 (10.23)	4.89
57 (13.8)	115 (46.1)	45.74 (13.41)	45.74 (13.41)	6.16	48.66 (14.26)	48.64 (14.26)	5.30
62 (16.6)	115 (46.1)	45.74 (13.41)	45.74 (13.41)	6.16	48.66 (14.26)	48.64 (14.26)	5.30
63 (17.2)	115 (46.1)	45.03 (13.20)	37.28 (10.93)	6.15	47.95 (14.05)	40.18 (11.78)	5.29
67 (19.4)	115 (46.1)	48.25 (14.14)	38.7 (11.34)	6.19	51.17 (15.00)	41.60 (12.19)	5.33
72 (22.2)	115 (46.1)	52.74 (15.46)	30.11 (8.82)	6.24	55.66 (16.31)	33.01 (9.67)	5.38
57 (13.8)	125 (51.7)	41.85 (12.27)	41.85 (12.27)	6.68	44.77 (13.12)	44.75 (13.11)	5.82

Table 34 Continued

Indoor WB	Outdoor DB	Net total cooling capacity*	Net sensible cooling capacity*	Total system power*	Gross total cooling capacity	Gross sensible cooling capacity	Condensing unit power
°F (°C)	°F (°C)	Btu/h (kW)	Btu/h (kW)	kW	Btu/h (kW)	Btu/h (kW)	kW
62 (16.6)	125 (51.7)	41.85 (12.27)	41.85 (12.27)	6.68	44.77 (13.12)	44.75 (13.11)	5.82
63 (17.2)	125 (51.7)	40.64 (11.91)	35.18 (10.31)	6.67	43.56 (12.77)	38.08 (11.16)	5.81
67 (19.4)	125 (51.7)	43.52 (12.75)	36.58 (10.72)	6.7	46.44 (13.61)	39.48 (11.57)	5.84
72 (22.2)	125 (51.7)	47.52 (13.93)	28.18 (8.26)	6.74	50.44 (14.78)	31.08 (9.11)	5.88

*Directly adopted from the manufacturer's catalog data.

APPENDIX D BLOWER PERFORMANCE TEST DATA

The test results of airflow, power, and efficiency over a pressure range of 0.1 to 1.2 in. w.g. (25 to 300 Pa) are presented in Figure 34 to Figure 69 for the twelve (12) blowers tested in this study.

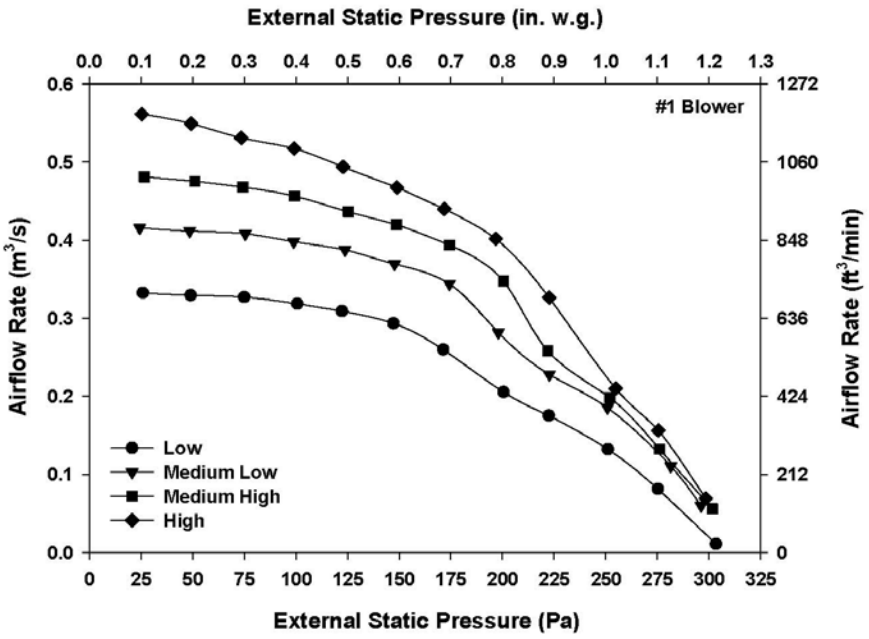

Figure 34 Measured airflow results for Blower #1

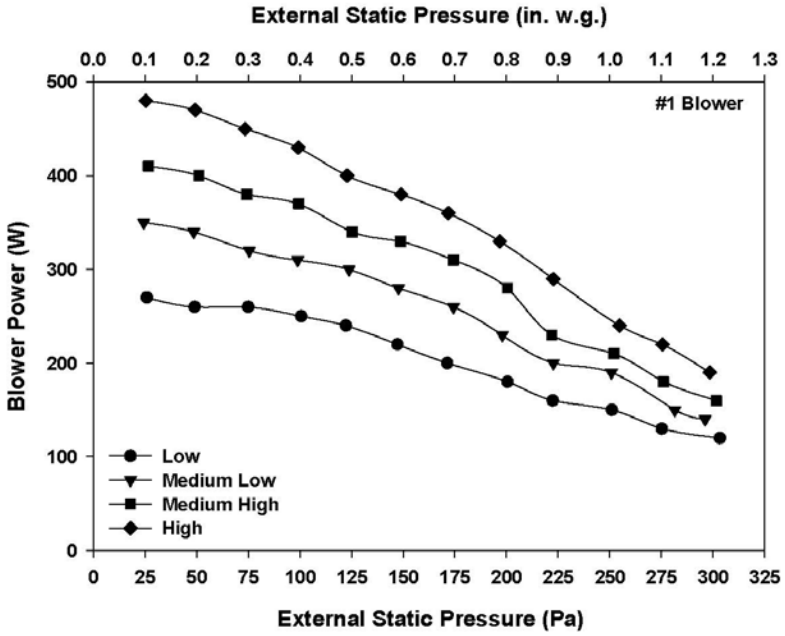

Figure 35 Measured power results for Blower #1

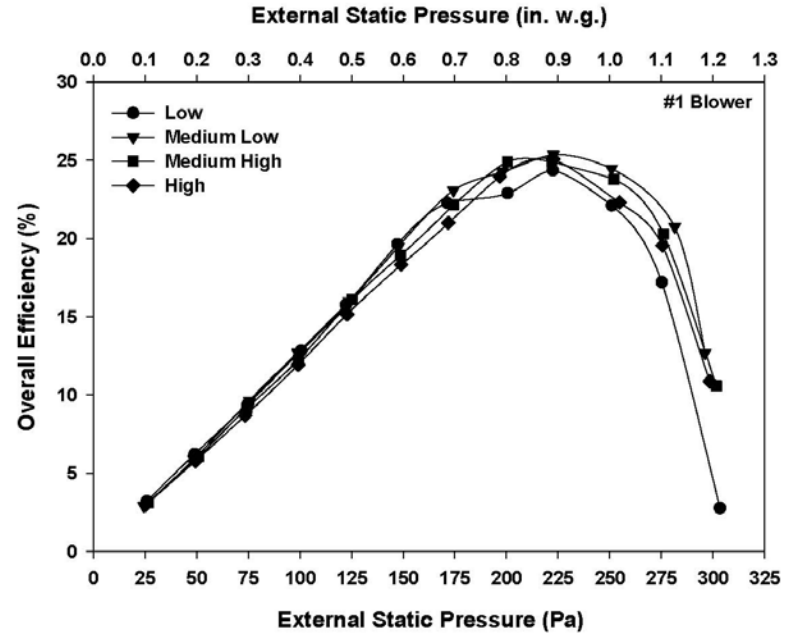

Figure 36 Efficiency results for Blower #1

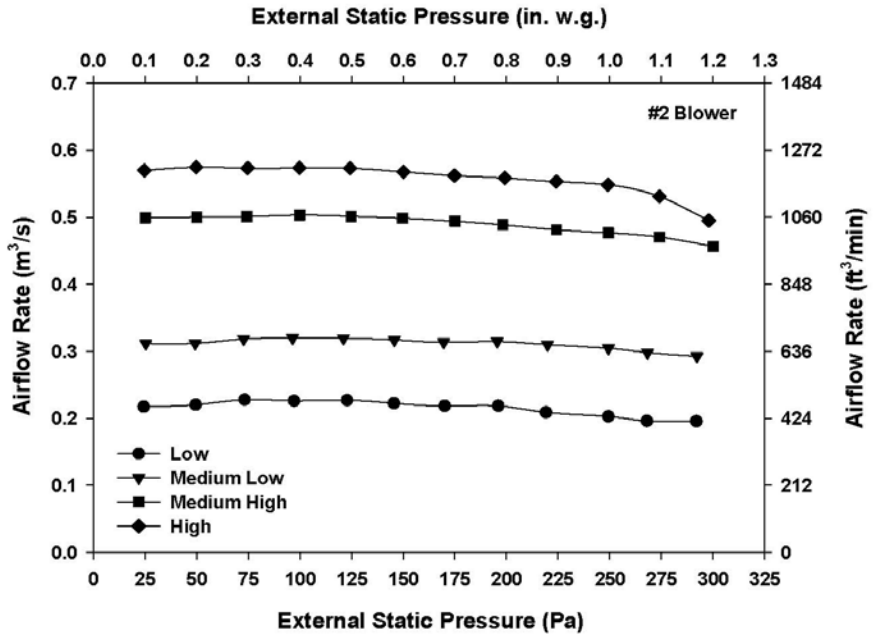

Figure 37 Measured airflow results for Blower #2

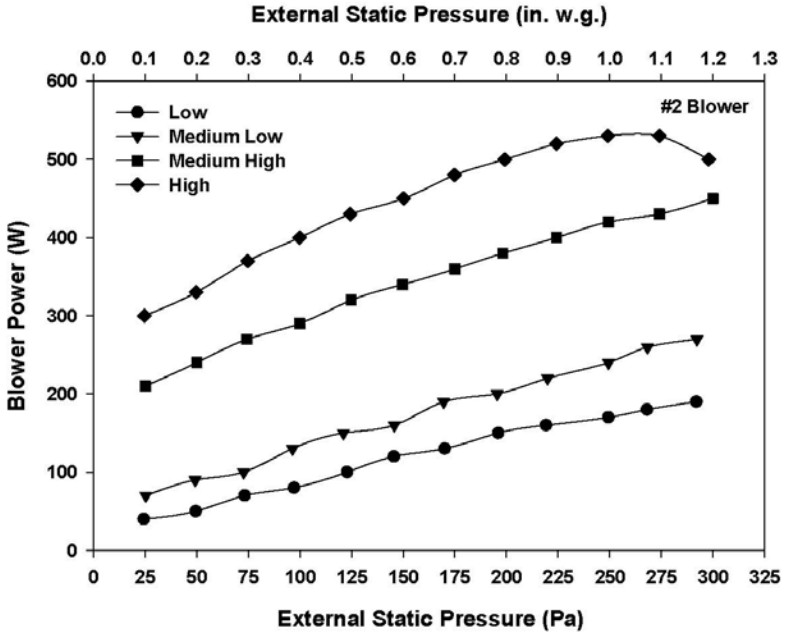

Figure 38 Measured power results for Blower #2

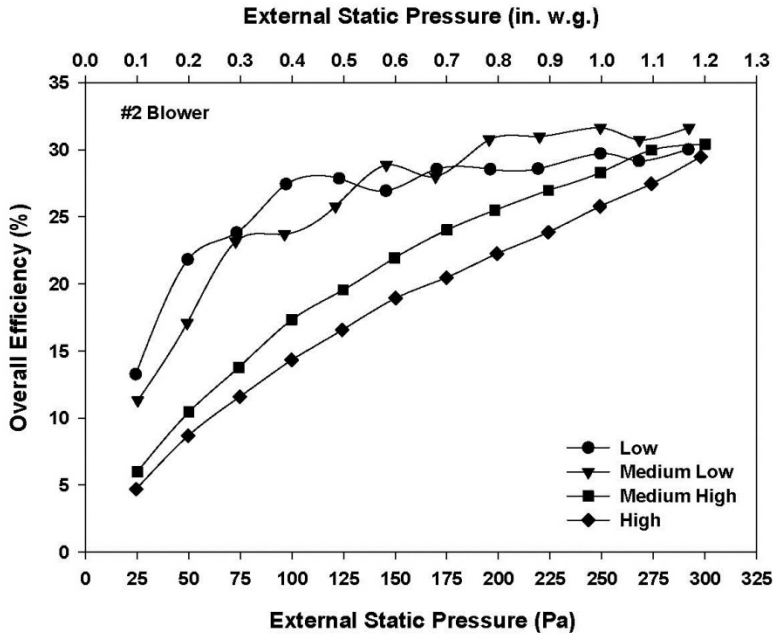

Figure 39 Efficiency results for Blower #2

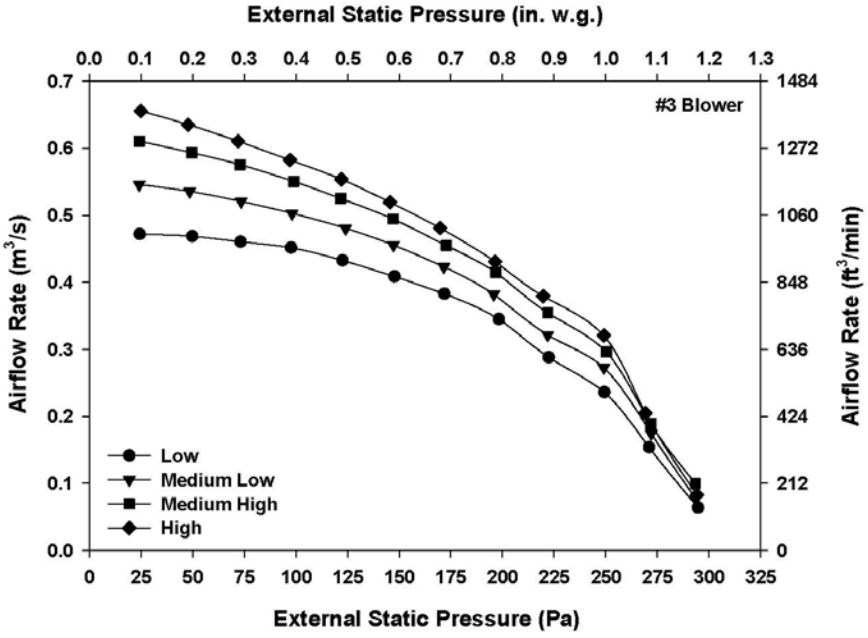

Figure 40 Measured airflow results for Blower #3

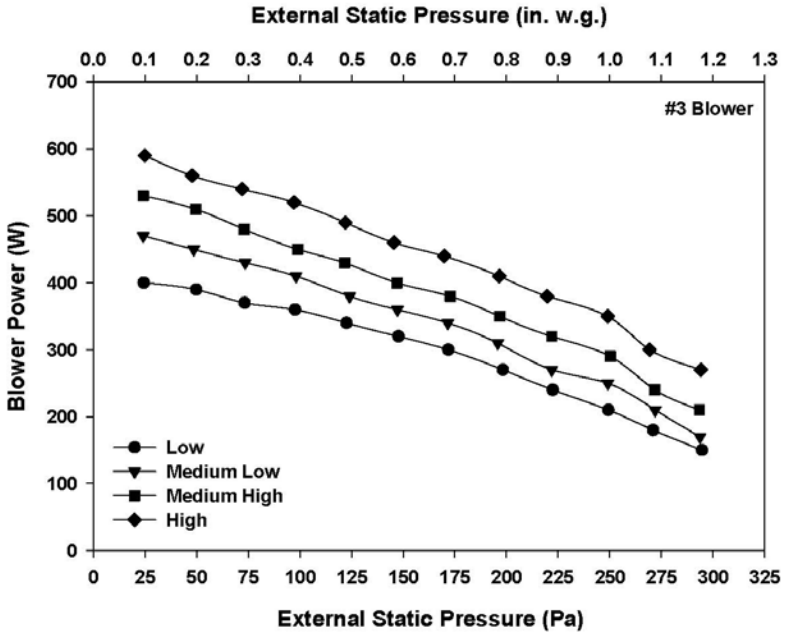

Figure 41 Measured power results for Blower #3

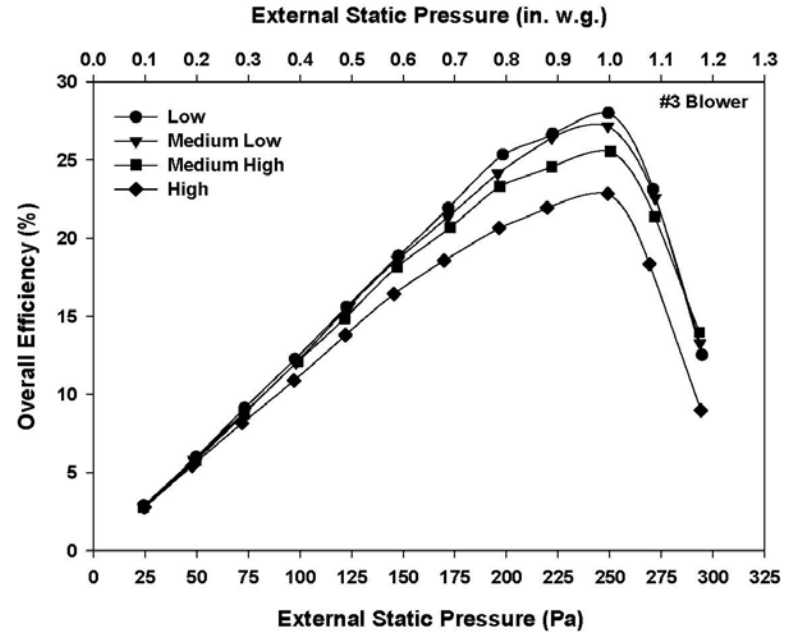

Figure 42 Efficiency results for Blower #3

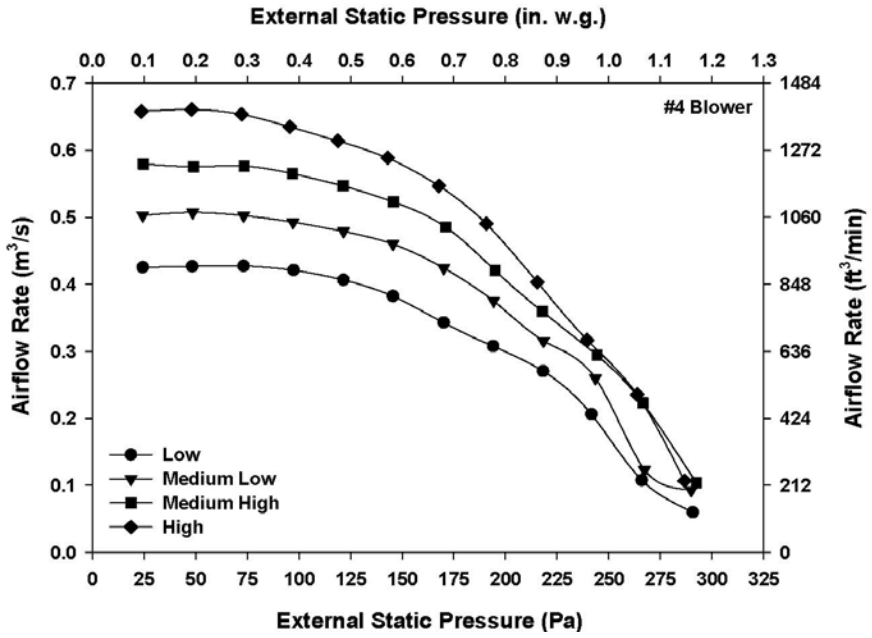

Figure 43 Measured airflow results for Blower #4

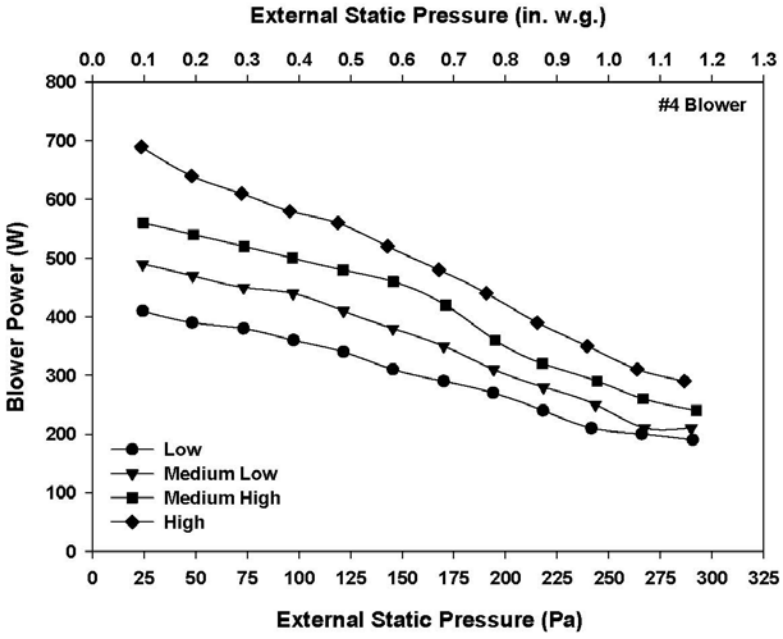

Figure 44 Measured power results for Blower #4

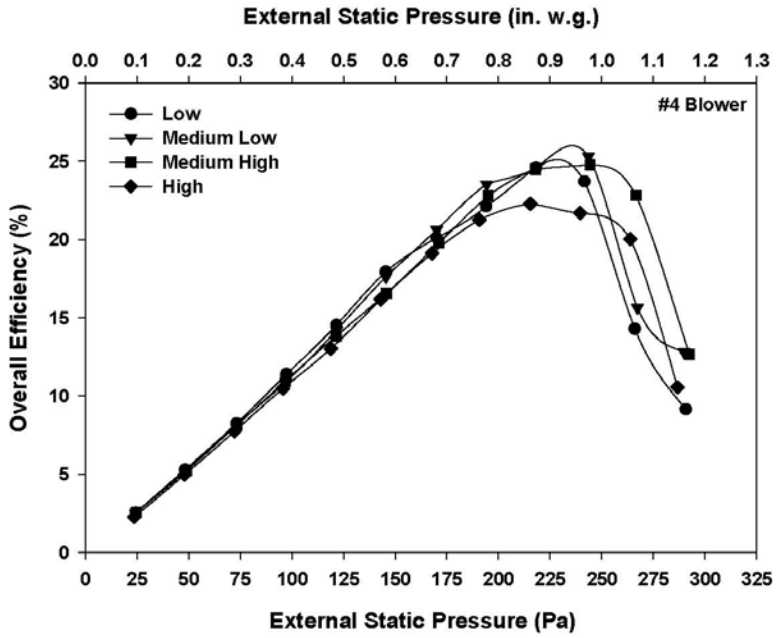

Figure 45 Efficiency results for Blower #4

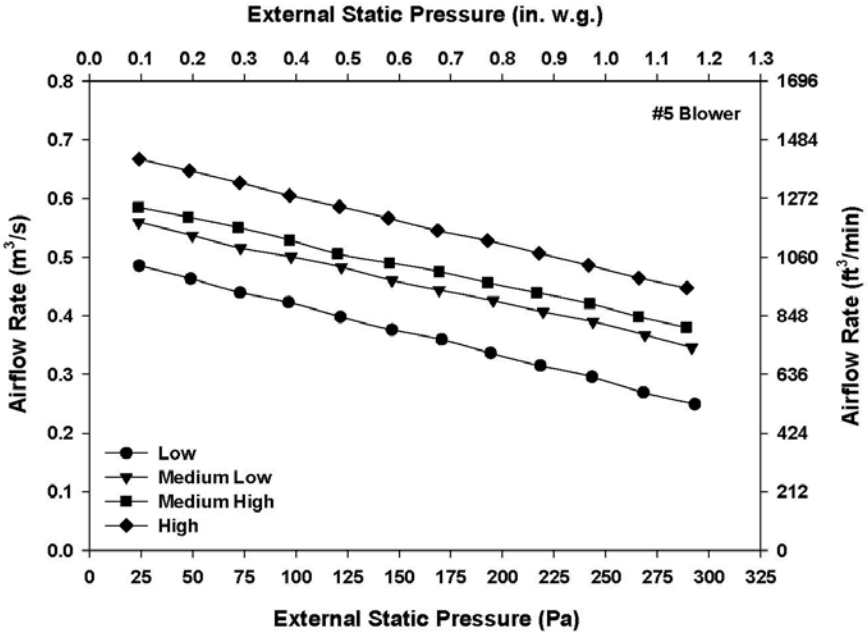

Figure 46 Measured airflow results for Blower #5

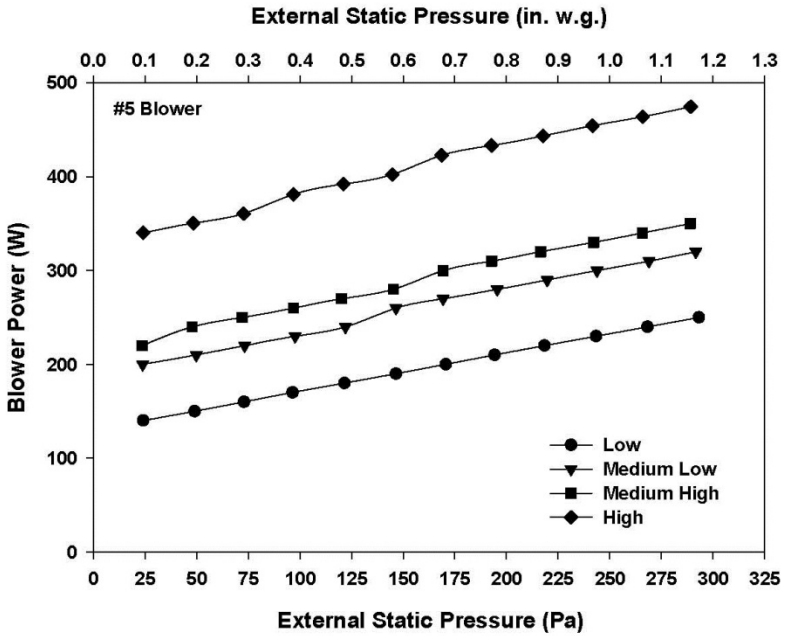

Figure 47 Measured power results for Blower #5

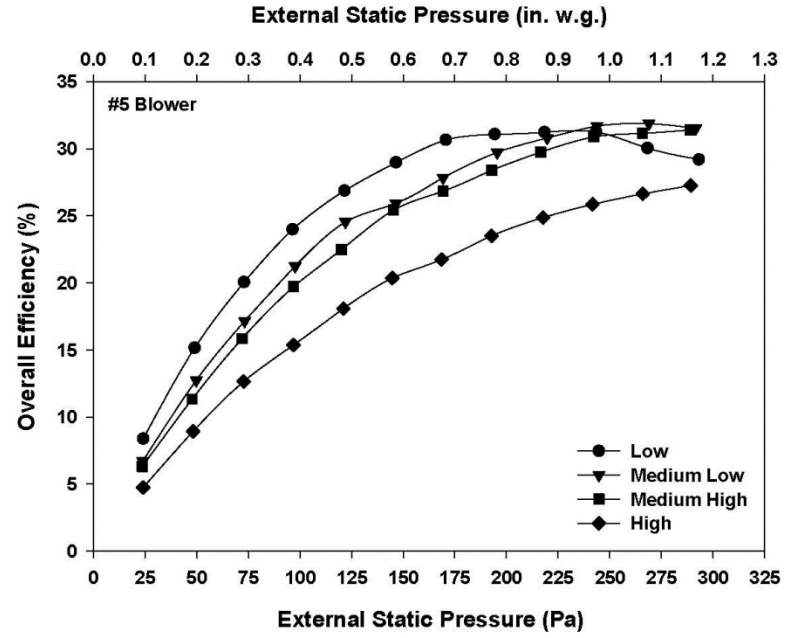

Figure 48 Efficiency results for Blower #5

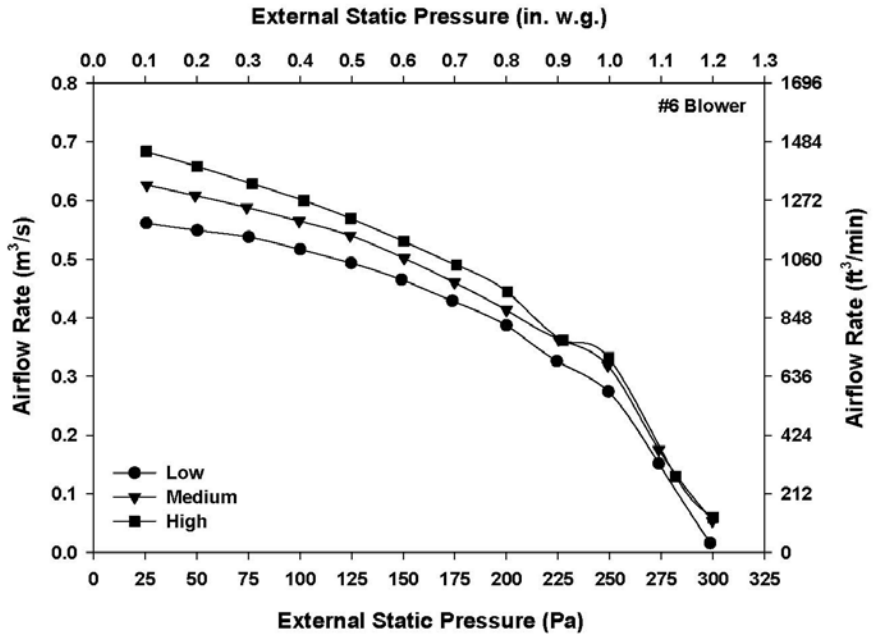

Figure 49 Measured airflow results for Blower #6

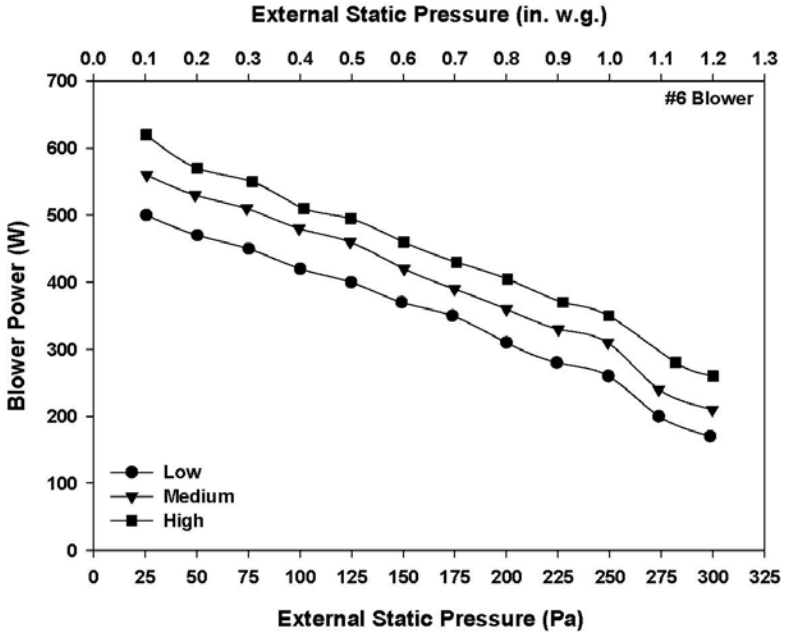

Figure 50 Measured power results for Blower #6

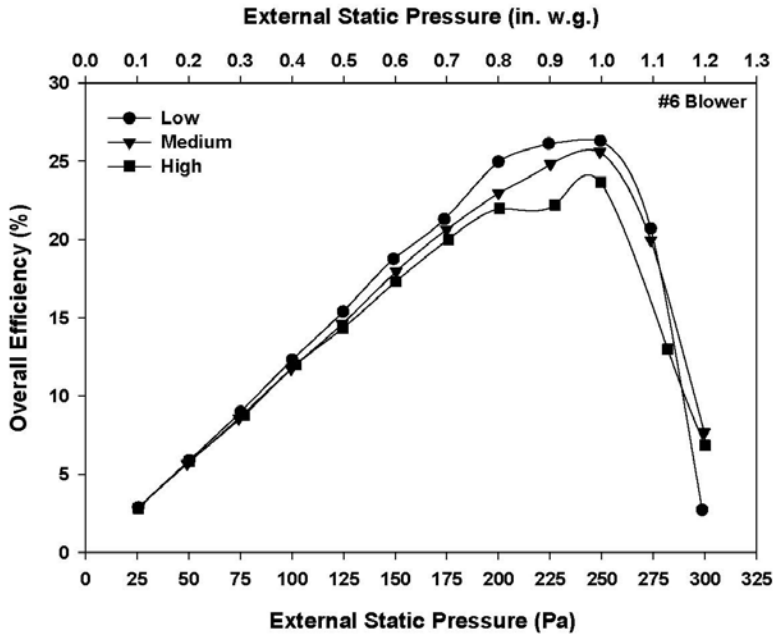

Figure 51 Efficiency results for Blower #6

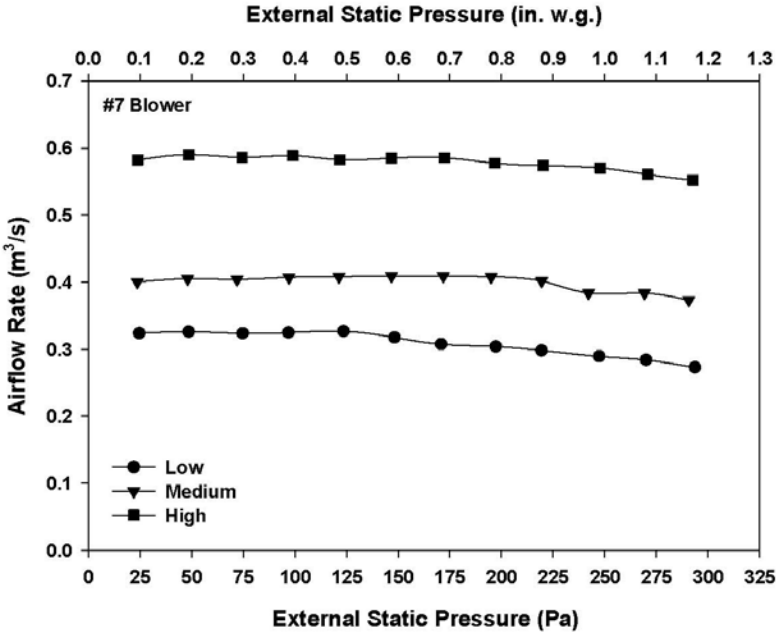

Figure 52 Measured airflow results for Blower #7

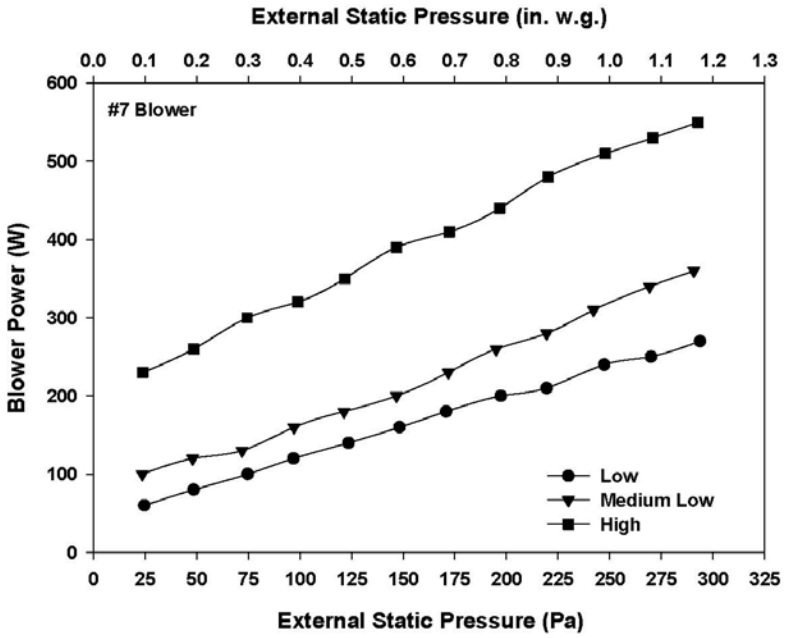

Figure 53 Measured power results for Blower #7

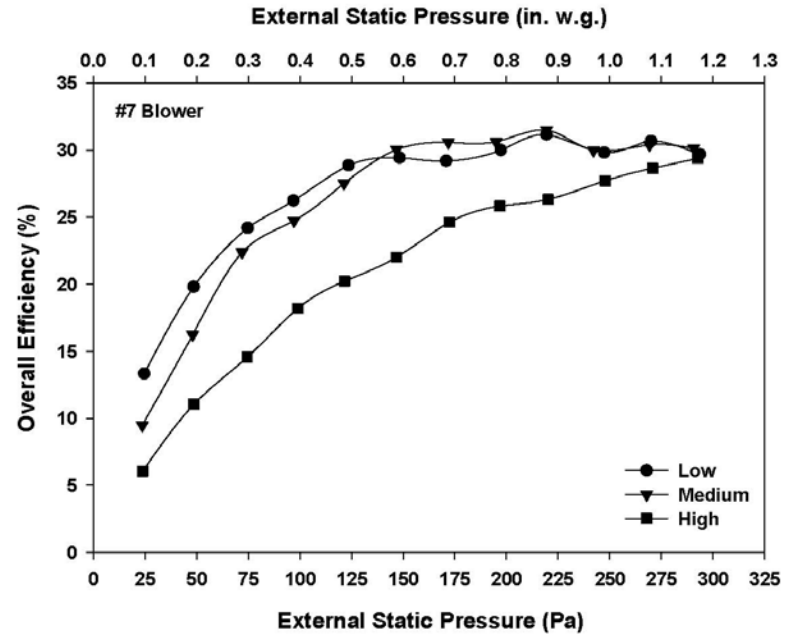

Figure 54 Efficiency results for Blower #7

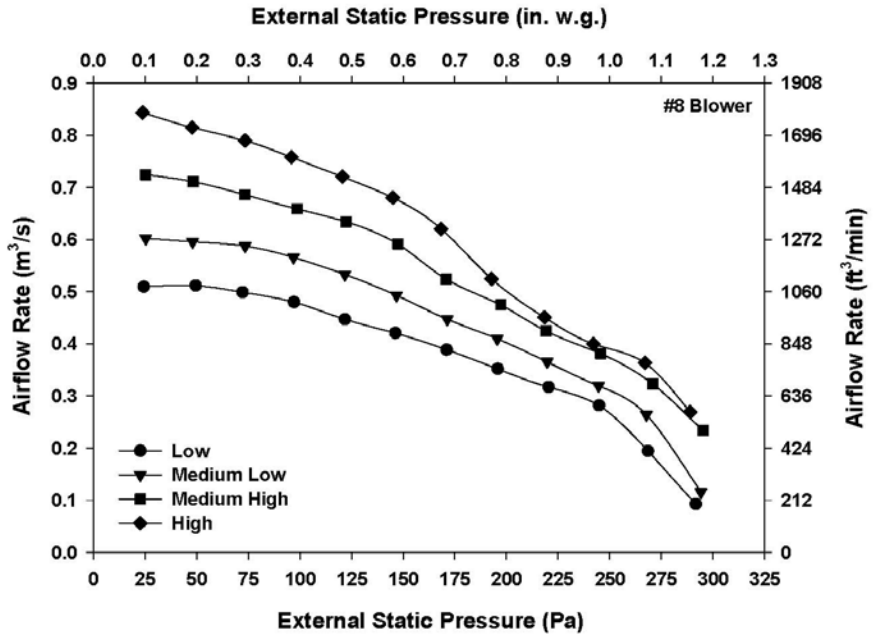

Figure 55 Measured airflow results for Blower #8

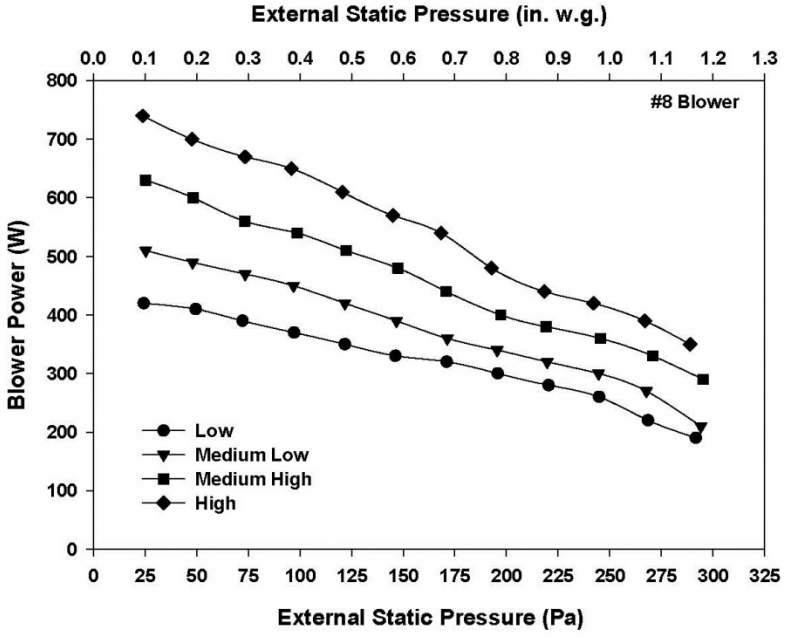

Figure 56 Measured power results for Blower #8

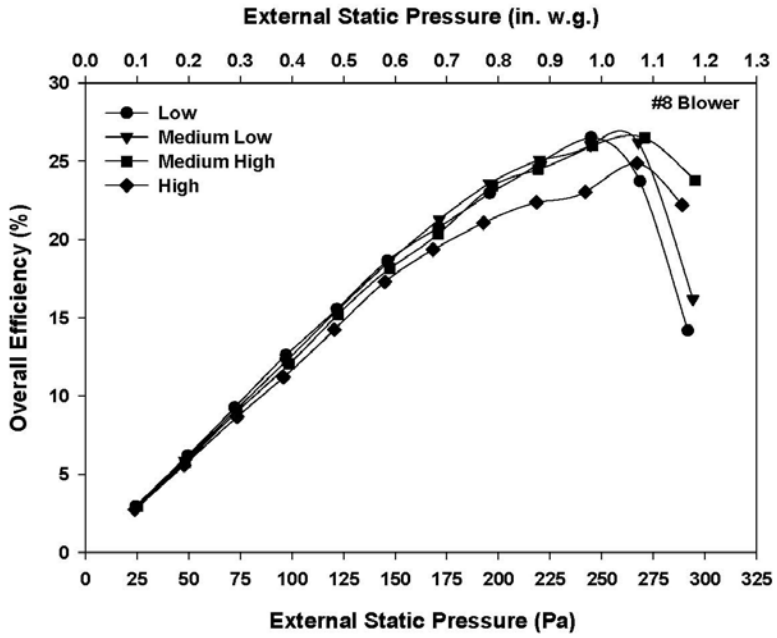

Figure 57 Efficiency results for Blower #8

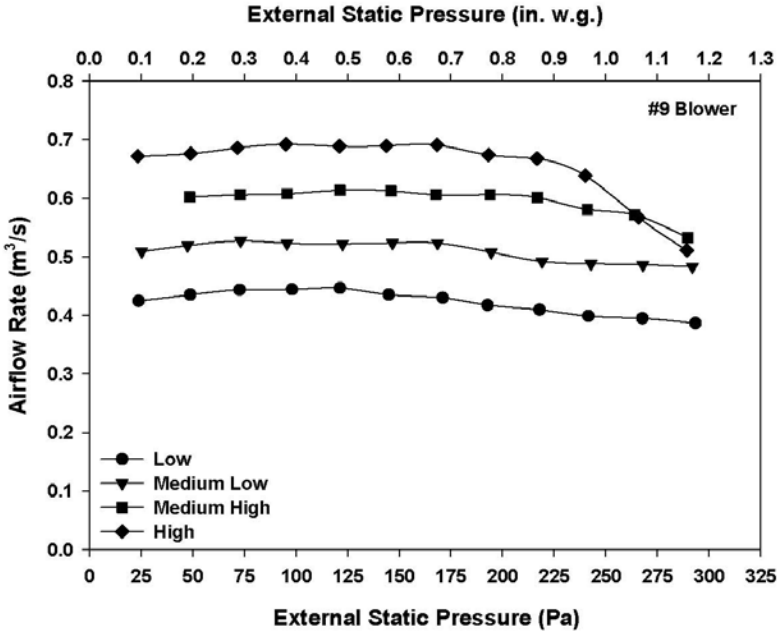

Figure 58 Measured airflow results for Blower #9

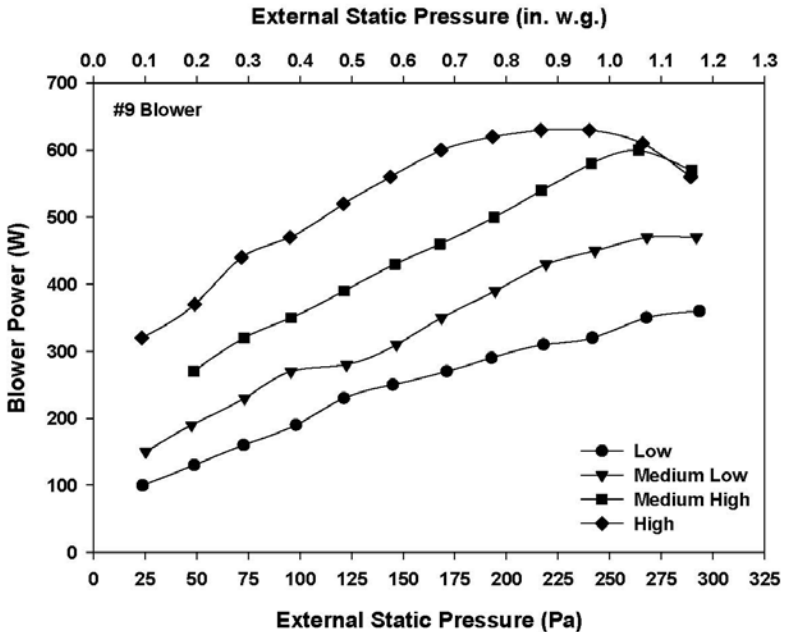

Figure 59 Measured power results for Blower #9

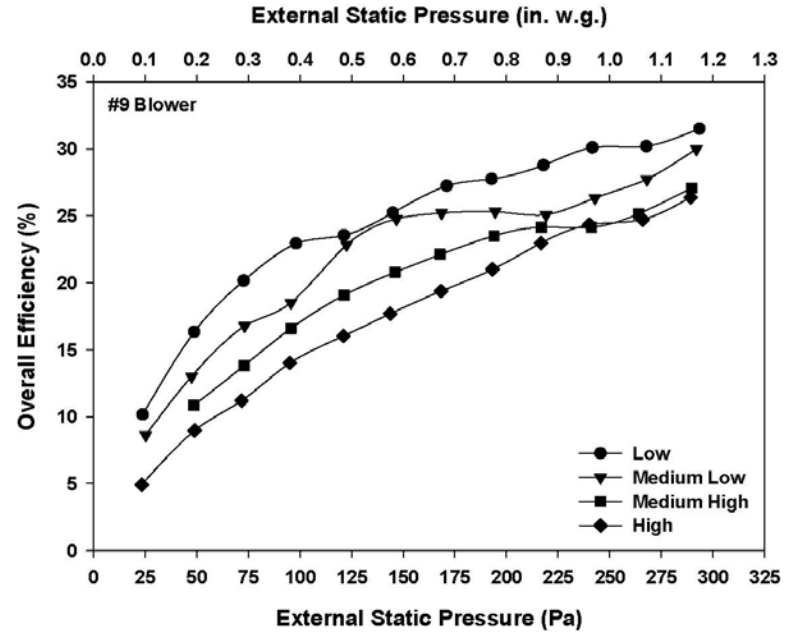

Figure 60 Efficiency results for Blower #9

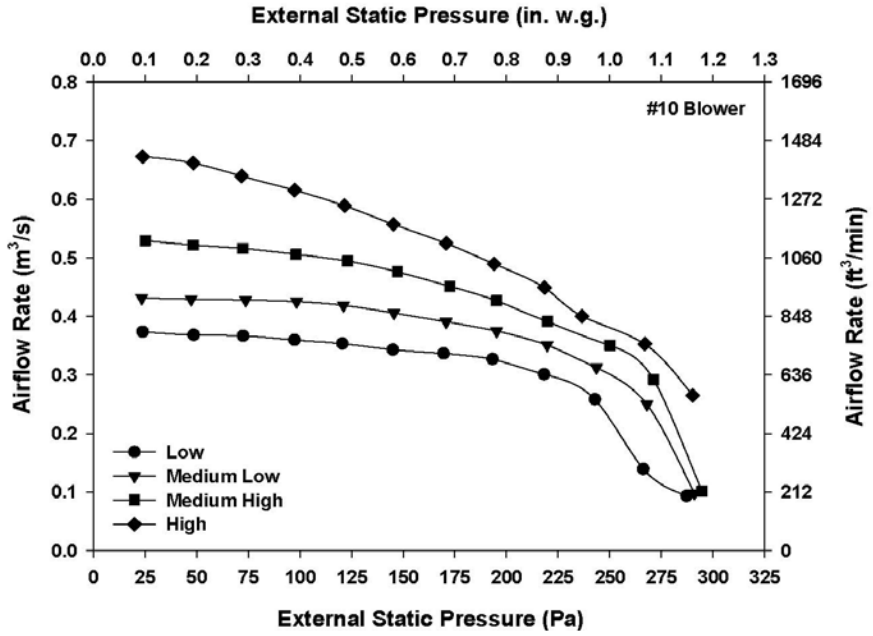

Figure 61 Measured airflow results for Blower #10

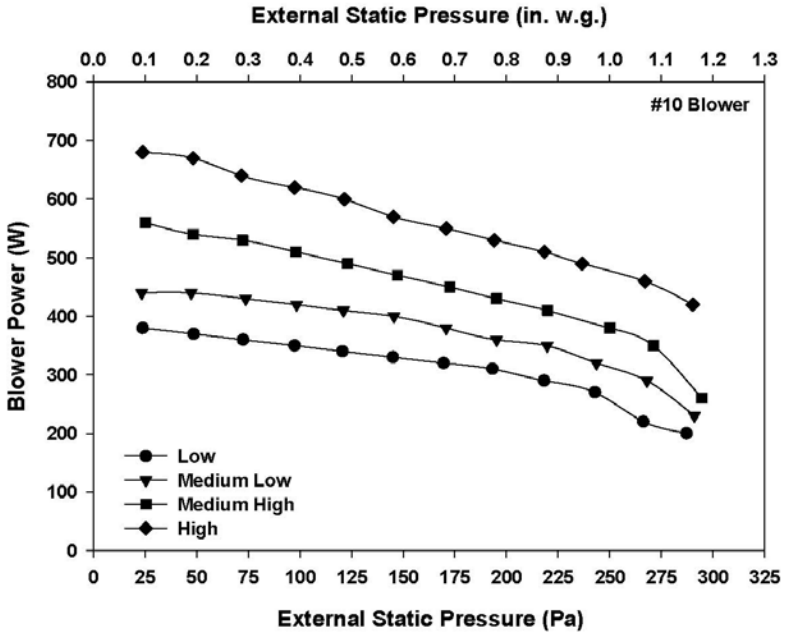

Figure 62 Measured power results for Blower #10

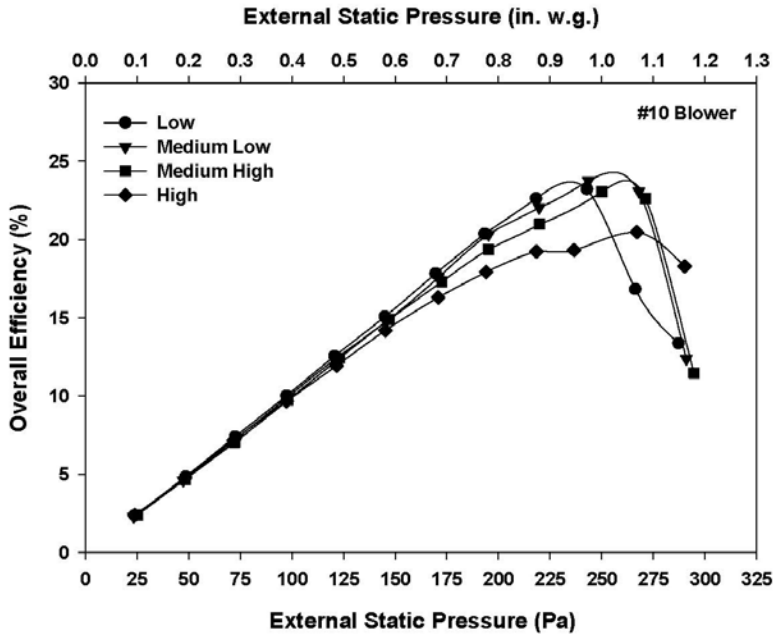

Figure 63 Efficiency results for Blower #10

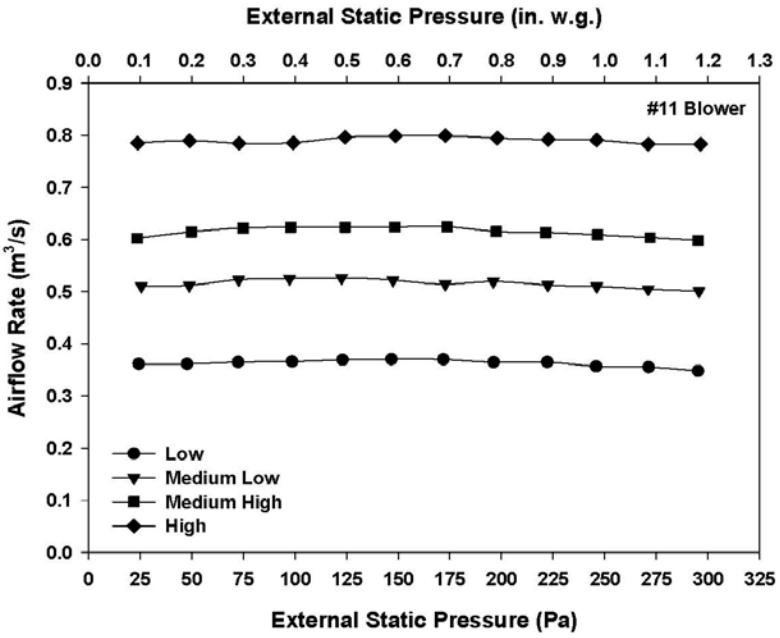

Figure 64 Measured airflow results for Blower #11

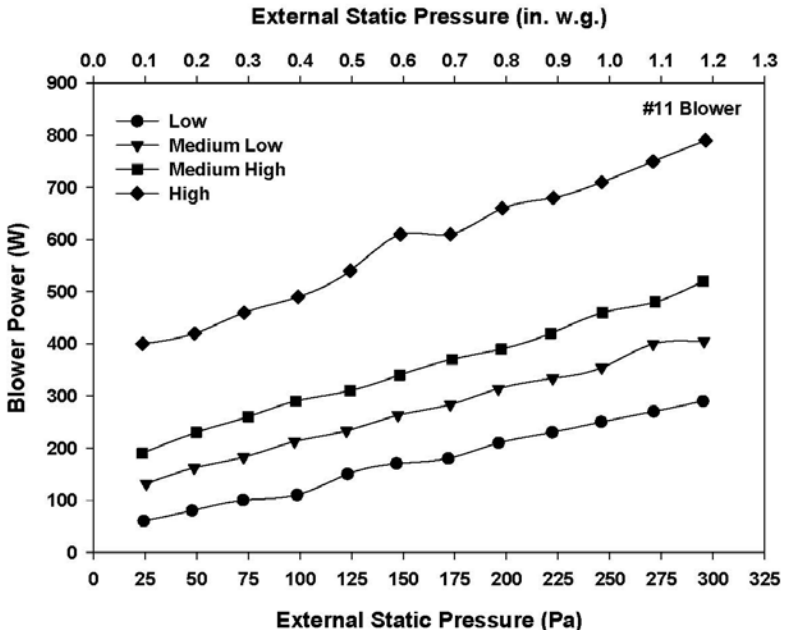

Figure 65 Measured power results for Blower #11

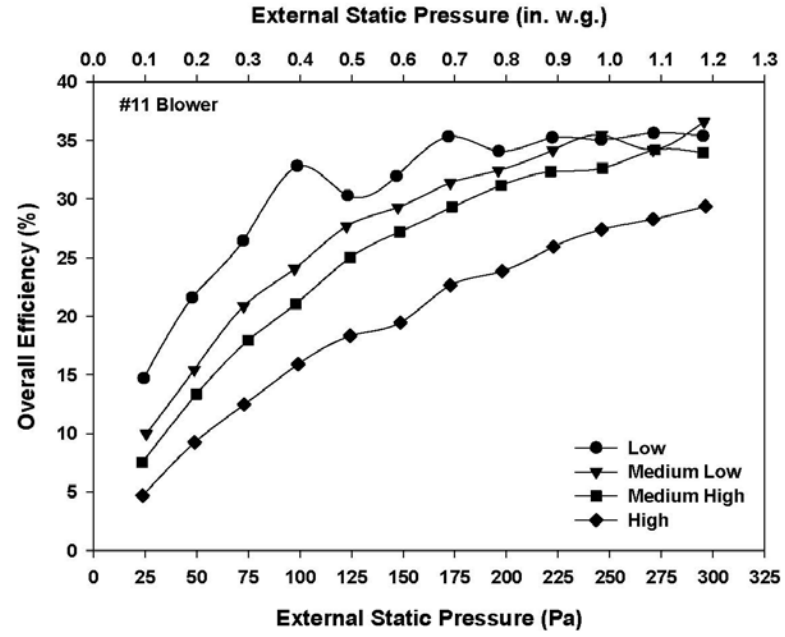

Figure 66 Efficiency results for Blower #11

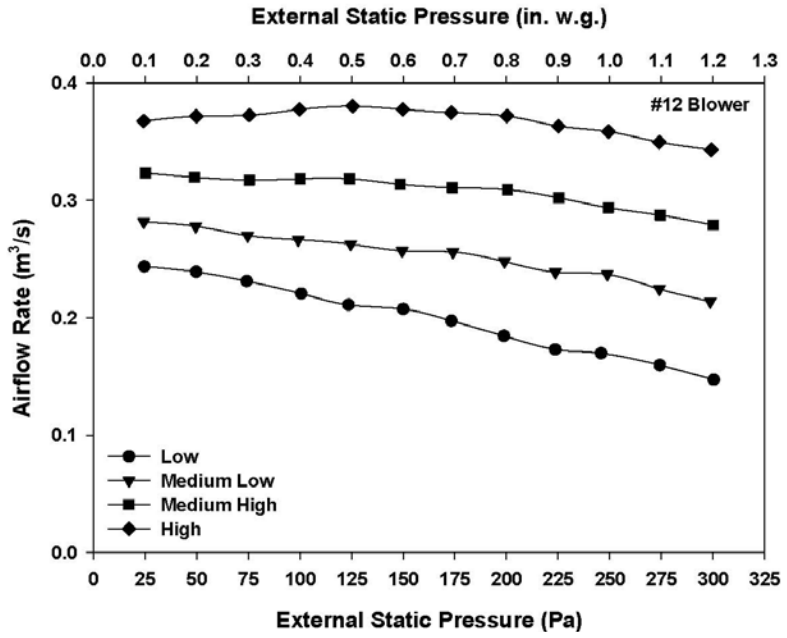

Figure 67 Measured airflow results for Blower #12

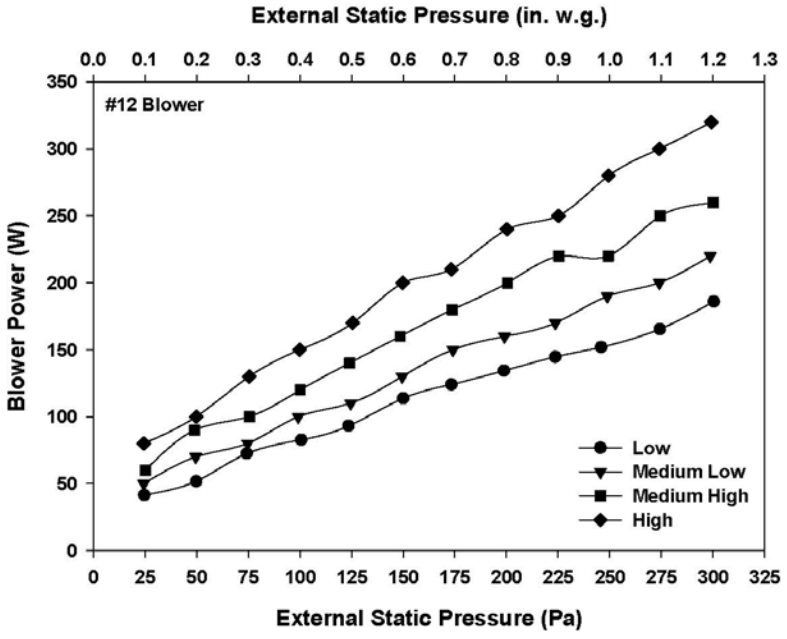

Figure 68 Measured power results for Blower #12

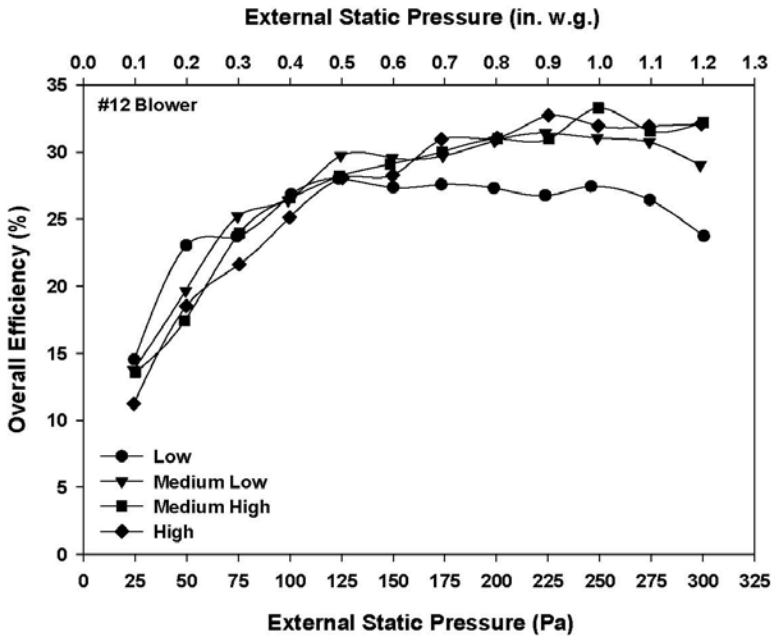

Figure 69 Efficiency results for Blower #12

APPENDIX E CORRELATION DEVELOPMENT BETWEEN ROTATIONAL SPEED AND EFFICACY FOR ECM BLOWERS

In addition to the overall efficiency that was discussed in Section 2, another index frequently used for evaluating blower energy performance is the efficacy (W per ft^3/min), which is the ratio of blower power to the airflow at a specific external static pressure. For example, the 2013 Building Energy Efficiency Standards for Residential and Nonresidential Buildings specifies a maximum efficacy of 0.58 W per ft^3/min for air handlers in residential central HVAC systems (CEC 2012). Also, the efficacy is used as the performance rating parameter in the new testing standard for residential furnace blowers issued by the Department of Energy in June 2014 (DOE 2014).

Efficacies were determined from the measured airflow and blower power data over a pressure range of 0.1 to 1.2 in. w.g. (25 to 300 Pa) for the six PSC blowers and the six ECM blowers tested in this study. As an example, Figure 70 compares efficacies for one PSC and one ECM blower over a range of blower speeds and external static pressures. It should be noted that the efficacy results in Figure 70 are the same PSC blower and the ECM blower that were shown as an example in Section 2 for airflow, power, and efficiency comparisons.

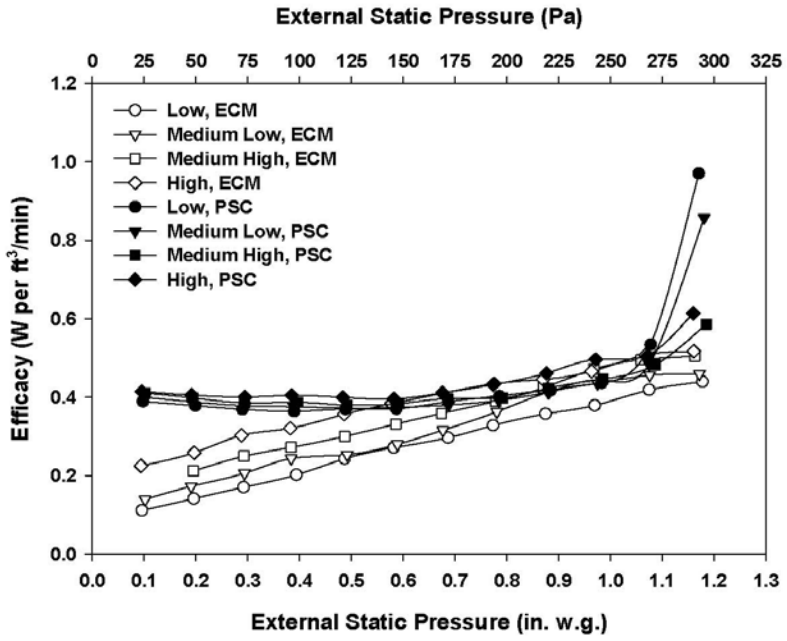

Figure 70 Efficacy comparison for one PSC blower and one ECM blower

As can be seen in Figure 70, the PSC blower and the ECM blower have different efficacy behaviors when the external static pressure is increased. For the PSC blower, all speeds have similar efficacy values that vary only slightly between 0.37 and 0.4 W per ft^3/min over a pressure range of 0.1 to 0.7 in. w.g. (25 to 175 Pa). At pressures above 0.7 in. w.g. (175 Pa), the efficacy gradually increases, indicating increasing blower power consumptions for the same airflow rate. However, a sharp efficacy increase occurs at even higher pressures above 1.1 in .w.g. (275 Pa), which is mainly caused by the sharp airflow decreases that were discussed in Section 2.

In contrast to the PSC blower, which has similar efficacy values for all speeds, the ECM blower always has higher efficacy values at lower blower speeds. For example,

at an external static pressure of 0.5 in. w.g. (125 Pa), the efficacy at the low speed is 0.24 W per ft^3/min that is 32% lower than the value of 0.36 W per ft^3/min at the high speed. Also, one can observe that the ECM blower has lower efficacies compared to the PSC blower at pressures below 0.5 in. w.g. (125 Pa), which shows the ECM blower's savings potential of using less power to deliver the same amount of air. For instance, under the most efficient operating condition of 0.1 in. w.g. (25 Pa) in the low speed, the efficacy for the ECM blower is about 32% lower than the value for the PSC blower at the same operating condition, showing 0.24 W per ft^3/min for the ECM blower and 0.37 W per ft^3/min for the PSC blower. However, the advantage of the ECM blower declines as the external static pressure is increased. At pressures above 0.8 in. w.g. (200 Pa), except for the low speed, efficacies of the PSC blower and the ECM blower falls into the same range of 0.4 to 0.5 W per ft^3/min.

As discussed earlier, Figure 70 shows that efficacies of both PSC and ECM blowers vary with external static pressures. For PSC blowers, the external static pressure can be used to predict the efficacy because efficacies are independent of blower speeds. However, the external static pressure alone is not enough as a predictor of efficacies for ECM blowers given the fact that a lower blower speed always has a higher efficacy value. Capturing the different efficacy behaviors of PSC and ECM blowers is of special importance to home energy auditors and field engineers, who have to frequently perform field measurements in residential buildings and need a reliable indicator of ECM blower performance.

An approach for using the blower rotational speed to predict the efficacy was developed for ECM blowers based on the experimental results for the six ECM blowers tested in this study. As the first step, the non-dimensional blower speed was calculated by using the blower speed and the maximum blower speed found over a range of pressures and speed settings. Then, the negative logarithm of the efficacy was plotted against the non-dimensional blower speed. A linear correlation was developed by taking the non-dimensional blower speed as the independent variable and the negative logarithm of the efficacy as the dependent variable. Figure 71 to Figure 76 compare the experimental data with developed correlations for the six ECM blowers tested in this study.

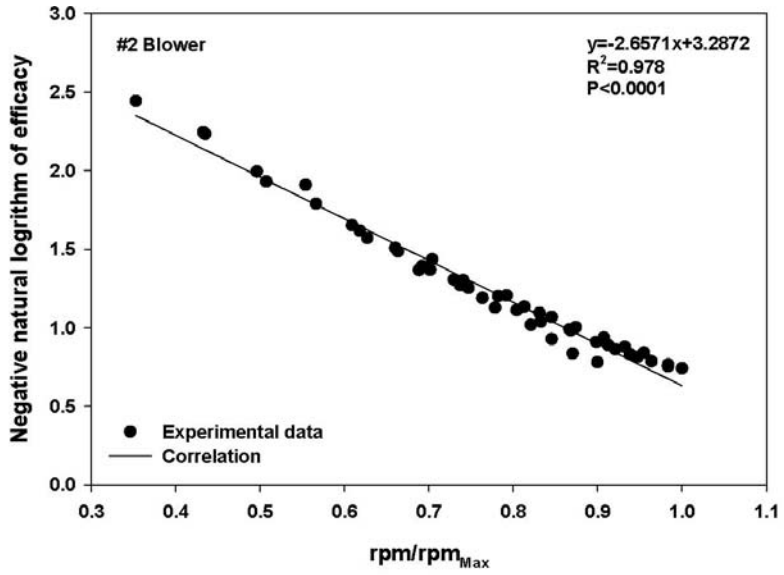

Figure 71 Correlation between blower speeds and efficacies for Blower #2

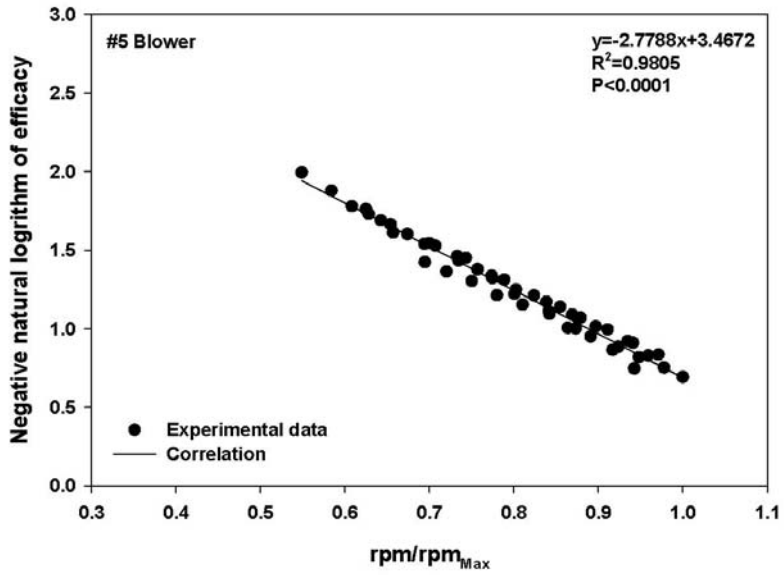

Figure 72 Correlation between blower speeds and efficacies for Blower #5

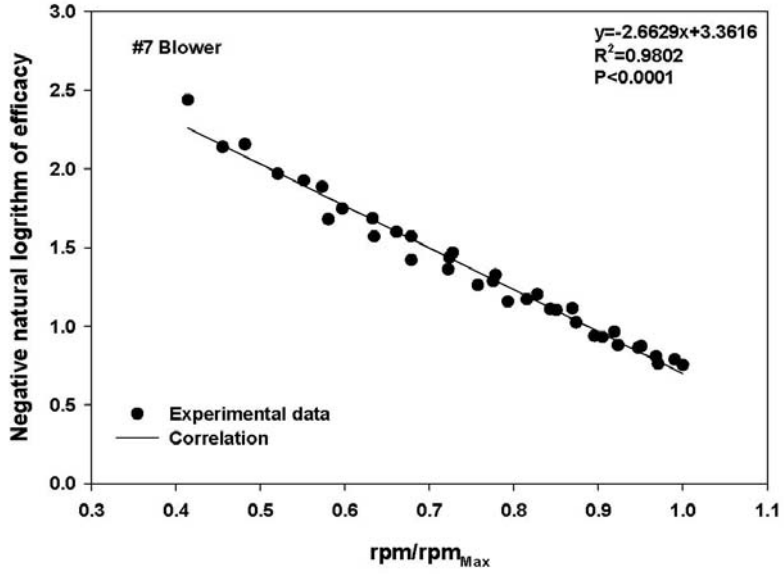

Figure 73 Correlation between blower speeds and efficacies for Blower #7

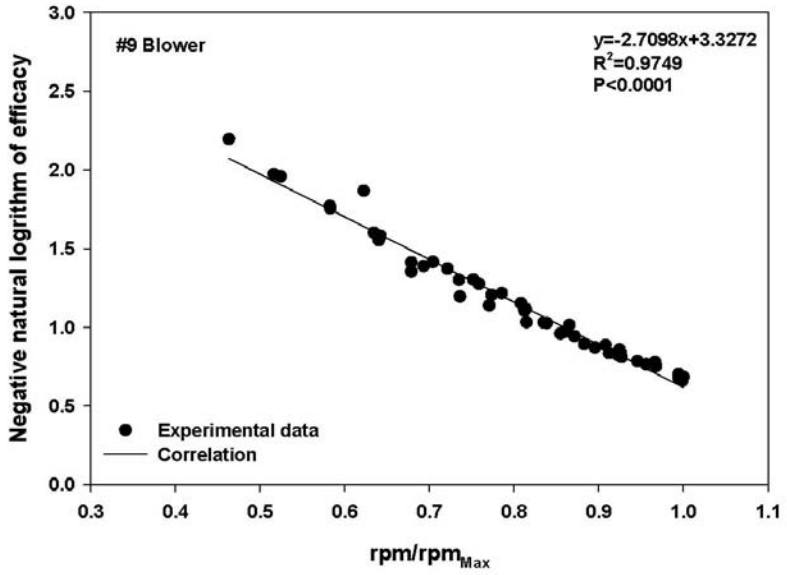

Figure 74 Correlation between blower speeds and efficacies for Blower #9

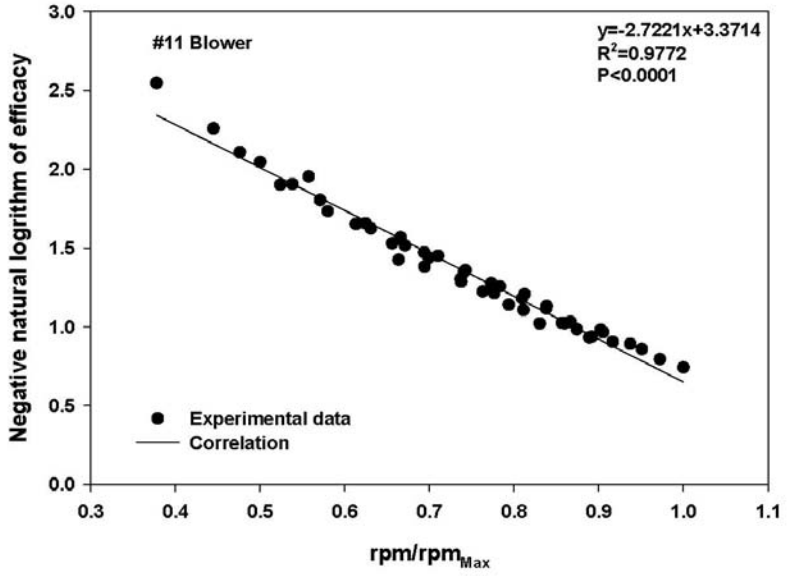

Figure 75 Correlation between blower speeds and efficacies for Blower #11

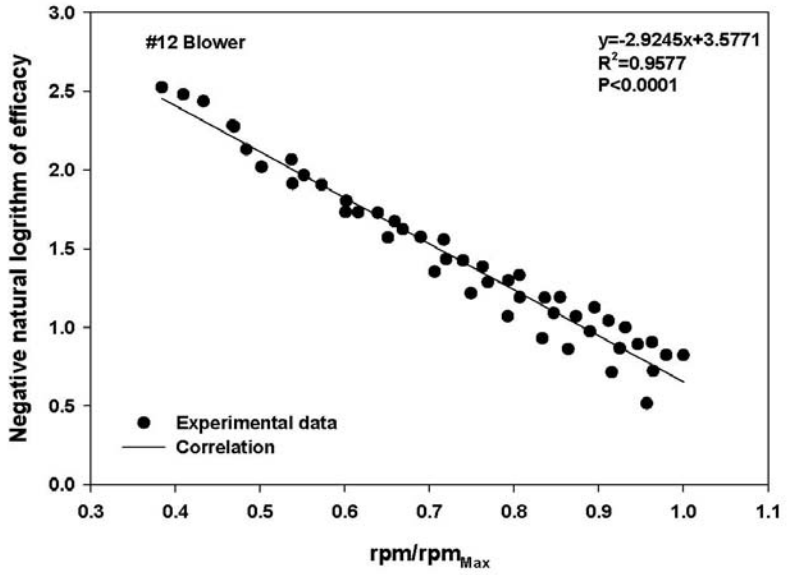

Figure 76 Correlation between blower speeds and efficacies for Blower #12

In addition to Figure 71 to Figure 76, Table 35 summarizes the coefficients and R^2 values for the developed correlations. As can be observed in Table 35, coefficients for the developed correlations vary from unit to unit, showing a range of -2.6571 to -2.9245 for the linear factor and a range of 3.2872 to 3.5771 for the offset factor. Variations in the coefficients may be attributable to various blower designs from different manufacturers, such as dimensions of housings and blower wheels, motor sizes, and speed control mechanisms.

Table 35 Coefficients and R^2 values for the developed correlations

Blower	Linear factor	Offset factor	R^2
#2	-2.6571	3.2872	0.978
#5	-2.7788	3.4672	0.9805
#7	-2.6629	3.3616	0.9802
#9	-2.7098	3.3272	0.9749
#11	-2.7221	3.3714	0.9772
#12	-2.9245	3.5771	0.9577

The good agreement between the experimental data and the correlations shown in Figure 71 to Figure 76 along with the R^2 values above 0.95 in Table 35 provide strong evidence for using rotational speeds as an indicator of ECM blower's efficacies. Specially, the developed approach can be used by field engineers to predict efficacies of ECM blowers based on the measurement of rotational speeds. The generated correlations can also be used to model the efficacy behaviors of ECM blowers at different operating conditions.

APPENDIX F BUILDING ENVELOP CONSTRUCTION AND MATERIAL PROPERTIES: THE CHICAGO HOME

Constructions and building material properties for the Chicago home are directly adopted from the residential prototype building models developed by the Pacific Northwest National Laboratory (2015) according to 2012 International Energy Conservation Code (ICC 2011). Table 36 and Table 37 summarize the thermal and physical properties of building materials used for modeling the Chicago home.

Table 36 Constructions and material properties for the Chicago home

Construction	Material	Roughness	Thickness	Conductivity	Density	Specific Heat
			m	W/m-K	kg/m^3	J/kg-K
Exterior Floor	floor_consol_layer	Rough	0.24	0.05	55	917
	Plywood_3/4in	Rough	0.02	0.12	545	675
	Carpet_n_pad	Medium Rough	0.03	0.06	32	837
Basement Wall	Plywood_3/4in	Rough	0.02	0.12	545	675
	bsmtwall_consol_layer	Rough	0.14	0.06	121	1036
	Plywood_3/4in	Rough	0.02	0.12	545	675
Exterior Wall	Stucco_1in	Medium Rough	0.03	1.4	1922	879
	Bldg_paper_felt*	Smooth	-	-	-	-
	sheathing_consol_layer	Rough	0.01	0.1	685	1172
	OSB_5/8in	Medium Rough	0.02	0.12	545	1213
	wall_consol_layer	Rough	0.14	0.06	121	1036
	Drywall_1/2in	Medium Rough	0.01	0.16	801	1088
Exterior Door	door_const	Smooth	0.03	0.07	513	768
Exterior Window	Glass**	-	-	-	-	-
Gable_end	Stucco_1in	Medium Rough	0.03	1.4	1922	879
	Bldg_paper_felt*	Smooth	-	-	-	-
	OSB_5/8in	Medium Rough	0.02	0.12	545	1213
	Air_4_in_vert***	-	-	-	-	-
	Drywall_1/2in	Medium Rough	0.01	0.16	801	1088

Table 36 Continued

Construction	Material	Roughness	Thickness	Conductivity	Density	Specific Heat
			m	W/m-K	kg/m^3	J/kg-K
Exterior Roof	Asphalt_shingle	Medium Rough	0.006	0.08	1121	1255
	OSB_1/2in	Rough	0.01	0.12	545	1213
Interior	ceil_consol_layer	Rough	0.37	0.06	42	776
Ceiling	Drywall_1/2in	Medium Rough	0.01	0.16	801	1088
Attic Floor	Drywall_1/2in	Medium Rough	0.01	0.16	801	1088
	ceil_consol_layer	Rough	0.37	0.06	42	776

*Object of Material:NoMass
**Object of WindowMaterial: SimpleGlazingSystem
***Object of Material: AirGap

Table 37 Properties of no-mass materials for the Chicago home

Material	Roughness	Thermal Resistance	U-Factor	Solar Heat Gain Coefficient	Visible Transmittance
		m^2-K/W	W/m^2-K	-	-
Bldg_paper_felt*	Smooth	0.01			
Glass**	-	-	1.8	0.4	0.88
Air_4_in_vert***	-	0.16		-	-

*Object of Material:NoMass
**Object of WindowMaterial: SimpleGlazingSystem
***Object of Material: AirGap

APPENDIX G BUILDING ENVELOP CONSTRUCTION AND MATERIAL PROPERTIES: THE AUSTIN HOME

Constructions and building material properties for the Austin home are directly adopted from the residential prototype building models developed by the Pacific Northwest National Laboratory (2015) according to 2012 International Energy Conservation Code (ICC 2011). Table 38 and Table 39 summarize the thermal and physical properties of building materials used for modeling the Austin home.

Table 38 Constructions and material properties for the Austin home

Construction	Material	Roughness	Thickness	Conductivity	Density	Specific Heat
			m	W/m-K	kg/m^3	J/kg-K
Exterior Floor	floor_consol_layer	Rough	0.09	0.05	55	917
	Plywood_3/4in	Rough	0.02	0.12	545	675
	Carpet_n_pad	Medium Rough	0.03	0.06	32	837
Exterior Wall	Stucco_1in	Medium Rough	0.03	1.4	1922	879
	Bldg_paper_felt*	Smooth	-	-	-	-
	sheathing_consol_layer	Rough	0.01	0.1	685	1172
	OSB_5/8in	Medium Rough	0.02	0.12	545	1213
	wall_consol_layer	Rough	0.09	0.06	121	1036
	Drywall_1/2in	Medium Rough	0.01	0.16	801	1088
Exterior Door	door_const	Smooth	0.03	0.07	513	768
Exterior Window	Glass**	-	-	-	-	-
Gable_end	Stucco_1in	Medium Rough	0.03	1.4	1922	879
	Bldg_paper_felt*	Smooth	-	-	-	-
	OSB_5/8in	Medium Rough	0.02	0.12	545	1213
	Air_4_in_vert***	-	-	-	-	-
	Drywall_1/2in	Medium Rough	0.01	0.16	801	1088
Exterior Roof	Asphalt_shingle	Medium Rough	0.006	0.08	1121	1255
	OSB_1/2in	Rough	0.01	0.12	545	1213
Interior Ceiling	ceil_consol_layer	Rough	0.32	0.06	42	776
	Drywall_1/2in	Medium Rough	0.01	0.16	801	1088

Table 38 Continued

Construction	Material	Roughness	Thickness	Conductivity	Density	Specific Heat
			m	W/m-K	kg/m^3	J/kg-K
Attic Floor	Drywall_1/2in	Medium Rough	0.01	0.16	801	1088
	ceil_consol_layer	Rough	0.32	0.06	42	776

*Object of Material:NoMass
**Object of WindowMaterial: SimpleGlazingSystem
***Object of Material: AirGap

Table 39 Properties of no-mass materials for the Austin home

Material	Roughness	Thermal Resistance	U-Factor	Solar Heat Gain Coefficient	Visible Transmittance
		m^2-K/W	W/m^2-K	-	-
Bldg_paper_felt*	Smooth	0.01			
Glass**	-	-	2.3	0.25	0.88
Air_4_in_vert***	-	0.16		-	-

*Object of Material:NoMass
**Object of WindowMaterial: SimpleGlazingSystem
***Object of Material: AirGap

APPENDIX H FLEXIBLE DUCTWORK DESIGNS FOR THE CHICAGO AND AUSTIN HOMES

Both the Chicago and Austin homes share the same ductwork layout, as shown in Figure 77. Duct sizing calculations strictly follow the design procedure in ACCA Manual D (Rutkowski 2011). As the first step, available static pressures (ASPs) are determined by subtracting component pressure drops from the design external static pressures of 0.3, 0.5, and 0.8 in. w.g. (75, 125, 200 Pa). The component pressure drops, such as pressure drops caused by filters, cooling coils, supply registers, and return grille, are assumed to be 0.26 in. w.g. (65 Pa) based on the values reported by Rutkowski (2011) and Wilcox (2006). Then, the total effective length (TEL) is calculated by summing the straight lengths of all duct sections and the fitting equivalent lengths for the run. It should be noted that calculations of the total effective length is only performed on the critical circulation path, which equals the sum of the longest supply run and the longest return run. With the knowledge of the available static pressure and the total effective length, the design friction rate (FR) can be calculated by using the following equation.

$$FR = \frac{ASP \times 100}{TEL} \quad (\text{in. w. g. per } 100 \text{ ft}) \tag{26}$$

The duct size is determined from the flexible duct friction chart (Chart 7) in Appendix 2 of ACCA Manual D (Rutkowski 2011) based on the design friction rate (FR) and the design airflow rate.

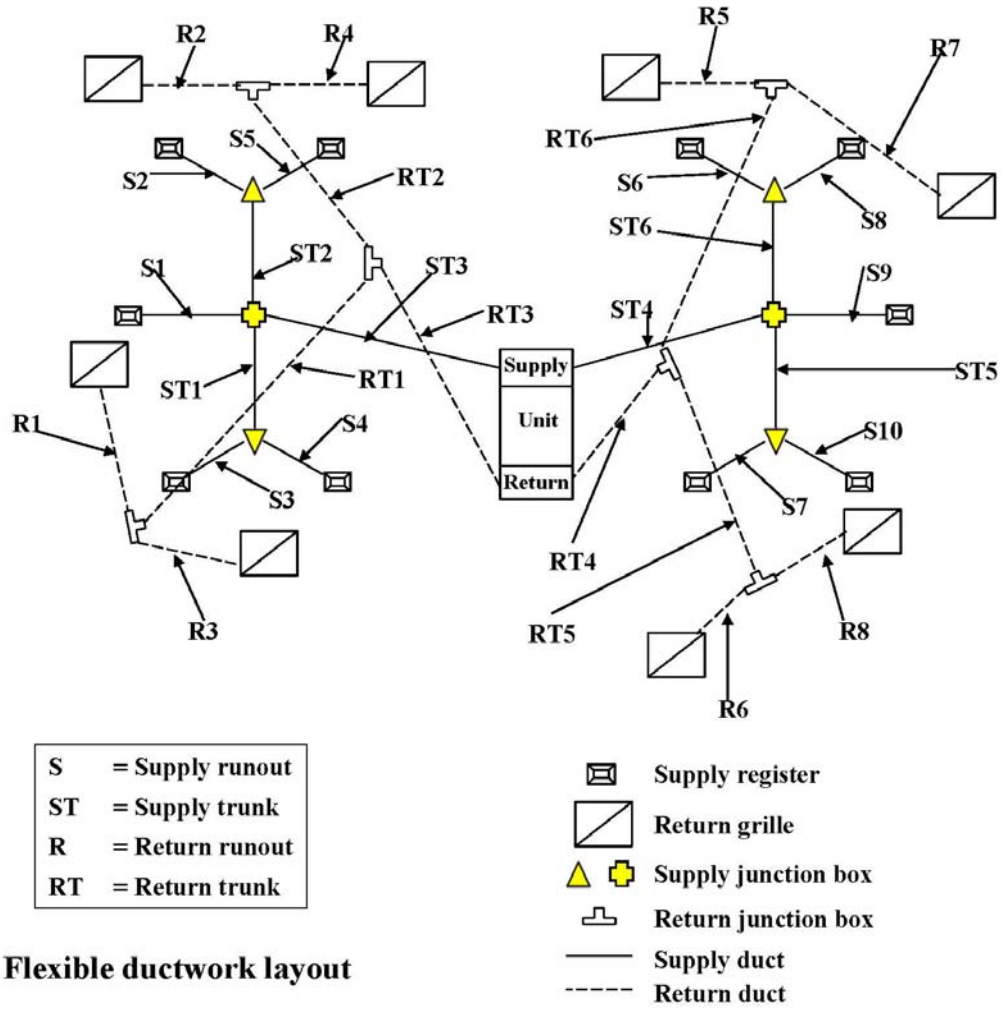

Figure 77 Flexible dutwork layout

The duct design procedures discussed above are incorporated into customized worksheets and used to design flexible ductworks with flow resistances of 0.3, 0.5, and 0.8 in. w.g. (75, 125, and 200 Pa) for both the Chicago home and the Austin home. Table 40 to Table 51 show the duct size and surface area calculations at various combinations of flow resistance and blower type for the Chicago home and the Austin home.

Table 40 Flexible duct sizing worksheet for the Chicago home (PSC+0.3 IWC)

Duct Sizing Worksheet (Chicago home Flex 0.3 IWC PSC)											
HF =	Blower CFM /		Heating Load =		1074	/	48000	=	0.022375	FR Value =	0.01
CF =	Blower CFM /		Cooling Load =		1074	/	30000	=	0.0358		
Supply Runout											
Name	H-Btu	C-Btu	H-Cfm	C-Cfm	Design Cfm	Round Size	Velocity	Final Size	Perimeter	Length	Surface Area
	Btu/hr	Btu/hr	cfm	cfm	cfm	inch	FPM	inch	ft	ft	ft^2
S1	4320	2460	97	88	97	**10**	177	**10**	2.62	10.00	26.18
S2	4032	2280	90	82	90	**10**	165	**10**	2.62	10.00	26.18
S3	3792	3000	85	107	107	**10**	197	**10**	2.62	10.00	26.18
S4	5376	3780	120	135	135	**12**	172	**12**	3.14	10.00	31.42
S5	6480	3600	145	129	145	**12**	185	**12**	3.14	10.00	31.42
S6	4272	2400	96	86	96	**10**	175	**10**	2.62	10.00	26.18
S7	4416	2580	99	92	99	**10**	181	**10**	2.62	10.00	26.18
S8	5760	3600	129	129	129	**10**	236	**10**	2.62	10.00	26.18
S9	3840	2400	86	86	86	**10**	158	**10**	2.62	10.00	26.18
S10	5712	3900	128	140	140	**12**	178	**12**	3.14	10.00	31.42
Supply Trunk											
			H-Cfm	C-Cfm	Design Cfm	Round Size	Velocity	Final Size	Perimeter	Length	Surface Area
			cfm	cfm	cfm	inch	FPM	inch	ft	ft	ft^2
ST 1	N/A		205	243	243	**14**	227	**14**	3.67	10.00	36.65
ST 2			235	211	235	**14**	220	**14**	3.67	10.00	36.65
ST 3			537	541	541	**20**	248	**20**	5.24	20.00	104.72
ST 4			537	533	537	**20**	246	**20**	5.24	20.00	104.72
ST 5			227	232	232	**14**	217	**14**	3.67	10.00	36.65
ST 6			224	215	224	**14**	210	**14**	3.67	10.00	36.65
Return Runout											
Name	Associated Supply run		H-Cfm	C-Cfm	Design Cfm	Round Size	Velocity	Final Size	Perimeter	Length	Surface Area
			cfm	cfm	cfm	inch	FPM	inch	ft	ft	ft^2
R1	S1		97	88	97	**10**	177	**10**	2.62	10.00	26.18
R2	S2		90	82	90	**10**	165	**10**	2.62	10.00	26.18
R3	S3, S4		205	243	243	**14**	227	**14**	3.67	10.00	36.65
R4	S5		145	129	145	**10**	266	**10**	2.62	10.00	26.18
R5	S6		96	86	96	**10**	175	**10**	2.62	10.00	26.18
R6	S7		99	92	99	**10**	181	**10**	2.62	10.00	26.18
R7	S8, S9		215	215	215	**14**	201	**14**	3.67	10.00	36.65
R8	S10		128	140	140	**10**	256	**10**	2.62	10.00	26.18
Return Trunk											
			H-Cfm	C-Cfm	Design Cfm	Round Size	Velocity	Final Size	Perimeter	Length	Surface Area
			cfm	cfm	cfm	inch	FPM	inch	ft	ft	ft^2
RT 1	N/A		302	331	331	**16**	237	**16**	4.19	10.00	41.89
RT 2			235	211	235	**12**	299	**12**	3.14	10.00	31.42
RT 3			537	541	541	**18**	306	**18**	4.71	15.00	70.69
RT 4			537	533	537	**18**	304	**18**	4.71	15.00	70.69
RT 5			227	232	232	**14**	217	**14**	3.67	10.00	36.65
RT 6			310	301	310	**16**	222	**16**	4.19	10.00	41.89

Table 41 Flexible duct sizing worksheet for the Chicago home (PSC+0.5 IWC)

Duct Sizing Worksheet (Chicago home Flex 0.5 IWC PSC)											
HF =	Blower CFM /		Heating Load =	997	/	48000	=	0.02077083	FR Value =	0.05	
CF =	Blower CFM /		Cooling Load =	997	/	30000	=	0.03323333			
Supply Runout											
Name	H-Btu	C-Btu	H-Cfm	C-Cfm	Design Cfm	Round Size	Velocity	Final Size	Perimeter	Length	Surface Area
	Btu/hr	Btu/hr	cfm	cfm	cfm	inch	FPM	inch	ft	ft	ft^2
S1	4320	2460	90	82	90	**7**	336	**7**	1.83	10.00	18.33
S2	4032	2280	84	76	84	**7**	313	**7**	1.83	10.00	18.33
S3	3792	3000	79	100	100	**7**	373	**7**	1.83	10.00	18.33
S4	5376	3780	112	126	126	**8**	360	**8**	2.09	10.00	20.94
S5	6480	3600	135	120	135	**8**	386	**8**	2.09	10.00	20.94
S6	4272	2400	89	80	89	**7**	332	**7**	1.83	10.00	18.33
S7	4416	2580	92	86	92	**7**	343	**7**	1.83	10.00	18.33
S8	5760	3600	120	120	120	**8**	343	**8**	2.09	10.00	20.94
S9	3840	2400	80	80	80	**7**	298	**7**	1.83	10.00	18.33
S10	5712	3900	119	130	130	**8**	371	**8**	2.09	10.00	20.94
Supply Trunk											
			H-Cfm	C-Cfm	Design Cfm	Round Size	Velocity	Final Size	Perimeter	Length	Surface Area
			cfm	cfm	cfm	inch	FPM	inch	ft	ft	ft^2
ST 1	N/A		190	225	225	**10**	413	**10**	2.62	10.00	26.18
ST 2			218	195	218	**10**	400	**10**	2.62	10.00	26.18
ST 3			499	502	502	**14**	470	**14**	3.67	20.00	73.30
ST 4			499	495	499	**14**	466	**14**	3.67	20.00	73.30
ST 5			210	215	215	**10**	395	**10**	2.62	10.00	26.18
ST 6			208	199	208	**10**	382	**10**	2.62	10.00	26.18
Return Runout											
Name	Associated Supply run		H-Cfm	C-Cfm	Design Cfm	Round Size	Velocity	Final Size	Perimeter	Length	Surface Area
			cfm	cfm	cfm	inch	FPM	inch	ft	ft	ft^2
R1	S1		90	82	90	**7**	336	**7**	1.83	10.00	18.33
R2	S2		84	76	84	**7**	313	**7**	1.83	10.00	18.33
R3	S3, S4		190	225	225	**10**	413	**10**	2.62	10.00	26.18
R4	S5		135	120	135	**8**	386	**8**	2.09	10.00	20.94
R5	S6		89	80	89	**7**	332	**7**	1.83	10.00	18.33
R6	S7		92	86	92	**7**	343	**7**	1.83	10.00	18.33
R7	S8, S9		199	199	199	**10**	366	**10**	2.62	10.00	26.18
R8	S10		119	130	130	**8**	371	**8**	2.09	10.00	20.94
Return Trunk											
			H-Cfm	C-Cfm	Design Cfm	Round Size	Velocity	Final Size	Perimeter	Length	Surface Area
			cfm	cfm	cfm	inch	FPM	inch	ft	ft	ft^2
RT 1	N/A		280	307	307	**12**	391	**12**	3.14	10.00	31.42
RT 2			218	195	218	**10**	400	**10**	2.62	10.00	26.18
RT 3			499	502	502	**14**	470	**14**	3.67	15.00	54.98
RT 4			499	495	499	**14**	466	**14**	3.67	15.00	54.98
RT 5			210	215	215	**9**	487	**9**	2.36	10.00	23.56
RT 6			288	279	288	**12**	367	**12**	3.14	10.00	31.42

Table 42 Flexible duct sizing worksheet for the Chicago home (PSC+0.8 IWC)

Duct Sizing Worksheet (Chicago home Flex 0.8 IWC PSC)												
HF =	Blower CFM /		Heating Load =		757	/	48000	=	0.01577083	FR Value =	0.12	
CF =	Blower CFM /		Cooling Load =		757	/	30000	=	0.02523333			
Supply Runout												
Name	H-Btu	C-Btu	H-Cfm	C-Cfm	Design Cfm	Round Size	Velocity	Final Size	Perimeter	Length	Surface Area	
	Btu/hr	Btu/hr	cfm	cfm	cfm	inch	FPM	inch	ft	ft	ft^2	
S1	4320	2460	68	62	68	**5**	500	**5**	1.31	10.00	13.09	
S2	4032	2280	64	58	64	**5**	466	**5**	1.31	10.00	13.09	
S3	3792	3000	60	76	76	**5**	555	**5**	1.31	10.00	13.09	
S4	5376	3780	85	95	95	**6**	486	**6**	1.57	10.00	15.71	
S5	6480	3600	102	91	102	**6**	520	**6**	1.57	10.00	15.71	
S6	4272	2400	67	61	67	**5**	494	**5**	1.31	10.00	13.09	
S7	4416	2580	70	65	70	**5**	511	**5**	1.31	10.00	13.09	
S8	5760	3600	91	91	91	**6**	463	**6**	1.57	10.00	15.71	
S9	3840	2400	61	61	61	**5**	444	**5**	1.31	10.00	13.09	
S10	5712	3900	90	98	98	**6**	501	**6**	1.57	10.00	15.71	
Supply Trunk												
			H-Cfm	C-Cfm	Design Cfm	Round Size	Velocity	Final Size	Perimeter	Length	Surface Area	
			cfm	cfm	cfm	inch	FPM	inch	ft	ft	ft^2	
ST 1	N/A		145	171	171	**7**	640	**7**	1.83	10.00	18.33	
ST 2			166	148	166	**7**	620	**7**	1.83	10.00	18.33	
ST 3			379	382	382	**10**	700	**10**	2.62	20.00	52.36	
ST 4			379	375	379	**10**	694	**10**	2.62	20.00	52.36	
ST 5			160	164	164	**7**	612	**7**	1.83	10.00	18.33	
ST 6			158	151	158	**7**	592	**7**	1.83	10.00	18.33	
Return Runout												
Name	Associated Supply run		H-Cfm	C-Cfm	Design Cfm	Round Size	Velocity	Final Size	Perimeter	Length	Surface Area	
			cfm	cfm	cfm	inch	FPM	inch	ft	ft	ft^2	
R1	S1		68	62	68	**5**	500	**5**	1.31	10.00	13.09	
R2	S2		64	58	64	**5**	466	**5**	1.31	10.00	13.09	
R3	S3, S4		145	171	171	**7**	640	**7**	1.83	10.00	18.33	
R4	S5		102	91	102	**6**	520	**6**	1.57	10.00	15.71	
R5	S6		67	61	67	**5**	494	**5**	1.31	10.00	13.09	
R6	S7		70	65	70	**5**	511	**5**	1.31	10.00	13.09	
R7	S8, S9		151	151	151	**7**	567	**7**	1.83	10.00	18.33	
R8	S10		90	98	98	**6**	501	**6**	1.57	10.00	15.71	
Return Trunk												
			H-Cfm	C-Cfm	Design Cfm	Round Size	Velocity	Final Size	Perimeter	Length	Surface Area	
			cfm	cfm	cfm	inch	FPM	inch	ft	ft	ft^2	
RT 1	N/A		213	233	233	**8**	668	**8**	2.09	10.00	20.94	
RT 2			166	148	166	**7**	620	**7**	1.83	10.00	18.33	
RT 3			379	382	382	**10**	700	**10**	2.62	15.00	39.27	
RT 4			379	375	379	**10**	694	**10**	2.62	15.00	39.27	
RT 5			160	164	164	**7**	612	**7**	1.83	10.00	18.33	
RT 6			219	212	219	**8**	627	**8**	2.09	10.00	20.94	

Table 43 Flexible duct sizing worksheet for the Chicago home (ECM+0.3 IWC)

Duct Sizing Worksheet (Chicago home Flex 0.3 ECM)											
HF =	Blower CFM /		Heating Load =		1000	/	48000	=	0.02083333	FR Value =	0.01
CF =	Blower CFM /		Cooling Load =		1000	/	30000	=	0.03333333		
Supply Runout											
Name	H-Btu	C-Btu	H-Cfm	C-Cfm	Design Cfm	Round Size	Velocity	Final Size	Perimeter	Length	Surface Area
	Btu/hr	Btu/hr	cfm	cfm	cfm	inch	FPM	inch	ft	ft	ft^2
S1	4320	2460	90	82	90	**9**	204	**9**	2.36	10.00	23.56
S2	4032	2280	84	76	84	**9**	190	**9**	2.36	10.00	23.56
S3	3792	3000	79	100	100	**10**	183	**10**	2.62	10.00	26.18
S4	5376	3780	112	126	126	**10**	231	**10**	2.62	10.00	26.18
S5	6480	3600	135	120	135	**10**	248	**10**	2.62	10.00	26.18
S6	4272	2400	89	80	89	**9**	201	**9**	2.36	10.00	23.56
S7	4416	2580	92	86	92	**9**	208	**9**	2.36	10.00	23.56
S8	5760	3600	120	120	120	**10**	220	**10**	2.62	10.00	26.18
S9	3840	2400	80	80	80	**9**	181	**9**	2.36	10.00	23.56
S10	5712	3900	119	130	130	**10**	238	**10**	2.62	10.00	26.18
Supply Trunk											
			H-Cfm	C-Cfm	Design Cfm	Round Size	Velocity	Final Size	Perimeter	Length	Surface Area
			cfm	cfm	cfm	inch	FPM	inch	ft	ft	ft^2
ST 1	N/A		191	226	226	**12**	288	**12**	3.14	10.00	31.42
ST 2			219	196	219	**12**	279	**12**	3.14	10.00	31.42
ST 3			500	504	504	**18**	285	**18**	4.71	20.00	94.25
ST 4			500	496	500	**18**	283	**18**	4.71	20.00	94.25
ST 5			211	216	216	**12**	275	**12**	3.14	10.00	31.42
ST 6			209	200	209	**12**	266	**12**	3.14	10.00	31.42
Return Runout											
Name	Associated Supply run		H-Cfm	C-Cfm	Design Cfm	Round Size	Velocity	Final Size	Perimeter	Length	Surface Area
			cfm	cfm	cfm	inch	FPM	inch	ft	ft	ft^2
R1	S1		90	82	90	**9**	204	**9**	2.36	10.00	23.56
R2	S2		84	76	84	**9**	190	**9**	2.36	10.00	23.56
R3	S3, S4		191	226	226	**12**	288	**12**	3.14	10.00	31.42
R4	S5		135	120	135	**10**	248	**10**	2.62	10.00	26.18
R5	S6		89	80	89	**9**	201	**9**	2.36	10.00	23.56
R6	S7		92	86	92	**9**	208	**9**	2.36	10.00	23.56
R7	S8, S9		200	200	200	**12**	255	**12**	3.14	10.00	31.42
R8	S10		119	130	130	**10**	238	**10**	2.62	10.00	26.18
Return Trunk											
			H-Cfm	C-Cfm	Design Cfm	Round Size	Velocity	Final Size	Perimeter	Length	Surface Area
			cfm	cfm	cfm	inch	FPM	inch	ft	ft	ft^2
RT 1	N/A		281	308	308	**16**	221	**16**	4.19	10.00	41.89
RT 2			219	196	219	**12**	279	**12**	3.14	10.00	31.42
RT 3			500	504	504	**18**	285	**18**	4.71	15.00	70.69
RT 4			500	496	500	**18**	283	**18**	4.71	15.00	70.69
RT 5			211	216	216	**12**	275	**12**	3.14	10.00	31.42
RT 6			289	280	289	**16**	207	**16**	4.19	10.00	41.89

Table 44 Flexible duct sizing worksheet for the Chicago home (ECM+0.5 IWC)

Duct Sizing Worksheet (Chicago home Flex 0.5 ECM)											
HF =	Blower CFM /		Heating Load =		1000	/	48000	=	0.02083333	FR Value =	0.05
CF =	Blower CFM /		Cooling Load =		1000	/	30000	=	0.03333333		
Supply Runout											
Name	H-Btu	C-Btu	H-Cfm	C-Cfm	Design Cfm	Round Size	Velocity	Final Size	Perimeter	Length	Surface Area
	Btu/hr	Btu/hr	cfm	cfm	cfm	inch	FPM	inch	ft	ft	ft^2
S1	4320	2460	90	82	90	**7**	337	**7**	1.83	10.00	18.33
S2	4032	2280	84	76	84	**7**	314	**7**	1.83	10.00	18.33
S3	3792	3000	79	100	100	**7**	374	**7**	1.83	10.00	18.33
S4	5376	3780	112	126	126	**8**	361	**8**	2.09	10.00	20.94
S5	6480	3600	135	120	135	**8**	387	**8**	2.09	10.00	20.94
S6	4272	2400	89	80	89	**7**	333	**7**	1.83	10.00	18.33
S7	4416	2580	92	86	92	**7**	344	**7**	1.83	10.00	18.33
S8	5760	3600	120	120	120	**8**	344	**8**	2.09	10.00	20.94
S9	3840	2400	80	80	80	**7**	299	**7**	1.83	10.00	18.33
S10	5712	3900	119	130	130	**8**	372	**8**	2.09	10.00	20.94
Supply Trunk											
			H-Cfm	C-Cfm	Design Cfm	Round Size	Velocity	Final Size	Perimeter	Length	Surface Area
			cfm	cfm	cfm	inch	FPM	inch	ft	ft	ft^2
ST 1	N/A		191	226	226	**10**	414	**10**	2.62	10.00	26.18
ST 2			219	196	219	**10**	402	**10**	2.62	10.00	26.18
ST 3			500	504	504	**14**	471	**14**	3.67	20.00	73.30
ST 4			500	496	500	**14**	468	**14**	3.67	20.00	73.30
ST 5			211	216	216	**10**	396	**10**	2.62	10.00	26.18
ST 6			209	200	209	**10**	383	**10**	2.62	10.00	26.18
Return Runout											
Name	Associated Supply run		H-Cfm	C-Cfm	Design Cfm	Round Size	Velocity	Final Size	Perimeter	Length	Surface Area
			cfm	cfm	cfm	inch	FPM	inch	ft	ft	ft^2
R1	S1		90	82	90	**7**	337	**7**	1.83	10.00	18.33
R2	S2		84	76	84	**7**	314	**7**	1.83	10.00	18.33
R3	S3, S4		191	226	226	**10**	414	**10**	2.62	10.00	26.18
R4	S5		135	120	135	**8**	387	**8**	2.09	10.00	20.94
R5	S6		89	80	89	**7**	333	**7**	1.83	10.00	18.33
R6	S7		92	86	92	**7**	344	**7**	1.83	10.00	18.33
R7	S8, S9		200	200	200	**10**	367	**10**	2.62	10.00	26.18
R8	S10		119	130	130	**8**	372	**8**	2.09	10.00	20.94
Return Trunk											
			H-Cfm	C-Cfm	Design Cfm	Round Size	Velocity	Final Size	Perimeter	Length	Surface Area
			cfm	cfm	cfm	inch	FPM	inch	ft	ft	ft^2
RT 1	N/A		281	308	308	**12**	392	**12**	3.14	10.00	31.42
RT 2			219	196	219	**10**	402	**10**	2.62	10.00	26.18
RT 3			500	504	504	**14**	471	**14**	3.67	15.00	54.98
RT 4			500	496	500	**14**	468	**14**	3.67	15.00	54.98
RT 5			211	216	216	**10**	396	**10**	2.62	10.00	26.18
RT 6			289	280	289	**12**	368	**12**	3.14	10.00	31.42

Table 45 Flexible duct sizing worksheet for the Chicago home (ECM+0.8 IWC)

Duct Sizing Worksheet (Chicago home Flex 0.8 IWC ECM)											
HF =	Blower CFM /		Heating Load =		1000	/	48000	=	0.02083333	FR Value =	0.12
CF =	Blower CFM /		Cooling Load =		1000	/	30000	=	0.03333333		
Supply Runout											
Name	H-Btu	C-Btu	H-Cfm	C-Cfm	Design Cfm	Round Size	Velocity	Final Size	Perimeter	Length	Surface Area
	Btu/hr	Btu/hr	cfm	cfm	cfm	inch	FPM	inch	ft	ft	ft^2
S1	4320	2460	90	82	90	**6**	458	**6**	1.57	10.00	15.71
S2	4032	2280	84	76	84	**6**	428	**6**	1.57	10.00	15.71
S3	3792	3000	79	100	100	**6**	509	**6**	1.57	10.00	15.71
S4	5376	3780	112	126	126	**7**	471	**7**	1.83	10.00	18.33
S5	6480	3600	135	120	135	**7**	505	**7**	1.83	10.00	18.33
S6	4272	2400	89	80	89	**6**	453	**6**	1.57	10.00	15.71
S7	4416	2580	92	86	92	**6**	469	**6**	1.57	10.00	15.71
S8	5760	3600	120	120	120	**7**	449	**7**	1.83	10.00	18.33
S9	3840	2400	80	80	80	**6**	407	**6**	1.57	10.00	15.71
S10	5712	3900	119	130	130	**7**	486	**7**	1.83	10.00	18.33
Supply Trunk											
			H-Cfm	C-Cfm	Design Cfm	Round Size	Velocity	Final Size	Perimeter	Length	Surface Area
			cfm	cfm	cfm	inch	FPM	inch	ft	ft	ft^2
ST 1	N/A		191	226	226	**8**	647	**8**	2.09	10.00	20.94
ST 2			219	196	219	**8**	627	**8**	2.09	10.00	20.94
ST 3			500	504	504	**12**	642	**12**	3.14	20.00	62.83
ST 4			500	496	500	**12**	637	**12**	3.14	20.00	62.83
ST 5			211	216	216	**8**	619	**8**	2.09	10.00	20.94
ST 6			209	200	209	**8**	599	**8**	2.09	10.00	20.94
Return Runout											
Name	Associated Supply run		H-Cfm	C-Cfm	Design Cfm	Round Size	Velocity	Final Size	Perimeter	Length	Surface Area
			cfm	cfm	cfm	inch	FPM	inch	ft	ft	ft^2
R1	S1		90	82	90	**6**	458	**6**	1.57	10.00	15.71
R2	S2		84	76	84	**6**	428	**6**	1.57	10.00	15.71
R3	S3, S4		191	226	226	**8**	647	**8**	2.09	10.00	20.94
R4	S5		135	120	135	**7**	505	**7**	1.83	10.00	18.33
R5	S6		89	80	89	**6**	453	**6**	1.57	10.00	15.71
R6	S7		92	86	92	**6**	469	**6**	1.57	10.00	15.71
R7	S8, S9		200	200	200	**8**	573	**8**	2.09	10.00	20.94
R8	S10		119	130	130	**7**	486	**7**	1.83	10.00	18.33
Return Trunk											
			H-Cfm	C-Cfm	Design Cfm	Round Size	Velocity	Final Size	Perimeter	Length	Surface Area
			cfm	cfm	cfm	inch	FPM	inch	ft	ft	ft^2
RT 1	N/A		281	308	308	**9**	697	**9**	2.36	10.00	23.56
RT 2			219	196	219	**8**	627	**8**	2.09	10.00	20.94
RT 3			500	504	504	**12**	642	**12**	3.14	15.00	47.12
RT 4			500	496	500	**12**	637	**12**	3.14	15.00	47.12
RT 5			211	216	216	**8**	619	**8**	2.09	10.00	20.94
RT 6			289	280	289	**9**	654	**9**	2.36	10.00	23.56

Table 46 Flexible duct sizing worksheet for the Austin home (PSC+0.3 IWC)

Duct Sizing Worksheet (Austin home Flex 0.3 IWC PSC)											
HF =	Blower CFM /		Heating Load =		1298	/	42000	=	0.030904762	FR Value =	0.01
CF =	Blower CFM /		Cooling Load =		1298	/	36000	=	0.036055556		
Supply Runout											
Name	H-Btu	C-Btu	H-Cfm	C-Cfm	Design Cfm	Round Size	Velocity	Final Size	Perimeter	Length	Surface Area
	Btu/hr	Btu/hr	cfm	cfm	cfm	inch	FPM	inch	ft	ft	ft^2
S1	3780	2952	117	106	117	**10**	214	**10**	2.62	10.00	26.18
S2	3528	2736	109	99	109	**10**	200	**10**	2.62	10.00	26.18
S3	3318	3600	103	130	130	**10**	238	**10**	2.62	10.00	26.18
S4	4704	4536	145	164	164	**12**	208	**12**	3.14	10.00	31.42
S5	5670	4320	175	156	175	**12**	223	**12**	3.14	10.00	31.42
S6	3738	2880	116	104	116	**10**	212	**10**	2.62	10.00	26.18
S7	3864	3096	119	112	119	**10**	219	**10**	2.62	10.00	26.18
S8	5040	4320	156	156	156	**10**	286	**10**	2.62	10.00	26.18
S9	3360	2880	104	104	104	**10**	190	**10**	2.62	10.00	26.18
S10	4998	4680	154	169	169	**12**	215	**12**	3.14	10.00	31.42
Supply Trunk											
			H-Cfm	C-Cfm	Design Cfm	Round Size	Velocity	Final Size	Perimeter	Length	Surface Area
			cfm	cfm	cfm	inch	FPM	inch	ft	ft	ft^2
ST 1	N/A		248	293	293	**16**	210	**16**	4.19	10.00	41.89
ST 2			284	254	284	**16**	204	**16**	4.19	10.00	41.89
ST 3			649	654	654	**20**	300	**20**	5.24	20.00	104.72
ST 4			649	644	649	**20**	297	**20**	5.24	20.00	104.72
ST 5			274	280	280	**16**	201	**16**	4.19	10.00	41.89
ST 6			271	260	271	**16**	194	**16**	4.19	10.00	41.89
Return Runout											
Name	Associated Supply run		H-Cfm	C-Cfm	Design Cfm	Round Size	Velocity	Final Size	Perimeter	Length	Surface Area
			cfm	cfm	cfm	inch	FPM	inch	ft	ft	ft^2
R1	S1		117	106	117	**10**	214	**10**	2.62	10.00	26.18
R2	S2		109	99	109	**10**	200	**10**	2.62	10.00	26.18
R3	S3, S4		248	293	293	**16**	210	**16**	4.19	10.00	41.89
R4	S5		175	156	175	**12**	223	**12**	3.14	10.00	31.42
R5	S6		116	104	116	**10**	212	**10**	2.62	10.00	26.18
R6	S7		119	112	119	**10**	219	**10**	2.62	10.00	26.18
R7	S8, S9		260	260	260	**14**	243	**14**	3.67	10.00	36.65
R8	S10		154	169	169	**12**	215	**12**	3.14	10.00	31.42
Return Trunk											
			H-Cfm	C-Cfm	Design Cfm	Round Size	Velocity	Final Size	Perimeter	Length	Surface Area
			cfm	cfm	cfm	inch	FPM	inch	ft	ft	ft^2
RT 1	N/A		365	400	400	**18**	226	**18**	4.71	10.00	47.12
RT 2			284	254	284	**16**	204	**16**	4.19	10.00	41.89
RT 3			649	654	654	**20**	300	**20**	5.24	15.00	78.54
RT 4			649	644	649	**20**	297	**20**	5.24	15.00	78.54
RT 5			274	280	280	**16**	201	**16**	4.19	10.00	41.89
RT 6			375	363	375	**16**	269	**16**	4.19	10.00	41.89

Table 47 Flexible duct sizing worksheet for the Austin home (PSC+0.5 IWC)

Duct Sizing Worksheet (Austin home Flex 0.5 IWC PSC)											
HF =	Blower CFM /		Heating Load =		1206	/	42000	=	0.028714286	FR Value =	0.05
CF =	Blower CFM /		Cooling Load =		1206	/	36000	=	0.0335		
Supply Runout											
Name	H-Btu	C-Btu	H-Cfm	C-Cfm	Design Cfm	Round Size	Velocity	Final Size	Perimeter	Length	Surface Area
	Btu/hr	Btu/hr	cfm	cfm	cfm	inch	FPM	inch	ft	ft	ft^2
S1	3780	2952	109	99	109	**7**	406	**7**	1.83	10.00	18.33
S2	3528	2736	101	92	101	**7**	379	**7**	1.83	10.00	18.33
S3	3318	3600	95	121	121	**8**	345	**8**	2.09	10.00	20.94
S4	4704	4536	135	152	152	**8**	435	**8**	2.09	10.00	20.94
S5	5670	4320	163	145	163	**8**	466	**8**	2.09	10.00	20.94
S6	3738	2880	107	96	107	**7**	402	**7**	1.83	10.00	18.33
S7	3864	3096	111	104	111	**7**	415	**7**	1.83	10.00	18.33
S8	5040	4320	145	145	145	**8**	415	**8**	2.09	10.00	20.94
S9	3360	2880	96	96	96	**7**	361	**7**	1.83	10.00	18.33
S10	4998	4680	144	157	157	**8**	449	**8**	2.09	10.00	20.94
Supply Trunk											
			H-Cfm	C-Cfm	Design Cfm	Round Size	Velocity	Final Size	Perimeter	Length	Surface Area
			cfm	cfm	cfm	inch	FPM	inch	ft	ft	ft^2
ST 1	N/A		230	273	273	**10**	500	**10**	2.62	10.00	26.18
ST 2			264	236	264	**10**	484	**10**	2.62	10.00	26.18
ST 3			603	608	608	**14**	569	**14**	3.67	20.00	73.30
ST 4			603	598	603	**14**	564	**14**	3.67	20.00	73.30
ST 5			254	260	260	**10**	478	**10**	2.62	10.00	26.18
ST 6			252	241	252	**10**	462	**10**	2.62	10.00	26.18
Return Runout											
Name	Associated Supply run		H-Cfm	C-Cfm	Design Cfm	Round Size	Velocity	Final Size	Perimeter	Length	Surface Area
			cfm	cfm	cfm	inch	FPM	inch	ft	ft	ft^2
R1	S1		109	99	109	**7**	406	**7**	1.83	10.00	18.33
R2	S2		101	92	101	**7**	379	**7**	1.83	10.00	18.33
R3	S3, S4		230	273	273	**10**	500	**10**	2.62	10.00	26.18
R4	S5		163	145	163	**8**	466	**8**	2.09	10.00	20.94
R5	S6		107	96	107	**7**	402	**7**	1.83	10.00	18.33
R6	S7		111	104	111	**7**	415	**7**	1.83	10.00	18.33
R7	S8, S9		241	241	241	**10**	442	**10**	2.62	10.00	26.18
R8	S10		144	157	157	**8**	449	**8**	2.09	10.00	20.94
Return Trunk											
			H-Cfm	C-Cfm	Design Cfm	Round Size	Velocity	Final Size	Perimeter	Length	Surface Area
			cfm	cfm	cfm	inch	FPM	inch	ft	ft	ft^2
RT 1	N/A		339	371	371	**12**	473	**12**	3.14	10.00	31.42
RT 2			264	236	264	**10**	484	**10**	2.62	10.00	26.18
RT 3			603	608	608	**14**	569	**14**	3.67	15.00	54.98
RT 4			603	598	603	**14**	564	**14**	3.67	15.00	54.98
RT 5			254	260	260	**10**	478	**10**	2.62	10.00	26.18
RT 6			349	338	349	**12**	444	**12**	3.14	10.00	31.42

Table 48 Flexible duct sizing worksheet for the Austin home (PSC+0.8 IWC)

Duct Sizing Worksheet (Austin home Flex 0.8 IWC PSC)											
HF =	Blower CFM /		Heating Load		915	/	42000	=	0.021785714	FR Value =	0.12
CF =	Blower CFM /		Cooling Load		915	/	36000	=	0.025416667		
Supply Runout											
Name	H-Btu	C-Btu	H-Cfm	C-Cfm	Design Cfm	Round Size	Velocity	Final Size	Perimeter	Length	Surface Area
	Btu/hr	Btu/hr	cfm	cfm	cfm	inch	FPM	inch	ft	ft	ft^2
S1	3780	2952	82	75	82	**6**	419	**6**	1.57	10.00	15.71
S2	3528	2736	77	70	77	**6**	391	**6**	1.57	10.00	15.71
S3	3318	3600	72	92	92	**6**	466	**6**	1.57	10.00	15.71
S4	4704	4536	102	115	115	**7**	431	**7**	1.83	10.00	18.33
S5	5670	4320	124	110	124	**7**	462	**7**	1.83	10.00	18.33
S6	3738	2880	81	73	81	**6**	415	**6**	1.57	10.00	15.71
S7	3864	3096	84	79	84	**6**	429	**6**	1.57	10.00	15.71
S8	5040	4320	110	110	110	**7**	411	**7**	1.83	10.00	18.33
S9	3360	2880	73	73	73	**6**	373	**6**	1.57	10.00	15.71
S10	4998	4680	109	119	119	**7**	445	**7**	1.83	10.00	18.33
Supply Trunk											
			H-Cfm	C-Cfm	Design Cfm	Round Size	Velocity	Final Size	Perimeter	Length	Surface Area
			cfm	cfm	cfm	inch	FPM	inch	ft	ft	ft^2
ST 1	N/A		175	207	207	**8**	592	**8**	2.09	10.00	20.94
ST 2			200	179	200	**8**	574	**8**	2.09	10.00	20.94
ST 3			458	461	461	**12**	587	**12**	3.14	20.00	62.83
ST 4			458	454	458	**12**	583	**12**	3.14	20.00	62.83
ST 5			193	198	198	**8**	566	**8**	2.09	10.00	20.94
ST 6			191	183	191	**8**	548	**8**	2.09	10.00	20.94
Return Runout											
Name	Associated Supply run		H-Cfm	C-Cfm	Design Cfm	Round Size	Velocity	Final Size	Perimeter	Length	Surface Area
			cfm	cfm	cfm	inch	FPM	inch	ft	ft	ft^2
R1	S1		82	75	82	**6**	419	**6**	1.57	10.00	15.71
R2	S2		77	70	77	**6**	391	**6**	1.57	10.00	15.71
R3	S3, S4		175	207	207	**9**	468	**9**	2.36	10.00	23.56
R4	S5		124	110	124	**7**	462	**7**	1.83	10.00	18.33
R5	S6		81	73	81	**6**	415	**6**	1.57	10.00	15.71
R6	S7		84	79	84	**6**	429	**6**	1.57	10.00	15.71
R7	S8, S9		183	183	183	**8**	524	**8**	2.09	10.00	20.94
R8	S10		109	119	119	**7**	445	**7**	1.83	10.00	18.33
Return Trunk											
			H-Cfm	C-Cfm	Design Cfm	Round Size	Velocity	Final Size	Perimeter	Length	Surface Area
			cfm	cfm	cfm	inch	FPM	inch	ft	ft	ft^2
RT 1	N/A		257	282	282	**9**	638	**9**	2.36	10.00	23.56
RT 2			200	179	200	**8**	574	**8**	2.09	10.00	20.94
RT 3			458	461	461	**12**	587	**12**	3.14	15.00	47.12
RT 4			458	454	458	**12**	583	**12**	3.14	15.00	47.12
RT 5			193	198	198	**8**	566	**8**	2.09	10.00	20.94
RT 6			264	256	264	**9**	599	**9**	2.36	10.00	23.56

Table 49 Flexible duct sizing worksheet for the Austin home (ECM+0.3 IWC)

Duct Sizing Worksheet (Austin home Flex 0.3 IWC ECM)											
HF =	Blower CFM /		Heating Load =		1200	/	42000	=	0.02857143	FR Value =	0.01
CF =	Blower CFM /		Cooling Load =		1200	/	36000	=	0.03333333		
Supply Runout											
Name	H-Btu	C-Btu	H-Cfm	C-Cfm	Design Cfm	Round Size	Velocity	Final Size	Perimeter	Length	Surface Area
	Btu/hr	Btu/hr	cfm	cfm	cfm	inch	FPM	inch	ft	ft	ft^2
S1	3780	2952	108	98	108	**10**	198	**10**	2.62	10.00	26.18
S2	3528	2736	101	91	101	**10**	185	**10**	2.62	10.00	26.18
S3	3318	3600	95	120	120	**10**	220	**10**	2.62	10.00	26.18
S4	4704	4536	134	151	151	**10**	277	**10**	2.62	10.00	26.18
S5	5670	4320	162	144	162	**10**	297	**10**	2.62	10.00	26.18
S6	3738	2880	107	96	107	**10**	196	**10**	2.62	10.00	26.18
S7	3864	3096	110	103	110	**10**	202	**10**	2.62	10.00	26.18
S8	5040	4320	144	144	144	**10**	264	**10**	2.62	10.00	26.18
S9	3360	2880	96	96	96	**10**	176	**10**	2.62	10.00	26.18
S10	4998	4680	143	156	156	**10**	286	**10**	2.62	10.00	26.18
Supply Trunk											
			H-Cfm	C-Cfm	Design Cfm	Round Size	Velocity	Final Size	Perimeter	Length	Surface Area
			cfm	cfm	cfm	inch	FPM	inch	ft	ft	ft^2
ST 1	N/A		229	271	271	**14**	254	**14**	3.67	10.00	36.65
ST 2			263	235	263	**14**	246	**14**	3.67	10.00	36.65
ST 3			600	605	605	**20**	277	**20**	5.24	20.00	104.72
ST 4			600	595	600	**20**	275	**20**	5.24	20.00	104.72
ST 5			253	259	259	**14**	242	**14**	3.67	10.00	36.65
ST 6			251	240	251	**14**	235	**14**	3.67	10.00	36.65
Return Runout											
Name	Associated Supply run		H-Cfm	C-Cfm	Design Cfm	Round Size	Velocity	Final Size	Perimeter	Length	Surface Area
			cfm	cfm	cfm	inch	FPM	inch	ft	ft	ft^2
R1	S1		108	98	108	**10**	198	**10**	2.62	10.00	26.18
R2	S2		101	91	101	**10**	185	**10**	2.62	10.00	26.18
R3	S3, S4		229	271	271	**14**	254	**14**	3.67	10.00	36.65
R4	S5		162	144	162	**10**	297	**10**	2.62	10.00	26.18
R5	S6		107	96	107	**10**	196	**10**	2.62	10.00	26.18
R6	S7		110	103	110	**10**	202	**10**	2.62	10.00	26.18
R7	S8, S9		240	240	240	**14**	225	**14**	3.67	10.00	36.65
R8	S10		143	156	156	**10**	286	**10**	2.62	10.00	26.18
Return Trunk											
			H-Cfm	C-Cfm	Design Cfm	Round Size	Velocity	Final Size	Perimeter	Length	Surface Area
			cfm	cfm	cfm	inch	FPM	inch	ft	ft	ft^2
RT 1	N/A		337	370	370	**16**	265	**16**	4.19	10.00	41.89
RT 2			263	235	263	**14**	246	**14**	3.67	10.00	36.65
RT 3			600	605	605	**20**	277	**20**	5.24	15.00	78.54
RT 4			600	595	600	**20**	275	**20**	5.24	15.00	78.54
RT 5			253	259	259	**14**	242	**14**	3.67	10.00	36.65
RT 6			347	336	347	**16**	248	**16**	4.19	10.00	41.89

Table 50 Flexible duct sizing worksheet for the Austin home (ECM+0.5 IWC)

Duct Sizing Worksheet (Austin home Flex 0.5 IWC ECM)											
HF =	Blower CFM /		Heating Load =		1200	/	42000	=	0.028571429	FR Value =	0.05
CF =	Blower CFM /		Cooling Load =		1200	/	36000	=	0.033333333		
Supply Runout											
Name	H-Btu	C-Btu	H-Cfm	C-Cfm	Design Cfm	Round Size	Velocity	Final Size	Perimeter	Length	Surface Area
	Btu/hr	Btu/hr	cfm	cfm	cfm	inch	FPM	inch	ft	ft	ft^2
S1	3780	2952	108	98	108	**7**	404	**7**	1.83	10.00	18.33
S2	3528	2736	101	91	101	**7**	377	**7**	1.83	10.00	18.33
S3	3318	3600	95	120	120	**8**	344	**8**	2.09	10.00	20.94
S4	4704	4536	134	151	151	**9**	342	**9**	2.36	10.00	23.56
S5	5670	4320	162	144	162	**9**	367	**9**	2.36	10.00	23.56
S6	3738	2880	107	96	107	**7**	400	**7**	1.83	10.00	18.33
S7	3864	3096	110	103	110	**7**	413	**7**	1.83	10.00	18.33
S8	5040	4320	144	144	144	**8**	413	**8**	2.09	10.00	20.94
S9	3360	2880	96	96	96	**7**	359	**7**	1.83	10.00	18.33
S10	4998	4680	143	156	156	**9**	353	**9**	2.36	10.00	23.56
Supply Trunk											
			H-Cfm	C-Cfm	Design Cfm	Round Size	Velocity	Final Size	Perimeter	Length	Surface Area
			cfm	cfm	cfm	inch	FPM	inch	ft	ft	ft^2
ST 1	N/A		229	271	271	**12**	345	**12**	3.14	10.00	31.42
ST 2			263	235	263	**12**	335	**12**	3.14	10.00	31.42
ST 3			600	605	605	**16**	433	**16**	4.19	20.00	83.78
ST 4			600	595	600	**16**	430	**16**	4.19	20.00	83.78
ST 5			253	259	259	**10**	475	**10**	2.62	10.00	26.18
ST 6			251	240	251	**10**	460	**10**	2.62	10.00	26.18
Return Runout											
Name	Associated Supply run		H-Cfm	C-Cfm	Design Cfm	Round Size	Velocity	Final Size	Perimeter	Length	Surface Area
			cfm	cfm	cfm	inch	FPM	inch	ft	ft	ft^2
R1	S1		108	98	108	**7**	404	**7**	1.83	10.00	18.33
R2	S2		101	91	101	**7**	377	**7**	1.83	10.00	18.33
R3	S3, S4		229	271	271	**12**	345	**12**	3.14	10.00	31.42
R4	S5		162	144	162	**9**	367	**9**	2.36	10.00	23.56
R5	S6		107	96	107	**7**	400	**7**	1.83	10.00	18.33
R6	S7		110	103	110	**7**	413	**7**	1.83	10.00	18.33
R7	S8, S9		240	240	240	**10**	440	**10**	2.62	10.00	26.18
R8	S10		143	156	156	**9**	353	**9**	2.36	10.00	23.56
Return Trunk											
			H-Cfm	C-Cfm	Design Cfm	Round Size	Velocity	Final Size	Perimeter	Length	Surface Area
			cfm	cfm	cfm	inch	FPM	inch	ft	ft	ft^2
RT 1	N/A		337	370	370	**12**	471	**12**	3.14	10.00	31.42
RT 2			263	235	263	**10**	482	**10**	2.62	10.00	26.18
RT 3			600	605	605	**16**	433	**16**	4.19	15.00	62.83
RT 4			600	595	600	**16**	430	**16**	4.19	15.00	62.83
RT 5			253	259	259	**10**	475	**10**	2.62	10.00	26.18
RT 6			347	336	347	**12**	442	**12**	3.14	10.00	31.42

Table 51 Flexible duct sizing worksheet for the Austin home (ECM+0.8 IWC)

Duct Sizing Worksheet (Austin home Flex 0.8 IWC ECM)											
HF =	Blower CFM /		Heating Load =		1200	/	42000	=	0.028571429	FR Value =	0.12
CF =	Blower CFM /		Cooling Load =		1200	/	36000	=	0.033333333		
Supply Runout											
Name	H-Btu	C-Btu	H-Cfm	C-Cfm	Design Cfm	Round Size	Velocity	Final Size	Perimeter	Length	Surface Area
	Btu/hr	Btu/hr	cfm	cfm	cfm	inch	FPM	inch	ft	ft	ft^2
S1	3780	2952	108	98	108	**6**	550	**6**	1.57	10.00	15.71
S2	3528	2736	101	91	101	**6**	513	**6**	1.57	10.00	15.71
S3	3318	3600	95	120	120	**7**	449	**7**	1.83	10.00	18.33
S4	4704	4536	134	151	151	**8**	433	**8**	2.09	10.00	20.94
S5	5670	4320	162	144	162	**8**	464	**8**	2.09	10.00	20.94
S6	3738	2880	107	96	107	**6**	544	**6**	1.57	10.00	15.71
S7	3864	3096	110	103	110	**6**	562	**6**	1.57	10.00	15.71
S8	5040	4320	144	144	144	**8**	413	**8**	2.09	10.00	20.94
S9	3360	2880	96	96	96	**6**	489	**6**	1.57	10.00	15.71
S10	4998	4680	143	156	156	**8**	447	**8**	2.09	10.00	20.94
Supply Trunk											
			H-Cfm	C-Cfm	Design Cfm	Round Size	Velocity	Final Size	Perimeter	Length	Surface Area
			cfm	cfm	cfm	inch	FPM	inch	ft	ft	ft^2
ST 1	N/A		229	271	271	**9**	614	**9**	2.36	10.00	23.56
ST 2			263	235	263	**9**	595	**9**	2.36	10.00	23.56
ST 3			600	605	605	**12**	770	**12**	3.14	20.00	62.83
ST 4			600	595	600	**12**	764	**12**	3.14	20.00	62.83
ST 5			253	259	259	**9**	587	**9**	2.36	10.00	23.56
ST 6			251	240	251	**9**	568	**9**	2.36	10.00	23.56
Return Runout											
Name	Associated Supply run		H-Cfm	C-Cfm	Design Cfm	Round Size	Velocity	Final Size	Perimeter	Length	Surface Area
			cfm	cfm	cfm	inch	FPM	inch	ft	ft	ft^2
R1	S1		108	98	108	**6**	550	**6**	1.57	10.00	15.71
R2	S2		101	91	101	**6**	513	**6**	1.57	10.00	15.71
R3	S3, S4		229	271	271	**9**	614	**9**	2.36	10.00	23.56
R4	S5		162	144	162	**8**	464	**8**	2.09	10.00	20.94
R5	S6		107	96	107	**6**	544	**6**	1.57	10.00	15.71
R6	S7		110	103	110	**6**	562	**6**	1.57	10.00	15.71
R7	S8, S9		240	240	240	**9**	543	**9**	2.36	10.00	23.56
R8	S10		143	156	156	**7**	584	**7**	1.83	10.00	18.33
Return Trunk											
			H-Cfm	C-Cfm	Design Cfm	Round Size	Velocity	Final Size	Perimeter	Length	Surface Area
			cfm	cfm	cfm	inch	FPM	inch	ft	ft	ft^2
RT 1	N/A		337	370	370	**10**	678	**10**	2.62	10.00	26.18
RT 2			263	235	263	**9**	595	**9**	2.36	10.00	23.56
RT 3			600	605	605	**12**	770	**12**	3.14	15.00	47.12
RT 4			600	595	600	**12**	764	**12**	3.14	15.00	47.12
RT 5			253	259	259	**9**	587	**9**	2.36	10.00	23.56
RT 6			347	336	347	**10**	636	**10**	2.62	10.00	26.18

APPENDIX I SHEET METAL DUCTWORK DESIGNS FOR THE CHICAGO AND AUSTIN HOMES

Similar to flexible ductwork designs, both the Chicago and Austin homes have the same layout for the rigid sheet metal ductwork, as shown in Figure 78. Again, ACCA Manual D (Rutkowski 2011) is used as the guideline for the duct sizing calculation. As the first step, available static pressures (ASPs) are determined by subtracting component pressure drops from the design external static pressures of 0.3, 0.5, and 0.8 in. w.g. (75, 125, 200 Pa). The component pressure drops, such as pressure drops caused by filters, cooling coils, supply registers, and return grille, are assumed to be 0.26 in. w.g. (65 Pa) based on the values reported by Rutkowski (2011) and Wilcox (2006). Then, the total effective length (TEL) is calculated by summing the straight lengths of all duct sections and the fitting equivalent lengths for the run. It should be noted that calculations of the total effective length is only performed on the critical circulation path, which equals the sum of the longest supply run and the longest return run. With the knowledge of the available static pressure and the total effective length, the design friction rate (FR) can be calculated by using Equation (26). The circular duct size is determined from the metal duct friction chart (Chart 1) in Appendix 2 of ACCA Manual D (Rutkowski 2011) based on the design friction rate (FR) and the design airflow rate. In addition, circular duct sizes of supply and return trunks are converted to rectangular duct sizes based on the equal friction rate by using the Chart 9 in Appendix 2 of ACCA Manual D (Rutkowski 2011).

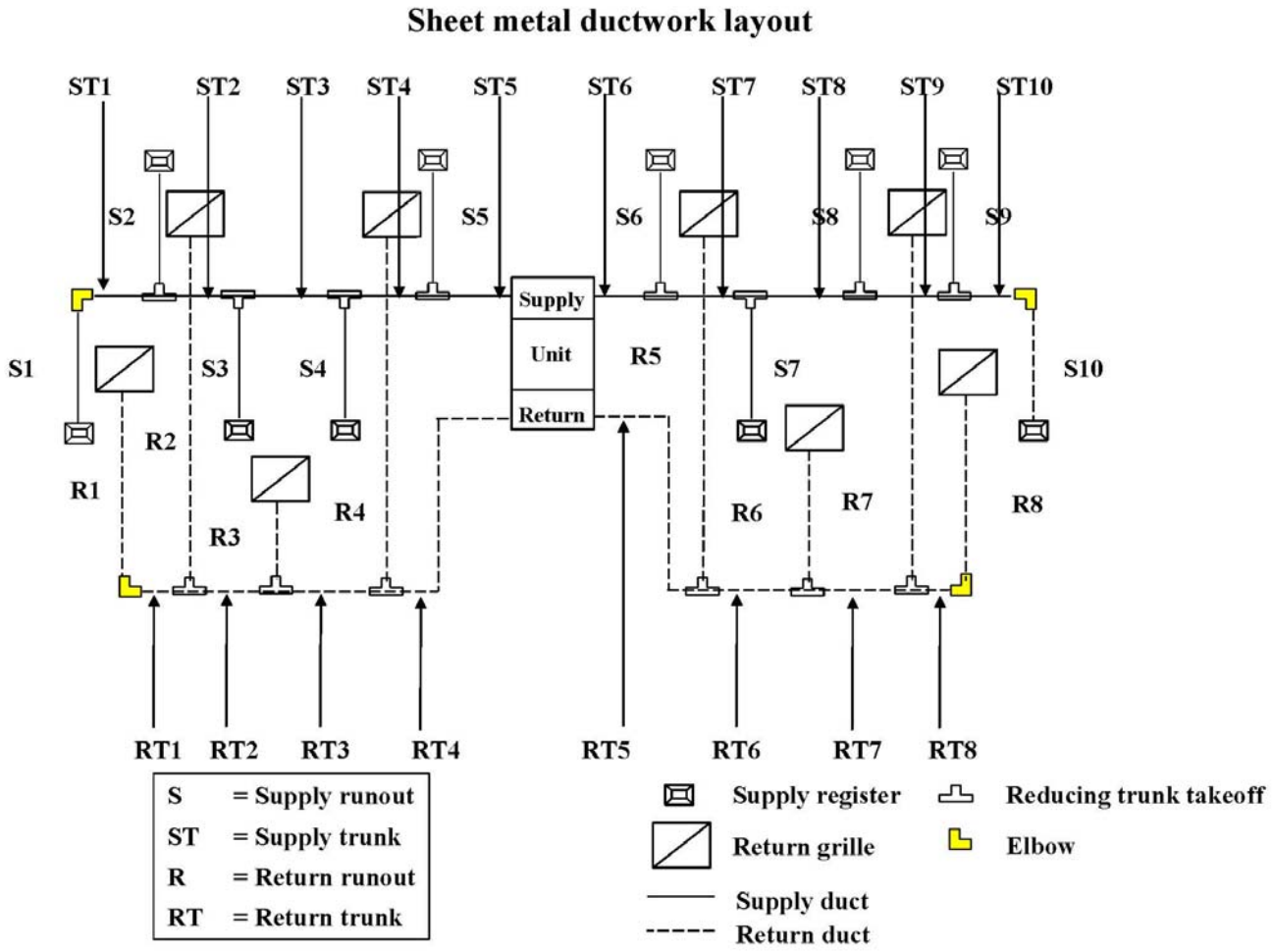

Figure 78 Sheet metal ductwork layout

Similar to the flexible ductwork design, customized worksheets are used to size sheet metal ducts at flow resistances of 0.3, 0.5, and 0.8 in. w.g. (75, 125, and 200 Pa) for both the Chicago and Austin homes. Table 52 to Table 63 show the results of sheet metal duct sizes and surface areas at various combinations of flow resistance and blower type.

Table 52 Sheet metal duct sizing worksheet for the Chicago home (PSC+0.3 IWC)

Duct Sizing Worksheet (Chicago home Rigid 0.3 IWC PSC)													
HF =	Blower CFM -		Heating Load =		1073	/	48000	=	0.02235417			FR Value =	0.01
CF =	Blower CFM -		Cooling Load =		1073	/	30000	=	0.03576667				
Supply Runout													
Name	H-Btu	C-Btu	H-Cfm	C-Cfm	Design Cfm	Round Size	Velocity	Final Size	Perimeter	Length	Surface Area		
	Btu/hr	Btu/hr	cfm	cfm	cfm	inch	FPM	inch	ft	ft	ft^2		
S1	4320	2460	97	88	97	**9**	219	**9**	2.36	10.00	23.56		
S2	4032	2280	90	82	90	**9**	204	**9**	2.36	10.00	23.56		
S3	3792	3000	85	107	107	**9**	243	**9**	2.36	13.00	30.63		
S4	5376	3780	120	135	135	**10**	248	**10**	2.62	13.00	34.03		
S5	6480	3600	145	129	145	**10**	266	**10**	2.62	13.00	34.03		
S6	4272	2400	95	86	95	**9**	216	**9**	2.36	13.00	30.63		
S7	4416	2580	99	92	99	**9**	223	**9**	2.36	15.00	35.34		
S8	5760	3600	129	129	129	**10**	236	**10**	2.62	15.00	39.27		
S9	3840	2400	86	86	86	**9**	194	**9**	2.36	15.00	35.34		
S10	5712	3900	128	139	139	**10**	256	**10**	2.62	13.00	34.03		
Supply Trunk													
			H-Cfm	C-Cfm	Design Cfm	Round Size	Velocity	Final Size			Perimeter	Length	Surface Area
			cfm	cfm	cfm	inch	FPM	H	×	W	ft	ft	ft^2
ST 1	N/A		97	88	97	**9**	219	**14**	×	**5**	3.17	5.00	15.83
ST 2			187	170	187	**12**	238	**14**	×	**9**	3.83	5.00	19.17
ST 3			271	277	277	**14**	259	**14**	×	**12**	4.33	10.00	43.33
ST 4			392	412	412	**16**	295	**14**	×	**15**	4.83	5.00	24.17
ST 5			537	541	541	**18**	306	**14**	×	**20**	5.67	5.00	28.33
ST 6			537	532	537	**18**	304	**14**	×	**20**	5.67	5.00	28.33
ST 7			441	446	446	**16**	320	**14**	×	**15**	4.83	10.00	48.33
ST 8			342	354	354	**14**	331	**14**	×	**12**	4.33	5.00	21.67
ST 9			214	225	225	**12**	287	**14**	×	**9**	3.83	5.00	19.17
ST 10			128	139	139	**10**	256	**14**	×	**6**	3.33	5.00	16.67
Return Runout													
Name	Associated Supply run		H-Cfm	C-Cfm	Design Cfm	Round Size	Velocity	Final Size	Perimeter	Length	Surface Area		
			cfm	cfm	cfm	inch	FPM	inch	ft	ft	ft^2		
R1	S1		97	88	97	**9**	219	**9**	2.36	5.00	11.78		
R2	S2		90	82	90	**9**	204	**9**	2.36	5.00	11.78		
R3	S3, S4		205	242	242	**14**	227	**14**	3.67	7.00	25.66		
R4	S5		145	129	145	**10**	266	**10**	2.62	6.00	15.71		
R5	S6		95	86	95	**9**	216	**9**	2.36	7.00	16.49		
R6	S7		99	92	99	**9**	223	**9**	2.36	8.00	18.85		
R7	S8, S9		215	215	215	**12**	273	**12**	3.14	7.00	21.99		
R8	S10		128	139	139	**10**	256	**10**	2.62	6.00	15.71		
Return Trunk													
			H-Cfm	C-Cfm	Design Cfm	Round Size	Velocity	Final Size			Perimeter	Length	Surface Area
			cfm	cfm	cfm	inch	FPM	H	×	W	ft	ft	ft^2
RT 1	N/A		97	88	97	**9**	219	**14**	×	**5**	3.17	5.00	15.83
RT 2			187	170	187	**12**	238	**14**	×	**9**	3.83	5.00	19.17
RT 3			392	412	412	**16**	295	**14**	×	**15**	4.83	5.00	24.17
RT 4			537	541	541	**18**	306	**14**	×	**20**	5.67	5.00	28.33
RT 5			537	532	537	**18**	304	**14**	×	**20**	5.67	5.00	28.33
RT 6			441	446	446	**16**	320	**14**	×	**15**	4.83	5.00	24.17
RT 7			342	354	354	**14**	331	**14**	×	**12**	4.33	5.00	21.67
RT 8			128	139	139	**10**	256	**14**	×	**6**	3.33	5.00	16.67

Table 53 Sheet metal duct sizing worksheet for the Chicago home (PSC+0.5 IWC)

Duct Sizing Worksheet (Chicago home Rigid 0.5 IWC PSC)													
HF =	Blower CFM -		Heating Load =	997	/	48000	=	0.02077083			FR Value =	0.06	
CF =	Blower CFM -		Cooling Load =	997	/	30000	=	0.03323333					
Supply Runout													
Name	H-Btu	C-Btu	H-Cfm	C-Cfm	Design Cfm	Round Size	Velocity	Final Size	Perimeter	Length	Surface Area		
	Btu/hr	Btu/hr	cfm	cfm	cfm	inch	FPM	inch	ft	ft	ft^2		
S1	4320	2460	90	82	90	**6**	457	**6**	1.57	10.00	15.71		
S2	4032	2280	84	76	84	**6**	427	**6**	1.57	10.00	15.71		
S3	3792	3000	79	100	100	**6**	508	**6**	1.57	13.00	20.42		
S4	5376	3780	112	126	126	**7**	470	**7**	1.83	13.00	23.82		
S5	6480	3600	135	120	135	**7**	504	**7**	1.83	13.00	23.82		
S6	4272	2400	89	80	89	**6**	452	**6**	1.57	13.00	20.42		
S7	4416	2580	92	86	92	**6**	467	**6**	1.57	15.00	23.56		
S8	5760	3600	120	120	120	**7**	448	**7**	1.83	15.00	27.49		
S9	3840	2400	80	80	80	**6**	406	**6**	1.57	15.00	23.56		
S10	5712	3900	119	130	130	**7**	485	**7**	1.83	13.00	23.82		
Supply Trunk													
			H-Cfm	C-Cfm	Design Cfm	Round Size	Velocity	Final Size			Perimeter	Length	Surface Area
			cfm	cfm	cfm	inch	FPM	H	×	W	ft	ft	ft^2
ST 1			90	82	90	**6**	457	**11**	×	**3**	2.33	5.00	11.67
ST 2			173	158	173	**8**	497	**11**	×	**5**	2.67	5.00	13.33
ST 3			252	257	257	**9**	582	**11**	×	**6**	2.83	10.00	28.33
ST 4			364	383	383	**12**	487	**11**	×	**11**	3.67	5.00	18.33
ST 5	N/A		499	502	502	**12**	640	**11**	×	**11**	3.67	5.00	18.33
ST 6			499	495	499	**12**	635	**11**	×	**11**	3.67	5.00	18.33
ST 7			410	415	415	**12**	528	**11**	×	**11**	3.67	10.00	36.67
ST 8			318	329	329	**14**	308	**11**	×	**15**	4.33	5.00	21.67
ST 9			198	209	209	**8**	600	**11**	×	**5**	2.67	5.00	13.33
ST 10			119	130	130	**7**	485	**11**	×	**4**	2.50	5.00	12.50
Return Runout													
Name	Associated Supply run		H-Cfm	C-Cfm	Design Cfm	Round Size	Velocity	Final Size	Perimeter	Length	Surface Area		
			cfm	cfm	cfm	inch	FPM	inch	ft	ft	ft^2		
R1	S1		90	82	90	**6**	457	**6**	1.57	5.00	7.85		
R2	S2		84	76	84	**6**	427	**6**	1.57	5.00	7.85		
R3	S3, S4		190	225	225	**8**	645	**8**	2.09	7.00	14.66		
R4	S5		135	120	135	**7**	504	**7**	1.83	6.00	11.00		
R5	S6		89	80	89	**6**	452	**6**	1.57	7.00	11.00		
R6	S7		92	86	92	**6**	467	**6**	1.57	8.00	12.57		
R7	S8, S9		199	199	199	**8**	571	**8**	2.09	7.00	14.66		
R8	S10		119	130	130	**7**	485	**7**	1.83	6.00	11.00		
Return Trunk													
			H-Cfm	C-Cfm	Design Cfm	Round Size	Velocity	Final Size			Perimeter	Length	Surface Area
			cfm	cfm	cfm	inch	FPM	H	×	W	ft	ft	ft^2
RT 1			90	82	90	**6**	457	**11**	×	**3**	2.33	5.00	11.67
RT 2			173	158	173	**8**	497	**11**	×	**5**	2.67	5.00	13.33
RT 3			364	383	383	**12**	487	**11**	×	**11**	3.67	5.00	18.33
RT 4	N/A		499	502	502	**12**	640	**11**	×	**11**	3.67	5.00	18.33
RT 5			499	495	499	**12**	635	**11**	×	**11**	3.67	5.00	18.33
RT 6			410	415	415	**10**	760	**11**	×	**8**	3.17	5.00	15.83
RT 7			318	329	329	**10**	603	**11**	×	**8**	3.17	5.00	15.83
RT 8			119	130	130	**7**	485	**11**	×	**4**	2.50	5.00	12.50

Table 54 Sheet metal duct sizing worksheet for the Chicago home (PSC+0.8 IWC)

Duct Sizing Worksheet (Chicago home Rigid 0.8 IWC PSC)													
HF =	Blower CFM -		Heating Load =		757	/	48000	=	0.01577083			FR Value =	0.13
CF =	Blower CFM -		Cooling Load =		757	/	30000	=	0.02523333				
Supply Runout													
Name	H-Btu	C-Btu	H-Cfm	C-Cfm	Design Cfm	Round Size	Velocity	Final Size	Perimeter	Length	Surface Area		
	Btu/hr	Btu/hr	cfm	cfm	cfm	inch	FPM	inch	ft	ft	ft^2		
S1	4320	2460	68	62	68	**5**	500	**5**	1.31	10.00	13.09		
S2	4032	2280	64	58	64	**5**	466	**5**	1.31	10.00	13.09		
S3	3792	3000	60	76	76	**5**	555	**5**	1.31	13.00	17.02		
S4	5376	3780	85	95	95	**6**	486	**6**	1.57	13.00	20.42		
S5	6480	3600	102	91	102	**6**	520	**6**	1.57	13.00	20.42		
S6	4272	2400	67	61	67	**5**	494	**5**	1.31	13.00	17.02		
S7	4416	2580	70	65	70	**5**	511	**5**	1.31	15.00	19.63		
S8	5760	3600	91	91	91	**6**	463	**6**	1.57	15.00	23.56		
S9	3840	2400	61	61	61	**5**	444	**5**	1.31	15.00	19.63		
S10	5712	3900	90	98	98	**6**	501	**6**	1.57	13.00	20.42		
Supply Trunk													
			H-Cfm	C-Cfm	Design Cfm	Round Size	Velocity	Final Size			Perimeter	Length	Surface Area
			cfm	cfm	cfm	inch	FPM	H	×	W	ft	ft	ft^2
ST 1			68	62	68	**5**	500	**7**	×	**3**	1.67	5.00	8.33
ST 2			132	120	132	**7**	493	**7**	×	**6**	2.17	5.00	10.83
ST 3			192	195	195	**8**	560	**7**	×	**8**	2.50	10.00	25.00
ST 4			276	291	291	**9**	658	**7**	×	**10**	2.83	5.00	14.17
ST 5	N/A		379	382	382	**12**	486	**7**	×	**18**	4.17	5.00	20.83
ST 6			379	375	379	**12**	482	**7**	×	**18**	4.17	5.00	20.83
ST 7			311	315	315	**9**	713	**7**	×	**10**	2.83	10.00	28.33
ST 8			241	250	250	**9**	565	**7**	×	**10**	2.83	5.00	14.17
ST 9			151	159	159	**7**	595	**7**	×	**6**	2.17	5.00	10.83
ST 10			90	98	98	**6**	501	**7**	×	**5**	2.00	5.00	10.00
Return Runout													
Name	Associated Supply run		H-Cfm	C-Cfm	Design Cfm	Round Size	Velocity	Final Size	Perimeter	Length	Surface Area		
			cfm	cfm	cfm	inch	FPM	inch	ft	ft	ft^2		
R1	S1		68	62	68	**5**	500	**5**	1.31	5.00	6.54		
R2	S2		64	58	64	**5**	466	**5**	1.31	5.00	6.54		
R3	S3, S4		145	171	171	**7**	640	**7**	1.83	7.00	12.83		
R4	S5		102	91	102	**6**	520	**6**	1.57	6.00	9.42		
R5	S6		67	61	67	**5**	494	**5**	1.31	7.00	9.16		
R6	S7		70	65	70	**5**	511	**5**	1.31	8.00	10.47		
R7	S8, S9		151	151	151	**7**	567	**7**	1.83	7.00	12.83		
R8	S10		90	98	98	**6**	501	**6**	1.57	6.00	9.42		
Return Trunk													
			H-Cfm	C-Cfm	Design Cfm	Round Size	Velocity	Final Size			Perimeter	Length	Surface Area
			cfm	cfm	cfm	inch	FPM	H	×	W	ft	ft	ft^2
RT 1			68	62	68	**5**	500	**7**	×	**3**	1.67	5.00	8.33
RT 2			132	120	132	**7**	493	**7**	×	**6**	2.17	5.00	10.83
RT 3			276	291	291	**10**	533	**7**	×	**12**	3.17	5.00	15.83
RT 4	N/A		379	382	382	**12**	486	**7**	×	**18**	4.17	5.00	20.83
RT 5			379	375	379	**12**	482	**7**	×	**18**	4.17	5.00	20.83
RT 6			311	315	315	**10**	577	**7**	×	**12**	3.17	5.00	15.83
RT 7			241	250	250	**9**	565	**7**	×	**10**	2.83	5.00	14.17
RT 8			90	98	98	**6**	501	**7**	×	**5**	2.00	5.00	10.00

Table 55 Sheet metal duct sizing worksheet for the Chicago home (ECM+0.3 IWC)

Duct Sizing Worksheet (Chicago home Rigid 0.3 IWC ECM)													
HF =	Blower CFM -		Heating Load =		1000	/	48000	=	0.02083333			FR Value =	0.01
CF =	Blower CFM -		Cooling Load =		1000	/	30000	=	0.03333333				
Supply Runout													
Name	H-Btu	C-Btu	H-Cfm	C-Cfm	Design Cfm	Round Size	Velocity	Final Size	Perimeter	Length	Surface Area		
	Btu/hr	Btu/hr	cfm	cfm	cfm	inch	FPM	inch	ft	ft	ft^2		
S1	4320	2460	90	82	90	**9**	204	**9**	2.36	10.00	23.56		
S2	4032	2280	84	76	84	**9**	190	**9**	2.36	10.00	23.56		
S3	3792	3000	79	100	100	**9**	226	**9**	2.36	13.00	30.63		
S4	5376	3780	112	126	126	**10**	231	**10**	2.62	13.00	34.03		
S5	6480	3600	135	120	135	**10**	248	**10**	2.62	13.00	34.03		
S6	4272	2400	89	80	89	**9**	201	**9**	2.36	13.00	30.63		
S7	4416	2580	92	86	92	**9**	208	**9**	2.36	15.00	35.34		
S8	5760	3600	120	120	120	**10**	220	**10**	2.62	15.00	39.27		
S9	3840	2400	80	80	80	**9**	181	**9**	2.36	15.00	35.34		
S10	5712	3900	119	130	130	**10**	238	**10**	2.62	13.00	34.03		
Supply Trunk													
			H-Cfm	C-Cfm	Design Cfm	Round Size	Velocity	Final Size			Perimeter	Length	Surface Area
			cfm	cfm	cfm	inch	FPM	H	×	W	ft	ft	ft^2
ST 1	N/A		90	82	90	**9**	204	**14**	×	**5**	3.17	5.00	15.83
ST 2			174	158	174	**12**	222	**14**	×	**9**	3.83	5.00	19.17
ST 3			253	258	258	**14**	241	**14**	×	**12**	4.33	10.00	43.33
ST 4			365	384	384	**16**	275	**14**	×	**15**	4.83	5.00	24.17
ST 5			500	504	504	**18**	285	**14**	×	**20**	5.67	5.00	28.33
ST 6			500	496	500	**18**	283	**14**	×	**20**	5.67	5.00	28.33
ST 7			411	416	416	**16**	298	**14**	×	**15**	4.83	10.00	48.33
ST 8			319	330	330	**14**	309	**14**	×	**12**	4.33	5.00	21.67
ST 9			199	210	210	**12**	267	**14**	×	**9**	3.83	5.00	19.17
ST 10			119	130	130	**10**	238	**14**	×	**6**	3.33	5.00	16.67
Return Runout													
Name	Associated Supply run		H-Cfm	C-Cfm	Design Cfm	Round Size	Velocity	Final Size	Perimeter	Length	Surface Area		
			cfm	cfm	cfm	inch	FPM	inch	ft	ft	ft^2		
R1	S1		90	82	90	**9**	204	**9**	2.36	5.00	11.78		
R2	S2		84	76	84	**9**	190	**9**	2.36	5.00	11.78		
R3	S3, S4		191	226	226	**12**	288	**12**	3.14	7.00	21.99		
R4	S5		135	120	135	**10**	248	**10**	2.62	6.00	15.71		
R5	S6		89	80	89	**9**	201	**9**	2.36	7.00	16.49		
R6	S7		92	86	92	**9**	208	**9**	2.36	8.00	18.85		
R7	S8, S9		200	200	200	**12**	255	**12**	3.14	7.00	21.99		
R8	S10		119	130	130	**10**	238	**10**	2.62	6.00	15.71		
Return Trunk													
			H-Cfm	C-Cfm	Design Cfm	Round Size	Velocity	Final Size			Perimeter	Length	Surface Area
			cfm	cfm	cfm	inch	FPM	H	×	W	ft	ft	ft^2
RT 1	N/A		90	82	90	**9**	204	**14**	×	**5**	3.17	5.00	15.83
RT 2			174	158	174	**12**	222	**14**	×	**9**	3.83	5.00	19.17
RT 3			365	384	384	**16**	275	**14**	×	**15**	4.83	5.00	24.17
RT 4			500	504	504	**18**	285	**14**	×	**20**	5.67	5.00	28.33
RT 5			500	496	500	**18**	283	**14**	×	**20**	5.67	5.00	28.33
RT 6			411	416	416	**16**	298	**14**	×	**15**	4.83	5.00	24.17
RT 7			319	330	330	**14**	309	**14**	×	**12**	4.33	5.00	21.67
RT 8			119	130	130	**10**	238	**14**	×	**6**	3.33	5.00	16.67

Table 56 Sheet metal duct sizing worksheet for the Chicago home (ECM+0.5 IWC)

Duct Sizing Worksheet (Chicago home Rigid 0.5 IWC ECM)													
HF =	Blower CFM -		Heating Load =		1000	/	48000	=	0.02083333			FR Value =	0.06
CF =	Blower CFM -		Cooling Load =		1000	/	30000	=	0.03333333				
Supply Runout													
Name	H-Btu	C-Btu	H-Cfm	C-Cfm	Design Cfm	Round Size	Velocity	Final Size		Perimeter	Length	Surface Area	
	Btu/hr	Btu/hr	cfm	cfm	cfm	inch	FPM	inch		ft	ft	ft2	
S1	4320	2460	90	82	90	**6**	458	**6**		1.57	10.00	15.71	
S2	4032	2280	84	76	84	**6**	428	**6**		1.57	10.00	15.71	
S3	3792	3000	79	100	100	**6**	509	**6**		1.57	13.00	20.42	
S4	5376	3780	112	126	126	**7**	471	**7**		1.83	13.00	23.82	
S5	6480	3600	135	120	135	**7**	505	**7**		1.83	13.00	23.82	
S6	4272	2400	89	80	89	**6**	453	**6**		1.57	13.00	20.42	
S7	4416	2580	92	86	92	**6**	469	**6**		1.57	15.00	23.56	
S8	5760	3600	120	120	120	**7**	449	**7**		1.83	15.00	27.49	
S9	3840	2400	80	80	80	**6**	407	**6**		1.57	15.00	23.56	
S10	5712	3900	119	130	130	**7**	486	**7**		1.83	13.00	23.82	
Supply Trunk													
			H-Cfm	C-Cfm	Design Cfm	Round Size	Velocity	Final Size			Perimeter	Length	Surface Area
			cfm	cfm	cfm	inch	FPM	H	×	W	ft	ft	ft2
ST 1	N/A		90	82	90	**6**	458	**11**	×	**3**	2.33	5.00	11.67
ST 2			174	158	174	**8**	498	**11**	×	**5**	2.67	5.00	13.33
ST 3			253	258	258	**9**	584	**11**	×	**6**	2.83	10.00	28.33
ST 4			365	384	384	**12**	489	**11**	×	**11**	3.67	5.00	18.33
ST 5			500	504	504	**12**	642	**11**	×	**11**	3.67	5.00	18.33
ST 6			500	496	500	**12**	637	**11**	×	**11**	3.67	5.00	18.33
ST 7			411	416	416	**12**	530	**11**	×	**11**	3.67	10.00	36.67
ST 8			319	330	330	**14**	309	**11**	×	**15**	4.33	5.00	21.67
ST 9			199	210	210	**8**	602	**11**	×	**5**	2.67	5.00	13.33
ST 10			119	130	130	**7**	486	**11**	×	**4**	2.50	5.00	12.50
Return Runout													
Name	Associated Supply run		H-Cfm	C-Cfm	Design Cfm	Round Size	Velocity	Final Size	Perimeter	Length	Surface Area		
			cfm	cfm	cfm	inch	FPM	inch	ft	ft	ft2		
R1	S1		90	82	90	**6**	458	**6**	1.57	5.00	7.85		
R2	S2		84	76	84	**6**	428	**6**	1.57	5.00	7.85		
R3	S3, S4		191	226	226	**8**	647	**8**	2.09	7.00	14.66		
R4	S5		135	120	135	**7**	505	**7**	1.83	6.00	11.00		
R5	S6		89	80	89	**6**	453	**6**	1.57	7.00	11.00		
R6	S7		92	86	92	**6**	469	**6**	1.57	8.00	12.57		
R7	S8, S9		200	200	200	**8**	573	**8**	2.09	7.00	14.66		
R8	S10		119	130	130	**7**	486	**7**	1.83	6.00	11.00		
Return Trunk													
			H-Cfm	C-Cfm	Design Cfm	Round Size	Velocity	Final Size			Perimeter	Length	Surface Area
			cfm	cfm	cfm	inch	FPM	H	×	W	ft	ft	ft2
RT 1	N/A		90	82	90	**6**	458	**11**	×	**3**	2.33	5.00	11.67
RT 2			174	158	174	**8**	498	**11**	×	**5**	2.67	5.00	13.33
RT 3			365	384	384	**12**	489	**11**	×	**11**	3.67	5.00	18.33
RT 4			500	504	504	**12**	642	**11**	×	**11**	3.67	5.00	18.33
RT 5			500	496	500	**12**	637	**11**	×	**11**	3.67	5.00	18.33
RT 6			411	416	416	**10**	763	**11**	×	**8**	3.17	5.00	15.83
RT 7			319	330	330	**10**	605	**11**	×	**8**	3.17	5.00	15.83
RT 8			119	130	130	**7**	486	**11**	×	**4**	2.50	5.00	12.50

Table 57 Sheet metal duct sizing worksheet for the Chicago home (ECM+0.8 IWC)

Duct Sizing Worksheet (Chicago home Rigid 0.8 IWC ECM)													
HF =	Blower CFM -		Heating Load =		1000	/	48000	=	0.02083333			FR Value =	0.13
CF =	Blower CFM -		Cooling Load =		1000	/	30000	=	0.03333333				
Supply Runout													
Name	H-Btu	C-Btu	H-Cfm	C-Cfm	Design Cfm	Round Size	Velocity	Final Size	Perimeter	Length	Surface Area		
	Btu/hr	Btu/hr	cfm	cfm	cfm	inch	FPM	inch	ft	ft	ft^2		
S1	4320	2460	90	82	90	**5**	660	**5**	1.31	10.00	13.09		
S2	4032	2280	84	76	84	**5**	616	**5**	1.31	10.00	13.09		
S3	3792	3000	79	100	100	**5**	733	**5**	1.31	13.00	17.02		
S4	5376	3780	112	126	126	**6**	642	**6**	1.57	13.00	20.42		
S5	6480	3600	135	120	135	**6**	688	**6**	1.57	13.00	20.42		
S6	4272	2400	89	80	89	**5**	653	**5**	1.31	13.00	17.02		
S7	4416	2580	92	86	92	**5**	675	**5**	1.31	15.00	19.63		
S8	5760	3600	120	120	120	**6**	611	**6**	1.57	15.00	23.56		
S9	3840	2400	80	80	80	**5**	587	**5**	1.31	15.00	19.63		
S10	5712	3900	119	130	130	**6**	662	**6**	1.57	13.00	20.42		
Supply Trunk													
			H-Cfm	C-Cfm	Design Cfm	Round Size	Velocity	Final Size			Perimeter	Length	Surface Area
			cfm	cfm	cfm	inch	FPM	H	×	W	ft	ft	ft^2
ST 1	N/A		90	82	90	**5**	660	**7**	×	**3**	1.67	5.00	8.33
ST 2			174	158	174	**7**	651	**7**	×	**6**	2.17	5.00	10.83
ST 3			253	258	258	**8**	739	**7**	×	**8**	2.50	10.00	25.00
ST 4			365	384	384	**9**	869	**7**	×	**10**	2.83	5.00	14.17
ST 5			500	504	504	**12**	642	**7**	×	**18**	4.17	5.00	20.83
ST 6			500	496	500	**12**	637	**7**	×	**18**	4.17	5.00	20.83
ST 7			411	416	416	**9**	942	**7**	×	**10**	2.83	10.00	28.33
ST 8			319	330	330	**9**	747	**7**	×	**10**	2.83	5.00	14.17
ST 9			199	210	210	**7**	786	**7**	×	**6**	2.17	5.00	10.83
ST 10			119	130	130	**6**	662	**7**	×	**5**	2.00	5.00	10.00
Return Runout													
Name	Associated Supply run		H-Cfm	C-Cfm	Design Cfm	Round Size	Velocity	Final Size	Perimeter	Length	Surface Area		
			cfm	cfm	cfm	inch	FPM	inch	ft	ft	ft^2		
R1	S1		90	82	90	**5**	660	**5**	1.31	5.00	6.54		
R2	S2		84	76	84	**5**	616	**5**	1.31	5.00	6.54		
R3	S3, S4		191	226	226	**7**	846	**7**	1.83	7.00	12.83		
R4	S5		135	120	135	**6**	688	**6**	1.57	6.00	9.42		
R5	S6		89	80	89	**5**	653	**5**	1.31	7.00	9.16		
R6	S7		92	86	92	**5**	675	**5**	1.31	8.00	10.47		
R7	S8, S9		200	200	200	**7**	748	**7**	1.83	7.00	12.83		
R8	S10		119	130	130	**6**	662	**6**	1.57	6.00	9.42		
Return Trunk													
			H-Cfm	C-Cfm	Design Cfm	Round Size	Velocity	Final Size			Perimeter	Length	Surface Area
			cfm	cfm	cfm	inch	FPM	H	×	W	ft	ft	ft^2
RT 1	N/A		90	82	90	**5**	660	**7**	×	**3**	1.67	5.00	8.33
RT 2			174	158	174	**7**	651	**7**	×	**6**	2.17	5.00	10.83
RT 3			365	384	384	**10**	704	**7**	×	**12**	3.17	5.00	15.83
RT 4			500	504	504	**12**	642	**7**	×	**18**	4.17	5.00	20.83
RT 5			500	496	500	**12**	637	**7**	×	**18**	4.17	5.00	20.83
RT 6			411	416	416	**10**	763	**7**	×	**12**	3.17	5.00	15.83
RT 7			319	330	330	**9**	747	**7**	×	**10**	2.83	5.00	14.17
RT 8			119	130	130	**6**	662	**7**	×	**5**	2.00	5.00	10.00

Table 58 Sheet metal duct sizing worksheet for the Austin home (PSC+0.3 IWC)

Duct Sizing Worksheet (Austin home Rigid 0.3 IWC PSC)													
HF =	Blower CFM -		Heating Load =		1298	/	42000	=	0.030904762			FR Value =	0.01
CF =	Blower CFM -		Cooling Load =		1298	/	36000	=	0.036055556				
Supply Runout													
Name	H-Btu	C-Btu	H-Cfm	C-Cfm	Design Cfm	Round Size	Velocity	Final Size	Perimeter	Length	Surface Area		
	Btu/hr	Btu/hr	cfm	cfm	cfm	inch	FPM	inch	ft	ft	ft^2		
S1	3780	2952	117	106	117	**10**	214	**10**	2.62	10.00	26.18		
S2	3528	2736	109	99	109	**9**	247	**9**	2.36	10.00	23.56		
S3	3318	3600	103	130	130	**10**	238	**10**	2.62	13.00	34.03		
S4	4704	4536	145	164	164	**12**	208	**12**	3.14	13.00	40.84		
S5	5670	4320	175	156	175	**12**	223	**12**	3.14	13.00	40.84		
S6	3738	2880	116	104	116	**10**	212	**10**	2.62	13.00	34.03		
S7	3864	3096	119	112	119	**10**	219	**10**	2.62	15.00	39.27		
S8	5040	4320	156	156	156	**12**	198	**12**	3.14	15.00	47.12		
S9	3360	2880	104	104	104	**10**	190	**10**	2.62	15.00	39.27		
S10	4998	4680	154	169	169	**12**	215	**12**	3.14	13.00	40.84		
Supply Trunk													
			H-Cfm	C-Cfm	Design Cfm	Round Size	Velocity	Final Size			Perimeter	Length	Surface Area
			cfm	cfm	cfm	inch	FPM	H	×	W	ft	ft	ft^2
ST 1			117	106	117	**10**	214	**24**	×	**4**	4.67	5.00	23.33
ST 2			226	205	226	**12**	288	**24**	×	**6**	5.00	5.00	25.00
ST 3			328	335	335	**14**	313	**24**	×	**7**	5.17	10.00	51.67
ST 4			474	498	498	**16**	357	**24**	×	**9**	5.50	5.00	27.50
ST 5	N/A		649	654	654	**20**	300	**24**	×	**14**	6.33	5.00	31.67
ST 6			649	644	649	**20**	297	**24**	×	**14**	6.33	5.00	31.67
ST 7			533	540	540	**18**	306	**24**	×	**12**	6.00	10.00	60.00
ST 8			414	428	428	**16**	307	**24**	×	**9**	5.50	5.00	27.50
ST 9			258	273	273	**14**	255	**24**	×	**7**	5.17	5.00	25.83
ST 10			154	169	169	**12**	215	**24**	×	**6**	5.00	5.00	25.00
Return Runout													
Name	Associated Supply run		H-Cfm	C-Cfm	Design Cfm	Round Size	Velocity	Final Size	Perimeter	Length	Surface Area		
			cfm	cfm	cfm	inch	FPM	inch	ft	ft	ft^2		
R1	S1		117	106	117	**10**	214	**10**	2.62	5.00	13.09		
R2	S2		109	99	109	**10**	200	**10**	2.62	5.00	13.09		
R3	S3, S4		248	293	293	**14**	274	**14**	3.67	7.00	25.66		
R4	S5		175	156	175	**12**	223	**12**	3.14	6.00	18.85		
R5	S6		116	104	116	**10**	212	**10**	2.62	7.00	18.33		
R6	S7		119	112	119	**10**	219	**10**	2.62	8.00	20.94		
R7	S8, S9		260	260	260	**14**	243	**14**	3.67	7.00	25.66		
R8	S10		154	169	169	**12**	215	**12**	3.14	6.00	18.85		
Return Trunk													
			H-Cfm	C-Cfm	Design Cfm	Round Size	Velocity	Final Size			Perimeter	Length	Surface Area
			cfm	cfm	cfm	inch	FPM	H	×	W	ft	ft	ft^2
RT 1			117	106	117	**10**	214	**24**	×	**4**	4.67	5.00	23.33
RT 2			226	205	226	**12**	288	**24**	×	**6**	5.00	5.00	25.00
RT 3			474	498	498	**16**	357	**24**	×	**9**	5.50	5.00	27.50
RT 4	N/A		649	654	654	**20**	300	**24**	×	**14**	6.33	5.00	31.67
RT 5			649	644	649	**20**	297	**24**	×	**14**	6.33	5.00	31.67
RT 6			533	540	540	**18**	306	**24**	×	**12**	6.00	5.00	30.00
RT 7			414	428	428	**16**	307	**24**	×	**9**	5.50	5.00	27.50
RT 8			154	169	169	**12**	215	**24**	×	**6**	5.00	5.00	25.00

Table 59 Sheet metal duct sizing worksheet for the Austin home (PSC+0.5 IWC)

Duct Sizing Worksheet (Austin home Rigid 0.5 IWC PSC)													
HF =	Blower CFM -		Heating Load =		1206	/	42000	=	0.02871429			FR Value =	0.06
CF =	Blower CFM -		Cooling Load =		1206	/	36000	=	0.0335				
Supply Runout													
Name	H-Btu	C-Btu	H-Cfm	C-Cfm	Design Cfm	Round Size	Velocity	Final Size	Perimeter	Length	Surface Area		
	Btu/hr	Btu/hr	cfm	cfm	cfm	inch	FPM	inch	ft	ft	ft^2		
S1	3780	2952	109	99	109	**7**	406	**7**	1.83	10.00	18.33		
S2	3528	2736	101	92	101	**7**	379	**7**	1.83	10.00	18.33		
S3	3318	3600	95	121	121	**7**	451	**7**	1.83	13.00	23.82		
S4	4704	4536	135	152	152	**8**	435	**8**	2.09	13.00	27.23		
S5	5670	4320	163	145	163	**8**	466	**8**	2.09	13.00	27.23		
S6	3738	2880	107	96	107	**7**	402	**7**	1.83	13.00	23.82		
S7	3864	3096	111	104	111	**7**	415	**7**	1.83	15.00	27.49		
S8	5040	4320	145	145	145	**8**	415	**8**	2.09	15.00	31.42		
S9	3360	2880	96	96	96	**7**	361	**7**	1.83	15.00	27.49		
S10	4998	4680	144	157	157	**8**	449	**8**	2.09	13.00	27.23		
Supply Trunk													
			H-Cfm	C-Cfm	Design Cfm	Round Size	Velocity	Final Size			Perimeter	Length	Surface Area
			cfm	cfm	cfm	inch	FPM	H	×	W	ft	ft	ft^2
ST 1	N/A		109	99	109	**7**	406	**11**	×	**4**	2.50	5.00	12.50
ST 2			210	191	210	**9**	475	**11**	×	**6**	2.83	5.00	14.17
ST 3			305	311	311	**10**	570	**11**	×	**8**	3.17	10.00	31.67
ST 4			440	463	463	**12**	590	**11**	×	**11**	3.67	5.00	18.33
ST 5			603	608	608	**12**	774	**11**	×	**11**	3.67	5.00	18.33
ST 6			603	598	603	**12**	768	**11**	×	**11**	3.67	5.00	18.33
ST 7			496	502	502	**12**	639	**11**	×	**11**	3.67	10.00	36.67
ST 8			385	398	398	**12**	507	**11**	×	**11**	3.67	5.00	18.33
ST 9			240	253	253	**9**	573	**11**	×	**6**	2.83	5.00	14.17
ST 10			144	157	157	**8**	449	**11**	×	**5**	2.67	5.00	13.33
Return Runout													
Name	Associated Supply run		H-Cfm	C-Cfm	Design Cfm	Round Size	Velocity	Final Size	Perimeter	Length	Surface Area		
			cfm	cfm	cfm	inch	FPM	inch	ft	ft	ft^2		
R1	S1		109	99	109	**7**	406	**7**	1.83	5.00	9.16		
R2	S2		101	92	101	**7**	379	**7**	1.83	5.00	9.16		
R3	S3, S4		230	273	273	**10**	500	**10**	2.62	7.00	18.33		
R4	S5		163	145	163	**8**	466	**8**	2.09	6.00	12.57		
R5	S6		107	96	107	**7**	402	**7**	1.83	7.00	12.83		
R6	S7		111	104	111	**7**	415	**7**	1.83	8.00	14.66		
R7	S8, S9		241	241	241	**9**	546	**9**	2.36	7.00	16.49		
R8	S10		144	157	157	**8**	449	**8**	2.09	6.00	12.57		
Return Trunk													
			H-Cfm	C-Cfm	Design Cfm	Round Size	Velocity	Final Size			Perimeter	Length	Surface Area
			cfm	cfm	cfm	inch	FPM	H	×	W	ft	ft	ft^2
RT 1	N/A		109	99	109	**7**	406	**11**	×	**4**	2.50	5.00	12.50
RT 2			210	191	210	**9**	475	**11**	×	**6**	2.83	5.00	14.17
RT 3			440	463	463	**12**	590	**11**	×	**11**	3.67	5.00	18.33
RT 4			603	608	608	**14**	569	**11**	×	**15**	4.33	5.00	21.67
RT 5			603	598	603	**14**	564	**11**	×	**15**	4.33	5.00	21.67
RT 6			496	502	502	**12**	639	**11**	×	**11**	3.67	5.00	18.33
RT 7			385	398	398	**12**	507	**11**	×	**11**	3.67	5.00	18.33
RT 8			144	157	157	**8**	449	**11**	×	**5**	2.67	5.00	13.33

Table 60 Sheet metal duct sizing worksheet for the Austin home (PSC+0.8 IWC)

Duct Sizing Worksheet (Austin home Rigid 0.8 IWC PSC)													
HF =	Blower CFM -		Heating Load =		915	/	42000	=	0.02178571			FR Value =	0.13
CF =	Blower CFM -		Cooling Load =		915	/	36000	=	0.02541667				
Supply Runout													
Name	H-Btu	C-Btu	H-Cfm	C-Cfm	Design Cfm	Round Size	Velocity	Final Size	Perimeter	Length	Surface Area		
	Btu/hr	Btu/hr	cfm	cfm	cfm	inch	FPM	inch	ft	ft	ft^2		
S1	3780	2952	82	75	82	**5**	604	**5**	1.31	10.00	13.09		
S2	3528	2736	77	70	77	**5**	564	**5**	1.31	10.00	13.09		
S3	3318	3600	72	92	92	**6**	466	**6**	1.57	13.00	20.42		
S4	4704	4536	102	115	115	**6**	587	**6**	1.57	13.00	20.42		
S5	5670	4320	124	110	124	**6**	629	**6**	1.57	13.00	20.42		
S6	3738	2880	81	73	81	**5**	597	**5**	1.31	13.00	17.02		
S7	3864	3096	84	79	84	**5**	617	**5**	1.31	15.00	19.63		
S8	5040	4320	110	110	110	**6**	559	**6**	1.57	15.00	23.56		
S9	3360	2880	73	73	73	**5**	537	**5**	1.31	15.00	19.63		
S10	4998	4680	109	119	119	**6**	606	**6**	1.57	13.00	20.42		
Supply Trunk													
			H-Cfm	C-Cfm	Design Cfm	Round Size	Velocity	Final Size			Perimeter	Length	Surface Area
			cfm	cfm	cfm	inch	FPM	H	×	W	ft	ft	ft^2
ST 1			82	75	82	**5**	604	**5**	×	**4**	1.50	5.00	7.50
ST 2			159	145	159	**7**	596	**5**	×	**8**	2.17	5.00	10.83
ST 3			231	236	236	**8**	676	**5**	×	**11**	2.67	10.00	26.67
ST 4			334	351	351	**9**	795	**5**	×	**14**	3.17	5.00	15.83
ST 5	N/A		458	461	461	**10**	846	**5**	×	**18**	3.83	5.00	19.17
ST 6			458	454	458	**10**	839	**5**	×	**18**	3.83	5.00	19.17
ST 7			376	381	381	**9**	862	**5**	×	**15**	3.33	10.00	33.33
ST 8			292	302	302	**8**	865	**5**	×	**11**	2.67	5.00	13.33
ST 9			182	192	192	**7**	719	**5**	×	**8**	2.17	5.00	10.83
ST 10			109	119	119	**6**	606	**5**	×	**6**	1.83	5.00	9.17
Return Runout													
Name	Associated Supply run		H-Cfm	C-Cfm	Design Cfm	Round Size	Velocity	Final Size	Perimeter	Length	Surface Area		
			cfm	cfm	cfm	inch	FPM	inch	ft	ft	ft^2		
R1	S1		82	75	82	**5**	604	**5**	1.31	5.00	6.54		
R2	S2		77	70	77	**5**	564	**5**	1.31	5.00	6.54		
R3	S3, S4		175	207	207	**7**	774	**7**	1.83	7.00	12.83		
R4	S5		124	110	124	**6**	629	**6**	1.57	6.00	9.42		
R5	S6		81	73	81	**5**	597	**5**	1.31	7.00	9.16		
R6	S7		84	79	84	**5**	617	**5**	1.31	8.00	10.47		
R7	S8, S9		183	183	183	**7**	685	**7**	1.83	7.00	12.83		
R8	S10		109	119	119	**6**	606	**6**	1.57	6.00	9.42		
Return Trunk													
			H-Cfm	C-Cfm	Design Cfm	Round Size	Velocity	Final Size			Perimeter	Length	Surface Area
			cfm	cfm	cfm	inch	FPM	H	×	W	ft	ft	ft^2
RT 1			82	75	82	**5**	604	**5**	×	**4**	1.50	5.00	7.50
RT 2			159	145	159	**7**	596	**5**	×	**8**	2.17	5.00	10.83
RT 3			334	351	351	**9**	795	**5**	×	**14**	3.17	5.00	15.83
RT 4	N/A		458	461	461	**10**	846	**5**	×	**18**	3.83	5.00	19.17
RT 5			458	454	458	**10**	839	**5**	×	**18**	3.83	5.00	19.17
RT 6			376	381	381	**10**	698	**5**	×	**18**	3.83	5.00	19.17
RT 7			292	302	302	**8**	865	**5**	×	**11**	2.67	5.00	13.33
RT 8			109	119	119	**6**	606	**5**	×	**6**	1.83	5.00	9.17

Table 61 Sheet metal duct sizing worksheet for the Austin home (ECM+0.3 IWC)

Duct Sizing Worksheet (Austin home Rigid 0.3 IWC ECM)													
HF =	Blower CFM -		Heating Load =	1200	/	42000	=	0.02857143			FR Value =	0.01	
CF =	Blower CFM -		Cooling Load =	1200	/	36000	=	0.03333333					
Supply Runout													
Name	H-Btu	C-Btu	H-Cfm	C-Cfm	Design Cfm	Round Size	Velocity	Final Size		Perimeter	Length	Surface Area		
	Btu/hr	Btu/hr	cfm	cfm	cfm	inch	FPM	inch		ft	ft	ft^2		
S1	3780	2952	108	98	108	**9**	244	**9**		2.36	10.00	23.56		
S2	3528	2736	101	91	101	**9**	228	**9**		2.36	10.00	23.56		
S3	3318	3600	95	120	120	**10**	220	**10**		2.62	13.00	34.03		
S4	4704	4536	134	151	151	**10**	277	**10**		2.62	13.00	34.03		
S5	5670	4320	162	144	162	**10**	297	**10**		2.62	13.00	34.03		
S6	3738	2880	107	96	107	**9**	242	**9**		2.36	13.00	30.63		
S7	3864	3096	110	103	110	**9**	250	**9**		2.36	15.00	35.34		
S8	5040	4320	144	144	144	**10**	264	**10**		2.62	15.00	39.27		
S9	3360	2880	96	96	96	**9**	217	**9**		2.36	15.00	35.34		
S10	4998	4680	143	156	156	**10**	286	**10**		2.62	13.00	34.03		
Supply Trunk														
			H-Cfm	C-Cfm	Design Cfm	Round Size	Velocity	Final Size			Perimeter	Length	Surface Area	
			cfm	cfm	cfm	inch	FPM	H	×	W	ft	ft	ft^2	
ST 1	N/A		108	98	108	**9**	244	**14**	×	**5**	3.17	5.00	15.83	
ST 2			209	190	209	**12**	266	**14**	×	**9**	3.83	5.00	19.17	
ST 3			304	310	310	**14**	290	**14**	×	**12**	4.33	10.00	43.33	
ST 4			438	461	461	**16**	330	**14**	×	**15**	4.83	5.00	24.17	
ST 5			600	605	605	**18**	342	**14**	×	**19**	5.50	5.00	27.50	
ST 6			600	595	600	**18**	340	**14**	×	**19**	5.50	5.00	27.50	
ST 7			493	499	499	**16**	358	**14**	×	**15**	4.83	10.00	48.33	
ST 8			383	396	396	**16**	284	**14**	×	**15**	4.83	5.00	24.17	
ST 9			239	252	252	**12**	321	**14**	×	**9**	3.83	5.00	19.17	
ST 10			143	156	156	**10**	286	**14**	×	**6**	3.33	5.00	16.67	
Return Runout														
Name	Associated Supply run		H-Cfm	C-Cfm	Design Cfm	Round Size	Velocity	Final Size	Perimeter	Length	Surface Area			
			cfm	cfm	cfm	inch	FPM	inch	ft	ft	ft^2			
R1	S1		108	98	108	**9**	244	**9**	2.36	5.00	11.78			
R2	S2		101	91	101	**9**	228	**9**	2.36	5.00	11.78			
R3	S3, S4		229	271	271	**12**	345	**12**	3.14	7.00	21.99			
R4	S5		162	144	162	**10**	297	**10**	2.62	6.00	15.71			
R5	S6		107	96	107	**9**	242	**9**	2.36	7.00	16.49			
R6	S7		110	103	110	**9**	250	**9**	2.36	8.00	18.85			
R7	S8, S9		240	240	240	**12**	306	**12**	3.14	7.00	21.99			
R8	S10		143	156	156	**10**	286	**10**	2.62	6.00	15.71			
Return Trunk														
			H-Cfm	C-Cfm	Design Cfm	Round Size	Velocity	Final Size			Perimeter	Length	Surface Area	
			cfm	cfm	cfm	inch	FPM	H	×	W	ft	ft	ft^2	
RT 1	N/A		108	98	108	**9**	244	**14**	×	**5**	3.17	5.00	15.83	
RT 2			209	190	209	**12**	266	**14**	×	**9**	3.83	5.00	19.17	
RT 3			438	461	461	**16**	330	**14**	×	**15**	4.83	5.00	24.17	
RT 4			600	605	605	**18**	342	**14**	×	**19**	5.50	5.00	27.50	
RT 5			600	595	600	**18**	340	**14**	×	**19**	5.50	5.00	27.50	
RT 6			493	499	499	**16**	358	**14**	×	**15**	4.83	5.00	24.17	
RT 7			383	396	396	**14**	370	**14**	×	**12**	4.33	5.00	21.67	
RT 8			143	156	156	**10**	286	**14**	×	**6**	3.33	5.00	16.67	

Table 62 Sheet metal duct sizing worksheet for the Austin home (ECM+0.5 IWC)

Duct Sizing Worksheet (Austin home Rigid 0.5 IWC ECM)													
HF =	Blower CFM -		Heating Load =		1200	/	42000	=	0.02857143			FR Value =	0.06
CF =	Blower CFM -		Cooling Load =		1200	/	36000	=	0.03333333				
Supply Runout													
Name	H-Btu	C-Btu	H-Cfm	C-Cfm	Design Cfm	Round Size	Velocity	Final Size	Perimeter	Length	Surface Area		
	Btu/hr	Btu/hr	cfm	cfm	cfm	inch	FPM	inch	ft	ft	ft^2		
S1	3780	2952	108	98	108	**7**	404	**7**	1.83	10.00	18.33		
S2	3528	2736	101	91	101	**7**	377	**7**	1.83	10.00	18.33		
S3	3318	3600	95	120	120	**7**	449	**7**	1.83	13.00	23.82		
S4	4704	4536	134	151	151	**8**	433	**8**	2.09	13.00	27.23		
S5	5670	4320	162	144	162	**8**	464	**8**	2.09	13.00	27.23		
S6	3738	2880	107	96	107	**7**	400	**7**	1.83	13.00	23.82		
S7	3864	3096	110	103	110	**7**	413	**7**	1.83	15.00	27.49		
S8	5040	4320	144	144	144	**8**	413	**8**	2.09	15.00	31.42		
S9	3360	2880	96	96	96	**7**	359	**7**	1.83	15.00	27.49		
S10	4998	4680	143	156	156	**8**	447	**8**	2.09	13.00	27.23		
Supply Trunk													
			H-Cfm	C-Cfm	Design Cfm	Round Size	Velocity	Final Size			Perimeter	Length	Surface Area
			cfm	cfm	cfm	inch	FPM	H	×	W	ft	ft	ft^2
ST 1	N/A		108	98	108	**7**	404	**11**	×	**4**	2.50	5.00	12.50
ST 2			209	190	209	**8**	598	**11**	×	**5**	2.67	5.00	13.33
ST 3			304	310	310	**10**	568	**11**	×	**8**	3.17	10.00	31.67
ST 4			438	461	461	**12**	587	**11**	×	**11**	3.67	5.00	18.33
ST 5			600	605	605	**14**	566	**11**	×	**15**	4.33	5.00	21.67
ST 6			600	595	600	**14**	561	**11**	×	**15**	4.33	5.00	21.67
ST 7			493	499	499	**12**	636	**11**	×	**11**	3.67	10.00	36.67
ST 8			383	396	396	**12**	504	**11**	×	**11**	3.67	5.00	18.33
ST 9			239	252	252	**9**	570	**11**	×	**6**	2.83	5.00	14.17
ST 10			143	156	156	**8**	447	**11**	×	**5**	2.67	5.00	13.33
Return Runout													
Name	Associated Supply run		H-Cfm	C-Cfm	Design Cfm	Round Size	Velocity	Final Size	Perimeter	Length	Surface Area		
			cfm	cfm	cfm	inch	FPM	inch	ft	ft	ft^2		
R1	S1		108	98	108	**7**	404	**7**	1.83	5.00	9.16		
R2	S2		101	91	101	**7**	377	**7**	1.83	5.00	9.16		
R3	S3, S4		229	271	271	**10**	497	**10**	2.62	7.00	18.33		
R4	S5		162	144	162	**8**	464	**8**	2.09	6.00	12.57		
R5	S6		107	96	107	**7**	400	**7**	1.83	7.00	12.83		
R6	S7		110	103	110	**7**	413	**7**	1.83	8.00	14.66		
R7	S8, S9		240	240	240	**9**	543	**9**	2.36	7.00	16.49		
R8	S10		143	156	156	**8**	447	**8**	2.09	6.00	12.57		
Return Trunk													
			H-Cfm	C-Cfm	Design Cfm	Round Size	Velocity	Final Size			Perimeter	Length	Surface Area
			cfm	cfm	cfm	inch	FPM	H	×	W	ft	ft	ft^2
RT 1	N/A		108	98	108	**7**	404	**11**	×	**4**	2.50	5.00	12.50
RT 2			209	190	209	**8**	598	**11**	×	**5**	2.67	5.00	13.33
RT 3			438	461	461	**12**	587	**11**	×	**11**	3.67	5.00	18.33
RT 4			600	605	605	**14**	566	**11**	×	**15**	4.33	5.00	21.67
RT 5			600	595	600	**14**	561	**11**	×	**15**	4.33	5.00	21.67
RT 6			493	499	499	**12**	636	**11**	×	**11**	3.67	5.00	18.33
RT 7			383	396	396	**12**	504	**11**	×	**11**	3.67	5.00	18.33
RT 8			143	156	156	**8**	447	**11**	×	**5**	2.67	5.00	13.33

Table 63 Sheet metal duct sizing worksheet for the Austin home (ECM+0.8 IWC)

Duct Sizing Worksheet (Austin home Rigid 0.8 IWC ECM)													
HF =	Blower CFM -		Heating Load =		1200	/	42000	=	0.02857143			FR Value =	0.13
CF =	Blower CFM -		Cooling Load =		1200	/	36000	=	0.03333333				
Supply Runout													
Name	H-Btu	C-Btu	H-Cfm	C-Cfm	Design Cfm	Round Size	Velocity	Final Size	Perimeter	Length	Surface Area		
	Btu/hr	Btu/hr	cfm	cfm	cfm	inch	FPM	inch	ft	ft	ft^2		
S1	3780	2952	108	98	108	**6**	550	**6**	1.57	10.00	15.71		
S2	3528	2736	101	91	101	**6**	513	**6**	1.57	10.00	15.71		
S3	3318	3600	95	120	120	**6**	611	**6**	1.57	13.00	20.42		
S4	4704	4536	134	151	151	**7**	566	**7**	1.83	13.00	23.82		
S5	5670	4320	162	144	162	**7**	606	**7**	1.83	13.00	23.82		
S6	3738	2880	107	96	107	**6**	544	**6**	1.57	13.00	20.42		
S7	3864	3096	110	103	110	**6**	562	**6**	1.57	15.00	23.56		
S8	5040	4320	144	144	144	**7**	539	**7**	1.83	15.00	27.49		
S9	3360	2880	96	96	96	**6**	489	**6**	1.57	15.00	23.56		
S10	4998	4680	143	156	156	**7**	584	**7**	1.83	13.00	23.82		
Supply Trunk													
			H-Cfm	C-Cfm	Design Cfm	Round Size	Velocity	Final Size			Perimeter	Length	Surface Area
			cfm	cfm	cfm	inch	FPM	H	×	W	ft	ft	ft^2
ST 1	N/A		108	98	108	**6**	550	**8**	×	**4**	2.00	5.00	10.00
ST 2			209	190	209	**7**	781	**8**	×	**5**	2.17	5.00	10.83
ST 3			304	310	310	**9**	701	**8**	×	**9**	2.83	10.00	28.33
ST 4			438	461	461	**10**	845	**8**	×	**11**	3.17	5.00	15.83
ST 5			600	605	605	**12**	770	**8**	×	**16**	4.00	5.00	20.00
ST 6			600	595	600	**12**	764	**8**	×	**16**	4.00	5.00	20.00
ST 7			493	499	499	**10**	915	**8**	×	**11**	3.17	10.00	31.67
ST 8			383	396	396	**10**	726	**8**	×	**11**	3.17	5.00	15.83
ST 9			239	252	252	**8**	722	**8**	×	**7**	2.50	5.00	12.50
ST 10			143	156	156	**7**	584	**8**	×	**5**	2.17	5.00	10.83
Return Runout													
Name	Associated Supply run		H-Cfm	C-Cfm	Design Cfm	Round Size	Velocity	Final Size	Perimeter	Length	Surface Area		
			cfm	cfm	cfm	inch	FPM	inch	ft	ft	ft^2		
R1	S1		108	98	108	**6**	550	**6**	1.57	5.00	7.85		
R2	S2		101	91	101	**6**	513	**6**	1.57	5.00	7.85		
R3	S3, S4		229	271	271	**9**	614	**9**	2.36	7.00	16.49		
R4	S5		162	144	162	**7**	606	**7**	1.83	6.00	11.00		
R5	S6		107	96	107	**6**	544	**6**	1.57	7.00	11.00		
R6	S7		110	103	110	**6**	562	**6**	1.57	8.00	12.57		
R7	S8, S9		240	240	240	**8**	688	**8**	2.09	7.00	14.66		
R8	S10		143	156	156	**6**	795	**6**	1.57	6.00	9.42		
Return Trunk													
			H-Cfm	C-Cfm	Design Cfm	Round Size	Velocity	Final Size			Perimeter	Length	Surface Area
			cfm	cfm	cfm	inch	FPM	H	×	W	ft	ft	ft^2
RT 1	N/A		108	98	108	**6**	550	**8**	×	**4**	2.00	5.00	10.00
RT 2			209	190	209	**7**	781	**8**	×	**5**	2.17	5.00	10.83
RT 3			438	461	461	**10**	845	**8**	×	**11**	3.17	5.00	15.83
RT 4			600	605	605	**12**	770	**8**	×	**16**	4.00	5.00	20.00
RT 5			600	595	600	**12**	764	**8**	×	**16**	4.00	5.00	20.00
RT 6			493	499	499	**10**	915	**8**	×	**11**	3.17	5.00	15.83
RT 7			383	396	396	**10**	726	**8**	×	**11**	3.17	5.00	15.83
RT 8			143	156	156	**7**	584	**8**	×	**5**	2.17	5.00	10.83

APPENDIX J ENERGYPLUS SIMULATION LAYOUT

A complete air loop in EnergyPlus (LBNL 2013a) includes a supply side branch and a demand side branch (LBNL 2014). The supply side branch (the branch between the "air loop inlet node" and the "air loop outlet node") is modeled as compound components, consisting of a blower, a direct expansion (DX) cooling coil, and a gas heating coil, as shown in Figure 79.

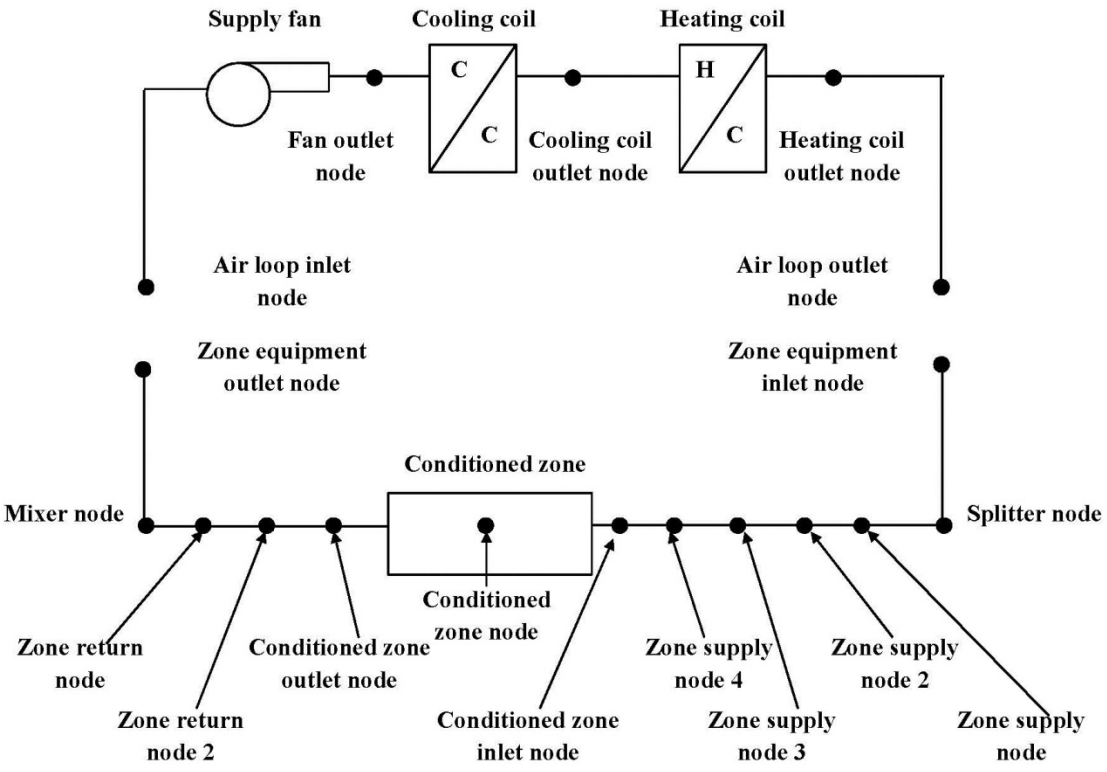

Figure 79 Node connections in EnergyPlus

The three EnergyPlus objects of Fan:OnOff, Coil:Cooling:DX:SingleSpeed, and Coil:Heating:Gas are first defined in the model group of fans and coils, and then assembled together in the object of AirLoopHVAC:Unitary:Furnace:HeatCool.

- Fan:OnOff

  This object models a constant air volume fan that is intended to cycle on and off in tandem with a cooling or heating system. The inputs of this object include fan/motor efficiency, maximum airflow rate, and fan pressure rise, all of which were provided by the developed empirical models of furnace blowers in Section 2.

- Coil:Cooling:DX:SingleSpeed

  This object represents the performance of a direct expansion (DX) cooling coil with a single capacity output. It uses performance information at the rating condition along with performance curves to determine capacities and power at part-load conditions. Sensible/latent capacity splits are determined by using the rated SHR and the SHR modifier curves. This DX cooling coil input requires the rated total cooling capacity, the rated SHR, the rated COP, and the rated air volume flow rate, all of which were experimentally determined at the rating condition (air entering the cooling coil at 80ºF dry-bulb/67°F wet-bulb (26.7°C dry-bulb/19.4°C wet-bulb) and air entering the outdoor condenser coil at 95°F dry-bulb (35°C dry-bulb)). In addition, this object requires a group of performance curves to estimate the actual capacities and power consumption at various airflow and temperature conditions. The capacity, power, and SHR modifier curves as a function of flow fractions were

determined from the air conditioner testing results over an airflow range of 1000 to 2250 ft^3/min (0.47 to 1.06 m^3/s), while the capacity, power, and SHR modifier curves as a function of temperatures were derived from the manufacturer's catalog data.

- Coil:Heating:Gas

  This object is a simple capacity model with the user-defined efficiency. The inputs include nominal capacity, user-defined efficiency, part load curve and parasitic electric or gas load. In this study, the efficiency of gas furnaces was assumed to be a constant of 80% and independent of airflows.

- AirLoopHVAC:Unitary:Furnace:HeatCool

  This object assembles all the previously defined EnergyPlus objects, namely Fan:OnOff, Coil:Cooling:DX:SingleSpeed and Coil:Heating:Gas, by connecting nodes that were defined with these components.

The branch between the "zone equipment inlet node" and the "zone equipment outlet node" is the supply side branch and represents the air distribution system. Supply and return ductworks in each duct design shown in Appendixes H and I were converted into single straight ducts by maintaining the same surface areas and pressure drops at design airflow rates. The equivalent duct cross-sectional areas and duct lengths of supply and return ductworks were assigned to the sectional branch between the "zone supply node 2" and the "zone supply node 3", which represents the supply ductwork, and the sectional branch between the "zone return node 2" and the "zone return node", which represents the return ductwork. The sectional branches between any other nodes in the

supply side branch were designed as idea ducts with no heat gains/losses through duct walls or pressure drops. A leakage level of 10% at a reference pressure of 0.1 in. w.g. (25 Pa) was assigned at the “zone supply node 2” and the “zone return node” to represent the supply and return leakages, respectively.

APPENDIX K COMPARISON OF ANNUAL ENERGY COSTS WITH AND WITHOUT LEAKAGES

The purpose of this section is to compare the impact of duct leakages on annual energy costs for both the Chicago home and the Austin home. In addition to the 24 building energy simulations that were performed and discussed in Section 4, another 24 simulations were conducted by maintaining the same input parameters but without modeling duct leakages. The annual energy costs without duct leakages were determined from the simulation results of electricity consumptions of blowers and condensing units as well as natural gas consumptions of furnaces at zero duct leakage, along with the same utility rates as used in Section 4 for the annual energy cost calculations for the Chicago home and the Austin home. Results of the annual energy cost with and without duct leakages are first grouped by the flow resistance magnitude and system configurations, and then shown in bar plots in Figure 80 and Figure 81 for the Chicago home and the Austin home, respectively. Also, the same results shown in Figure 80 and Figure 81 are summarized in Table 64, along with the percentage increase in the annual energy cost relative to the no-leakage scenario.

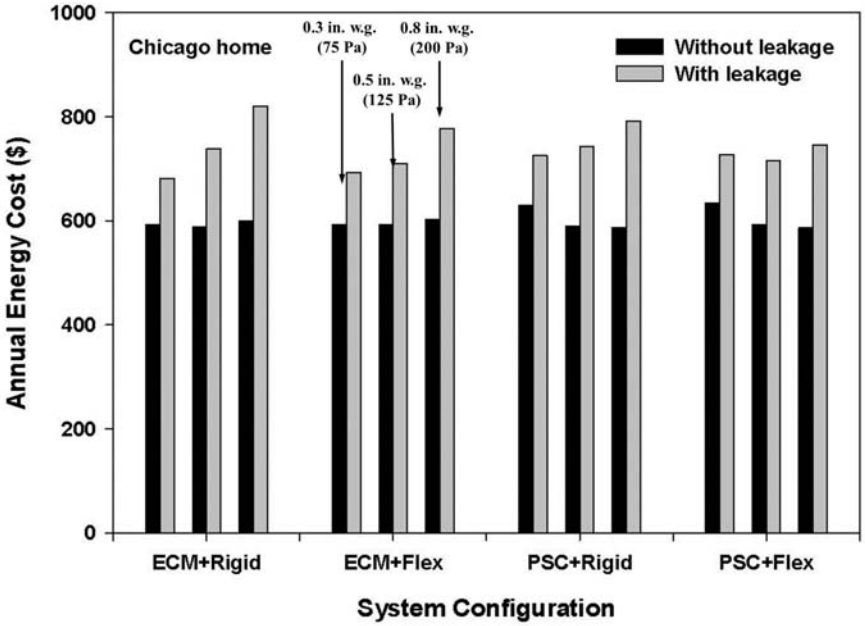

Figure 80 Comparison of annual energy cost for the Chicago home with and without duct leakages

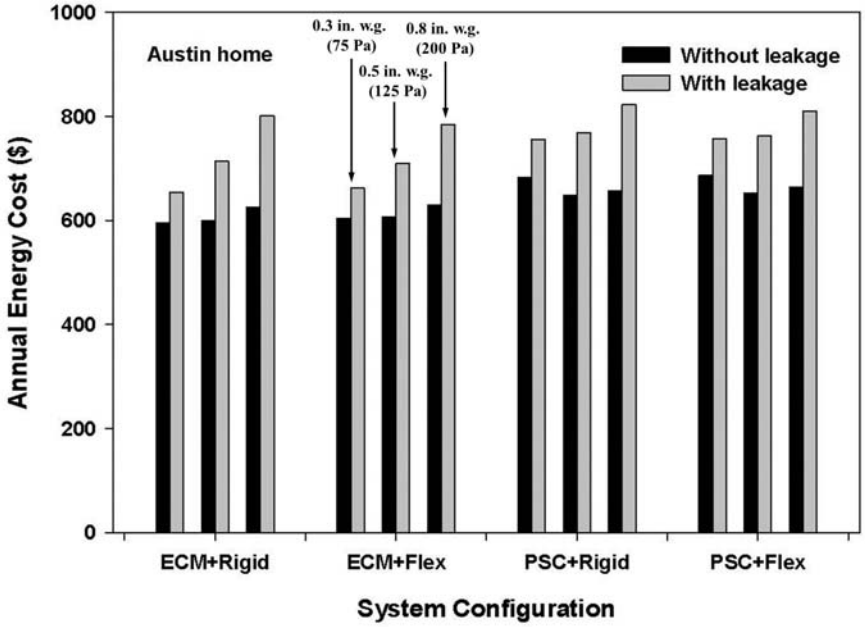

Figure 81 Comparison of annual energy cost for the Austin home with and without duct leakages

Table 64 Results of annual energy costs with and without duct leakages

Location	Blower	Ductwork	Flow resistance, in. w.g. (Pa)	Annual energy cost		
				No leakage, USD	With leakage, USD	Percentage increase, %
Chicago home	ECM	Sheet metal	0.3 (75)	593	681	13
			0.5 (125)	589	738	20
			0.8 (200)	599	820	27
		Flexible	0.3 (75)	593	693	14
			0.5 (125)	592	710	17
			0.8 (200)	602	777	22
	PSC	Sheet metal	0.3 (75)	629	725	13
			0.5 (125)	590	742	21
			0.8 (200)	588	792	26
		Flexible	0.3 (75)	634	727	13
			0.5 (125)	593	716	17
			0.8 (200)	586	746	21
Austin home	ECM	Sheet metal	0.3 (75)	596	654	9
			0.5 (125)	601	714	16
			0.8 (200)	625	801	22
		Flexible	0.3 (75)	605	662	9
			0.5 (125)	607	709	14
			0.8 (200)	630	785	20
	PSC	Sheet metal	0.3 (75)	683	755	10
			0.5 (125)	648	769	16
			0.8 (200)	658	822	20
		Flexible	0.3 (75)	687	757	9
			0.5 (125)	653	762	14
			0.8 (200)	664	810	18

Comparing the results with and without duct leakages in Figure 80 and Figure 81 along with Table 64 shows that the annual energy cost is increased with duct leakages in all simulated scenarios for both the Chicago home and the Austin home. For example, in the combination of ECM+Flex for the Chicago home, the annual energy cost at the low flow resistance of 0.3 in. w.g. (75 Pa) is increased by 14% from $593 to $693 as the effect of duct leakages is modeled. Increases in the annual energy cost are also observed in the other system configurations at all levels of flow resistances but with different magnitudes.

In addition, Table 64 shows that systems with higher flow resistances have greater percentage increases in the annual energy cost due to duct leakages compared to systems with lower flow resistances. For instance, in the combination of PSC+Rigid for the Austin home, the percentage increase in the annual energy cost is increased from 10% to 20% as a result of increasing the flow resistance from 0.3 to 0.8 in. w.g. (75 to 200 Pa). The same trend is also observed in all simulated scenarios for both the Chicago home and the Austin home. Table 64 shows that compared to the results without duct leakages, the annual energy cost with leakages for the Chicago home is increased by 13-14% at the low flow resistance of 0.3 in. w.g. (75 Pa), 17-21% at the medium flow resistance of 0.5 in. w.g. (125 Pa), and 21-27% at the high flow resistance of 0.8 in. w.g. (200 Pa). For the Austin home, the annual energy cost is increased by 9-10% at the low flow resistance of 0.3 in. w.g. (75 Pa), 14-16% at the medium flow resistance of 0.5 in. w.g. (125 Pa), and 18-22% at the high flow resistance of 0.8 in. w.g. (200 Pa), depending on duct designs and blower types.

Higher annual energy costs at higher duct flow resistances are mainly caused by increased duct leakages considering the fact that the leakage airflow is modeled proportionally to the differential pressure between the interior and exterior of the duct wall. The leakage airflow results in a loss of the conditioned air to the outside on the supply side and the infiltration of unconditioned air into the system on the return side. Therefore, greater energy use and higher annual costs occur in systems with both PSC and ECM blowers as the consequences of using ductworks of higher flow resistance.